

IDENTIFICATION OF HIV-1 REACTIVATING QUINOLINE COMPOUNDS AS BROMODOMAIN INHIBITORS

Erik Abner

TESI DOCTORAL UPF / 2016

Director:

Dr. Albert Jordan Vallès

Molecular Genomics Department

Molecular Biology Institute of Barcelona (IBMB) – CSIC

DEPARTMENT OF EXPERIMENTAL AND HEALTH SCIENCES - UPF



"If you torture the data long enough, it will confess."

Ronald H. Coase

ACKNOWLEDGEMENTS

Whoa. Writing these words now, it's finally hitting me how this stage of my life is almost over. It's been a journey beyond of what I expected, both in good and bad, but I imagine that's one of the main purposes of getting a PhD. Throughout my time here in Barcelona I feel like I've changed quite a lot, which is largely due to the amazing people that I've met here. You've all left a mark on me. Guess that's what I deserve for choosing the red pill.

First of course I want to thank my supervisor Albert Jordan, for allowing me to carry out this project, for his guidance, assistance and ideas. For going along with my stubborn nature and challenging me. Though it took some years to get the project moving, we finally got it done!

Thank you all who you've ever called me a polar bear. It was a real pleasure working with you guys. I can only imagine how satisfied you are that you can finally set the temperature in the lab back to the Mediterranean standards and won't have to wear sweaters to work in June any more. Especially I'm grateful to Carles, Andrea and Regi – you were always there to brainstorm with, giving me tips and introducing me new tricks.

Thank you Dr. Chiara Mencarelli, you've always been super supportive and believed in me even when I didn't myself. Being among my first mentors, you became a paragon to me on how a scientist should be and throughout the years I tried to mimic your attitude and persistence. I'd also like to thank some others from my Maastricht times. And I'd like to thank Dr. Willem Voncken and Dr. Frank Stassen for their personal support and for being among the most enthusiastic and stimulating professors I've had. Thank you Carla, David, Elke, Anne - I still miss burger Tuesdays and quiz nights...

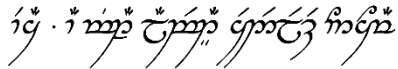
I want to thank Gabriela Uffert, my first mentor back in Estonia. You basically showed me how to hold a pipette, explained me what is transformation, witnessed my first infection and set me on the right path. All the best with your dissertation and defense as well!

I would like to thank Dr. Monty Montano, my mentor during my research stay in Harvard Med. Your California style ability to push and motivate people is something I hope to learn some day myself. While I'm at the Boston topic, I also want to thank Brian, it was a real pleasure working with you. Although my time in the lab was short, your professionalism and

über-postdoc-salesman-skills are characteristics I took with me as an inspiration from my time there.

Thank you Joana for all those late night cereals and wines and sharing labstories. And for letting me beg/borrow/steal stuff from your lab constantly. Just remember, as your Sagan put it: *"It pays to keep an open mind, but not so open your brains fall out."*

Thank you Alex, your well timed tea-breaks were able to keep me sane at times I could have flipped. Thank you Marcos for taking me to the best gigs of Barcelona. All the best to you guys with little Eliana, I'm sure you'll cultivate an epic biologist out of her eventually (even if you don't want to admit it yourself yet!).

Thank you Francisco and Jordi, you hopeless eternal nerds. 

I want to thank Maria, for pulling me out of the science stuff to all the non-science stuff. I promise to get my revenge somehow with the GFP prank you pulled on me once. And I want to thank my padawans Elisa, Lorenza and Julia. I learned from you as much as you hopefully learned from me.

I also want to thank Kadri and Arzu for your friendship and for reminding me once in a while what speaking your mother tongue feels like. Sticking to the roots kept me oriented. You two deserve a cold slow northern pokerfaced hug.

And then there's the long list of people I who've I've crossed paths with, but who all had a role in my journey. Let's start with you IRBians, who accepted me as one even though I was the mole in your institute: Berta, Claire, Craig, Emre, Felipe, Giorgia, Aina, Helena, Johan, Laura, Lorenzo, Natalia, Ninja, Pancho, Patrick, Petra, Sandra, Suvi, Salva. Make SHARC great again! The same goes for the CRGians: Adam, Alba, Alsu, André, Lucho, Michael. Special awesome awards go to the SCUBA divers, Gemma and Adrian. Rosa and Francisca also deserve to be pointed out, for reminding me that living in Barcelona is definitely more breathtaking than the previous rainy countries I used to live in. Thank you Robbi and Siragan from Boston, who definitely spiced up my "fruit salad of life". May you live long and prosper! I also can't get by without thanking Wikipedia, coffee machine, 9gag, Youtube, PhD comics, amazon.es, TED talks, indian cuisine, Phenomena cinema *etc.*

Thank you all who are back in Estonia and still remember me. Janis and Priit, years may pass, but luckily some people just won't change. Thank you BESTies, especially Jürgen and Tuuli.

Even if I sometimes feel like a tourist when I return to my own country, you two always manage to make me feel at home again.

I want to thank Aaron, Beta, Luis and Vika for those movie marathons, chino dinners, karaokes, hikes, Costa Brava weekends, trips all around world *etc.* Thank you for the company, for the friendship, for all the good times and the good vibes.

Finally, and with complete seriousness now, my deepest appreciation goes to all of my family. Not a day goes by that I remember how grateful I am to my parents for how they've raised their kids. Thank you for all the advice, all the help, for criticizing and scolding when needed (usually well deserved) and for always being understanding. Thank you for all the support and the unconditional love.

ABSTRACT

Upon HIV-1 infection, a reservoir of HIV latently infected resting T cells prevents the eradication of the virus from patients. To achieve eradication, the existing virus suppressing antiretroviral therapy must be combined with drugs that reactivate the dormant viruses. Our group previously described a novel chemical scaffold compound, MMQO (8-methoxy-6-methylquinolin-4-ol), which is capable of reactivating viral transcription through an unknown mechanism. The objective of this project was to identify the molecular binding partners of MMQO and elaborate their role in the reactivation of HIV-1.

We established that MMQO is capable of inducing HIV-1 independently of viral proteins by inducing transcription from proviral minigenomes lacking genes for viral components, allowing us to hypothesize that the compound primarily functions through host factors. Characterizing MMQO's transcriptional profiles with total mRNA expression microarrays, we were able to identify numerous traits provoked by the drug. MMQO displayed a robust immunosuppressive nature, it affected cell proliferation by diminishing cMyc and Bcl-2 protein levels and increased the dysregulation of acetylation sensitive genes. These hallmarks indicated that MMQO mimics acetylated lysines of core histones and functions as a bromodomain and extraterminal domain (BET) protein family inhibitor. Further gene expression and proteomic analysis confirmed this supposition and we demonstrated that MMQO dislodges the BET family member Brd4 from global chromatin and antagonizes the pro-latent role of Brd4 near the transcription start site of HIV-1. Computational docking models also confirmed MMQO's specificity towards the BET family bromodomains and an *in vitro* screening against the family members by FRET identified MMQO to have the highest affinity towards the Brd9 protein. Finally, we established that the inhibition of Brd9 had minimal effect on the proviral expression, suggesting that the primary function of MMQO on HIV-1 can be attributed to the displacement of Brd4.

Due to the broad range of properties characteristic to BET family inhibitors, these molecules are currently being evaluated in clinical trials against various types of cancers and immune conditions. The dual functioning scaffold compound MMQO is a new member of this class of drugs. The minimalistic structure of MMQO shows promise for it to be further optimized for higher affinities towards Brd9 / 4 and could potentially be of use in research against a variety of diseases, including HIV.

RESUMEN

Tras la infección por VIH-1, el establecimiento de un depósito de células T en reposo infectadas latentemente con VIH impide la erradicación del virus en pacientes. Para lograr la erradicación, la terapia retroviral existente debe combinarse con medicamentos que reactiven los virus latentes. Previamente, nuestro grupo describió un nuevo compuesto químico, MMQO (8-metoxi-6-metilquinolin-4-ol) que es capaz de reactivar la transcripción viral a través de un mecanismo desconocido. El objetivo de este proyecto fue identificar las proteínas que interactúan con MMQO e investigar su papel en la reactivación del VIH-1.

Hemos establecido que MMQO es capaz de inducir la transcripción de minigenomas provirales que carecen de genes para los componentes virales, lo que nos permite plantear la hipótesis de que el compuesto funciona principalmente a través de factores del huésped. La caracterización de los perfiles de transcripción de MMQO mediante *microarrays* de expresión nos permitió identificar numerosos rasgos provocados por el compuesto. MMQO muestra una robusta naturaleza inmunosupresora que afecta a la proliferación celular debido a la disminución de los niveles proteicos de cMyc y Bcl-2 y la desregulación de genes sensibles a acetilación. Estas características indican que MMQO imita las lisinas acetiladas de histonas y funciona como un inhibidor de bromodominio y dominio extraterminal (BET). Análisis adicionales de la expresión génica y proteómica confirmaron esta hipótesis y demostramos que MMQO desplaza de la cromatina a Brd4, un miembro de la familia BET y antagoniza el papel pro-latente de Brd4 cerca del sitio de inicio de la transcripción de VIH-1. Modelos computacionales de *docking* también confirmaron la especificidad de MMQO hacia los bromodominios de la familia BET y un ensayo *in vitro* mediante FRET contra los miembros de la familia, identificó que MMQO tiene una mayor afinidad hacia la proteína Brd9. Por último, hemos establecido que la inhibición de Brd9 tiene un mínimo efecto sobre la expresión proviral, lo que sugiere que la principal función de MMQO sobre VIH-1 se puede atribuir al desplazamiento de Brd4.

Debido a la amplia gama de propiedades de los inhibidores de la familia BET, estas moléculas se están evaluando actualmente en ensayos clínicos contra diversos tipos de cáncer y afecciones inmunitarias. MMQO, con un funcionamiento dual, es un nuevo miembro de esta clase de medicamentos. La estructura minimalista de MMQO puede ser muy prometedora ya que puede ser modificada para optimizar la afinidad hacia Brd9 / 4 y, potencialmente,

podría ser de utilidad en la investigación contra una gran variedad de enfermedades, incluyendo el VIH.

PREFACE

The nuclear bromodomain containing protein 4 (Brd4) functions as a transcriptional regulator by binding the acetylated lysines of the chromatin interacting proteins. These include transcription factors, nucleosomes and members of the transcriptional machinery. In doing so, Brd4 primarily facilitates transcription initiation, elongation and mediates the assignment of chromatin modifications. Due to its broad scope of action, Brd4 is not only implicated in a number of roles in normal cellular responses, but also in numerous diseases, which include autoimmune disorders, a wide array of cancer subtypes and in latency of HIV.

Bromodomain inhibition has recently surged as an optimistic solution against these maladies, largely due to the „open access“ approach performed with the pilot drug JQ1. Though a chemical inhibition against Brd4 was only first described in 2010 in an immunosuppressive context, within the previous five years the open disclosure of the structure of JQ1 led to the filing of over 200 patents for similarly structured compounds and for a variety of uses. At the moment there are already ongoing clinical trials with Brd4 inhibitors against atherosclerosis, coronary artery disease, diabetes, tumors of the hematopoietic tissues, to name a few. In the process of developing structures against Brd4, numerous other sideline products against other bromodomains have been developed, thus further elucidating the roles of bromodomain proteins in cell physiology, all while displaying clinical potential.

Our group previously demonstrated how the experimental compound MMQO was able to revert HIV-1 latency by an unknown process. The goal of this project was to establish the molecular mechanism of MMQO and determine its potential for further development. Combining both *in vitro* and *in silico* methods, we determined MMQO to interact directly with various bromodomains, primarily with Brd4 and Brd9.

The results of this thesis will not only be applicable in the context of treating HIV-1, but could additionally be employed in the development of cancer therapeutics. The dual functioning characteristic of MMQO could be further optimized for higher affinities against its targets, thus applying it against cell types mutually sensitive towards Brd9 and Brd4 inhibition.

CONTENTS

CONTENTS	15
<hr/>	
INTRODUCTION	21
<hr/>	
1. HIV.....	23
1.1 HIV-1 structure.....	23
1.2 HIV-1 viral life cycle.....	25
1.3 HAART.....	26
1.4 HIV-1 latency.....	28
1.4.1 HIV-1 transcription.....	29
1.4.2 HIV-1 <i>trans</i> -dominant latency.....	30
2. Bromodomain proteins.....	32
2.1 BET proteins.....	33
2.2 SWI/SNF complex.....	34
2.3 Brd7 and Brd9.....	35
3. Curing from HIV infection.....	36
3.1 The “shock and kill” therapy.....	37
3.1.1 NF-κB activators.....	39
3.1.2 Chromatin modulators.....	40
3.1.3 A new latency reversing agent.....	42
RESULTS	47
<hr/>	
1. Characterization of MMQO.....	49
1.1 Effect of MMQO treatment on the transcriptome.....	49
1.2 Time-course dysregulation of gene expression by MMQO.....	53
1.3 cMyc decrease in response MMQO.....	55
1.4 MMQO increases apoptosis and inhibits proliferation.....	59
1.5 Regulation of immunogenicity related genes.....	60
2. MMQO as a noise enhancer on HIV-1 transcription.....	64
2.1 MMQO as an HDAC inhibitor?.....	65
2.2 Comparing MMQO and TSA transcriptomes.....	71
2.3 Analysis of MMQO specific genes.....	74
3. MMQO as a bromodomain inhibitor.....	75
3.1 Comparison between MMQO and the BET inhibitor JQ1 transcriptomes..	75

3.2 Evidence of MMQO binding to Brd4.....	78
3.3 Comparison of MMQO and JQ1 experimentally.....	80
3.4 BETi function in response to Brd4 knockdown.....	84
3.5 MMQO affects Brd4 binding to HIV-1 minigenome promoter.....	85
3.6 MMQO specificity towards the different bromodomains of Brd4.....	87
3.7 MMQO targets BETi specific genes.....	90
3.8 Biotin tagging MMQO.....	91
3.9 Testing MMQO derivatives.....	94
3.10 MMQO has a higher affinity for Brd9.....	96
3.11 Effect of Brd9 inhibition on HIV-1 expression.....	97
3.12 Comparing Brd4 and Brd9 inhibition by gene expressions.....	99
DISCUSSION	101
1. MMQO as a dual bromodomain inhibitor.....	103
2. MMQO as an anticancer drug.....	105
3. Role of bromodomains and MMQO in HIV-1 reactivation.....	108
CONCLUSIONS	115
MATERIALS AND METHODS	119
1. Materials.....	121
1.1 Reagents.....	121
1.2 Plasmids.....	121
1.3 Primers.....	121
1.4 Antibodies.....	124
1.5 shRNA sequences.....	124
2. Methods.....	125
2.1 Cell culturing.....	125
2.2 Microarray.....	125
2.3 Microarray analysis.....	126
2.4 RNA extraction, reverse transcription and Real Time PCR.....	127
2.5 Protein extraction, gel electrophoresis, and immunoblotting.....	127
2.6 Virus production and infection.....	128
2.7 Flow cytometry.....	128

2.8 Bliss independence model..... 128

2.9 *In silico* docking.....129

2.10 Nuclear Magnetic Resonance of MMQO with Brd4-BD1..... 129

2.11 Homogeneous Time Resolved Fluorescence..... 129

2.12 Chromatin immunoprecipitation..... 129

ANNEX _____ **131**

1. Comparison of MMQO target genes to MAPK pathway target genes..... 133

2. The lack of response by MAPKs following MMQO treatment.....135

3. MMQO in combination with MAPK inhibitors..... 136

4. Cross-reaction of MMQO and PI3K/Akt pathway in HIV expression and
T cell receptor signaling..... 142

ABBREVIATIONS _____ **149**

REFERENCES _____ **155**

INTRODUCTION

1. HIV

The on-going Human Immunodeficiency Virus (HIV) pandemic has claimed more than 35 million lives since its discovery in 1981 and the World Health Organization estimates that currently about 36,7 million people are infected by the retrovirus (UNAIDS Report 2016). Although it is estimated that the HIV epidemic started already in the early 1900s, the virus was only isolated and described for the first time in 1983, from a patient with symptoms that precede the Acquired Immunodeficiency Syndrome (AIDS) (Barré-Sinoussi et al. 1983; Faria et al. 2014). HIV is categorized into two different subtypes: HIV subtype 1 (HIV-1) and HIV-2. Both of these viruses originate from different Simian Immunodeficiency Virus (SIV) subtypes, with HIV-1 being the globally spread subtype. The disease primarily attacks CD4+ T-lymphocytes, and in a smaller proportion also macrophages, dendritic cells, astrocytes and within a few years it severely deteriorates a patient's immune system if left untreated, leading to AIDS. Patients with AIDS succumb to other opportunistic infections due to dysfunctional defense mechanisms of their organism, by infections that are normally not considered lethal if occurring in a healthy individual.

1.1 HIV-1 structure

HIV-1 is a member of the genus *lentivirus*, which is characterized by positively oriented single-stranded RNA (ssRNA) viruses (Ratner et al. 1985). The viral particle of HIV-1 contains

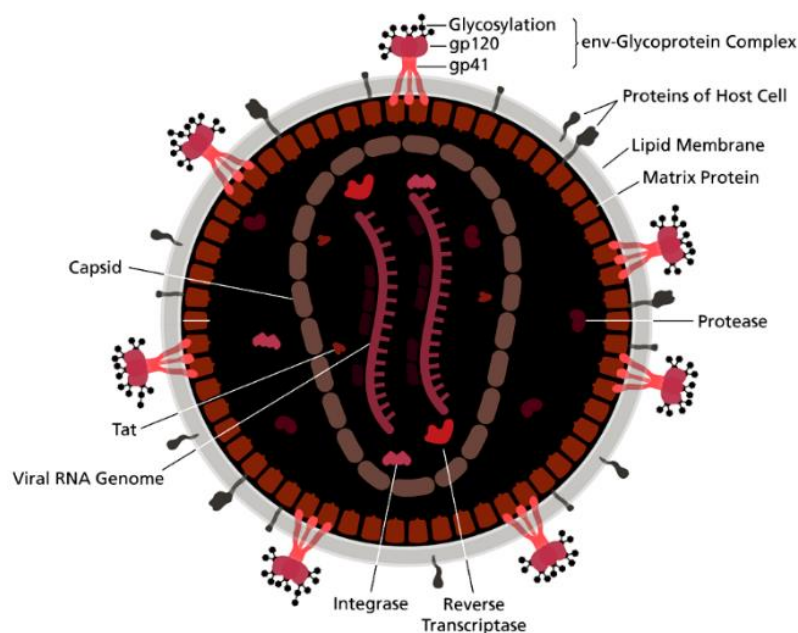


Figure 1: HIV-1 viral particle. Image adapted from Thomas Splettstößer's collection.

two copies of a 9,7kb long genome, which are surrounded by an inner conical-shaped capsid. This core is further covered by a spherical matrix structure, consisting of viral proteins that form a stable virion. The matrix itself is enveloped in a host-derived lipid membrane, which also expresses host proteins and viral glycoproteins responsible for interacting with host cells (Figure 1).

The HIV-1 genome consists of 5' and 3' long terminal repeats (LTR) regions and nine viral genes in-between (Figure 2). The viral genes can be transcribed in three different open reading frames (ORFs) and the translated precursor proteins can be further cleaved into mature components for the infectious virion. The genes can be categorized into three subclasses: structural protein coding, essential regulatory element coding and accessory regulatory protein coding (described in detail in Los Alamos National Laboratory HIV Databases).

Structural proteins:

- *gag*: primarily encodes for the physical infrastructure proteins like p17 (matrix) and p24 (capsid)
- *pol*: this genomic region encodes the viral protease, reverse transcriptase and integrase
- *env*: encodes for the glycoproteins gp120 and gp41 necessary to interact with host CD4 and CCR5 / CXCR4 receptors and assisting with the fusion with the host cell

Essential regulatory elements:

- *tat*: trans-activator of transcription (Tat) is a protein crucial for efficient viral genome transcription initiation
- *rev*: regulator of expression of virion (*rev*) encodes for a nuclear protein responsible for the stabilization and nuclear export of viral mRNA

Accessory regulatory elements:

- *nef*: negative regulatory factor (*nef*) a multifunctional protein capable of interacting and inhibiting with various cytosolic host proteins, thus further promoting viral spread and survivability

- *vpr*: viral protein R (*vpr*) assists in the nuclear import of the pre-integration complex. Is also known to induce cell cycle arrest of host cells, to further assist in the viral integration process
- *vif*: viral infectivity factor (*vif*) protects viral mRNA from the host antiviral mechanisms by inhibiting the APOBEC3G protein
- *vpu*: viral protein unique (*vpu*) is a protein necessary for viral envelope assembly and enhancing viral release from the host cell membrane

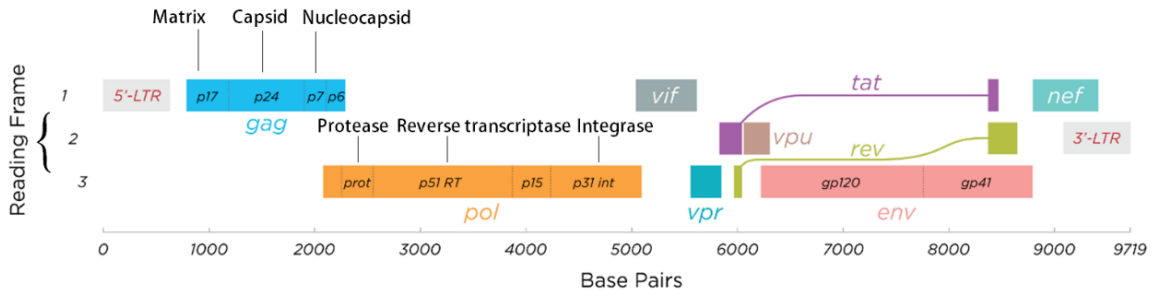


Figure 2: Genome structure of HIV-1. Image adapted from Thomas Spletstößer’s collection.

1.2 HIV viral life cycle

The viral life-cycle begins with the receptor-mediated merging of the viral envelope and the host cell membrane, after which the viral capsid is released into the cytoplasm. First the viral gp120 glycoprotein binds to the host membrane CD4 receptor, which in turn leads to a

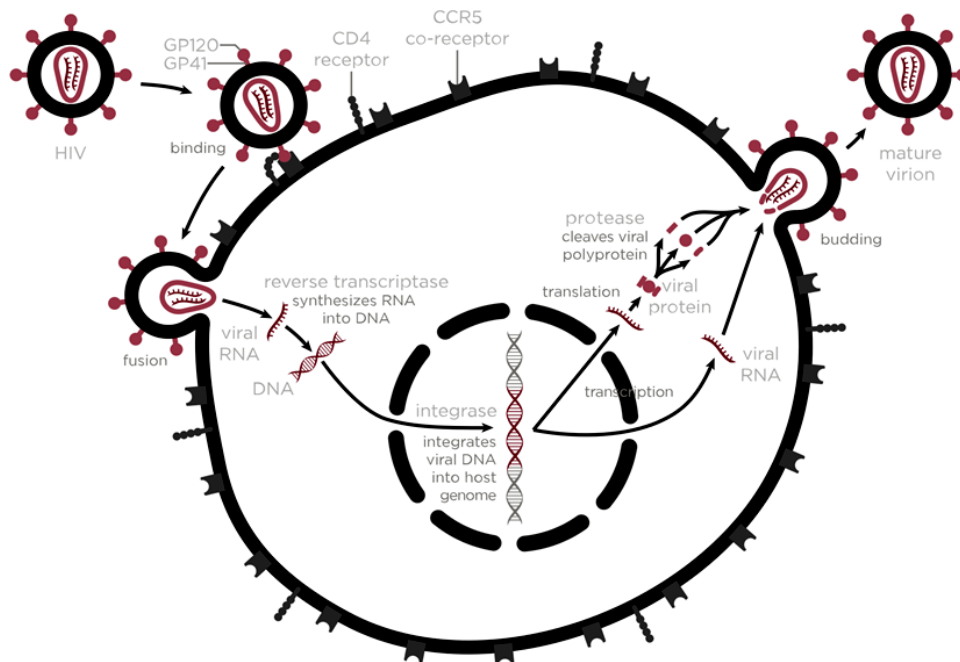


Figure 3: Simplified model of HIV life cycle. Image adapted from Thomas Spletstößer’s collection.

cascade that results in the fusion of viral and cellular membranes. Once in the cytosol, the matrix and capsid structures are partially uncoated and the HIV-1 ssRNA genomes are then reverse transcribed into double stranded DNA molecules by the reverse transcriptases included in the viral capsid. Together with various other viral components, like integrase, Vpr and matrix proteins and host factors, the pre-integration complex is formed in combination with the newly synthesized DNA. Utilizing host factors like Lens Epithelium-Derived Growth Factor (LEDGF/p75) this complex then enters the host nucleus, where the viral DNA is integrated preferentially into open chromatin. This integrated provirus then serves as a template for the production for a new generation of viral mRNA molecules utilizing host transcriptional factors and machinery, with viral Tat protein supporting the process as a catalyst. The newly transcribed mRNA is then either spliced for translation or left intact for packaging into new virions. Ultimately the new virions are assembled from the intact mRNA, together with various viral and host proteins and budded out of the cell (Figure 3) (reviewed in Engelman & Cherepanov, 2012).

1.3 HAART

CD4+ T cells are an essential component of the human adaptive immune system against pathogens, while also playing a key role in sustaining a long lasting immunological memory after the initial infection has been eliminated. In case of HIV-1, the initial acute stage of infection is suppressed in the first months, being followed by a chronic phase where virus slowly but progressively exhausts the immune system by eliminating the CD4+ T cells. This process can proceed for years, characterized by a low amount of plasma viremia. If left uncontrolled, the CD4+ cells will decrease to critical levels and the immune system loses the capability of responding adequately to other opportunistic diseases, resulting in AIDS and eventually death (Figure 4).

A major breakthrough in controlling HIV came with the introduction of the highly active antiretroviral therapy (HAART or ART). The main benefit of ART arises by potent inhibitory antiviral mechanisms targeting against various stages of the viral lifecycle and eventually leading up to an undetectable viral load. Azidothymidine (AZT), the first drug that was directly used against HIV as an reverse-transcriptase inhibitor, was clinically approved for use in 1986. The development of antiretrovirals has since then surged, additionally targeting

viral binding to host cells, fusion, integrase or protease functions (reviewed in Volberding & Deeks, 2010).

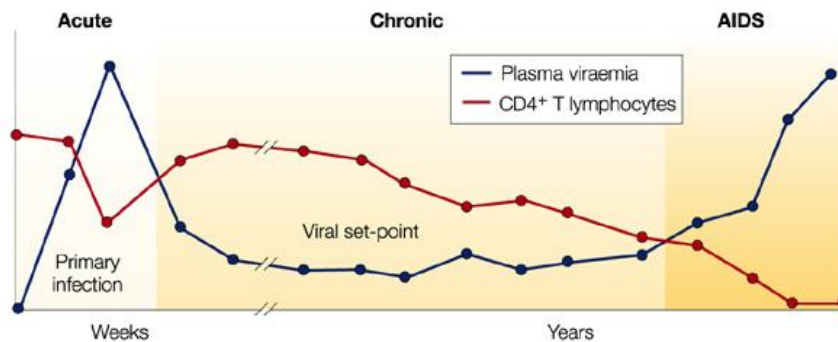


Figure 4: Typical disease course of individual with HIV. Image adapted from Simon & Ho, 2003.

Modern HAART was established in 1996, which consists of daily doses of a three-drug cocktail regimen targeting different stages of the viral life cycle. The drugs are prescribed in combination to ensure optimal synergy, thus allowing minimal viral expression in blood serum and preserving the cells of the immune system. The development of ART not only dramatically increased the survival rates of the infected subjects, but also decreased the transmission probability to uninfected sexual partners by 92-96% (Donnell et al. 2010) and decreased dramatically the rate of mother-to-child transmission to less than 1% (Coutsoudis et al. 2010).

The disadvantages of ART are the side-effects induced by the long period of therapy and that modern medications are not capable of a total viral eradication, thus a complete recovery remains unachieved. Furthermore, the reverse-transcription mechanism of HIV-1 is notably error-prone, since the viral transcriptase is lacking a proofreading ability (Gianotti et al. 1999). The imprecise reverse transcription induces a high mutation rate of the viral genomes and eventually allows the virus to develop resistance to drugs used in ART. Consequently, patients receiving ART have to be monitored regularly to ensure that the number of viral particles remains low in serum.

While ART is considered a major breakthrough in combating HIV, it is still not capable of fully clearing out the viral reservoir since it only targets the virus in the replicating phase. Even though the viral load remains undetectable during the therapy, it is prone to recover within a few weeks / months upon interruption of ART. Although various experimental techniques have been carried out in order to establish a cure, as of late 2016 only one person can be considered functionally cured from HIV-1 (Figure 5).

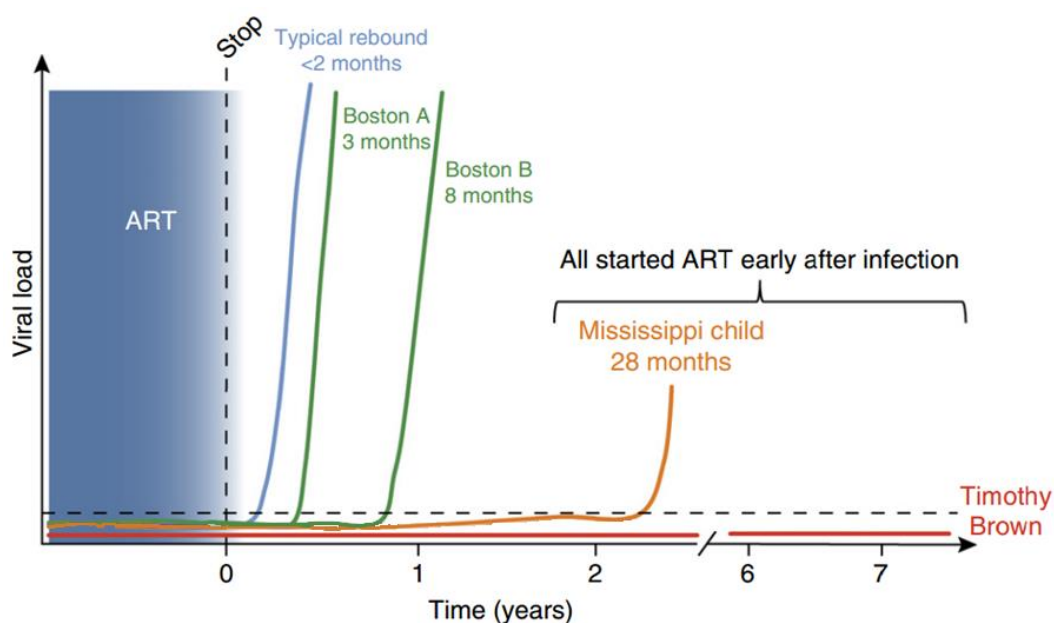


Figure 5: Typical disease course of individual with HIV. Cessation of ART causes a viral rebound within weeks. Stem cell transplantation from a CCR5 Δ 32 negative donor allows Timothy Brown to survive without ART and without any detectable virus from blood or tissue. Boston patients A and B received normal stem cell transplantations without any mutations, which delayed the viral rebound following the cessation of ART. Mississippi baby contracted HIV-1 at her birth from the mother, was treated with intense ART immediately thereafter but was later off the regimen for 28 months until viral rebound. Image adapted from Deeks et al. 2016.

1.4 HIV-1 latency

Most of the infected CD4⁺ T cells die rapidly in response to HIV-1 infection, yet a small but a significant number of infected cells survive. Active CD4⁺ T cells are able to revert to a quiescent state with minimal HIV-1 gene expression following the proviral integration and persist as long-lived central or transition memory T cells sheltering latent HIV-1 genomes. These T cell populations harboring the latent reservoirs cannot be detected by the immune surveillance, since viral antigens are not presented to immune effector cells and ART remains ineffective against an already integrated provirus. Opposite to active T-lymphocytes, which have a short half-life, in a dormant state the memory T cells possess an estimated half-life of approximately 44 months, and are thus considered to be the primary barrier why the disease remains a chronic affliction (reviewed in Van Lint et al. 2013). Mathematical models predict that the eradication of a reservoir consisting of 10^6 cells would take 73 years *in vivo* (Persaud et al. 2003). Extensive efforts have been carried out within the last 25 years to characterize these cells and understand how HIV-1 is regulated after integration and why it can remain transcriptionally latent.

1.4.1 HIV-1 transcription

HIV-1 makes use of cellular transcription factors for its expression and a few dozen binding motifs have been identified in the 5' LTR end of the HIV-1 genome (reviewed in Colin & Van Lint 2009). The most crucial elements upstream of the transcription start site (TSS) are the TATA-responsive element and the three tandem Sp1-binding sites. These are followed by dual motifs for Nuclear factor kappa-light-chain-enhancer of activated B cells (NF- κ B) binding, Nuclear factor of activated T-cells (NFAT), Activator Protein 1 (AP-1), Lymphoid Enhancer Binding Factor 1 (LEF-1) and CREB binding protein (CBP) to name a few. In addition to harboring a large variety of motifs for binding host factors, transcription factors like cMyc, YY1 and CTIP2 also play a role in viral transcription. Since HIV-1 transcription depends highly on the chromatin state, various epigenetic regulators like the SWI/SNF complex, histone deacetylase (HDAC) and bromodomain protein family members are also known to coordinate viral gene expression (reviewed in Mbonye & Karn, 2014). Arguably the most crucial factor for HIV-1 transcription, aside from its viral Tat protein, is the positive transcription elongation factor (P-TEFb).

P-TEFb is a heterodimer consisting of cyclin-dependent kinase 9 (Cdk9) and one of its regulatory subunits, Cyclin T1, T2, or K (Zhou et al. 2012). As the name of the complex suggests, the primary role of P-TEFb is to elongate the transcriptional process, which is achieved by phosphorylating C-terminal domain of RNA Polymerase II (Pol II), DRB sensitivity inducing factor (DSIF) and negative elongation factor (NELF). Normally after the initiation of transcription, Pol II is prohibited from elongating by the NELF and DSIF factors, an obstruction that can be overridden by P-TEFb leading to the synthesis of mRNAs. The intracellular abundance and function of P-TEFb is tightly regulated either by the bromodomain containing 4 (Brd4) protein or by the repressive 7SK small nuclear ribonucleoprotein (7SK snRNP) complex. While the 7SK snRNP complex is considered strictly an inhibitory structure rendering P-TEFb catalytically inactive, the Brd4 functions primarily by mobilizing the P-TEFb to the TSS and facilitating the elongation. However in case of HIV-1, P-TEFb is incapable of carrying out the elongation process in absence of the viral Tat protein, thus it is hijacked by the Tat protein from either the 7SK snRNP or Brd4 protein and sequestered for viral transcription (reviewed in Barboric & Lenasi, 2010).

Deletion analysis of viral LTR has revealed that immediately following the TSS a hairpin structured 59-nucleotide long RNA structure is encoded, called the trans-activation

response element (TAR). Following analyses proved that TAR is a crucial element for Tat functioning in the viral protein by facilitating its specific localization, since Tat itself lack DNA-binding capability. In doing so, Tat is able to introduce the P-TEFb complex to Super Elongation Complex (SEC) and facilitate efficient proviral elongation (Figure 6).

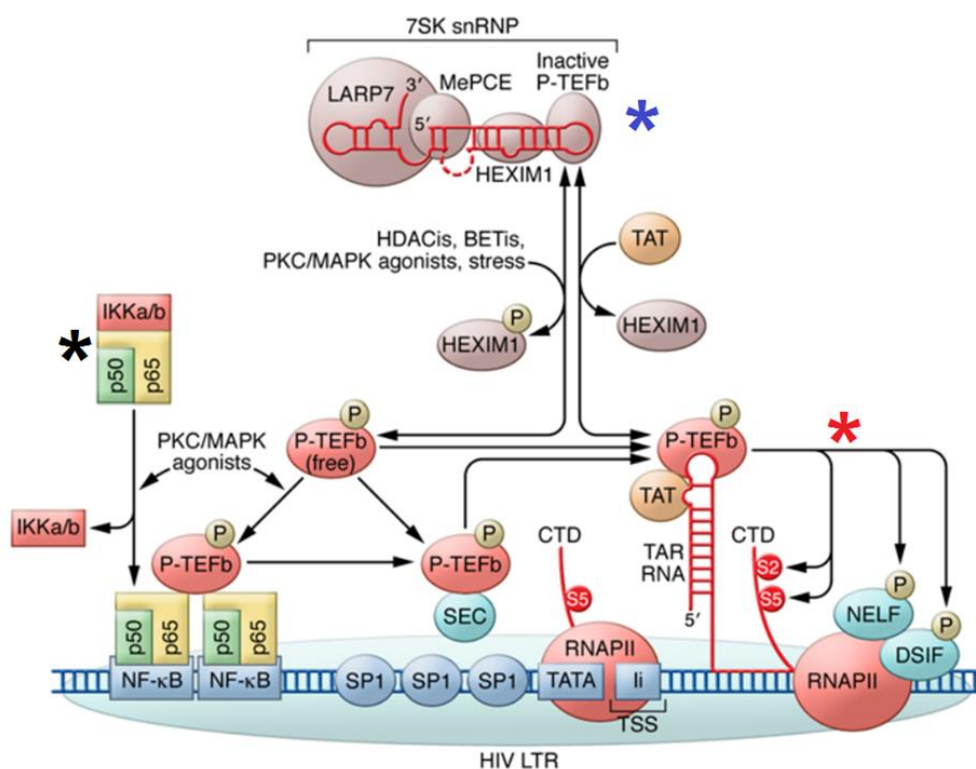


Figure 6: Transcriptional mechanisms of HIV-1. (Black asterisk) An initial signal, such as introduction of NF- κ B to the viral promoter initiates viral transcription. Any unassigned P-TEFb can synergistically assist in this process by being recruited to the promoter by NF- κ B or the super elongation complex (Blue asterisk) Structure and sequestration of P-TEFb by the repressive 7SK snRNP complex. P-TEFb can be abducted by viral Tat protein or released chemically with chemical modulators. HDAC and BET family protein inhibitors, along with PKC pathway agonists are known to release HEXIM1 from the 7SK snRNP complex, thus freeing up additional P-TEFb for viral Tat. (Red asterisk) The released P-TEFb is hijacked by Tat, which mobilizes to the viral 5'LTR to form a complex with TAR. This allows P-TEFb to elongate the transcription by phosphorylating the C-terminal domain of Pol II, NELF and DSIF. Image adapted from Cary et al. 2016.

1.4.2 HIV-1 *trans*-dominant latency

HIV repression can be categorized into two fundamental groups: the *cis*-dominant and the *trans*-dominant mechanisms (Hamer, 2004). The *cis*-dominant dependent latency is caused by restricted access and faulty functionality of transcriptional machinery to the promoter, caused by the integration site of provirus. HIV-1 transcription models imply how a high

genome expression of HIV-1 is related to a high CD4⁺ T-lymphocyte activity during an immune response. Since the provirus integrates itself typically into active genes, it has higher chances of coming in contact with the Pol II transcriptional machinery. Hence, integration in the vicinity of a highly potent promoter or in opposing orientation of the competitive host gene, in heterochromatic or intergenic regions, introns or in a gene desert will diminish the chance of viral replication (Stellbrink et al. 2002, Coiras et al. 2007). The *trans*-dominant mechanisms are characterized by expression affecting elements like lack of cellular transcription factors. For example, the NF- κ B heterodimer is only mobilized to the nucleus following T cell activation and extracellular proinflammatory signals, further supporting the low incidence of viral expression in resting memory CD4⁺ T cells (Figure 7A).

Repressive chromatin structure is additionally known to drastically affect viral transcription, since HIV-1 provirus is highly dependent on its nucleosomal structure. During the integration process, HIV-1 establishes a strict nucleosomal conformation at the 5' LTR, with Nuc-0 residing at the start of the genome and Nuc-1 being localized immediately after the TSS (Verdin et al. 1993). In doing so, the virus creates a ~250bp long nucleosome-free zone that can be accessed by chromatin modifiers and transcription factors, thus facilitating a dominant expression witnessed in active viruses (Figure 7B). In case of latency, access to the LTR becomes restricted by repressive transcription factors and HDACs, DNA or histone tail methylations or by sterically compact chromatin structure. For example, the suppressive HDACs are known to localize on the transcription factors on the NF- κ B, Sp1, AP-4 and LSF motifs around the TSS (reviewed in Hakre et al. 2012). Bromodomain proteins, like Brd4 and Brd2, have also been demonstrated to inhibit viral transcription by masking the already acetylated lysines on Nuc-0, Nuc-1 and NF- κ B, while the chromatin remodeling BAF complex immobilizes Nuc-1 (reviewed in Boehm et al. 2013).

Another possibility for viral latency is the lack of viral Tat protein, since the initial signal for HIV-1 transcription will then depend on the host transcription factors. Although Tat proteins are encapsulated within the mature virion and participate in the reverse transcription, the protein levels are too low to assist the proviral genome in early stage transcription (Goodsell, 2012; Romani et al. 2010). Due to the low amount of Tat at these early stages of viral life cycle, HIV-1 transcription is known to consist of two phases: first, in an initial phase, when only short mRNAs are produced for reaching a threshold of TAR RNA and Tat protein, while the second phase is characterized by Tat-P-TEFb dependent elongation, production of

full length viral sequences and continuation of normal viral life cycle (reviewed in D'Orso & Frankel, 2010).

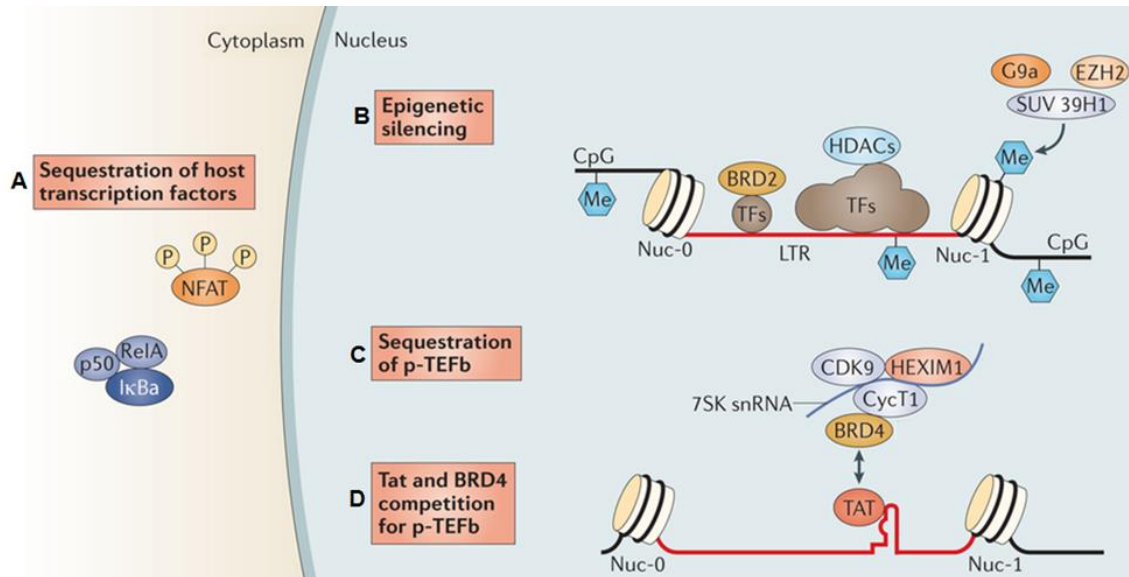


Figure 7: Examples of molecular mechanisms that maintain post-integrational latency. (A) Cytosolic sequestration of HIV-1 activating host transcription factors like NFAT and NF- κ B. (B) Epigenetic modifications like methylations and acetylations on these nucleosomes can lead to a repressive chromatin state. Other epigenetic characteristics like DNA hypermethylation or hindering the function of TFs with HDAC or BET proteins can further factor into viral expression. (C) P-TEFb sequestration by the 7SK snRNP complex (depicted by the complex members Brd4 and HEXIM1) (D) Brd4 is thought to compete with viral Tat for the P-TEFb complex. Image adapted from Archin et al. 2014.

2. Bromodomain proteins

A prominent role in HIV-1 regulation is carried out by the bromodomain family proteins, primarily functioning as chromatin readers, transcriptional mediators and histone acetyltransferases. A bromodomain structure consists of about 110 amino acids, which are organized as a “bundle” of four alpha helices separated by variable loop regions. This superstructure creates a hydrophobic core that can recognize acetylated lysine residues (KAc) (Dhalluin et al. 1999) (Figure 8A-B). The human genome encodes 61 bromodomains present in 46 different proteins (neglecting splice variants), where differences in the amino acid residues around the acetyl-lysine binding site impart ligand specificity (Filippakopoulos et al. 2012) (Figure 8C). The bromodomain family primarily facilitates protein-protein interactions on the chromatin, thus regulating the epigenetic structure and function of the chromatin (Smith & Zhou 2015). Due to their role in various biological processes and diseases, the members of the bromodomain family have been identified as having a

moderately high druggability, leading to a surge in the development of chemical inhibitors against these chromatin readers (Filippakopoulos & Knapp, 2014).

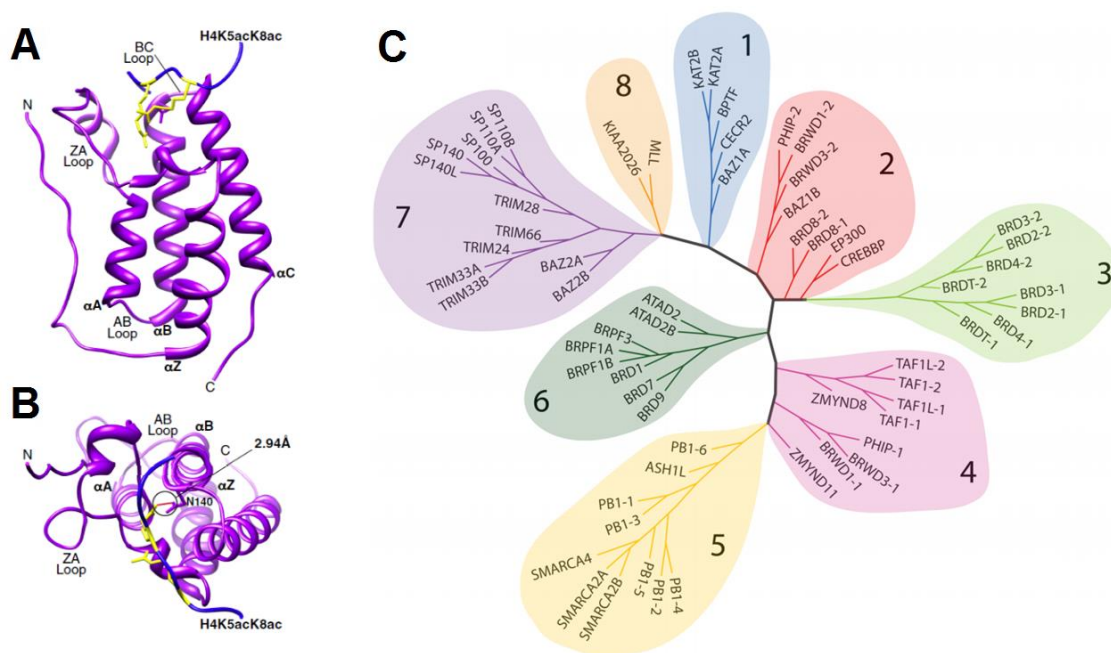


Figure 8: Example of a bromodomain structure and phylogenetic tree of the human bromodomains. (A) Crystal structure of the first bromodomain of Brd4. KAc residue is highlighted in yellow. (B) Top view of image (A). The hydrogen bond between the highly conserved asparagine residue is shown in red. PDB: 3UVW (C) Sequence similarity-based phylogenetic tree of the 61 human bromodomains from the 46 different bromodomain proteins divided into eight groups. Illustrations adapted from Boehm et al. 2013 and Smith & Zhou, 2015.

2.1 BET proteins

The bromodomain and extra-terminal domain (BET) family of adaptor protein subfamily is comprised of Brd2, Brd3, Brd4, and the testis-specific BrdT. Common to all four BET proteins are two conserved N-terminal bromodomains (BD1 and BD2), which are chromatin interaction domains that recognize acetylated lysine residues on histone tails and other nuclear proteins (Figure 9). Bromodomain-mediated interactions with acetylated chromatin result in the localization of BET proteins to discrete locations along the chromosome, where they recruit other regulatory complexes and transcription factors to influence gene expression (Dey et al. 2003). BETs are transcriptional regulators that control expression of genes that with regulatory roles in cellular proliferation, cell cycle progression, and apoptosis (Maruyama et al. 2002, Dey et al. 2009) and also in other processes such as transcriptional elongation (Bartholomeeusen et al. 2012, Zhang et al. 2012), replication (Chen et al. 2011), hematopoiesis (Gamsjaeger et al. 2011), adipogenesis (Denis, 2010;

Wang et al. 2010), and spermatogenesis (Shang et al. 2007). Dysfunction of BET proteins has been associated with the development of aggressive tumors. Importantly, BET family proteins play a critical role in tumorigenesis by driving the expression of genes and proteins that are essential for tumor growth and survival, such as cMyc and Bcl-2 (Rahl et al. 2010, Dawson et al. 2011, Delmore et al. 2011, Mertz et al. 2011, Zuber et al. 2011).

Due to their crucial role on chromatin regulation, bromodomains also have an effect on HIV-1 on expression. The well-studied member of the BET family is Brd4, whose role in transcriptional regulation was first suggested by its interaction with P-TEFb. It has been shown to be a latency promoting factor by interfering with Tat localization to the viral promoter (Jang et al. 2005, Bisgrove et al. 2007). At least two regions of Brd4 bind directly to P-TEFb: the C-terminal domain (CTD) interacts with Cyclin T1 and Cdk9, while BD2 recognizes an acetylated region of Cyclin T1 (Chen et al. 2014). The interaction with Brd4 will prevent P-TEFb from associating with HEXIM1, a member of 7SK snRNP complex that sequesters P-TEFb in a kinase-inactive state. Importantly, the Brd4 additionally promotes the phosphorylation of CDK9, leading to the inhibition of its kinase activity and further promoting viral quiescence (Zhou et al. 2009). Both the knockdown and chemical inhibition of Brd4 have been shown to rescue HIV-1 from latency (Boehm et al. 2013, Li et al. 2013).

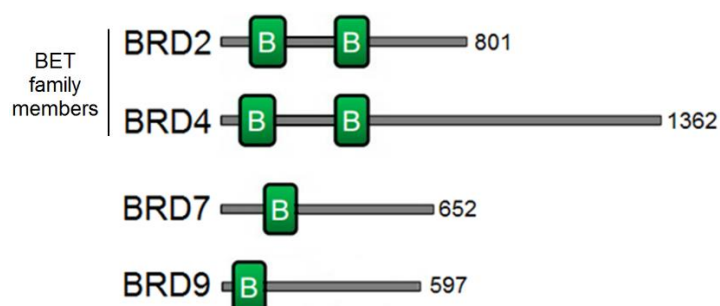


Figure 9: Domain organization of Brd2, Brd4, Brd7 and Brd9. Protein length in amino acids is shown at the right of each protein. Figure adapted from Philpott et al. 2014.

2.2 SWI/SNF complex

Bromodomain proteins also form part of the SWItch/Sucrose Non-Fermentable (SWI/SNF) complexes. SWI/SNF complexes are considered among the main players involved in nucleosome remodeling and their role has been conserved from prokaryotes to eukaryotes. In mammals, the SWI/SNF complexes regulate a broad range of genetic programs, such as

proliferation, differentiation, cell migration, hormone receptor signaling, *etc* (reviewed in Wilson et al. 2011). The main function of these complexes is to focus on altering the nucleosomal architecture in relation to DNA, thus inducing either transcriptional repression or activation (Whitehouse et al. 1999). The unwrapping, mobilizing, exchanging and ejecting of nucleosomes is considered to be primary mechanisms by which SWI/SNF exerts its effect in target promoters. Due to the large number of subunits (around 12-15 per complex) a variety of combinations can form, but in general two mechanistically different master complexes are observed in mammals – the BAF and PBAF. These two main complexes share the nine core subunits, but differ in the additional 3-5 subunits (Figure 10). The PBAF complex is specified by the PBRM1, ARID2 and Brd7 proteins, while the BAF complex is limited to interaction with the Bcl-7 family, Bcl-11 family, SS18, ARID1A/B and Brd9 (Middeljans et al. 2012, Zinzalla, 2016). These subunits have been suggested to be responsible for targeting the complexes to distinct loci within the genome (Thompson, 2009). Though the SWI/SNF complexes consist of various bromodomain proteins, this project focuses only on Brd7 and Brd9.

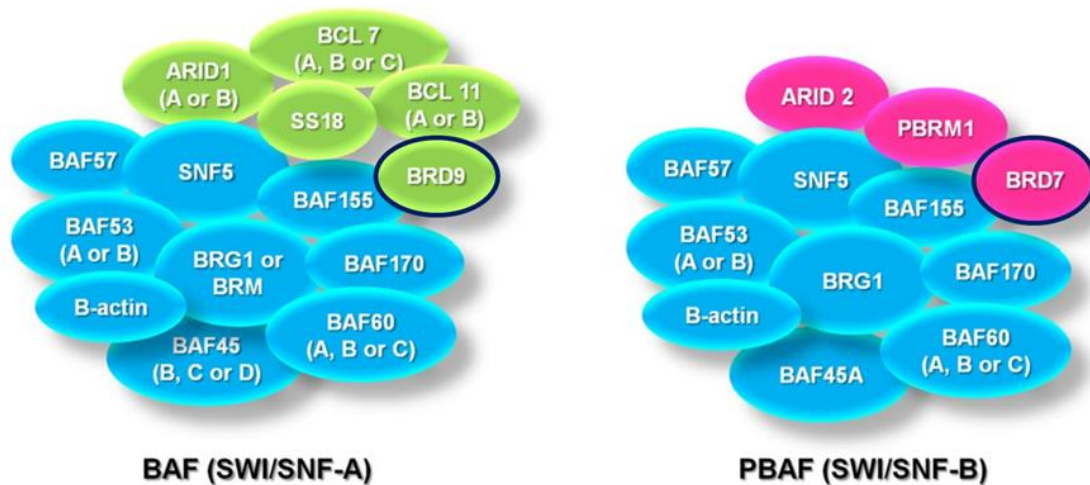


Figure 10: The two major families of SWI/SNF complexes present in humans. Common/core subunits are depicted in light blue, BAF complex specific members are shown in green, and the subunits only found in PBAF complexes shown in pink. Brd7 and Brd9 subunits are highlighted in dark blue. Illustration adapted from Zinzalla, 2016.

2.3 Brd7 and Brd9

Similarly to other bromodomain containing proteins, the bromodomains in Brd7 and Brd9 are known to be highly conserved and they have been demonstrated to interact with acetylated core histones (Peng et al. 2006, Filippakopoulos et al. 2012). This fact suggests

that both of these bromodomains might play a role in the migration of the SWI/SNF complexes and can be responsible for the interactions with other transcriptional regulators *in situ*. Indeed, Brd7 was first described to be crucial for the transcription of certain subsets of genes in embryonic stem cells (Kaesler et al. 2008). Like Brd4, both Brd7 and Brd9 have been shown to play relevant roles in different types of cancers, albeit through separate mechanisms. For example, on the one hand, Brd7 has been described to interact directly with p53 and the histone acetyltransferase p300 and to induce the transcription of their target genes, thus suppressing tumorigenicity (Drost et al. 2010). On the other hand, Brd9 has been recently shown to be necessary for the survival of certain tumors. For example, in acute myeloid leukemia (AML), chronic myelogenous leukemia (CML) and T-cell acute lymphoblastic leukemia (T-ALL) cell lines Brd9 is used to sustain the upregulation of *MYC* and the knockdown of *BRD9* is detrimental to the differentiation of AML (Hohmann et al. 2016).

In what concerns of HIV-1, the PBAF complex has also been shown to be recruited to the proximal end of Nuc-1 and facilitate the nucleosomal depletion (Henderson et al. 2004), while the BAF complex is described to maintain HIV-1 latency by stabilizing the Nuc-1 in the internucleosomal region of the 5' LTR (Rafati et al. 2011). Interestingly, BAF has been suggested as to be a putative therapeutic target to deplete the HIV-1 reservoir (Stoszko et al. 2016). Both of the SWI/SNF complexes have been shown to interact with Tat, and it has been suggested that Tat might function in replacing the repressive BAF complex with the activating PBAF complex (reviewed in Boehm et al. 2013).

3. Curing from HIV infection

In order to cure a patient infected with HIV a variety of different strategies have been proposed and tested. In 1995 David Ho pushed for the “Hit HIV early and hard” concept with conventional antiretroviral compounds and this approach has shown potential throughout the years (Ho, 1995). Modern post-exposure prophylaxis (PEP) consists of a month long heavy dose ART course, which is initiated within hours or days after initial exposure. PEP has been shown to be highly effective, but it does not provide total protection from HIV-1 (reviewed in Krakower et al. 2015). Another example of effective early stage therapy is the Visconti cohort. This is a small group of HIV-positive patients who started ART during the

acute stage of the infection and remained on medication for at least three years, but then stopped. Curiously these patients are able to contain the viral load without developing any adverse effects and only a few of them have relapsed throughout the years (Sáez-Cirión et al. 2013). Unlike Timothy Brown, these patients still display detectable viral reservoirs, thus they can only be considered functionally cured until they experience a viral rebound.

Though the precedents of Timothy Brown and the Visconti cohort serve as examples in controlling the viral infection without antiretrovirals, these cases are not to be considered the clinical normality. Establishing an early ART regimen is not an option in most cases and curing HIV-1 with stem cell transplantations is deemed to be too unfeasible due to safety concerns. At the moment, the common consensus is that the viral reservoir will either have to be completely eradicated or at least depleted to a level where a viral rebound is considered unlikely (Deeks et al. 2016). A hypothetical model used currently in clinical trials to achieve this objective is called the “shock and kill” therapy.

3.1 The “shock and kill” therapy

To achieve HIV eradication from infected patients, HAART has been suggested to be combined with drugs that “shock” the proviral transcription into activity and flush out the dormant viruses (Hamer, 2004). Following the reactivation of latent proviruses, the immune system and cytopathogenicity will be responsible for “killing” the infected cells, while the continuous HAART guarantees protection against further infection (Figure 11).

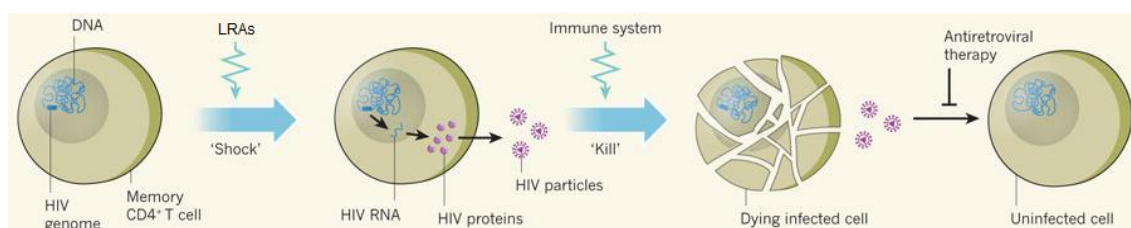


Figure 11: Concept of “shock and kill” therapeutic approach. First the virus is reactivated with latency reactivating agents and then the infected cells are either eliminated by the immune system or they die during the viral replication process. Sustained HAART will avoid further reinfection. Image adapted from Deeks, 2012.

Though the reported pilot studies utilizing “shock” type drugs thus far have proven less efficient than expected, there still is potential (Table 1). Most of the completed clinical trials

have shown an increase in intracellular viral transcription and in some cases also a higher viral load, but none of them have reported a decrease of viral reservoir size.

	Drug dosing (doses)	HIV-1 transcription (fold > baseline)	Plasma HIV-1	Post Dosing Viral Effect	T-cell Activation	Reservoir Size
Vorinostat						
Archin <i>et al.</i> 2012	400mg (1)	4,8	NC	ND	ND	ND
Elliot <i>et al.</i> 2014	400mg daily (14)	2,7	NC	Yes	NC	NC
Archin <i>et al.</i> 2014	400mg TIW (22)	1,3	NC	ND	ND	NC
Panobinostat						
Rasmussen <i>et al.</i> 2014	20mg TIW (12)	2,9	Increased	Yes	Increased	NC
Romidepsin						
Sogaard <i>et al.</i> 2015	5mg/m ² (3)	3,8	Increased	No	Increased	NC
Disulfiram						
Spivak <i>et al.</i> 2014	500mg daily (14)	ND	Increased	Yes	ND	NC
Elliot <i>et al.</i> 2015	Dose escalation (3)	~2	Increased	Yes	ND	ND

Table 1: Reported clinical trials of latency reversing agents. Table adapted from Rasmussen *et al.* 2016. Abbreviations: ND, not determined; TIW, three times a week; NC, no change.

Perhaps the most intriguing clinical trial is the ongoing phase II RIVER trial, which is far among the most complex human subjects based project (RIVER trial protocol). In addition to reactivating the latent reservoirs similarly to the trials listed in Table 1, the RIVER trial will additionally include a priming phase of the immune system against HIV-1 infected cells with two different vaccines. This preliminary boost to the immune system is expected to assist in the clearance of infected populations.

Small molecule inhibitors are commonly considered the preferred method in forcing molecular regulations. Due to technical reasons like membrane penetration, mechanical simplicity, rapid function, cost efficiency, *in vivo* stability (to name a few), the research field in HIV-1 is currently concentrating on the development of small molecule latency reversing agents (LRAs). At least thirteen different types of molecular mechanisms are known to reactivate HIV-1 transcription *in vitro*, listed in Table 2.

Reactivating axis	Example activator	Reference for anti-HIV activity
TCR engagement	αCD3	Chun <i>et al.</i> 1998
TLR agonists	MGN1703, GS-9620	Offersen <i>et al.</i> 2016 ; Cohen <i>et al.</i> 2015
ILR agonists	IL-2, IL-7	Chun <i>et al.</i> 1999 ; Scripture-Adams <i>et al.</i> 2002
TNFR agonists	TNFα	Duh <i>et al.</i> 1989
PKC / NFκB	PMA, Prostratin	Kaufman <i>et al.</i> 1987 ; Kulkosky <i>et al.</i> 2001
PI3K / AKT	Disulfiram	Xing <i>et al.</i> 2011
Wnt / LEF1	Lithium chloride	Sheridan <i>et al.</i> 1995
P-TEFb release	HMBA	Tsatsanis <i>et al.</i> 1992
HDAC inhibition	Vorinostat, Valproic acid	Contreras <i>et al.</i> 2009 ; Lehman <i>et al.</i> 2007
BET inhibition	JQ1	Banerjee <i>et al.</i> 2012
HMT inhibition	BIX01294	Imai <i>et al.</i> 2010
DNA MTase inhibition	5-AzadC	Bouchat <i>et al.</i> 2016
BAF depletion	Pyrimethamine	Stoszko <i>et al.</i> 2016

Table 2: Known latency reactivating mechanisms. Directly activating mechanisms are marked in blue, while the yellow cells highlight the virus transcription enhancing mechanisms.

It has been suggested that HIV gene expression reactivators can be grouped into two categories: direct activators and noise enhancers (Dar et al. 2014). Direct activators (such as PMA, TNF- α , α -CD3, etc.) are responsible for introducing transcription factors to the promoter and activating the transcription process (such as NF- κ B), while noise enhancers (e.g. HDAC inhibitors) are responsible for modulating the chromatin state and easing the access of transcription factors to the viral promoter and ultimately assisting the elongation process. The reasoning for this type of categorization is that the two groups of drugs tend to synergize when combined together, due to their different mechanisms on viral promoters (Wong et al. 2014). Both groups display specific advantages and disadvantages, which will be briefly introduced in the following paragraphs.

3.1.1 NF- κ B activators

One of the main strategies initially was to activate the infected resting T-lymphocytes with immunoregulatory proteins. Experiments with cytokines Interleukin-2 (IL-2), Interleukin-7 (IL-7) or tumor necrosis factor alpha (TNF- α) in combination with HAART have shown to reduce the number of CD4+ T cells and activate the expression of latent viruses in infected cells (Chun et al. 1999, Brooks et al. 2003). The downside of those modulators is their aggressiveness. These proteins are incapable of discriminating between infected and uninfected cells, leading to a massive T cell activation, a decrease in patient's immunological memory and oftentimes to a cytokine storm.

Mitogenic phorbol esters, such as phorbol-12-myristate-13-acetate (PMA), as well as the non-tumor-promoting phorbol esters prostratin and bryostatin-1, also activate the dormant HIV-1 promoter through the activation of protein kinase C (PKC) axis and, ultimately, NF- κ B and NFAT transcription factors. Although these small molecule PKC pathway agonists are known to lead to a cytokine storm in clinical trials against cancer, the doses needed for viral reactivation result in minimal cytokine release from T cells in *ex vivo* conditions (Laird et al. 2015). These compounds will have to be further investigated in clinical settings to establish their efficacy and safety. In research settings, they have proven to be extremely advantageous as positive controls for testing novel therapeutics against viral latency on *in vitro* models.

Other uncanonical and novel mechanisms activating NF- κ B-dependent HIV-1 transcription are the Toll-like receptor (TLR) agonists and the phosphatase and tensin homolog (PTEN)

inhibitor disulfiram. For example, the TLR9 agonist MGN1703, a compound currently in phase III clinical trials against colorectal cancer, was recently demonstrated to both promote potent HIV-1 transcription in patient derived CD4+ T cells and boost natural killer (NK) cell-mediated suppression of viral particle production in the CD4+ cells *ex vivo* (Offersen et al. 2016). Disulfiram on the other hand reduces the PTEN protein levels, which in turn leads to hyperphosphorylation of protein kinase B (Akt) and activation of the Akt pathways. This activity is known to moderately induce the NF- κ B activity and release P-TEFb from the 7SK snRNP complex, thus combating viral latency (Xing et al. 2011, Doyon et al. 2013). Most importantly, disulfiram has already been for decades in clinical use against alcoholism, suggesting its application in HIV-1 patients could be well tolerated and it is currently undergoing clinical trials to estimate its efficacy in reactivating HIV-1 in physiological settings.

3.1.2 Chromatin modulators

The solution against a global T cell activation is the use of less invasive compounds that are still capable of inducing a proviral response. Loosening of chromatin at the transcription start site of HIV-1 by removing repressive markers has been suggested as possible mechanism (Hamer, 2004). According to recent observations, once HIV-1 transcription passes the first phase of Tat production, HIV-1 expression can function autonomously of cellular relaxation due to the potency of the positive feedback loop of Tat (Razooky et al. 2015). This fact suggests that HIV-1 reactivation should be possible in resting CD4+ T cells also in a clinical setting. More importantly, it implies that for an efficient therapy activating only the first block of viral transcription (Tat-TAR production) should be enough to initiate the “shock” cascade.

The inhibitors of histone deacetylases (HDACi) like valproic acid (VPA), trichostatin-A (TSA) and suberoylanilide hydroxamic acid (SAHA) have been shown to increase HIV-1 promoter expression and yet keep the activation of resting T cells at a minimal level (Figure 12). Yet the use of those agents as alternatives to NF- κ B activation produces another problem – a general effect on transcription of non-target genes, potentially causing a multitude of side-effects (reviewed in Shirakawa et al. 2013).

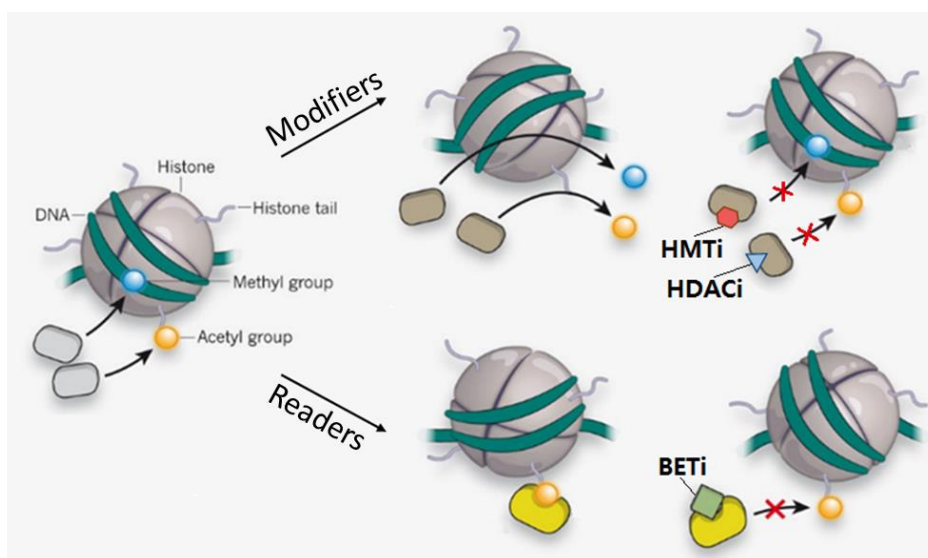


Figure 12: Fundamental players of epigenetic regulation. Three categories of mediators – writers, erasers and readers – orchestrate protein and histone modifications, the chemical instructions responsible for gene expression. (Above) For example addition of acetyl groups by epigenetic writers by histone acetyltransferases (HAT) causes histones to be more negatively charged, thus decreasing their affinity to DNA. Hyperacetylated nucleosomes are generally linked to transcriptional activation. An acetylated or methylated state can be reversed by epigenetic erasers, such as HDACs or histone methyltransferases (HMT), whose activity in turn can be prohibited with chemical inhibitors. (Below) Acetylated histones can interact with chromatin readers, such as bromodomain proteins like Brd4. Inhibition of BET bromodomains releases them from acetylated histones allowing other readers to interact with the nucleosomes. Image adapted from Maxmen, 2012.

In the last four years numerous studies have shown that BET bromodomain inhibitors can trigger HIV transcription in latently infected cells, thus activating viral replication (Banerjee et al. 2012, Zhu et al. 2012, Li et al. 2013). JQ1 was described as the first of its class as small-molecule inhibitor of Brd4, displaying the highest affinity for the first bromodomain of Brd4 and it has received much attention for its therapeutic potential against multiple myeloma and other cancer types addicted to the cMyc oncogene (Filippakopoulos et al. 2010, Delmore, Mertz et al. 2011, Zuber et al. 2011). The effect of JQ1 in viral reactivation can be explained by tilting the competition between Brd4 and Tat for their association with P-TEFb in Tat's favor (Yang et al. 2005). By inhibiting Brd4 with JQ1, a larger pool of P-TEFb becomes available to associate with Tat to activate transcription elongation of the HIV genome (Figure 13). In line with the activator-enhancer drug type hypothesis, bromodomain inhibition has been shown to confirm the premise of chromatin loosening drugs synergizing with direct NF- κ B activators to reactivate viral transcription, both in laboratory Jurkat models and patient derived *ex vivo* conditions (Jiang et al. 2015, Laird et al. 2015).

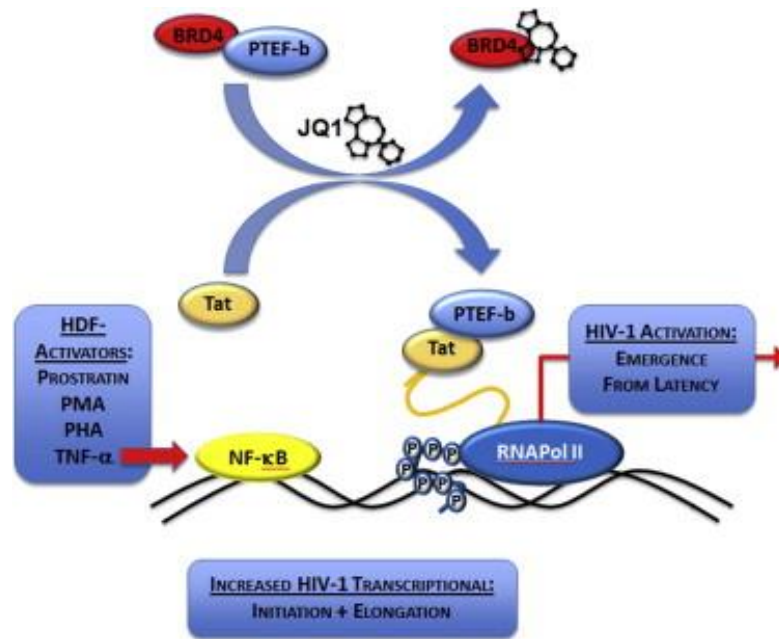


Figure 13: Model depicting canonical mechanism of Brd4 inhibition having an effect on HIV-1 latency. Brd4 generally sequesters the PTEF-b complex necessary for RNA Pol-II, NELF and DSIF phosphorylation. Upon inhibition by bromodomain inhibitors, such as JQ1, PTEF-b becomes hijacked by Tat. This process in turn assists the regular NF- κ B dependent initiation and furthers the elongation. Illustration adapted from Zhu et al. 2012.

However, it has been proposed that JQ1 reactivates HIV-1 from latency through a mechanism independent from Tat (Boehm et al. 2013). It is hypothesized that this could be due to unspecific targeting of Brd2 by JQ1 in the nucleosome free core of 5'LTR, resulting in the recruitment of histone modification enzymes, transcriptional activator complexes and chromatin modeling factors to the promoter, thereby activating viral transcription. Still, as a counterargument Boehm et al. demonstrated how JQ1 is still capable of reactivating latent HIV-1 minigenome even in cell lines where both Brd4 and Brd2 have been knocked down so the exact mechanism of how bromodomain inhibitors affect the latent proviral chromatin remains somewhat elusive.

3.1.3 A new latency reversing agent

CD4⁺ T cells are known to migrate and reside, besides blood, in different organs, including brain, lymph nodes, gut, lungs and female reproductive tract, to name a few (Sheridan & Lefrançois, 2011). Since only 2-5% of the total CD4⁺ T cell population resides in blood, it is crucial that the proposed new LRAs possess the capability to migrate to and function in the different tissues. In addition to participating in different physiological roles, the migrated T

cells might also possess different phenotypes, which might further interfere with drug specificities. The uneven results due to the differences of individual compounds in case of “shock and kill” therapies have already been observed – even though the HDAC inhibitors romidepsin and panobinostat increased plasma viremia and T cell activation, vorinostat failed to do so (Table 1). Due to the complicated nature of the infected cells, a large variety of LRAs have to be identified and developed for tissue specificity, efficacy and safety. Furthermore, drug related factors that have to be taken into consideration during lead compound identification are drug potency, half-life in physiological settings, ease of extraction or synthesis, molecular weight (smaller molecules diffuse better), and number of reactive hydrogen bonds, amongst others (reviewed in Zhang & Wilkinson 2007).

An excellent approach for discovering new antiretrovirus activating compounds is using cell lines that harbor a minimal provirus genome. An example of a viral latency model is the J-Lat A2 clone, described by Jordan *et al.* 2003. A four kilobase long sequence, consisting of various elements from the full length HIV-1 genome and a green fluorescence protein (GFP) sequence (5’LTR-Tat-IRES-GFP-3’LTR), was integrated into an intron of the *UTX* gene of a Jurkat T cell line (Figure 14).

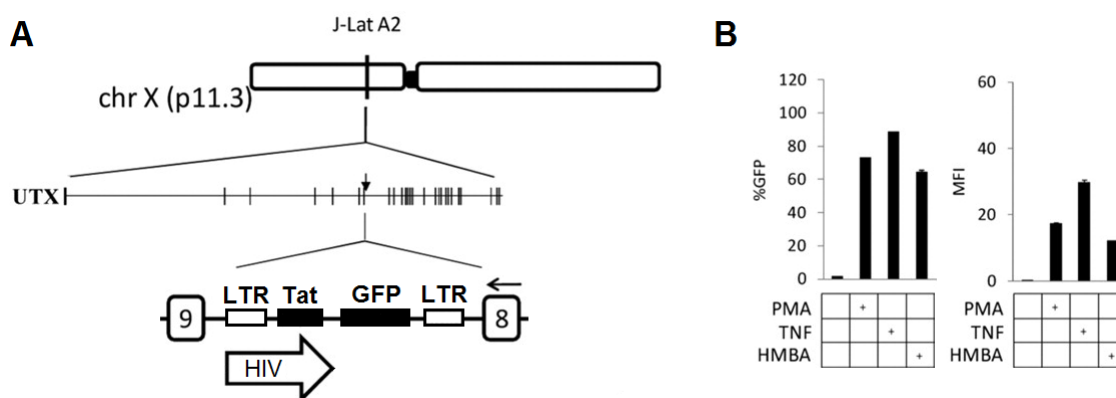


Figure 14: The location of the HIV-1 minigenome in J-Lat A2 cellular model and its response to LRAs (A) The minigenome in Jurkat J-Lat A2 clones is integrated at intron 8 of UTX gene in the opposite transcriptional orientation of the host gene. Cells were previously described in Jordan *et al.* 2003. **(B)** Flow cytometry analysis of A2 responsiveness to PMA (10nM), TNF (10ng/ml) and HMBA (10mM) after 24 hour treatment. Figure adapted from Gallastegui *et al.* 2011.

In search of new LRAs, our group previously screened a library of 6000 small molecules to identify basic compounds capable of reactivating the latent HIV-1 minigenome from A2 cells. Cells were treated for 24 hours with 40µM and analysed for GFP-expression. In total eight different compounds were considered to reactivate GFP expression, from which three compounds shared an 8-hydroxyquinoline (8-HQ) skeleton. Virtual screening for further

similar compounds and additional substitutions of the functional groups in these compounds led to the identification of 8-methoxy-6-methylquinolin-4-ol (MMQO) (Figure 15A). MMQO displayed the highest activity against viral latency with an EC₅₀ of 80 μ M and displayed first signs of toxicity at 160 μ M (Figure 15B). Furthermore, it was observed that MMQO synergizes with other known activating agents like PMA, TNF- α and prostratin and has additive effects with TSA and HMBA, suggesting that its cellular target is different from the known targets for these compounds (Figure 15C). Moreover, it was shown that MMQO alone does not induce the transcriptional activity of minimal promoters containing binding sites for typical HIV-1 activating transcription factors NF- κ B, NFAT, AP-1 and Sp1. Finally the authors demonstrated that in addition to inducing HIV-LTR transactivation, MMQO is also able to display immunosuppressive activity by repressing CD3-induced IL-2 and TNF- α promoter activation (Figure 15D).

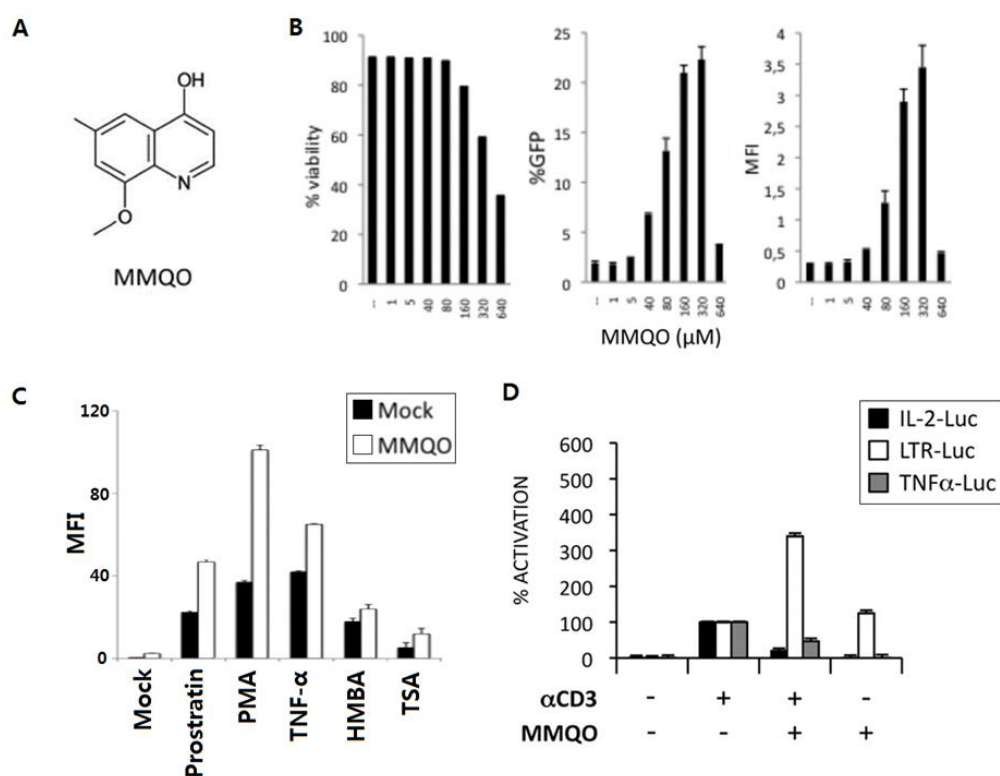


Figure 15: Structure and function of MMQO on HIV-1 minigenome. (A) Structure of the scaffold compound MMQO. (B) Dose dependence of minigenome in response to MMQO. Flow cytometry analysis of a J-Lat heterogeneous population responsiveness to increasing doses of MMQO after 24 hour treatment. Cells were analyzed by forward scatter (FSC) and side scatter (SSC), by the GFP expressing percentage among the viable sample and their GFP expression intensity (MFI, depicted in arbitrary units). (C) MMQO activity in combination with other viral activators. Flow cytometry analysis of J-Lat E27 or H2 clones following 36h treatment with the designated compound(s). (D) Differential effects of MMQO on IL-2 and TNF- α promoters and HIV-LTR transactivation. Jurkat cells were transiently transfected with the plasmids IL-2-Luc, TNF- α -Luc, and LTR-Luc, and 24 h later they were stimulated with coated anti-CD3 (1 μ g/ml) in the absence or the presence MMQO (160 μ M) for 24 h. The results are expressed as the percentage of activation considering CD3-induced transactivation as 100% activation. Figure adapted from Gallastegui et al. 2012.

The quinoline scaffolds have been called previously a “privileged structure” with rich diversity for biological properties (Song et al. 2014). Numerous quinoline structured chemotherapeutics are currently available on the market (e.g. lenvatinib, topotecan and irinotecan) and they have been found to be applicable in research settings. Quinolines are applied as DNA intercalators, G-quadruplex structure stabilizers, androgen receptor antagonists, metal-ion chelators and anti-mitotic agents. A large variety of inhibitory compounds against tubulin polymerization, histone acetyltransferases, topoisomerases, kinesins, mTOR, PARP, proteasomes and MAPKs have also been developed. Immunomodulatory effects of quinolones have been described with HDAC, sirtuin, STAT3 and NF- κ B inhibitory compounds (reviewed in Afzal et al. 2014). The 8-HQ structures, that MMQO is based on, are specifically known to present excellent scaffold compound characteristics and have shown promise in development of anticancer, antifungal, antiparasitic agents, and even as HIV integrase inhibitors (Serrao et al. 2013).

RESULTS

The primary objective of this thesis project was to identify the molecular mechanism of the antiviral compound MMQO. Based on the preliminary results with α -CD3 antibody treatments we hypothesized that MMQO functions through a pathway that exhibits immunosuppressive properties. Considering that the drug affects proviral transcription, a process that is highly dependent on cellular host factors, it is plausible that it will also affect the cell's transcriptome on a global scale.

1. Characterization of MMQO

1.1 Effect of MMQO treatment on the transcriptome

Recognizing that the final output of the drug's functionality is measured in mRNA production, we decided to follow up the characterization of MMQO by utilizing a genome-wide Agilent RNA expression microarray platform with transcripts extracted from Jurkat and HeLa cells treated with or without MMQO. Creating a profile of the compound's transcriptome on the different cell types would help us identify the overlapping pathways and determine the common denominators. In order to identify MMQO's mechanism of action without the possible interference from the HIV-1 minigenome, specifically by the Tat protein that has been described to reprogram the cellular epigenetic landscape (Reeder et al. 2015), we opted to use unmanipulated Jurkat and HeLa cells for the microarray experiment. We confirmed that MMQO indeed does activate HIV independently of the viral transcriptional factor Tat, by measuring the GFP expression from MMQO treated latent Jurkat cells infected with Tat-negative HIV minigenomes (Figure 16).

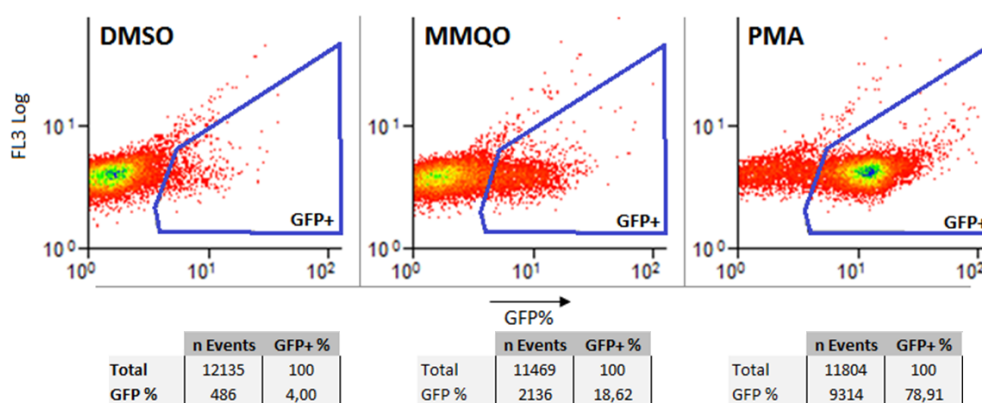


Figure 16: MMQO elicits its effect on the minigenome independently of viral Tat protein. Flow cytometry analysis of previously established latent Jurkat E89 clones, which are infected with Tat-negative GFP-expressing minigenomes, described in (Jordan et al. 2001). Cells were treated 24h either with MMQO (160 μ M), PMA (10nM) or equivalent volume of solvent (DMSO). The events displayed only includes cells that were considered viable according to forward and side scatter gating. Blue gates/boxes highlight the percentage of GFP expressing cells.

Considering that MMQO induces the minigenome expression to about an 8-10 fold increase after eight hours of treatment at EC₅₀ doses (Gallastegui et al. 2012), we concluded it to be a pragmatic treatment time to carry out the microarrays, since the specific target genes of MMQO might respond similarly to HIV-1 promoter stimulation and be sufficiently differentially regulated. In addition, this relatively short treatment time should minimize excessive changes on the protein level, which could otherwise cause unwanted secondary response in the transcriptome. Since this experiment was carried out with the purpose of creating more specific hypotheses about the functioning of the drug, we resolved to apply a minimal setup with only six samples: two replicates of Jurkat cells treated with MMQO, two replicates of untreated Jurkat cells, one sample of HeLa cells treated with MMQO and one sample of untreated HeLa cells. Examining at the correlations between the individual probes we observed an acceptable overlap between the associated samples (Figure 17A). In addition we were able to identify hundreds of up- and downregulated transcripts reliably (Figure 17B). Based on the volcano plot it can be concluded that MMQO causes considerably more potent downregulation as opposed to upregulation of genes. This trait is visualized in the following bar graph, where the percentage of differently expressed transcripts are sorted by fold change cut-offs (Figure 17C).

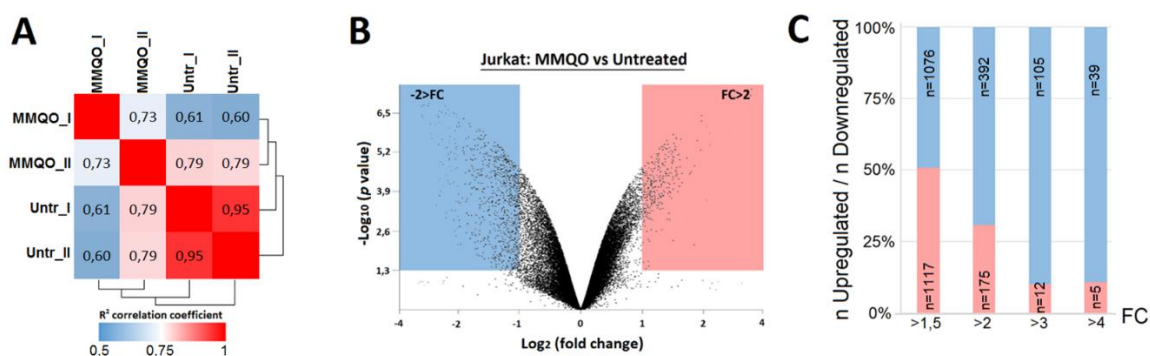


Figure 17: General characteristics of the RNA expression microarrays performed on MMQO treated cells. (A) Heat map showing R correlation for the simplicate and duplicate microarray samples from cells treated 8h with MMQO (80µM) or left untreated. Expression data were obtained by hybridization with an Agilent Human microarray platform. Calculations for the correlation matrix were performed by Andrea Izquierdo-Bouldstridge. (B) Volcano plot of gene expression differences between the Jurkat samples. Blue square includes all the statistically significant downregulated genes, pink square includes all the upregulated genes (p -value<0,05). (C) Gene expression profiles of MMQO. The total number of protein coding genes significantly up- or downregulated by MMQO 8h ($n=2193$) were categorized into four groups based on their mean fold change compared to the untreated genes. The number of upregulated genes was divided by the number of downregulated genes in each expression group that is displayed in the percentage ratio.

The fold change of all transcripts between the untreated control groups and the MMQO treated groups was considered differentially expressed if the genes present a fold-change of at least 1,5 and also surpass a p -value<0,05 after adjustment for multiple testing (McCarthy & Smyth, 2009). We determined that in total MMQO regulated 2193 transcripts at a fold change cut-off of 1,5 and 549 transcripts with a fold change of 2,0 (Figure 18A-B). This broad transcriptional response was unexpected, since we were initially anticipating to identify precise pathways with low number but specifically regulated genes and predict the factors involved. The top 50 differentially upregulated and downregulated genes are depicted in the heat map (Figure 18C). The genes marked with asterisks will later be tested by qPCR.

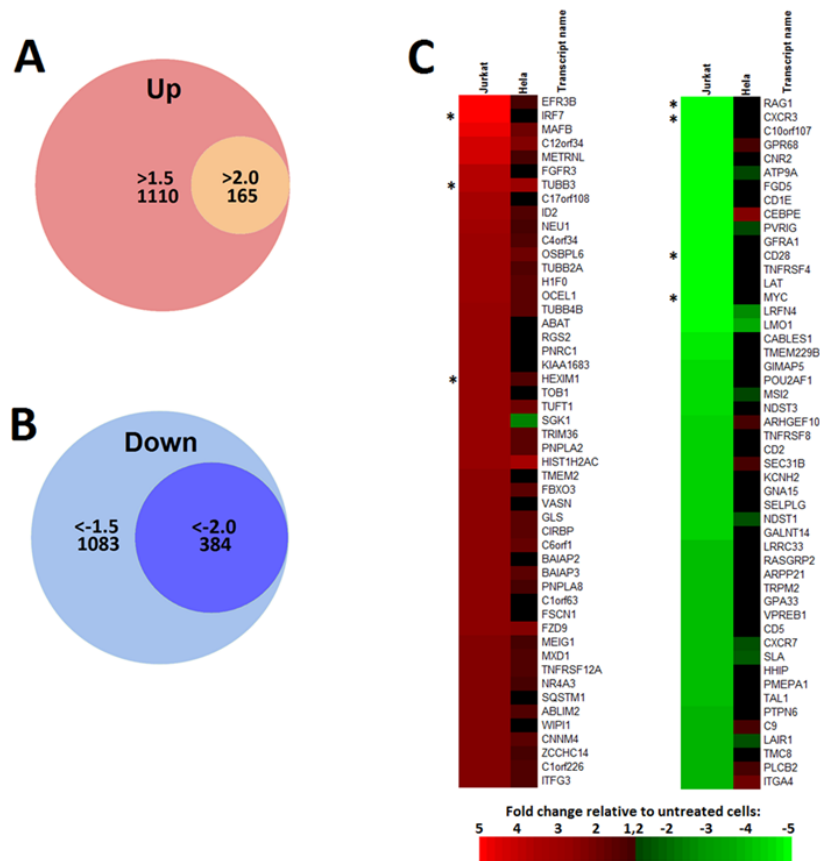


Figure 18: Top regulated genes in MMQO treated Jurkat and HeLa cells. (A-B) Venn diagrams of statistically significant ($q < 0,05$) differential expression of genes that are up- or downregulated with a 1,5-fold or 2-fold change (or greater) when Jurkat cells are treated with MMQO (8h, 80 μ M). Circles in (A) and (B) are depicted proportional in size to each other. (C) Heat map of the top 50 up- and downregulated genes detected in MMQO treated cells compared to the untreated populations. The values in simplicate HeLa samples for the corresponding genes are also shown. Each gene row is normalized to mean expression level. *IRF7*, *TUBB3*, *HEXIM1*, *RAG1*, *CXCR3*, *CD28* and *MYC* were further validated by qPCR showing concordant results.

A potential pitfall of the microarray setup was the fact that the negative controls were not treated with the vehicle compound, but were left untreated instead. Considering the specificity of microarrays and the possibility of possible side-effects from DMSO we decided to confirm the results with various target genes by qPCR (Figure 19). Most of the genes tested didn't show strong response to DMSO treatment alone, except for RAG1 that was adversely regulated to MMQO.

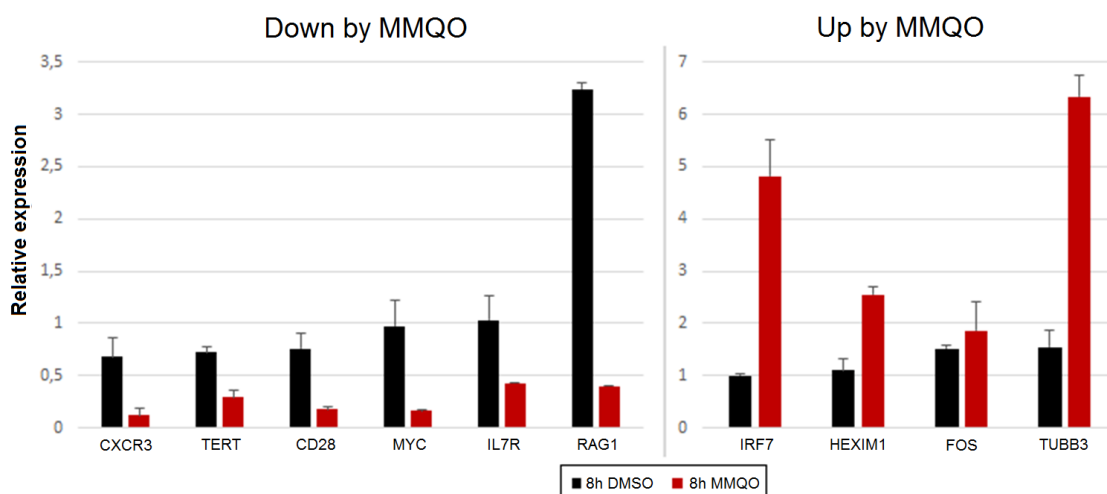


Figure 19: Confirmation of microarray results by qPCR. For a small collection of genes we performed an independent validation on Jurkat cells that were treated 8h with MMQO (80 μ M), equivalent volume of DMSO or left untreated. The bars on the left represent genes that were downregulated, while the bars on the right represent genes upregulated by MMQO. Glyceraldehyde-3-phosphate dehydrogenase (GAPDH) was measured for normalization and results are represented relative to results from untreated cells. The means and S.D. values (error bars) are shown from a representative experiment measured in duplicate.

Curiously the overlap between HeLa and Jurkat cells is minimal (Figure 18C). We estimate that 174 genes were upregulated mutually in both Jurkat and HeLa cell lines ($FC > 1,5$), while 173 genes were downregulated with a fold change below $-1,5$. The exact number of implicated genes in HeLa cells is impossible to determine due to lack of replicates in HeLa sample group. Of the possible 6875 long intergenic non-coding RNAs (lincRNAs) available on the array only 91 were differentially regulated in Jurkat cells, but most of the particular lincRNAs have not been previously described in detail and will not be further investigated within the framework of the present study.

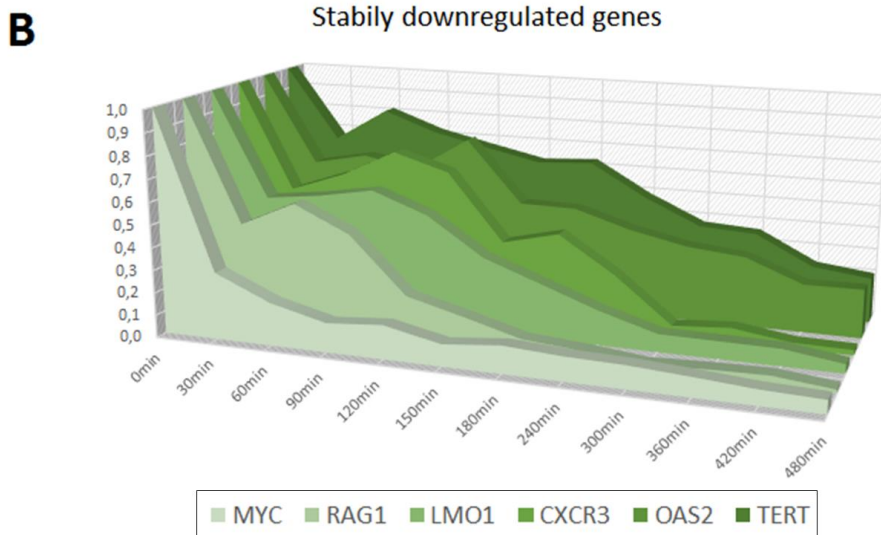
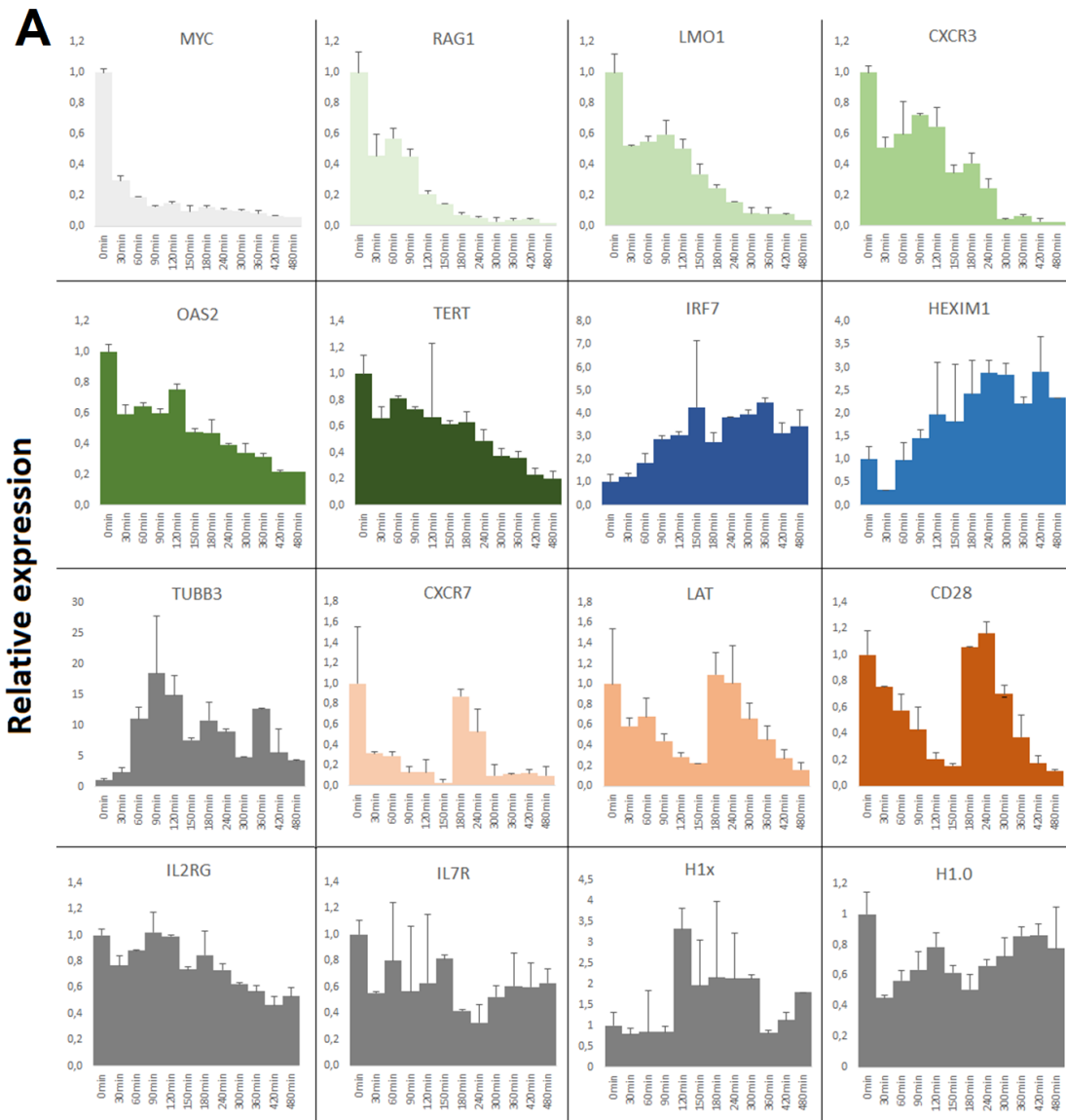
Following the previously described results by Gallastegui et al. 2012, we initially hypothesized MMQO to function via the mitogen-activated protein kinase (MAPK) pathways and concentrated on elaborating the role of c-Jun N-terminal kinase (JNK) and other MAPKs in viral reactivation in response to MMQO treatment. Thorough microarray analysis with

the g:profiler, DAVID and Gene Set Enrichment Analysis (GSEA) toolkits didn't show strong support towards the activity of any MAP kinases – according to GSEA out of the total 198 gene sets positively correlating datasets with MMQO, only 3 were related to mitogenic pathways. Additional gene expression and immunoblotting experiments comparing MMQO to known mitogens in combination with various chemical inhibitors against different stages of the MAPK-axis also contradicted the results described in Gallastegui et al. 2012. Due to their connections with mitogenic pathways and HIV transcriptional activity, we also considered the possibility of MMQO functioning via alternative pathways, such as the protein kinase A (PKA), Akt and Wnt signaling pathways. All of these pathways did present enrichments in the microarray data, but were nevertheless experimentally shown to play negligible roles in response to MMQO. Akt protein remained inactive following MMQO treatments, while the positive controls disulfiram and insulin caused a rapid and specific phosphorylation of Akt. Lithium chloride (LiCl), a Wnt signaling pathway stimulator, synergistically activated HIV-1 transcription in combination with MMQO Tat-dependently in latent models, but curiously MMQO inhibited the upregulation of canonical LiCl target gene expressions. In none of the experiments carried out did we witness any antagonistic or less than additive effects between MMQO and the chemical activators of these pathways. We eventually concluded that the MAPK pathways do not participate directly in the functioning of MMQO and were forced to reevaluate the possible molecular functions of the compound. The experiments and results reported in this paragraph are described in higher detail in the Annex (page 131), since they did not contribute significantly to the central theme of this dissertation or remained inconclusive.

1.2 Time-course dysregulation of gene expression by MMQO

To improve our comprehension on the effect MMQO has on its target genes we decided to examine their time dependent kinetics. Understanding the consistency of their dysregulation should help us hypothesize which pathways might be implicated directly by MMQO. To that end we extracted mRNA from Jurkat cells treated at twelve different time points with MMQO (up to eight hours) and analyzed the target genes by qPCR. In total we studied the expression changes of sixteen genes that were up- or downregulated in the microarray analysis (Figure 20A). We identified six genes that were stably decreased (Figure 20B), two genes that increased consistently (Figure 20C), five genes that didn't show a clear

pattern of regulation and three downregulated genes that displayed a curious rescuing peak after three hours of treatment (Figure 20D).



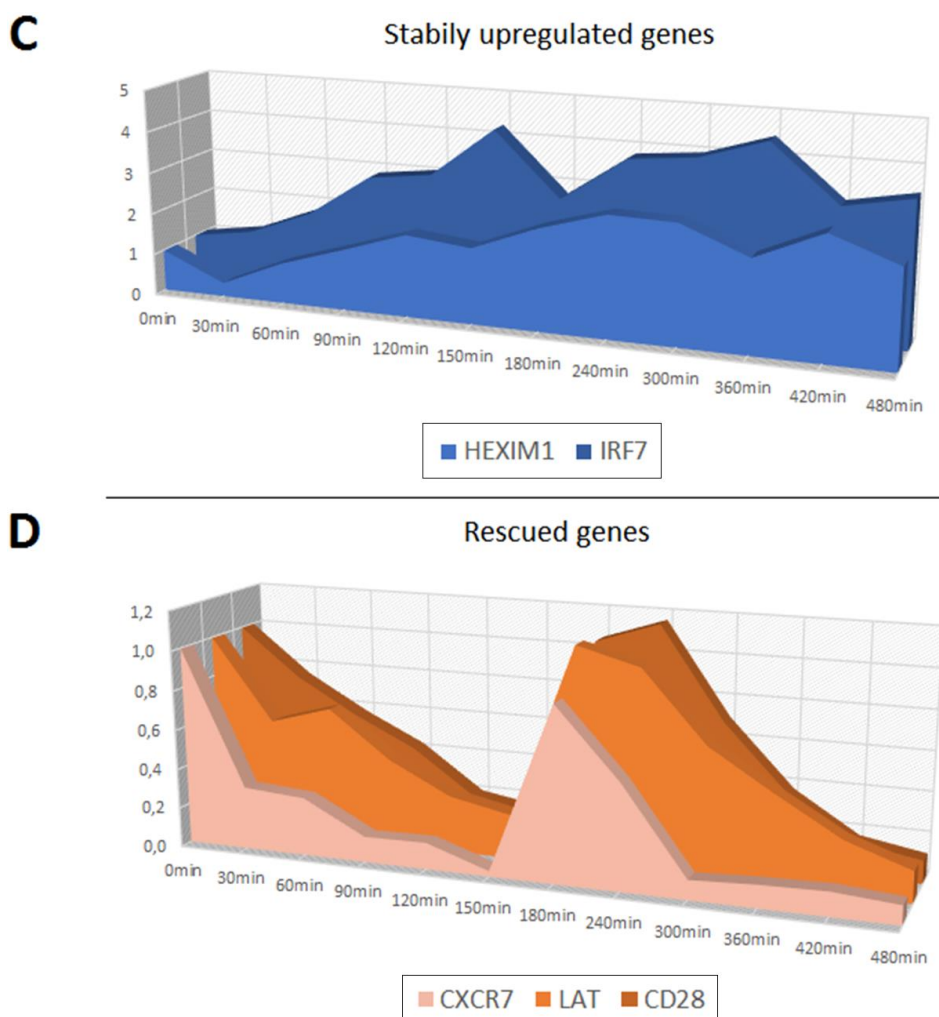


Figure 20: qPCR of target gene differential regulations by MMQO in a time dependent manner. (A) Jurkat cells were treated at eleven different time points with MMQO (160 μ M) or left untreated. Genes were chosen based on their specificity towards MMQO in microarray. *GAPDH* was measured for normalization and results are represented relative to results from untreated cells. The means and S.D. values (error bars) are shown from a representative experiment measured in duplicate. (B-D) Visualization of the kinetics of three different gene subgroups. Color coding overlaps with figure (A).

1.3 cMyc decrease in response MMQO

Among the persistently downregulated genes *MYC* emerges as the most intriguing target – it exhibits a potent decline already after 15 minutes of MMQO treatment and remains continuously repressed, even until five days after initial treatment (data not shown). Additional kinetics experiments with shorter time points and varying doses of MMQO confirm its high responsiveness to the drug (Figure 21A-C).

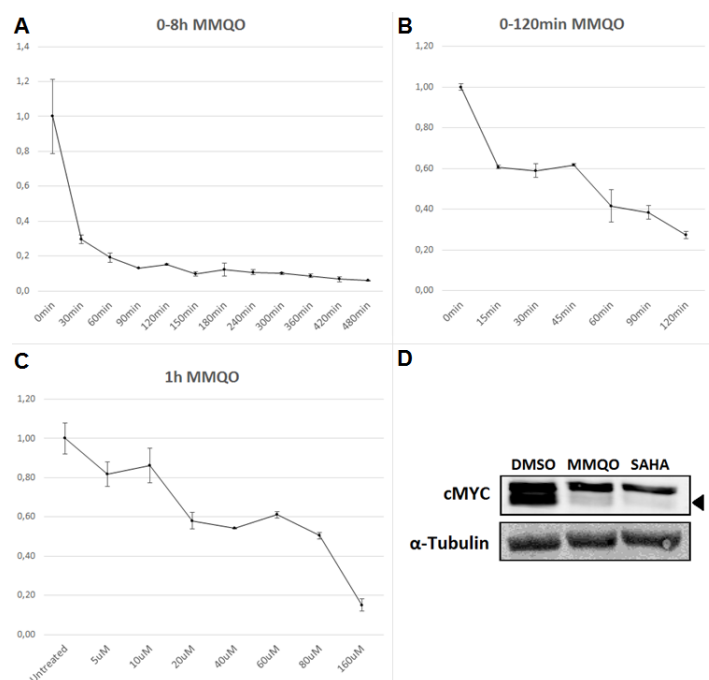


Figure 21: Downregulation of cMyc. (A-C) qPCR results depicting how *MYC* downregulation is time and dose sensitive. (A-B) Native Jurkat cells were treated at different time points with either MMQO (160 μ M) or left untreated. (C) Native Jurkat cells were treated with varying doses of MMQO for 1 hour or left untreated. *GAPDH* was measured for normalization and results are represented relative to results from the untreated cells. The means and S.D. values (error bars) are shown from a representative experiment measured in duplicate. (B) Western blot analysis of cMyc protein expression. Jurkat cells were incubated 12 hours with MMQO (160 μ M), SAHA (5 μ M) or left untreated. Total protein was extracted with RIPA buffer and analyzed by immunoblotting against various cMyc and α -Tubulin as a loading control. Triangle designates the correct cMyc band.

The sequence-specific transcriptional regulator cMyc protein canonically participates in cell cycle progression, apoptosis and is considered a quintessential oncogene (Nilsson & Cleveland, 2003). It is also noteworthy to mention that depending on the cell line *MYC* has been shown to be present in 11-25% of human gene promoters, with especially higher rates in lymphomas (Fernandez et al. 2003). As a transcriptional factor cMyc is known to autoregulate its own gene expression, which could explain the rapid decline we witness in response to MMQO. This assumption is supported by the fact that the cMyc protein half-life is known to be about 11-18 minutes long, while the half-life of the mature mRNA of *MYC* is known to be about thirty minutes long (Gregory & Hann, 2000; Herrick & Ross, 1994). The drastic decline of the *MYC* gene by MMQO translates also to protein level, similarly to the previously published decrease caused by histone deacetylase inhibitors in Jurkat cells (Figure 21D) (Mu et al. 2014).

The drastic obstruction of cMyc can most prominently be demonstrated by GSEA – from the top 10 gene sets that correlated most with the downregulated genes by MMQO, six were directly cMyc reliant and two to gene sets related to *MYC* disrupting HDAC inhibitors (Figure 22A-B).

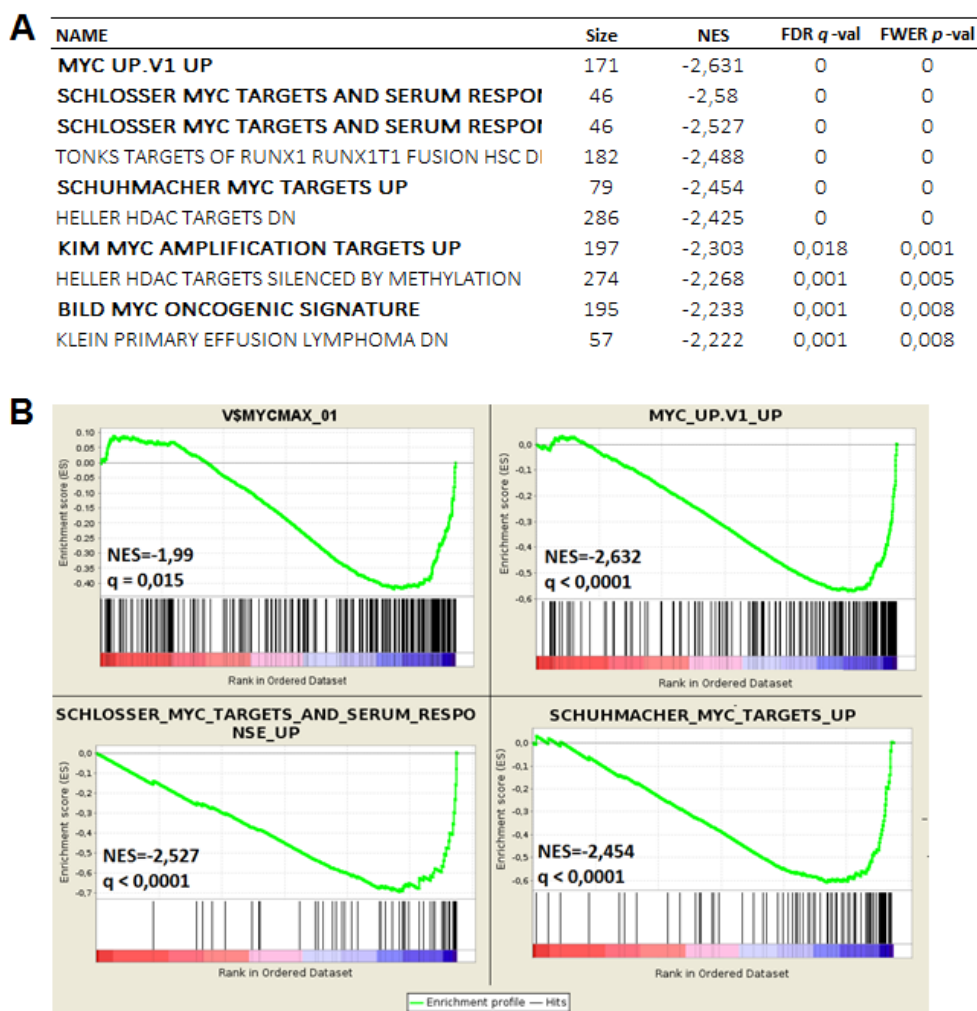


Figure 22: *MYC* downregulation according to GSEA. (A) Table of top 10 gene sets enriched among genes downregulated by MMQO in Jurkat cell line based on GSEA. In total 85 gene sets correlated negatively with MMQO treatment. Gene sets related to *MYC* are marked in bold. (NES, normalized enrichment score) (B) GSEA showing downregulation of three cMyc-dependent gene sets and a representative set of genes with proximal promoter regions containing cMyc-binding sites in the transcriptional profiles of cells treated with MMQO. Depicted is the plot of the running sum for the molecular signatures database v.5.2 gene set within the MMQO dataset, including the maximum enrichment score and the leading edge subset of enriched genes.

Among all the significantly enriched gene sets only one DNA-binding motif module was negatively correlated with MMQO treatment – V\$MYCMAX_01, which is the designation for the most common cMyc binding sites (Table 3).

Gene set	Size	NES	FDR <i>q</i> -val	FWER <i>p</i> -val
MYC UP.V1 UP	171	-2,631	0,000	0,000
SCHLOSSER MYC TARGETS AND SERUM RESPONSE DN	46	-2,580	0,000	0,000
SCHLOSSER MYC TARGETS AND SERUM RESPONSE UP	46	-2,527	0,000	0,000
SCHUHMACHER MYC TARGETS UP	79	-2,454	0,000	0,000
KIM MYC AMPLIFICATION TARGETS UP	197	-2,303	0,018	0,001
BILD MYC ONCOGENIC SIGNATURE	195	-2,233	0,001	0,008
COLLER MYC TARGETS UP	25	-2,143	0,005	0,054
SCHLOSSER MYC AND SERUM RESPONSE SYNERGY	31	-2,098	0,006	0,101
SCHLOSSER MYC TARGETS REPRESSED BY SERUM	156	-2,031	0,011	0,251
V\$MYCMAX 01	250	-1,989	0,015	0,379
DANG REGULATED BY MYC UP	70	-1,985	0,015	0,400
ACOSTA PROLIFERATION INDEPENDENT MYC TARGETS	82	-1,919	0,026	0,665
MENSSEN MYC TARGETS	53	-1,860	0,040	0,892

Table 3: Table of MYC related gene sets (*q*-value<0,05) among the genes regulated by MMQO in Jurkat cells based on GSEA. The only dataset which was enriched among all the transcription factor motif gene sets (GSEA: C3) is highlighted in bold.

The transcriptional regulation by cMyc is considered a hallmark for both cancer initiation and maintenance and the loss of its transcriptional control renders the affected cells apoptotic (Gabay et al. 2014). Indeed, we also found a positive correlation between MMQO treatment and enrichment of proapoptotic GSEA gene sets (Table 4).

NAME	Size	NES	FDR <i>q</i> -val	FWER <i>p</i> -val
GNF2_H2AFX	31	1,936	0,013	0,311
REACTOME_INTRINSIC_PATHWAY_FOR_APOPTOSIS	29	1,869	0,016	0,658
CASPASE_ACTIVATION	26	1,859	0,018	0,713
POSITIVE_REGULATION_OF_CASPASE_ACTIVITY	30	1,827	0,025	0,866
APOPTOTIC_PROGRAM	59	1,714	0,047	1,000

Table 4: Table of apoptosis related gene sets (*q*-value<0,05) among the genes regulated by MMQO in Jurkat cells based on GSEA. In total 198 gene sets correlated positively with MMQO treatment.

This interpretation is in parallel supported by the microarray analysis software Ingenuity Pathway Analysis (IPA) physiological functions prediction, where only five datasets correlated positively with MMQO treatment and three from those were directly linked to apoptosis (falling under the category “Cell Death”) (Table 5).

Functions Annotation	Category	p-Value	Z-score	# Molecules
Apoptosis of lymphocytes	Cell Death	<0,0001	2,131	97
Apoptosis of mononuclear leukocytes	Cell Death	<0,0001	2,220	98
Infection of mammalia	Infectious Disease	<0,0001	2,786	81
Apoptosis of hematopoietic progenitor cells	Cell Death	<0,0005	2,029	45
Differentiation of leukemia cell lines	Cellular Development	<0,005	2,404	31

Table 5: Molecular and cellular functions and physiological activities enriched for genes affected by MMQO in Jurkat cells. Shown are the only five hits with a positive regulation z-score using IPA, together with significance scores (*p*-values) and the number of genes included in each class.

1.4 MMQO increases apoptosis and inhibits proliferation

The antiproliferative effect of MMQO was validated by counting cells in culture over a course of five day treatment period. Noticeable reduction of proliferation was detected already after two days of high-dose MMQO treatment (Figure 23A). The increase of proapoptotic DNA damage related signals also increased already after twelve hours of MMQO treatment in HeLa cells, though not as potently as with the cytotoxic topoisomerase inhibitor Camptothecin (Figure 23B). The cleaved p25 form of PARP is considered to be a marker for caspase-3 activity and single stranded DNA breaks, while the phosphorylated Ser-139 of H2Ax (γ -H2AX) is a marker for double stranded DNA breaks (Kinner et al. 2008, Chaitanya et al. 2010). We did not witness any additional cleavage of caspase-3, another

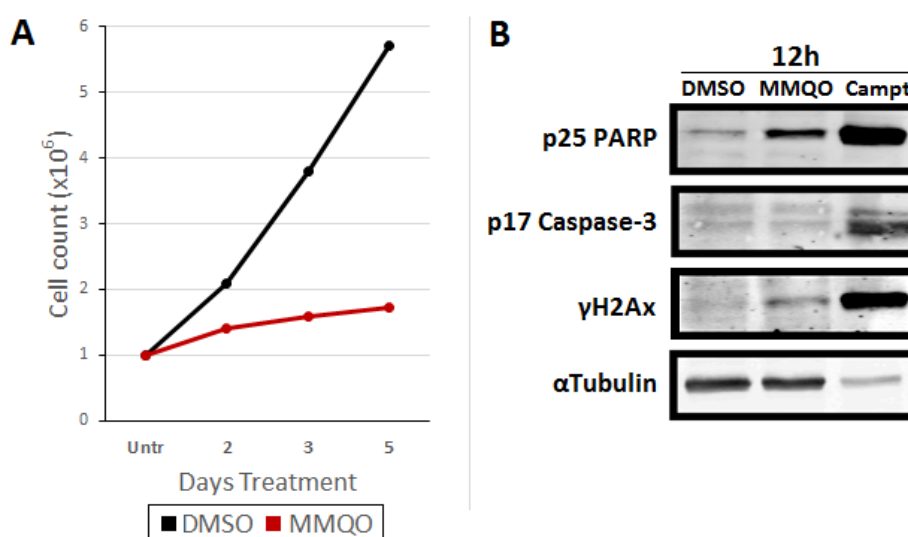


Figure 23: MMQO affects cell proliferation and induces proapoptotic signaling. (A) Jurkat cell numbers with MMQO (160 μ M) treatment or equivalent volume of the vehicle DMSO. Results normalized to time = 0 levels. (B) Western blot analysis of various apoptotic markers. HeLa cells were incubated 12 hours with MMQO (160 μ M), Camptothecin (5 μ M) or equivalent volume of DMSO. Total protein was extracted with RIPA buffer and analyzed by immunoblotting against listed targets and α -Tubulin was as a loading control.

marker for proapoptotic signaling, but this could be explained by the timing of the experiment or by the poor quality of the antibody. It is important to note here that the dose of MMQO used for this experiment (160 μ M) doesn't normally present any change in viability after 24-hour treatment in flow cytometry based detection methods.

While the dysregulation of *MYC* is a peculiar hallmark of MMQO and it helps us describe the drug-induced decrease in proliferation, these facts alone won't be able to help us determine the detailed mechanism of MMQO. *MYC* regulation has been under investigation already for more than thirty years and numerous different compounds and mechanisms have been shown to have an effect on its expression in carcinogenic cells. The chemical downregulators of the *MYC* gene include tricyclic antidepressants (serotonin transporter inhibitors), FUSE binding protein inhibitors (a transcription factor necessary for *MYC* expression), quinoline structures that stabilize the *MYC* promoter into an inert G-quadruplex structure, specific inhibitors cMyc protein targeting inhibitors like 10058-F4, bromodomain and HDAC inhibitors that disrupt the super enhancer of *MYC*, to name a few (Xia et al. 1994, Huth et al. 2004, Huang et al. 2006, Ou et al. 2007, Lovén et al. 2013, Thomas & Tansey, 2015).

1.5 Regulation of immunogenicity related genes

Perhaps coincidentally the three genes that presented the rescuing peak earlier on in the kinetics experiment can be considered immunogenicity regulating members (Figure 20D). Linker for Activation of T-Cells (*LAT*) and Cluster of Differentiation 28 (*CD28*) participate in T cell activation, while C-X-C chemokine Receptor type 7 (*CXCR7*) is considered to participate in the migration process of lymphocytes (Hartmann et al. 2008, Acuto & Michel, 2013, Lin et al. 2014). All these three genes are known to contain NF- κ B motifs at their proximal transcription start site and the expression of *CD28* and *CXCR7* has indeed been shown to be NF- κ B responsive (Jin et al. 2009, Banerjee et al. 2012). In fact, based on the MMQO microarray the IPA software did predict an inhibition of the NF- κ B complex activity, due to the downregulation of various target genes, which included several of the stably decreasing genes as well (e.g. *CXCR3*, *IL7R*, *TERT*) (Table 6). IPA transcription factor prediction supported this inhibitory effect also in HeLa cells (z-score -2,79). Moreover, many of these genes aren't known to contain cMyc motifs near their TSS. In fact, the most significantly enriched data sets like "MYC_UP.V1_UP" mostly do not contain any genes related to the

immune system, suggesting that an alternative mechanism independent from cMyc dependent transcription must regulate the immunosuppression witnessed following MMQO treatment.

Gene	FC	Gene	FC	Gene	FC	Gene	FC
<i>CXCR3</i>	-9,351	<i>TNFSF4</i>	-2,595	<i>CCND2</i>	-2,028	<i>CD86</i>	-1,579
<i>MYC</i>	-6,279	<i>TNFSF10</i>	-2,484	<i>NFKB1</i>	-1,951	<i>CD82</i>	-1,578
<i>VPREB1</i>	-4,857	<i>CD83</i>	-2,475	<i>CFLAR</i>	-1,932	<i>HDGF</i>	-1,565
<i>SELPLG</i>	-4,263	<i>C1R</i>	-2,404	<i>RFTN1</i>	-1,821	<i>CST7</i>	-1,559
<i>STAT5A</i>	-3,478	<i>BCL11A</i>	-2,383	<i>KIT</i>	-1,815	<i>ERAP2</i>	-1,554
<i>LTB</i>	-3,363	<i>ITGAL</i>	-2,213	<i>IL15</i>	-1,796	<i>CCR7</i>	-1,553
<i>LSP1</i>	-2,859	<i>RUNX1</i>	-2,194	<i>CBR3</i>	-1,743	<i>CASP4</i>	-1,492
<i>CD40LG</i>	-2,838	<i>GZMK</i>	-2,190	<i>IL23A</i>	-1,734	<i>RGS16</i>	-1,479
<i>TERT</i>	-2,609	<i>BATF</i>	-2,093	<i>SPIB</i>	-1,637	<i>ICOS</i>	-1,461
<i>IL7R</i>	-2,603	<i>CFTR</i>	-2,083	<i>IKBKE</i>	-1,618	<i>BCL2</i>	-1,457

Table 6: IPA prediction of top 40 NF- κ B complex target genes that were downregulated by MMQO. All the forty targets listed here should be upregulated by NF- κ B. Based on 80 different target genes the NF- κ B complex was downregulated by a z-score of -2,363.

The immunosuppressive pattern can also be corroborated by examining the pathway enrichments from downregulated genes in the microarray. Analysis with the Gene Ontology (GO), TRANSFAC and Reactome (REAC) database terms with the g:profiler toolkit generates nine different negative correlations to MMQO treatment, with all of them featuring immunogenic characteristics (Table 7). In total 30,5% of the downregulated genes (n = 313, FC < -2) are among the Reactome dataset “Immune system”, indicating anew the high proportion of immune genes among the MMQO dataset. The dataset “Regulation of α - β -T-cell proliferation” was among the most greatly inflicted by the MMQO treatment – 21,7% of the members from that pathway are included among the downregulated genes in the

NAME	Term ID	p-Value	Q&T/Q	Q&T/T
cell activation	GO:0001775	<0,0001	0,166	0,045
antigen processing and presentation, exogenous lipid antigen via MHC class Ib	GO:0048007	0,003	0,016	0,571
mast cell activation	GO:0045576	0,017	0,028	0,130
Immunoregulatory interactions between a Lymphoid and a non-Lymphoid cell	REAC:198933	0,020	0,078	0,065
cytokine production	GO:0001816	0,020	0,091	0,037
Cell surface interactions at the vascular wall	REAC:202733	0,027	0,062	0,079
regulation of alpha-beta T cell proliferation	GO:0046640	0,027	0,020	0,217
immunoglobulin production	GO:0002377	0,035	0,032	0,096
Immune System	REAC:168256	0,041	0,305	0,025

Table 7: Enrichment of Gene Ontology (GO) and Reactome (REAC) datasets among the genes downregulated by MMQO. Q = number of query genes. T = number of term genes. Q&T/Q denotes how many percent from the 313 MMQO downregulated genes belong to this gene set (FC<-2). Q&T/T denotes how many percent do the MMQO regulated genes overlap with the full dataset. Data obtained with g:profiler toolkit analysis.

MMQO microarray, coinciding with the results from the proliferation experiment on Jurkat cells (Figure 23A). It should be noted that GSEA did not show any positive significant enrichment of gene sets related to the immune system, while there were seven immune system datasets overrepresented among the downregulated genes, such as “IMMUNE_SYSTEM_PROCESS”, “HUMORAL_IMMUNE_RESPONSE” and “B_CELL_ACTIVATION”.

Based on the microarray data, the extensive and rapid downregulation of various genes of the immune system and on the immunosuppressive properties described by Gallastegui et al. 2012, we hypothesize that MMQO can inhibit the functioning of NF- κ B complex. Unfortunately we cannot yet propose a specific mechanism, nor the specific site affected by the compound. Among the possibilities could be direct modifiers of NF- κ B itself, its binding partners, inhibitors of upstream regulators, DNA-binding inhibitors, NF- κ B expression inhibitors *etc.* Nevertheless, it is crucial that we understand the mechanism of the witnessed immunosuppression, since that pathway will probably lead us to the specific binding partner of MMQO and will hopefully be shared with HIV-1 transcriptional induction.

From the possibilities listed as NF- κ B inhibitory we can exclude a few options. It's highly probable that if NF- κ B binding motif was not affected by MMQO, since we would have witnessed an increased motif enrichment among the downregulated genes from the transcription factor analysis. Neither was there any NF- κ B motif enrichment among the GSEA gene sets (q -value 0,519, NES=1,06). Thus far the indications for immunosuppression have been more global and not NF- κ B specific, as was highlighted by the fact that only ~30% of the downregulated genes were considered to be part of the “Immune System” dataset.

The fact that *MYC* gene can be rapidly downregulated within fifteen minutes after initial treatment, suggests a direct downregulatory pathway action by MMQO, yet NF- κ B is only considered to be a positively contributing factor to *MYC* expression (Qin et al. 1999, Barkett & Gilmore, 1999). Knowing this we can also exclude the possibility of MMQO inhibiting directly the NF- κ B complex, thus narrowing the possibilities for its function. Based on the microarray data we can consider two different mechanisms that might contribute either up- or downstream of NF- κ B to the immunosuppression – either tubulin polymerization or histone deacetylase functioning (Table 8).

NAME	Size	NES	FDR <i>q</i> -val	FWER <i>p</i> -val
PEART_HDAC_PROLIFERATION_CLUSTER_UP	56	2,451	0,000	0,000
HELLER_HDAC_TARGETS_UP	299	2,240	0,000	0,000
HELLER_HDAC_TARGETS_SILENCED_BY_METHYLATION_UP	446	2,090	0,003	0,016
N_ACETYLTRANSFERASE_ACTIVITY	21	1,937	0,013	0,308
ZHONG_RESPONSE_TO_AZACITIDINE_AND_TSA_UP	177	1,919	0,013	0,393
MICROTUBULE_ASSOCIATED_COMPLEX	47	1,903	0,014	0,486
MICROTUBULE_MOTOR_ACTIVITY	16	1,897	0,014	0,507
MICROTUBULE_CYTOSKELETON	149	1,880	0,015	0,598
ACETYLTRANSFERASE_ACTIVITY	25	1,871	0,016	0,652
ESTABLISHMENT_OF_ORGANELLE_LOCALIZATION	17	1,776	0,032	0,987
SPINDLE_MICROTUBULE	16	1,776	0,032	0,988
PID_HDAC_CLASSIII_PATHWAY	25	1,767	0,032	0,994
HISTONE_ACETYLTRANSFERASE_ACTIVITY	16	1,726	0,043	1,000
N_ACYLTRANSFERASE_ACTIVITY	24	1,711	0,048	1,000
PEART_HDAC_PROLIFERATION_CLUSTER_DN	75	-2,071	0,008	0,155
HELLER_HDAC_TARGETS_SILENCED_BY_METHYLATION_DN	274	-2,268	0,008	0,005
HELLER_HDAC_TARGETS_DN	286	-2,425	0,000	0,000

Table 8: Table of selected HDAC and tubulin related gene sets (*q*-value<0,05) among all the genes regulated by MMQO in Jurkat cells based on GSEA. In total 283 gene sets correlated either positively or negatively with MMQO treatment. Gene sets related to HDACs are marked in blue, while gene sets related to tubulins are depicted with orange.

The regulation of NF- κ B transcription and nuclear translocation has been described previously to be partially dependent on cytoskeletal stability (Spencer et al. 1999, Jung et al. 2003). Besides showing positive enrichment in regulating the tubulin dependent gene sets, MMQO treatment also upregulated four tubulin family members that were not included in the GSEA results – *TUBB3*, *TUBB2A*, *TUBB4B* and *TUBB8* (with fold changes of +3,93; +3,12; +2,97; +2,14 respectively). Tubulin binding compounds are known to induce mitotic arrest, apoptosis and upregulate β -tubulin family members (Saussede-Aim et al. 2009). Furthermore, numerous quinoline scaffold tubulin polymerization inhibitors have been already described, so there is a possibility for MMQO to directly function on the cytoskeleton and consequently inhibit NF- κ B activity (Afzal et al. 2014). However, there are a few counterarguments against MMQO inhibition of tubulin polymerization. A largely disagreeing fact is that according to the author's knowledge, none of the numerous extensively studied tubulin inhibitors are known to induce HIV-1 transcription while still retaining minimal toxicity on the target cells as witnessed by MMQO treatment. A lack of oversight of that scale would be highly unlikely since anti-microtubule natural agents like vinblastine and vincristine have been in clinical use as chemotherapeutic agents for about

five decades, while the synthetic paclitaxel was approved for clinical use 25 years ago (Torres et al. 2015). Nevertheless, we decided to measure effect of nocodazole, a known tubulin polymerization inhibitor, has on the expression of MMQO target genes. We didn't witness any relevant effect of nocodazole at very high dose on the genes *TUBB3*, *IRF7* nor *MYC* (Figure 24).

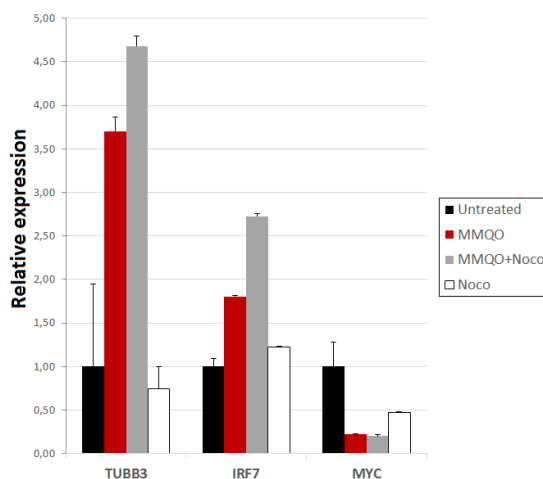


Figure 24: qPCR for target gene dysregulations by MMQO and Nocodazole in Jurkat cells. Cells were treated for 3h with MMQO (160 μ M), Nocodazole (50ng/ml), their combination or left untreated. Genes were chosen based on their specificity towards MMQO. *GAPDH* was measured for normalization and results are represented relative to results from untreated cells. The means and S.D. values (error bars) are shown from a representative experiment measured in duplicate.

Though we can't yet be sure if the mechanism that control NF- κ B dependent transcription and regulates *MYC* are the same, we can speculate them to be regulated by the same factors. Though the possibility of an NF- κ B inhibiting compound to activate HIV-1 transcription sounds paradoxical to say the least, we could speculate on one similarly functioning mechanism – namely through the inhibition of histone deacetylases.

2. MMQO as a noise enhancer on HIV-1 transcription

The fact that MMQO synergizes with known viral activators as published by Gallastegui et al. 2012 (PMA, prostratin, α -CD3), has thousands of targets as seen by microarray data and the lack of MFI increase in Tat-negative cell lines indicates that MMQO probably functions more as an enhancer of viral transcription. This presumption is also supported by MMQO's rapid synergy with PMA on the viral promoter (Figure 25). The Tat-negative E89 Jurkat clones, exhibit a potent synergy between those two drugs already after one hour, whereas

if MMQO would only function via alternative mechanisms such as cMyc downregulation, the cells wouldn't have time to express enough viral mRNA for a significant difference. In general MMQO starts to exhibit a notable effect on the viral promoter after three to four hours (Gallastegui et al. 2012).

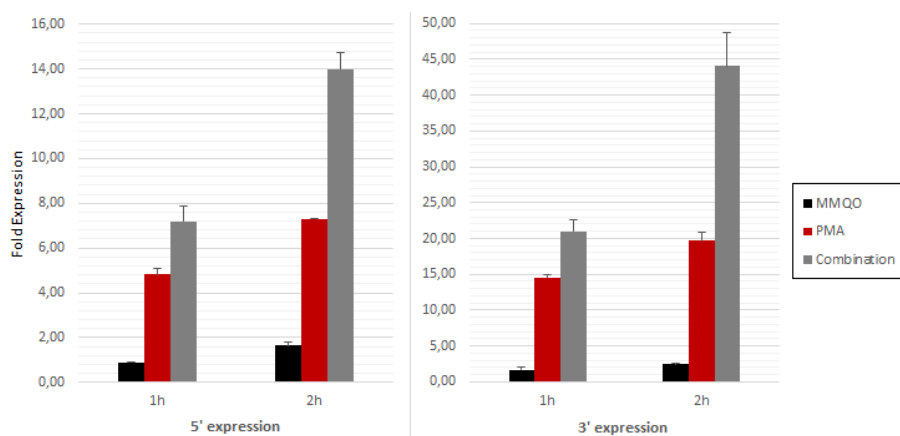


Figure 25: qPCR results depicting the rapid synergy between PMA and MMQO. E89 Jurkat clones were treated for 1h or 2h either with MMQO (160 μ M), PMA (10nM), their combination or equivalent volume of DMSO as vehicle. *GAPDH* was measured for normalization and results are represented relative to results from the DMSO treated cells. Primers to detect the amplicons from 5' LTR and 3' LTR were used. Means and S.D. values (error bars) are shown from a representative experiment measured in duplicate.

2.1 MMQO as an HDAC inhibitor?

Among the GSEA results, HDAC related gene sets were largely enriched, with nine gene sets correlating positively and three gene sets correlating negatively with MMQO treatment (Table 8). It should be noted that these HDAC datasets contain nearly a thousand genes, while the tubulin associated gene sets encompassed only about ~200 genes, further demonstrating the plausibility of MMQO being an HDAC inhibitor (HDACi). A large proportion of the genes encompassed in these data sets are related to the immune system, thus finally providing a possible explanation for the broad immunosuppression that we have witnessed by MMQO. This observation also is in agreement with previously published data that describe HDAC inhibitors to exert an immunosuppressive impact on both Jurkat cells and regulatory immune cells in general (Januchowski & Jagodzinski, 2007, Kroesen et al. 2014).

Various studies have also linked HDACi to HIV-1 reactivation through different mechanisms

– HDAC inhibitors are known to induce general chromatin decondensation that is crucial for efficient viral transcription, to release the repressive p50 homodimer from the canonical NF- κ B binding motifs and to release the repressive cMyc protein from the Sp1-complex on the viral promoter (Figure 26).

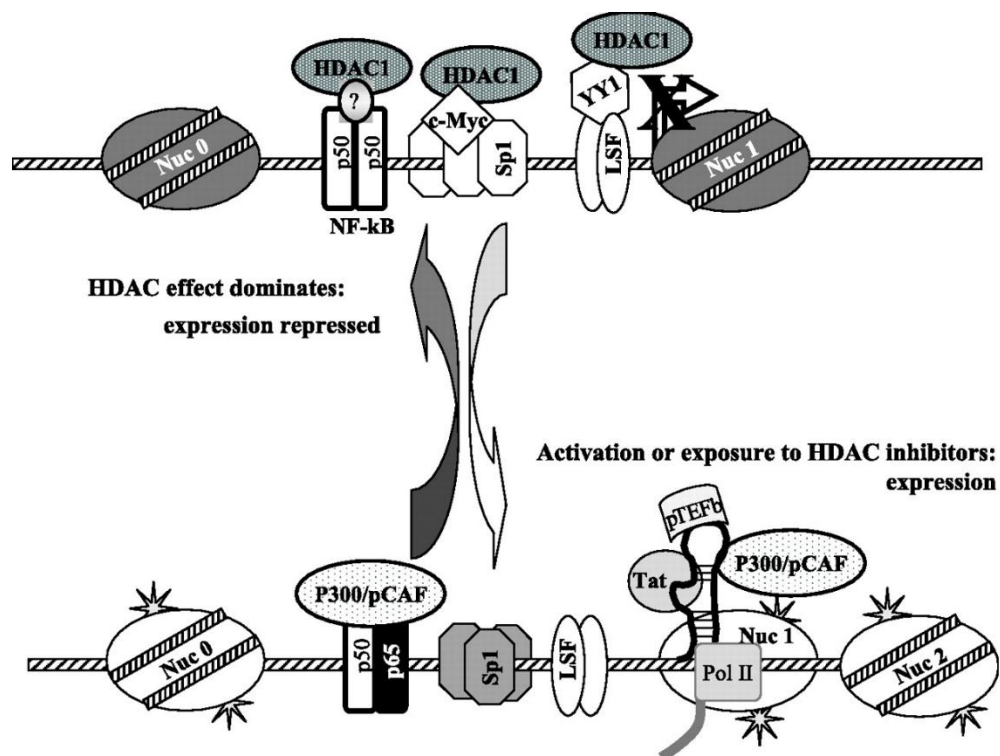


Figure 26: Model of how HDAC inhibitors affect viral latency. HDAC proteins are able to suppress the viral transcription through various repressive factors and core histone deacetylation. The addition of histone deacetylase inhibitors decreases the occupancy of repressors and loosens the chromatin. Figure adapted from Jiang et al. 2007.

Importantly, several quinoline structured compounds have been described to inhibit HDACs directly (Afzal et al. 2014). Clioquinol, a known anti-malarial compound, has been shown to cause global hyperacetylation by blocking the active site of HDAC proteins directly (Cao et al. 2013). This hindrance is shown to take place directly through a binding to the Zn^{2+} ion within the active pocket, a compulsory characteristic for efficient inhibition of the enzyme's function (Figure 27A). Utilizing *in silico* molecular docking we were able to affirm the possibility of MMQO being an HDAC inhibitor, with a docking score of -7,018 (Figure 27B). The prediction model shows a stable interaction between the ketone group of MMQO and the Zn^{2+} , with a secondary stabilizing interaction forming at the methoxy group with the 308-Tyrosine residue. The docking score mimics the potential energy change between the ligand and the protein, meaning a negative score corresponds to a strong binding, while a less negative or even a positive score corresponds to a weak or non-existing binding.

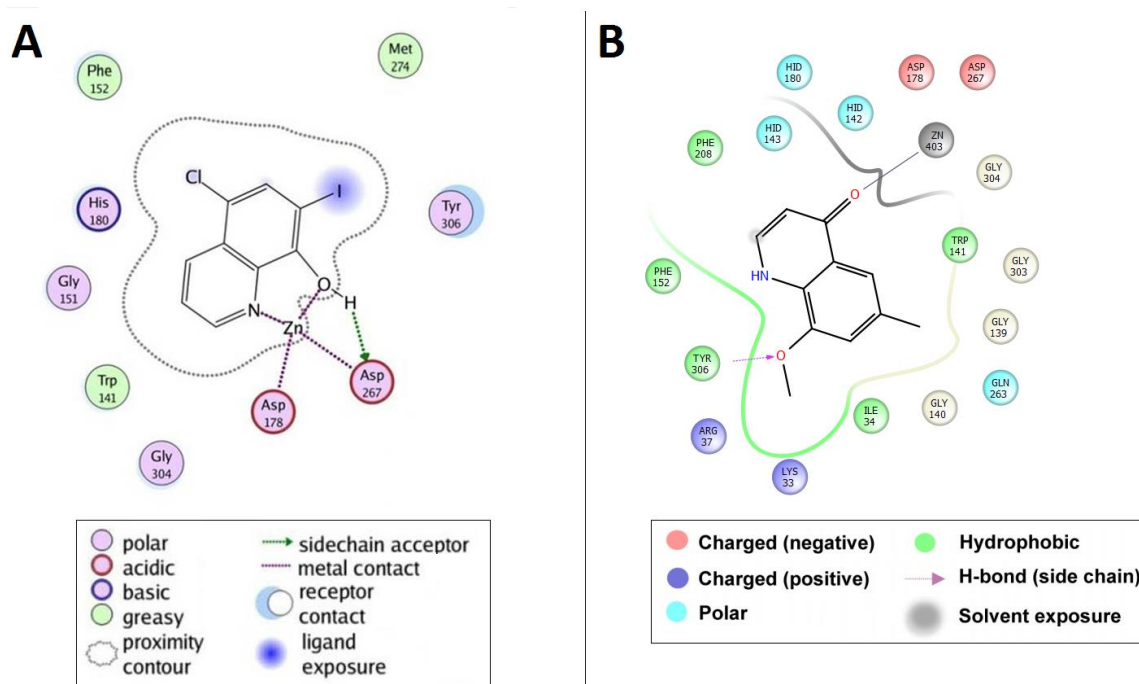


Figure 27: *In silico* docking models of clioquinol and MMQO in the HDAC8 active site. (A) Previously published example of clioquinol forming a stable binding with the Zn^{2+} and interacts with residues in the active site of HDAC8 protein (PDB code: 1T64). Figure adapted from Cao et al. 2013. (B) Docking of MMQO in the same HDAC8 model. Note the contact made by the ketone group to the Zn^{2+} . Illustration created by Salvador Guardiola, Institute for Research in Biomedicine (IRB).

HDAC inhibition is known to cause an oscillatory transcription in immunoresponsive genes, notable especially during the first hours after treatment (Peart et al. 2005). Prompted by the docking model, we decided to compare the immunosuppressive effects of MMQO in comparison to SAHA (a pan HDAC inhibitor) and BAY-11-7085 (an inhibitor of NF- κ B signaling pathway). We witnessed an almost identical effect by MMQO and SAHA when blocking the effect of PMA, a known and potent NF- κ B activator, affirming the rationale about MMQO's

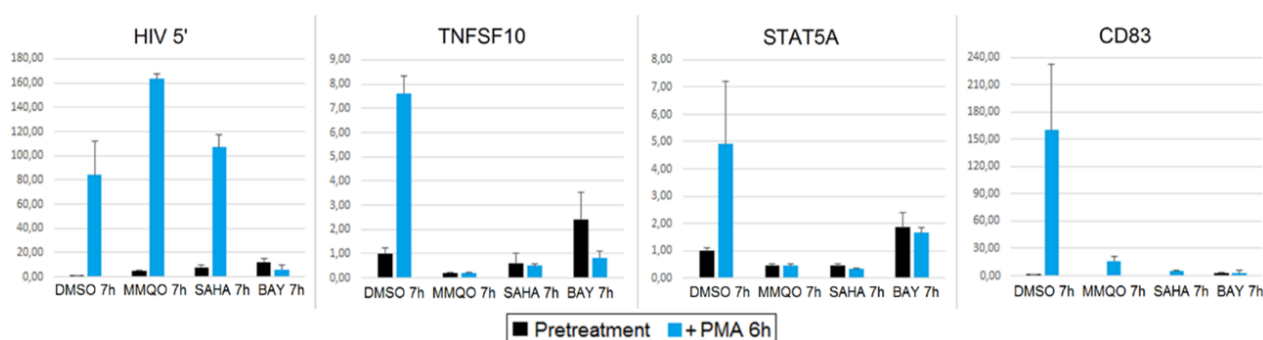


Figure 28: qPCR results depicting the effect of various drugs on NF- κ B target genes. E89 Jurkat clones were pretreated for 1h either with MMQO (160 μ M), SAHA (5 μ M), BAY-11-7085 (20 μ M) or equivalent volume of DMSO as vehicle. Subsequently the cells were treated for 6h with PMA (10nM). *GAPDH* was measured for normalization and results are represented relative to results from the DMSO treated cells. The genes were chosen based on the list of targets genes predicted by IPA. The means and S.D. values (error bars) are shown from a representative experiment measured in duplicate.

molecular mechanism as an HDAC inhibitor (Figure 28). In addition to blocking the target genes of PMA in the E89 Jurkat clones, like *TNFSF10*, *STAT5A* and *CD83*, we expectedly also witnessed a synergistic activation of the provirus by SAHA and MMQO.

The similarities between the HDAC inhibitors and MMQO can also be observed via flow cytometry. As opposed to the potent induction to PMA, MMQO and SAHA only cause a minute increase in the fraction of GFP-positive cells and their fluorescence intensity (Figure 29A). Moreover, in combination with each other the effects of both SAHA and MMQO largely overlap in terms of number of GFP-positive cells induced (Figure 29B). This further confirms the concept that both of the compounds are only able to loosen the chromatin around the LTR, rather than causing direct activation on the minigenome. This overlapping result was also obtained with TSA, another pan HDAC inhibitor (Figure 29C).

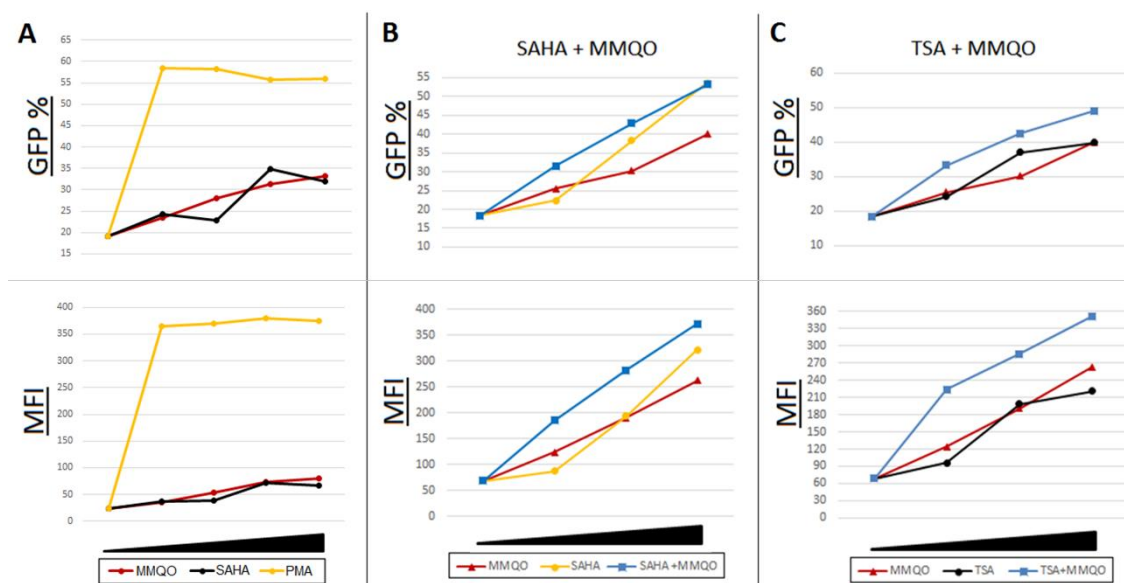


Figure 29: Dose dependent GFP expression profilers of MMQO, SAHA, TSA and PMA in flow cytometry. Latent heterogeneously infected Jurkat population containing the minigenome were treated with various doses of MMQO (80-320 μ M), TSA (20-200nM), SAHA (0,5-5 μ M), PMA (2-10nM) or left untreated for 24h. Cells were analyzed by forward scatter (FSC) and side scatter (SSC), by the GFP expressing percentage among the viable sample and their GFP expression intensity (MFI, depicted in arbitrary units). The inclining triangle in bottom indicates the intensity of the treatment. (A) Cells were treated separately. (B) MMQO and SAHA treatments were done alone or in combination with each other (C) MMQO and TSA treatments were done alone or in combination with each other.

Since MMQO generally starts to exhibit its positive effect on the viral promoter after three hours by mRNA detection methods, it was logical to also compare the gene expression of other MMQO target genes in response to HDAC inhibitors in that timeframe. In terms of target gene kinetics, HDAC inhibitors and MMQO again present considerable similarities. The main target genes of MMQO, such as *CXCR3*, *CD28*, *MYC* and *TUBB3* show almost

identical expression levels after both three hour and eight hour treatments by TSA or MMQO (Figure 30A). Nevertheless, there were considerable differences as well, such as the expression patterns of *IL7R*, *FOS*, *RAG1*, to name a few. These differences suggest that probably MMQO presents alternative mechanisms or that TSA and MMQO do not share the same class of protein targets.

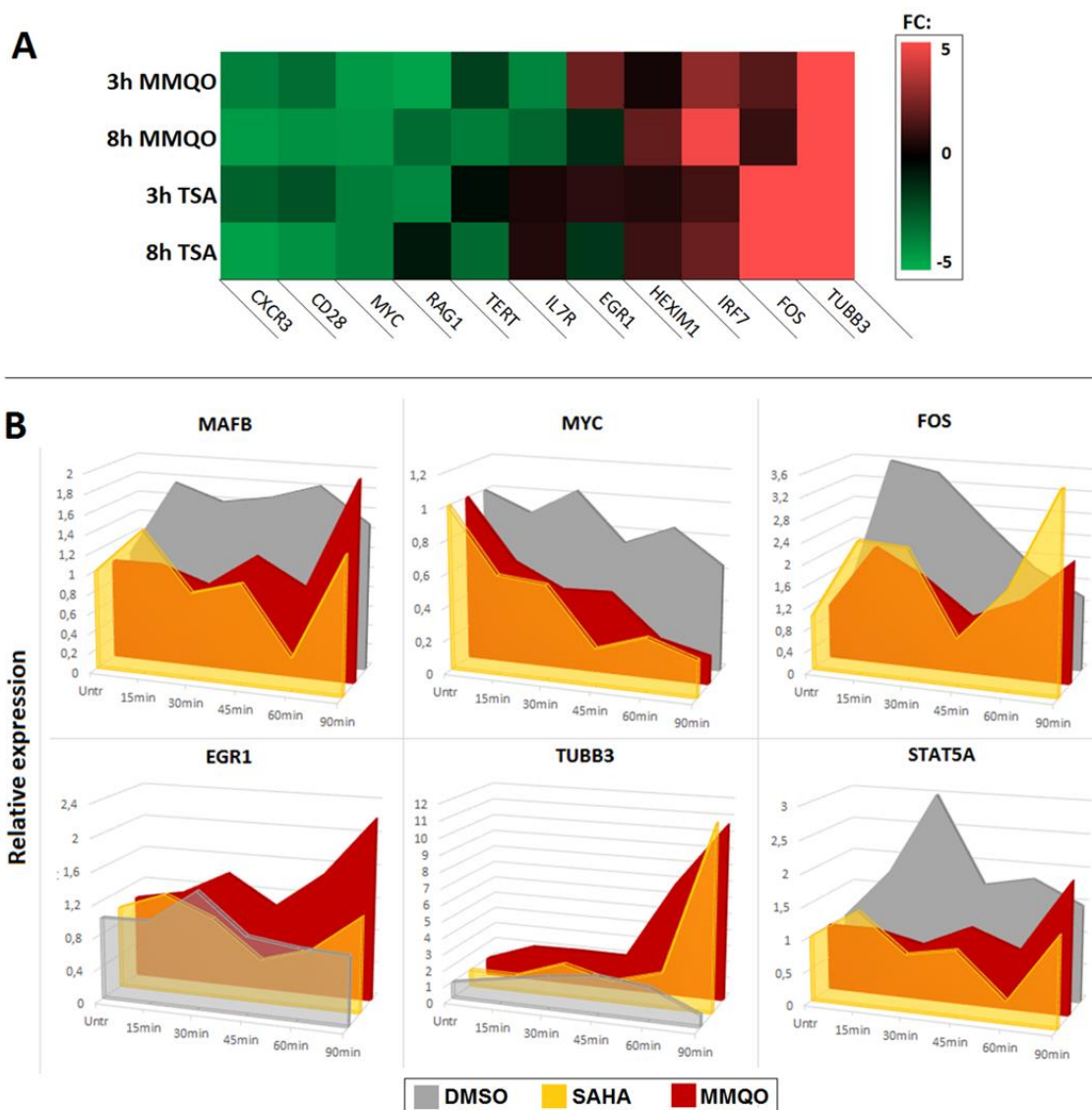
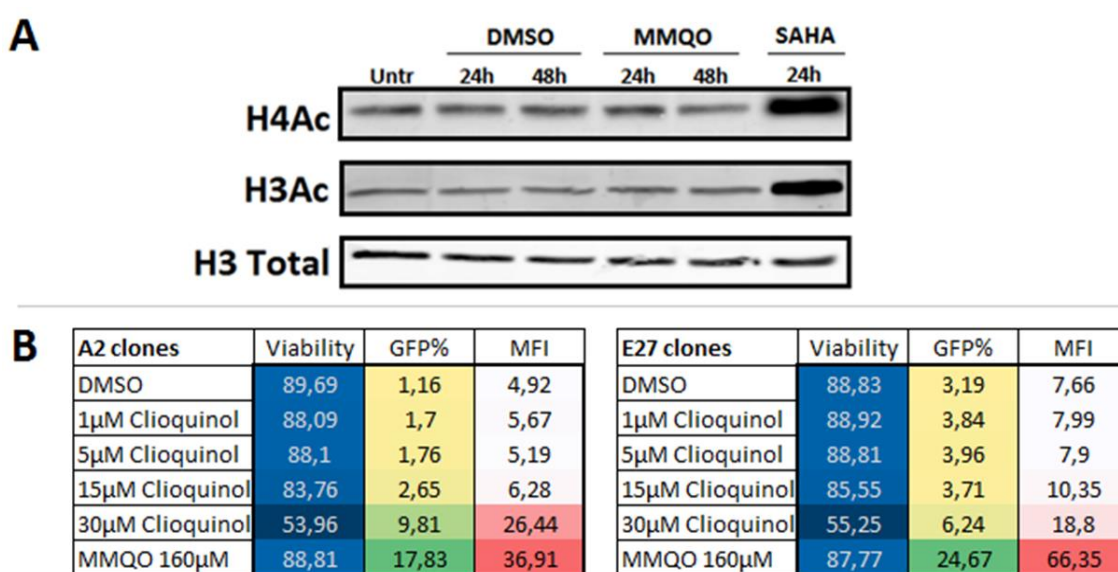


Figure 30: qPCR results the kinetics of MMQO target genes in response to HDAC inhibitors. (A) Jurkat cells were treated for either 3h or 8h with MMQO (160 μ M), TSA (200nM) or left untreated. *GAPDH* was measured for normalization and results are represented relative to results from the untreated cells. Heat map results were measured in duplicate and only genes that had reliable S.D. values are depicted in the figure. (B) Jurkat cells were treated for with MMQO (160 μ M), SAHA (5 μ M) or equivalent volume of DMSO during listed time points. *GAPDH* was measured for normalization and results were measured in duplicate.

The regulation of early response genes like *MYC* and *FOS* are known to depend delicately on the chromatin architecture and any tampering with the balanced transcriptional state leads to rapid dysregulation of these target genes (Fowler et al. 2011). Kinetic analysis with SAHA and MMQO on six different early response genes again confirm how MMQO treatment and SAHA induced hyperacetylation result in comparable regulation patterns (Figure 30B).

Though HDAC inhibitors and MMQO share considerable similarities in terms on gene expression kinetics and in their ability to regulate the activity of NF- κ B, other impermissible differences counter charge MMQO's role as an HDAC targeting compound. Notably we were not able to observe any changes in global core histone acetylation by MMQO, while SAHA treated Jurkat cells exhibited potent total H3 and H4 acetylation in whole cell extracts (Figure 31A). This observation was re-confirmed various times and in different cell lines. In addition to failing to observe the principal hallmark of histone deacetylase inhibition by MMQO, we neither witnessed any effect of clioquinol alone on the A2 and E27 clones, nor in combination with MMQO (Figure 31B-C). Clioquinol was previously described to inhibit both class I and II HDACs, and induce apoptosis in leukemia cell lines (Cao et al. 2013). Due to its minimal structure and functional similarities to MMQO, we initially used it as a model compound to build up the hypothesis for HDAC inhibition. Subsequent *in silico* molecular docking on HDAC1 and HDAC2 further proved our suspicions – MMQO wasn't able to enter the tight active pocket of different HDAC proteins, while SAHA as a positive control was able to dock as previously described (data not shown).



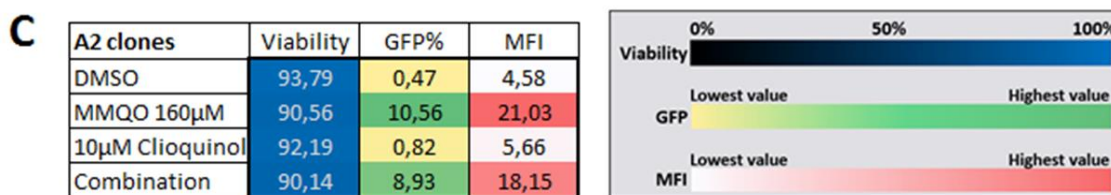


Figure 31: MMQO does not cause global hyperacetylation. (A) Jurkat cells were incubated for 24 or 48 hours with MMQO (160µM), SAHA (5µM), equivalent volume of DMSO or left untreated. Total protein was extracted with RIPA buffer and analyzed by immunoblotting against acetylated histone H4 or H3 or total H3 as a loading control. (B) Flow cytometry results of MMQO and clioquinol at different doses on two different GFP-expressing latent Jurkat clones. (C) A2 clones with MMQO and clioquinol combinations. Cells were analyzed by forward scatter (FSC) and side scatter (SSC), by the GFP expressing percentage among the viable sample and their GFP expression intensity (MFI, depicted in arbitrary units). The color code in bottom indicates the intensity of the value within the datasets.

The differences on the kinetics of MMQO target genes by TSA presented in Figure 30A could hypothetically be caused by distinct specificities towards different family members of HDAC proteins. Nevertheless, the lack of hyperacetylation in response to MMQO is an irrefutable argument against the compound functioning as an HDAC inhibitor directly. This observation was further substantiated by the shortcomings of the proposed hypothesis based on clioquinol. Though MMQO presents considerable similarities with HDAC inhibitors like SAHA and TSA, we're forced to conclude that it is not an HDAC inhibitor.

However, both HDAC inhibitors and MMQO still present considerable similarities – in the microarray MMQO targeted known acetylation sensitive genes, both MMQO and SAHA presented potent immunosuppressive traits and in combination MMQO and HDAC inhibitors exhibit less than additive effects on the viral promoter.

2.2 Comparing MMQO and TSA transcriptomes

Taking into account the likeness of the two classes of compounds, we decided to further investigate the differences between them. Considering that we already have extensively examined MMQO by RNA expression microarrays, it made sense to carry out similar analysis where we compare effects on transcriptome by TSA to MMQO. We decided to decrease the treatment time only three hours this time around, since it's the time point when the HIV-1 based minigenome usually begins to respond to MMQO. Furthermore, we previously already demonstrated how at a three hour treatment we were able to discriminate between similarities and differences of MMQO target gene expression by TSA (Figure 30A). Most

importantly, the short treatment time should restrict the side effects and minimize transcriptional background noise from factors like cMyc. For increased statistical significance we included three untreated Jurkat samples, three MMQO treated samples (160 μ M) and two TSA treated samples (200nM). The positive correlations between the individual probes were confirmed by the high overlap between the associated samples (Figure 32A). The correlation between the TSA and MMQO datasets was $R=0,695$, confirming the previous notion of HDAC inhibitors having a different target than MMQO, yet still being able to affect the transcriptome to a similar level (Figure 32B).

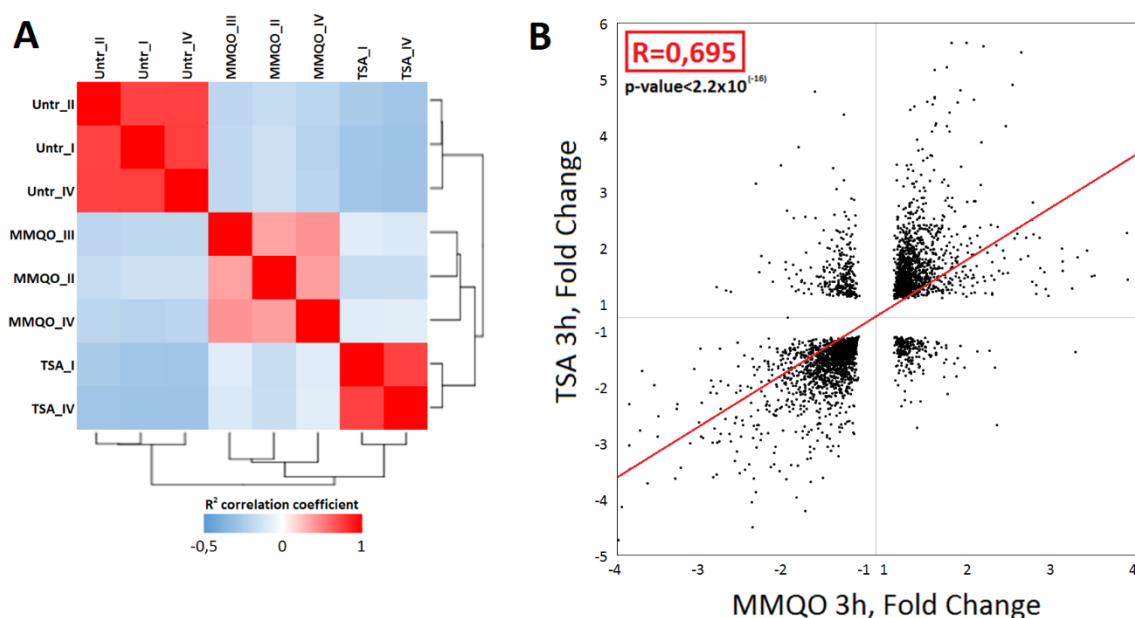


Figure 32: Correlations between MMQO and TSA treatments from RNA expression microarrays (A) Heat map depicting R^2 correlation (or is it just regular Pearson/R correlation?) for the triplicate and duplicate microarray samples from Jurkat cells treated 3h with MMQO (160 μ M), TSA (200nM) or left untreated. Expression data were obtained by hybridization with an Agilent Human microarray platform. (B) Scatterplot of fold changes for the 3376 significant genes ($q < 0,05$) from the TSA and MMQO 3h datasets. Calculations for the correlation matrix and scatterplot were performed by Andrea Izquierdo-Bouldstridge.

Most of the MMQO regulated genes are also regulated by TSA, but only a minority of TSA regulated genes are dependent on MMQO. In total 892 genes were differentially regulated by MMQO, while TSA treatment affected 1594 genes (FC cutoff $\pm 1,5$). The overlaps between those two datasets are depicted in the Venn diagrams, with up- and downregulated genes depicted separately (Figure 33A-C). In accordance with the previous microarray, qPCR and western blot results, we witnessed the same target genes of MMQO being dysregulated.

Among the most upregulated genes were again *IRF7*, *TUBB3* and *HEXIM1*, while the most severely downregulated genes included *CXCR3*, *MYC*, *CXCR7* and *RAG1*, to name a few.

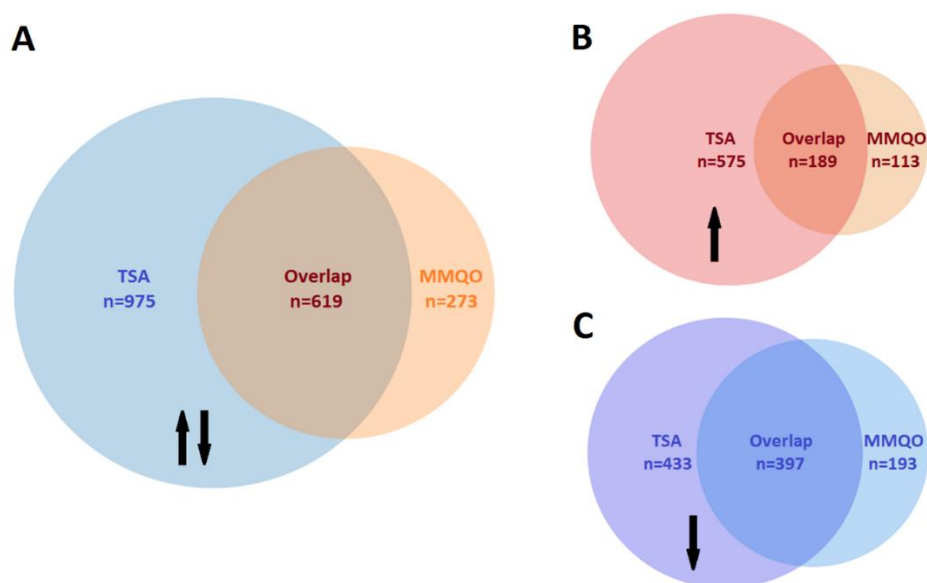


Figure 33: Genes differentially regulated by MMQO and TSA Jurkat cells. (A) Venn diagram of statistically significant ($q < 0,05$) differential expression of genes that are up- or downregulated with a 1,5x fold change (or greater) when Jurkat cells are treated with MMQO or TSA. (B) Venn diagram of genes mutually upregulated by MMQO or TSA (C) Venn diagram of genes mutually downregulated by MMQO or TSA. Circles in the figure are depicted proportional in size to each other.

An in depth GSEA analysis revealed that TSA treated cells correlated positively with 394 datasets, with five most significant datasets being directly linked to the functions of HDACs. This proves that the microarrays were carried out correctly and that GSEA is an efficient tool to analyze the acquired data, but it also further demonstrates the broad effect an HDAC inhibitor can have already after three hours.

To our surprise GSEA analysis revealed no significant positively correlating enrichments with the three hour MMQO treatment, while previously after eight hour stimulation we witnessed the presence of 198 gene sets. This further confirms the peculiar character of MMQO and its independence from typical activating pathways or canonic pan-HDAC inhibition. GSEA did reconfirm the repressive traits of MMQO – 28 pathway related gene sets were downregulated, most of them again related to immune pathways, HDAC functioning and cancer viability, thus showing no functional difference from HDAC inhibitor treatment. Among the negatively correlating transcription factor motifs we witnessed the enrichment of numerous transcription factors sites, but none presented a normalized

enrichment score below -2 and were not considered reliable enough. It still should be noted that these gene sets included the motifs also for NF- κ B and cMyc.

2.3 Analysis of MMQO specific genes

From the 892 differentially expressed genes by MMQO, 306 genes were not affected by the TSA treatment – 113 of those were upregulated, while 193 were downregulated. GO analysis of those genes did not support any pathway enrichment among the up- or downregulated gene sets (data not shown). We did witness an enrichment of GC-rich motifs among the downregulated genes, which included binding sites for the AP-2 and Sp transcription factor families (Table 9). Both the AP- and Sp-family proteins play a significant role in HIV-1 expression and have been shown directly to interact in a dualistic repressive and activating manner with the promoter (Perkins et al. 1994, Jiang et al. 2007).

NAME	term ID	p-value	Q&T/Q	Q&T/T
AP-2α; motif: NSCCNCRGGSN	TF:M07348	<0,0001	0,694	0,011
ZIC1; motif: VGGGGAGS	TF:M07344	<0,0001	0,689	0,011
E2F-3; motif: GGCGGGN	TF:M02089	0,0001	0,732	0,011
AP-2γ; motif: GCCYNNGGG	TF:M00470	0,0001	0,579	0,012
AP-2γ; motif: GCCYNCRGSN	TF:M03811	0,0005	0,683	0,011
AP-2α; motif: NGCCYSNNGSN	TF:M01857	0,0007	0,732	0,01
Spz1; motif: DNNGGRGGGWNNNN	TF:M00446	0,0013	0,913	0,009
Sp1; motif: GGGGCGGGGT	TF:M00008	0,0013	0,71	0,01
MAZ; motif: GGGGAGGG	TF:M00649	0,0014	0,552	0,011
AP-2β; motif: GCN NNGGSCNGVGGGN	TF:M01858	0,0015	0,579	0,011
Sp1; motif: NNGGGCGGGGNN	TF:M00932	0,0018	0,798	0,01
CKROX; motif: SCCCTCCCC	TF:M01175	0,0031	0,399	0,013
Sp6; motif: WGGGCGG	TF:M05361	0,0103	0,678	0,01
CPBP; motif: NGGGCGG	TF:M05444	0,0103	0,678	0,01
Sp2; motif: WGGGCGG	TF:M05332	0,0103	0,678	0,01
Kaiso; motif: GCMGGGRGCRGS	TF:M03876	0,0126	0,721	0,01
AP-2α; motif: GCCNNNRGS	TF:M00469	0,0189	0,339	0,013
GKLF; motif: NNRRGRRNGNSNNN	TF:M07040	0,0210	0,852	0,009
Sp1; motif: NGGGGCGGGGN	TF:M07395	0,0233	0,776	0,01

Table 9: Enrichment of TRANSFAC datasets among the genes specifically downregulated by MMQO. Q = number of query genes. T = number of term genes. Q&T/Q denotes how many percent from the 193 uniquely MMQO downregulated genes belong to this gene set (FC<-1,5). Q&T/T denotes how many percent do the MMQO regulated genes overlap with the full dataset. Sp and AP-2 transcription family members are highlighted in bold. Analysis performed with the g:profiler toolkit.

Nevertheless, it is possible that the divergence of the TRANSFAC transcription factor analysis results is a consequence of similar and/or overlapping nucleotide sequences, with which the computational algorithms are forced to present false-positive results. It is also important to note that most mammalian promoters are known to contain GC-rich areas or CpG islands, as can be witnessed by the fact that the Sp1 and AP-2 specific motifs are highly abundant in thousands of promoters (Sharif et al. 2010, Fenouil et al. 2012).

Due to the lack of conclusive results from the GO, KEGG, TRANSFAC and GSEA analysis we were forced to concentrate individually on the 306 differently regulated genes by MMQO. We prioritized the search by the prominence of certain genes based on their effect on immune function (*CX3CR1*, *CCR7*, *IL7R* etc.), HIV-1 pathogenesis, transcription and latency (*BRD2*, *BCL11A*, *BACH2* etc.), by their generally well described status in literature (*CD69*, *TLR3*, *IFIT1* etc.) and by their continuous differential regulation by MMQO in both of the microarrays (*LAT*, *ETS2*, *TMEM121* etc.). During the literature research we also acknowledged the previously established aspects of MMQO, such as *MYC* downregulation, functional similarities to HDAC inhibition in terms of effect on transcriptome, induction of apoptosis, decrease in proliferation and the potent immunosuppression. A thorough review of the existing literature based on our experimental data led us to believe that MMQO might function as a bromodomain inhibiting protein, specifically by targeting directly the protein Bromodomain-containing protein 4 (Brd4).

3. MMQO as a bromodomain inhibitor

3.1 Comparison between MMQO and the BET inhibitor JQ1 transcriptomes

Besides reactivating HIV transcription both Tat dependently and independently, downregulating cMyc and playing a role in proliferation and apoptosis, bromodomain inhibitors like JQ1 have also been described to mimic HDAC inhibitors in their function on the transcriptome of cells from lymphoma lineages (Bhadury et al. 2014). In addition to targeting a similar set of genes, BET family inhibitors also have been shown to cause severe immunosuppression by disabling NF- κ B's ability to locate gene enhancer regions through a

direct interaction with Lys-310 of the RelA subunit (Nicodeme et al. 2010, Belkina et al. 2013, Brown et al. 2014, Huang et al. 2008).

In terms of specific MMQO target genes, bromodomain inhibitors have also been shown to target specifically *IL4R* and *IL7R* (Ott et al. 2012), *ADM* (Mazur et al. 2015), *APOE* (Bailey et al. 2010), *TLR3* and *CD69* (Nicodeme et al. 2010). Data mining of the datasets from EMBL-EBI Expression Atlas consortium confirms a similarity between the target genes of MMQO and JQ1. From the 125 genes that were specifically differentially regulated by MMQO after the three and eight hour therapies, 58 were also considered to be target genes of JQ1 (Table 10).

Gene	FC log2	Gene	FC log2	Gene	FC log2	Gene	FC log2	Gene	FC log2	Gene	FC log2
<i>SRC</i>	3,1	<i>CCR7</i>	1,4	<i>USP11</i>	1,1	<i>GRIN2D</i>	-1,0	<i>TMEM121</i>	-1,2	<i>KCNH2</i>	-1,9
<i>CREM</i>	2,7	<i>MGEA5</i>	1,3	<i>DNAJB6</i>	1,0	<i>NPRL3</i>	-1,0	<i>TNFSF10</i>	-1,3	<i>NPR3</i>	-2,0
<i>SQSTM1</i>	1,9	<i>CHML</i>	1,3	<i>ZC3H6</i>	1,0	<i>PNN</i>	-1,0	<i>GALNT6</i>	-1,3	<i>PSTPIP1</i>	-2,0
<i>DNAJB4</i>	1,7	<i>TAF12</i>	1,3	<i>ZBTB43</i>	-0,6	<i>IFIT1</i>	-1,0	<i>GNA15</i>	-1,3	<i>ZBTB1</i>	-2,2
<i>TMEM2</i>	1,7	<i>SIRT1</i>	1,2	<i>CTSC</i>	-0,6	<i>BACH2</i>	-1,1	<i>NOP16</i>	-1,3	<i>AIM1</i>	-2,3
<i>TRIB1</i>	1,7	<i>PMEPA1</i>	1,2	<i>ARL4C</i>	-0,6	<i>DHRS3</i>	-1,1	<i>TNFRSF25</i>	-1,4	<i>PTPRN2</i>	-2,3
<i>DCXR</i>	1,6	<i>KIF1B</i>	1,2	<i>EPB41L4B</i>	-0,6	<i>PARP8</i>	-1,1	<i>LGALS1</i>	-1,4	<i>KCNN4</i>	-2,3
<i>STOX1</i>	1,5	<i>MOB3A</i>	1,1	<i>AMPD3</i>	-0,6	<i>SLAMF6</i>	-1,1	<i>KBTD11</i>	-1,5	<i>IL7R</i>	-3,1
<i>ZMIZ1</i>	1,4	<i>RNF213</i>	1,1	<i>RIMS2</i>	-0,7	<i>TANK</i>	-1,1	<i>ATP10A</i>	-1,7		
<i>BRD2</i>	1,4	<i>SPG20</i>	1,1	<i>CMTM7</i>	-1,0	<i>PEX13</i>	-1,2	<i>SPRY1</i>	-1,7		

Table 10: List of genes mutually dysregulated by MMQO and JQ1 in the EMBL-EBI Expression Atlas arrays. The 15 JQ1 specific array datasets on EMBL-EBI were analyzed for the expression of the 125 MMQO specific genes. Listed are the genes that were only expressed in *Homo Sapiens* and had a fold change of ± 2 .

The JQ1 specific datasets made available by EMBL are mostly based on melanoma cell lines like OMM1 and C918, which bear little resemblance to the leukemic derived Jurkat cells used in our experiments. We therefore performed a more thorough analysis with data from a microarray (Affymetrix platform) performed with 24-hour JQ1 treated latent Jurkat population (Banerjee et al. 2012). Even though there was a considerable difference between the setups of the MMQO and JQ1 experiments (24h JQ1 vs 8h MMQO / Native Jurkat vs Tat-expressing J-Lat / Agilent vs Affymetrix platform), a significant overlap can be witnessed between the transcriptomes of both drugs (Figure 34A). The correlation $R=0,841$ acquired is higher than the comparison between TSA and MMQO ($R=0,695$) and resembles more the previously calculated correlation between the two different MMQO datasets ($R=0,860$).

Profiling of the transcriptomes by their fold changes further substantiates the similarities between the two drugs and opposes them against HDAC inhibition or proinflammatory α -

CD3 signaling. Following an 8 hour treatment by MMQO or 24 hour treatment by JQ1, Jurkat cells exhibit predominantly downregulatory effects on the transcriptome, while the 24 hour treatment with T cell receptor activating α -CD3 demonstrates a strong upregulation of the transcripts (Figure 34B).

The almost identical profiles of JQ1 and MMQO 8 hour treatment again confirm their similarity, since these curves are plotted independently of each other with different datasets. Similarly to α -CD3 treatment HDAC inhibition also displays more upregulation, which is also to be expected since histone deacetylation is commonly considered a repressive mark and the inhibition of HDACs is supposed to relieve that transcriptional repression. The outlying curve of the 3 hour MMQO treated cells show a constantly 40% upregulated genes, with no tendency towards any change. This could most probably be explained by the lack of negative effect MMQO has on cMyc dependent transcription at such short time. Indeed, HeLa cells that were treated for 8 hours displayed considerably more upregulated transcripts than downregulated, but neither the *MYC* gene nor the cMyc protein are affected by MMQO in HeLa cells (data not shown) and *MYC* has been described to be resistant to JQ1 treatment (Mertz et al. 2011, Fowler et al. 2014).

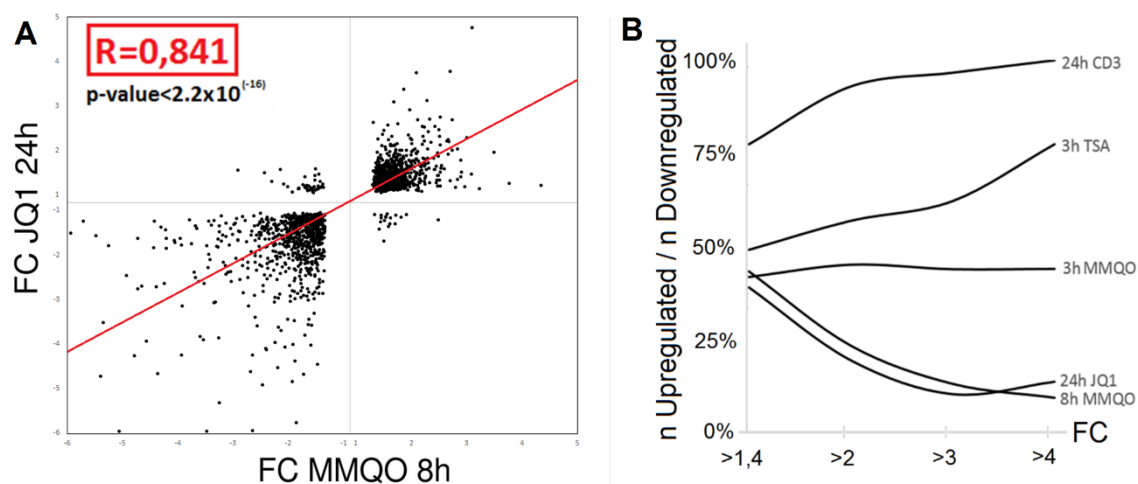


Figure 34: Correlation between MMQO and JQ1 treatments from RNA expression microarrays. (A) Scatterplot of fold changes for the 1774 significant genes ($q < 0,05$) from the JQ1 24h and MMQO 8h datasets. Calculations for the scatterplot were performed by Andrea Izquierdo-Bouldstridge. The JQ1 treated Jurkat cell based dataset was previously published by Banerjee et al. 2012. (B) Transcript expression profiles of TSA, MMQO, JQ1 and α -CD3 in Jurkat cells. The total number of transcripts significantly up- or downregulated by MMQO 3h ($n=2571$), MMQO 8h ($n=4160$), TSA 3h ($n=4851$), JQ1 24h ($n=2358$) and α -CD3 24h ($n=528$) were categorized into four groups based on their fold change compared to the untreated genes. The number of upregulated genes was divided by the number of downregulated genes in each expression group that is displayed in the percentage ratio.

3.2 Evidence of MMQO binding to Brd4

Brd4 inhibition as a mechanism provides potential for suppression of tumorigenesis and immunomodulatory clinical applications and since the discovery of the first Brd4 inhibitor in 2010 numerous different compounds besides JQ1 have been designed. The most successful compounds are based around the triazolodiazepine structure (such as JQ1, CPI-203, OTX-015, I-BET-762), but other scaffolds have been suggested as well (Vidler et al. 2013). Though quinoline structures have been the basis for Brd4 inhibition as well, none of the compounds have been developed to a final commercially available successful product (Chung et al. 2012).

BET family inhibitors function in a dualistic manner on the acetylated lysine binding sites of their target proteins – a reactive domain of the compound is responsible for interacting with an asparagine residue (such as the Asp-140 in Brd4 BD1 domain), while the exterior lipophilic WPF shelf (named after residues W81, P82 and F83, Nicodeme et al. 2010) is used as a stabilizing site to keep the compound lodged within the pocket. Based on *in silico* molecular docking we were able to confirm an efficient binding of MMQO into the first bromodomain pocket of the Brd4 protein, with a stable docking score of -6,402 (Figure 35A). This interaction is anchored by the previously mentioned Asp-140, which is further stabilized by the WPF cleft (Pro-82) and the inert methyl groups of MMQO face the outside of the pocket (Figure 35B). JQ1 interacted with the BD1 domain in our assays exactly as previously described, with a docking score of -6,41. Unlike previously with the different HDAC family members, additional *in silico* docking with other Brd4-BD1 crystal structures available on the Protein Data Bank always confirmed the validity of MMQO's specific docking. This structural prediction model affirms MMQO's role as a bromodomain inhibitor, since it demonstrates how MMQO is capable of presenting the dualistic function previously described necessary for a BET inhibitor (BETi) (Figure 35C).

Following the promising results based on the microarray and computational techniques, the *in vitro* binding of MMQO to the BD1 pocket was confirmed by nuclear magnetic resonance (NMR). As shown in two-dimensional ^1H - ^{15}N -heteronuclear single quantum coherence (HSQC) spectra, the first bromodomain of Brd4 (Brd4-BD1) exhibited similar chemical shift perturbations upon binding to both MMQO and MS417, an inhibitor designed specifically

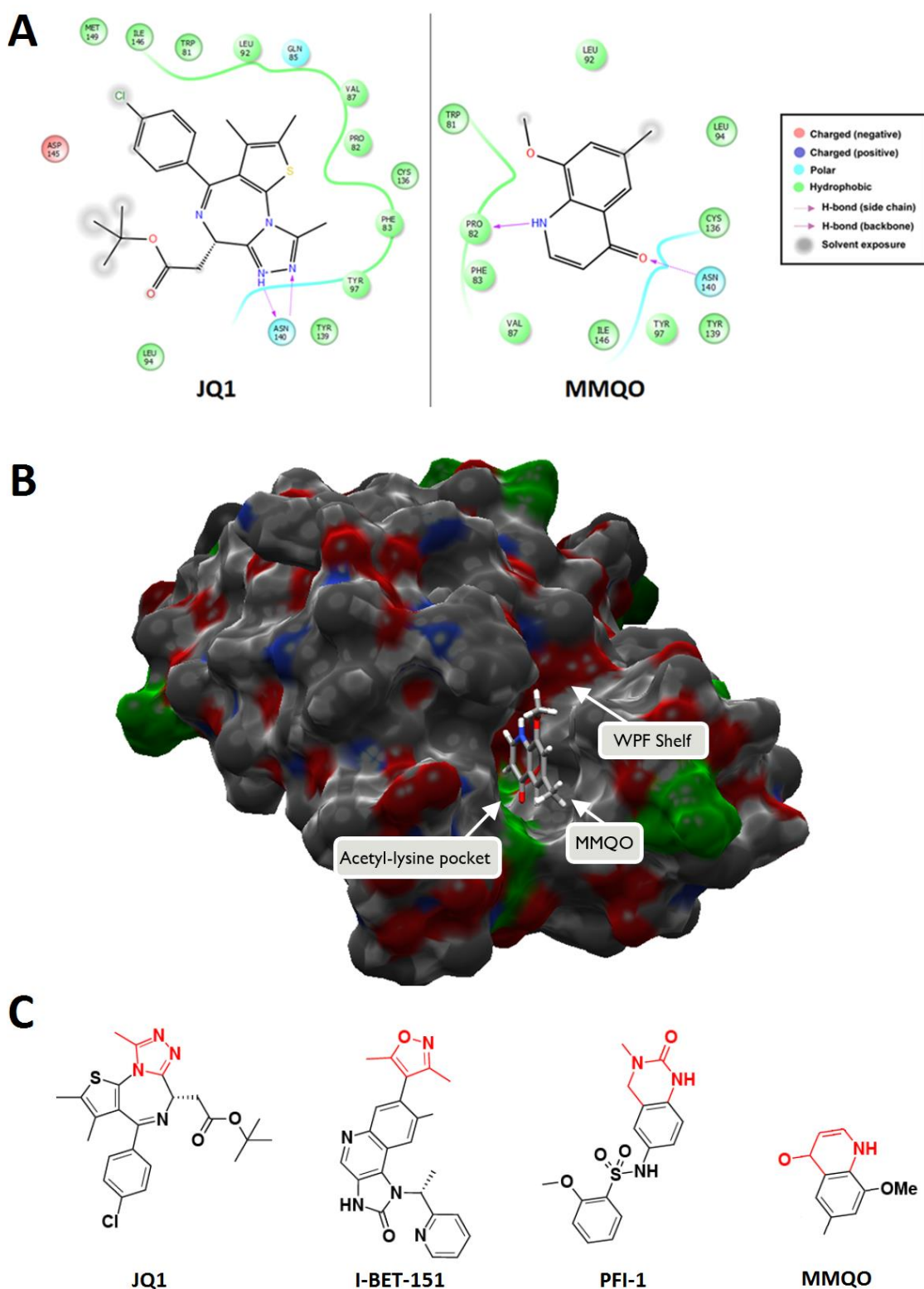


Figure 35: *In silico* docking models of JQ1 and MMQO in the Brd4-BD1. (A) MMQO was docked in the Brd4-BD1 domain (right). JQ1 was docked as control (left). PDB code: 3MXF. Illustration created by Salvador Guardiola, IRB. (B) Surface-filled representation of the same docking. Asparagine residues are marked in green, positively charged features are in red, negatively charged features are in blue and gray areas designate neutral charges. (C) Illustration depicting three commercially available bromodomain inhibitors and MMQO. Red area designates the active Asn-140 interacting KAc mimetic site, while black region corresponds for the core region responsible for stabilization of the drug.

against the bromodomains of Brd4 (Zhang et al. 2012) (Figure 36A-B). The NMR assay was carried out by Dr. Ming-Ming Zhou's group in Mount Sinai School of Medicine, United States of America. Thus far this is the first setting where MMQO has been found to interact directly with a protein.

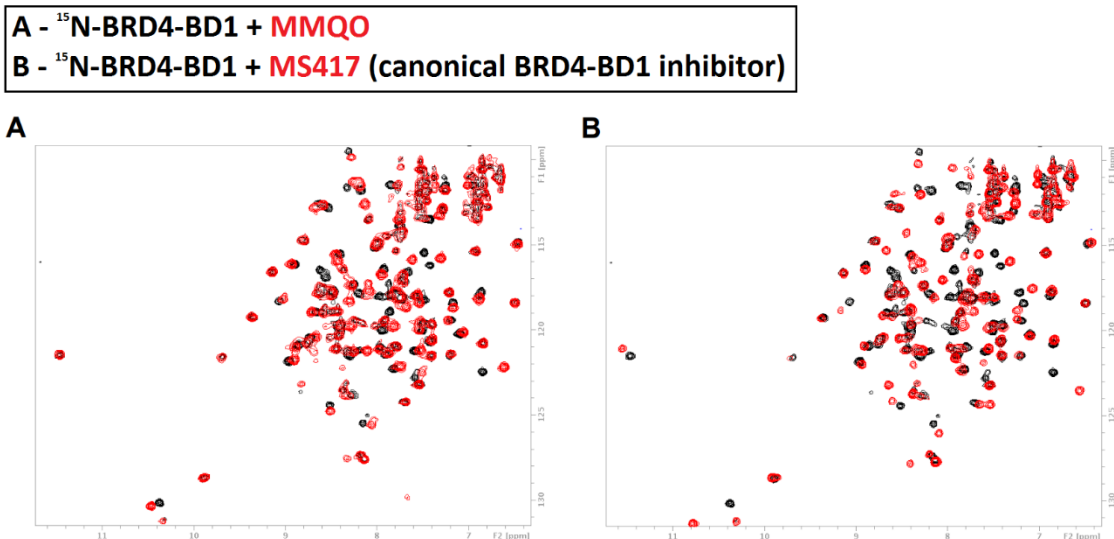


Figure 36: Binding of MMQO and MS-417 to the BD1 domain of Brd4 as evaluated by NMR. Superposition of 2D ^1H - ^{15}N HSQC spectra of human Brd4-BD1 in the free form (black signals) and in the presence of MMQO (A) or MS-417, a previously described Brd4 inhibitor as a positive control (B). The protein concentration was 0,1mM and the molar concentration of MMQO was 0,5mM. Experiments carried out by the laboratory of Ming-Ming Zhou in Mount Sinai School of Medicine, New York, United States of America.

3.3 Comparison of MMQO and JQ1 experimentally

To validate the *in silico*, microarray and NMR results we had to prove MMQO's functionality also in our cellular models. To that end we first decided to examine how bromodomain inhibitors such as JQ1 function on MMQO's target genes, like the HIV-1 minigenome and *MYC*, and if they present similar characteristics to MMQO.

Based on the microarray data, we chose strongly up- and downregulated genes by MMQO as controls. In particular, we were interested in the effect of both drugs on genes that can be considered MMQO specific (*ZBTB1*, *CCR7*) or generally acetylation and bromodomain inhibition sensitive (*MYC*, *IRF7*, *RAG1*, *CXCR7*). Confirming the previous microarray results, we saw a strong upregulation of *IRF7*, *HEXIM1*, *ZBTB1* and *CCR7* and a marked downregulation of *MYC*, *RAG1* and *CXCR7* by MMQO. As expected, the same genes that were dysregulated by MMQO, were similarly regulated by JQ1. The effect of the drugs is

almost identical for both of them (Figure 37A). This long treatment also serves as a proof of the long lasting effect of both drugs, since the genes like *CCR7* and *ZBTB1* can be considered to be highly specific target genes of Brd4 inhibition in these cells. In parallel we also wanted to confirm that the effect of both drugs translates to protein level in Jurkat cells. We performed a Western blot testing two different proteins, cMyc and Bcl-2. It has been shown that both of these proteins are established Brd4-dependent targets and that treatment with JQ1 markedly reduced their protein expression, inducing growth arrest and apoptosis in different cell types (Wyce et al. 2013, Knoechel et al. 2014). We performed a total protein extraction from Jurkat cells treated two to five days with MMQO or JQ1 and confirmed that MMQO is persistently able to downregulate cMyc also at protein level, throughout the extensive treatment. Similarly to cMyc we also observed a time-dependent down regulation of Bcl-2, albeit at lower levels than with the JQ1 treatment (Figure 37B).

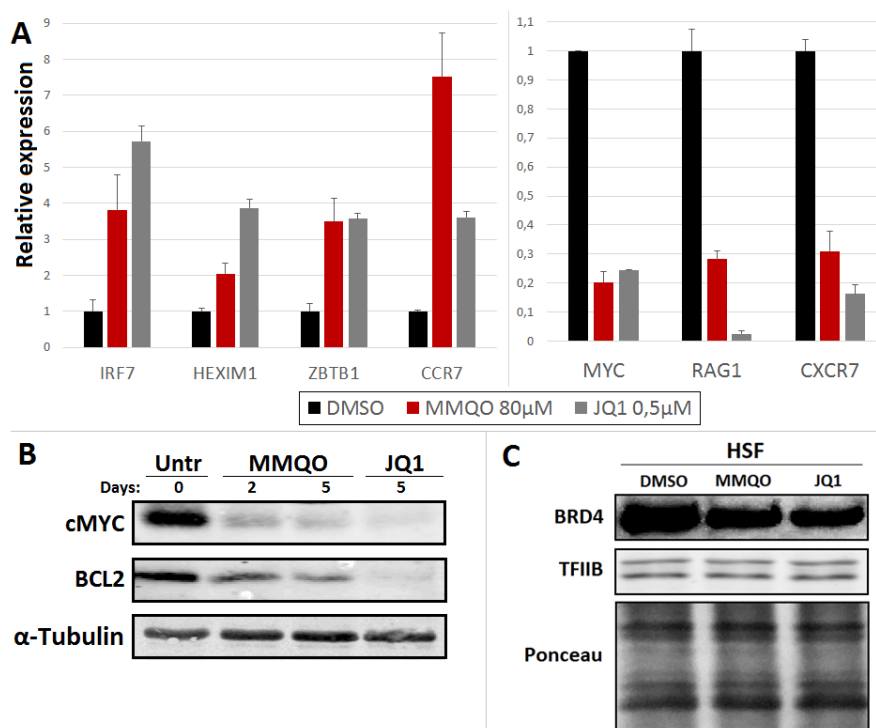


Figure 37: qPCR and immunoblot results depicting long term effects of MMQO or JQ1 on MMQO target genes and Brd4. (A) Uninfected Jurkat cells were treated for 5 days either with MMQO (80µM), JQ1 (0,5µM) or equivalent volume of DMSO as vehicle. *GAPDH* was measured for normalization and results are represented relative to results from the DMSO treated cells. Genes were chosen by their specificity to MMQO in the microarrays. Means and S.D. values (error bars) are shown from a representative experiment measured in duplicate. (B) Cells were incubated 2 to 5 days with MMQO (80µM), JQ1 (0,5µM) MMQO or left untreated. Total protein was extracted with RIPA buffer and immunoblotted against total cMyc, Bcl-2 or α-Tubulin as a loading control. (C) High salt nuclear fractionation from HeLa cells treated with MMQO (160µM), JQ1 (1µM) or equivalent volume of DMSO for 8h. High salt fraction protein was immunoblotted against total Brd4. TFIIB detection was included as a control to ensure that the high salt wash was performed at an even level in all the samples and a Ponceau staining image is included as a loading control.

To measure the effect MMQO might have on nuclear Brd4 protein, we performed a nucleoplasm extraction, from where the chromatin was extracted, followed by a high salt wash on the chromatin. The first step was performed to remove all the free protein from the nucleus so we could concentrate the immunoblotting to the chromatin-bound material itself. As expected, following the high salt treatment, we witnessed that less Brd4 was released from the chromatin following MMQO or JQ1 treatment than from the negative control sample, indicating that there was less Brd4 bound to chromatin following the treatments with either of the drugs (Figure 37C).

As anticipated, the effect of JQ1 on the minigenome was similar to MMQO and in combination the two different drugs completely overlapped in their effect (Figure 38). This observation was made in both Tat-positive and Tat-deficient Jurkat cells. As previously, JQ1 did present a more potent signal on the target gene. Altogether, this data strongly suggests that the two mechanisms are probably overlapping in their effect on the latent minigenome.

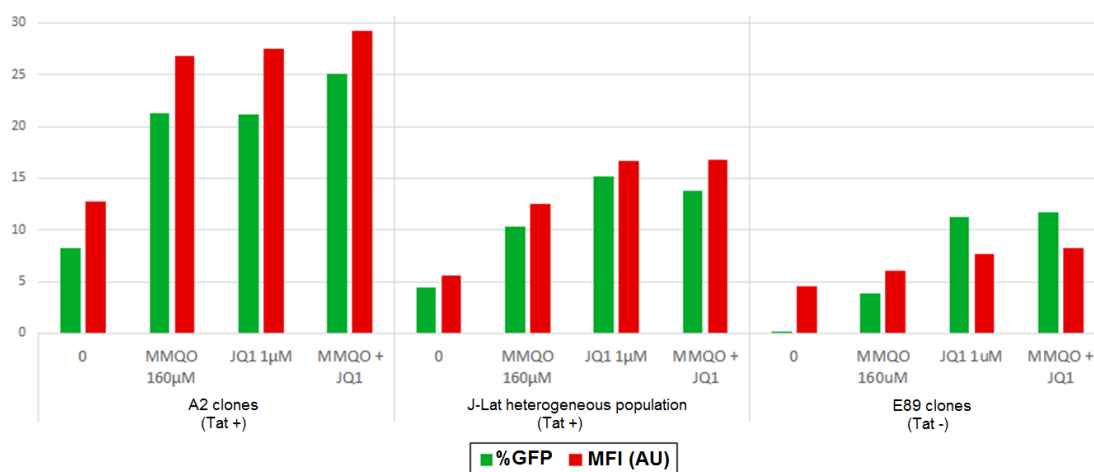


Figure 38: MMQO and JQ1 treatments overlap in their effect on the HIV-1 minigenome by flow cytometry. Listed infected latent Jurkat cells were treated with MMQO (160μM), JQ1 (1μM), their combination or left untreated for 24h and the cells were analyzed by forward scatter (FSC) and side scatter (SSC), by the GFP expressing percentage among the viable sample and their GFP expression intensity (MFI, depicted in arbitrary units).

In order to further characterize the effect both drugs have on the viral transcription reactivation, we explored their response in combination with other known viral reactivators - PMA as a direct activating NF-κB inducer, or SAHA (HDAC inhibitor) and HMBA (Akt pathway activator, Contreras et al. 2007) as compounds that prime the HIV-1 for

reactivation. Similarly to earlier results, MMQO and JQ1 behaved almost identically. In combination with the enhancers HMBA and SAHA both of the drugs functioned in an additive manner, while with PMA we witnessed a substantial synergy (Figure 39). In all the cases the percentages of GFP-expressing cells and their fluorescence intensities were analogous. These results further substantiate the similarities between the two compounds.

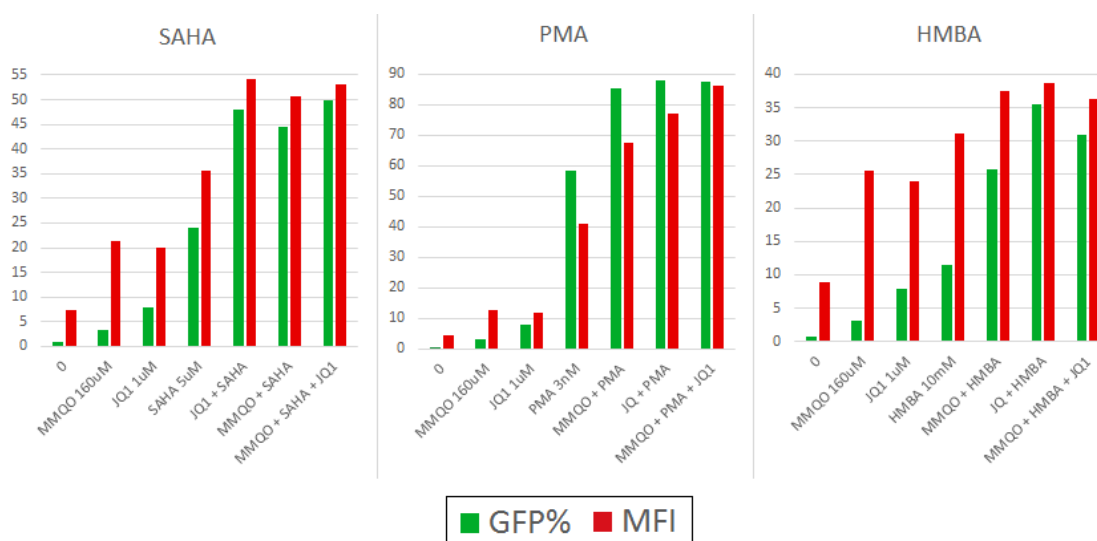


Figure 39: MMQO and JQ1 treatments in combination with other viral reactivators by flow cytometry. Latent A2 Jurkat clones were treated with MMQO (160µM), JQ1 (1µM), left untreated or treated in combination with the listed drug for 24h and the cells were analyzed by forward scatter (FSC) and side scatter (SSC), by the GFP expressing percentage among the viable sample and their GFP expression intensity (MFI, depicted in arbitrary units).

To quantitate the interaction between JQ1 and MMQO, we compared the experimentally obtained expression to the effects predicted under the Bliss independence model for combined drug effects. This model assumes that the stimulants act through different mechanisms, so that their effects multiply when administered in combination. A drug combination whose effect significantly exceeds that predicted by the Bliss model can be said to exhibit synergy. We reconfirmed that JQ1 and MMQO combinations did not exhibit synergy, but rather conformed to the predictions of the Bliss independence model (Figure 40). Though a synergy was apparent at the lowest doses, it is to be expected since JQ1 is known to inhibit also the second bromodomain of Brd4 (Brd4-BD2) and the BET family (Deeney et al. 2016). If the drug can target multiple sites simultaneously, even if on the same protein, then according the Bliss model it can be considered to have different mechanisms.

Nevertheless, at higher doses this synergy dissipates, suggesting that the effect on the latent minigenome can easily be saturated and the alternative BET inhibitory mechanisms are overwhelmed. It is important to note that this experiment was carried out in latently infected Tat-negative minigenome, to avoid any additional transcriptional interference from the catalytic Tat protein. An alternative explanation for the synergy at low doses could be that MMQO is affecting those same sites and causing unspecific signals.

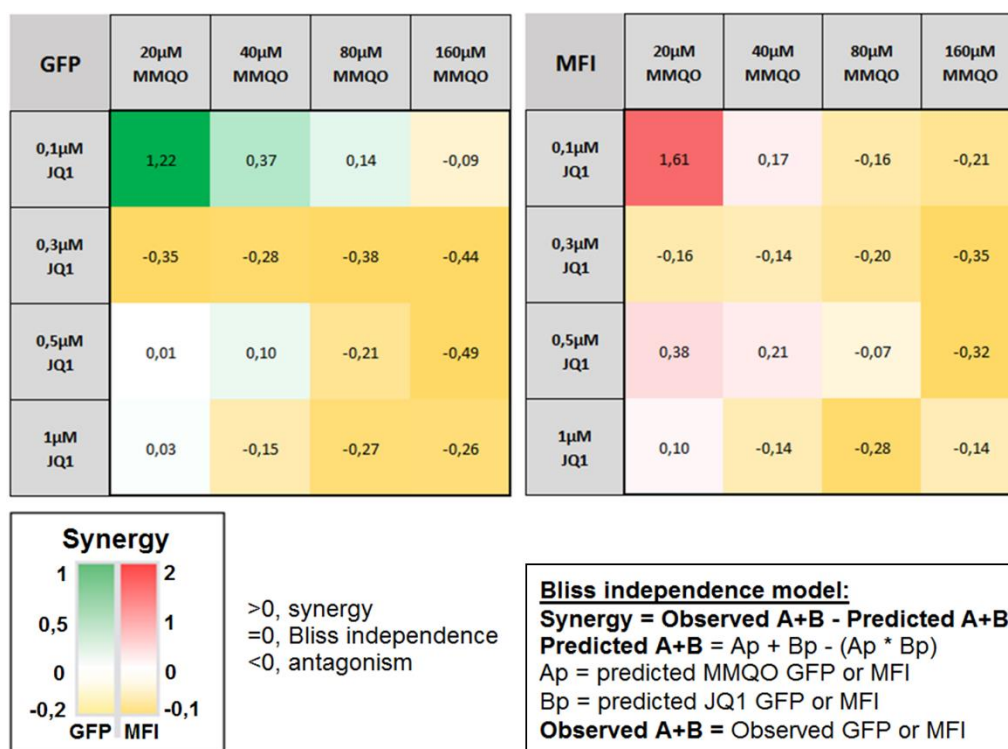


Figure 40: MMQO and JQ1 do not present synergy according to the Bliss independence model. Infected latent Tat-deficient HeLa cells were treated with varying doses of MMQO (20-160µM), JQ1 (0,1-1µM), their combination or left untreated for 24h and the cells were analyzed by forward scatter (FSC) and side scatter (SSC), by the GFP expressing percentage among the viable sample and their GFP expression intensity (MFI, depicted in arbitrary units). Calculation of synergy for the combinations using the Bliss independence model. Data are presented in a heat map model as the difference between the observed and predicted fractional response relative to a single PMA (10nM) treatment.

3.4 BETi function in response to Brd4 knockdown

Considering the possible unspecific targeting by the two compounds, we decided to knock down the expression of both Brd4 and Brd2 proteins by short hairpin RNA (shRNA), the two BET proteins that have been shown to affect HIV-1 latency. Unfortunately both Jurkat and HeLa cells went into cell cycle arrest following the successful infection, so setting up double

knockdown cells proved to be impossible and acquiring reliable results from MMQO response experiments became challenging. Nevertheless, we were able to confirm the previously published results of Boehm et al. 2012, where the authors demonstrated that the knockdown of Brd4 alone might not be sufficient to release HIV-1 from transcriptional latency. In response to knockdown of Brd4, but not Brd2, we witnessed an increase of the basal state of the viral expression and an enhanced response to MMQO, JQ1 or PMA (Figure 41). Considering the limitations of this method and the previously published fragmentary results, we decided to continue utilizing more direct methods in order to prove that MMQO specifically targets Brd4.

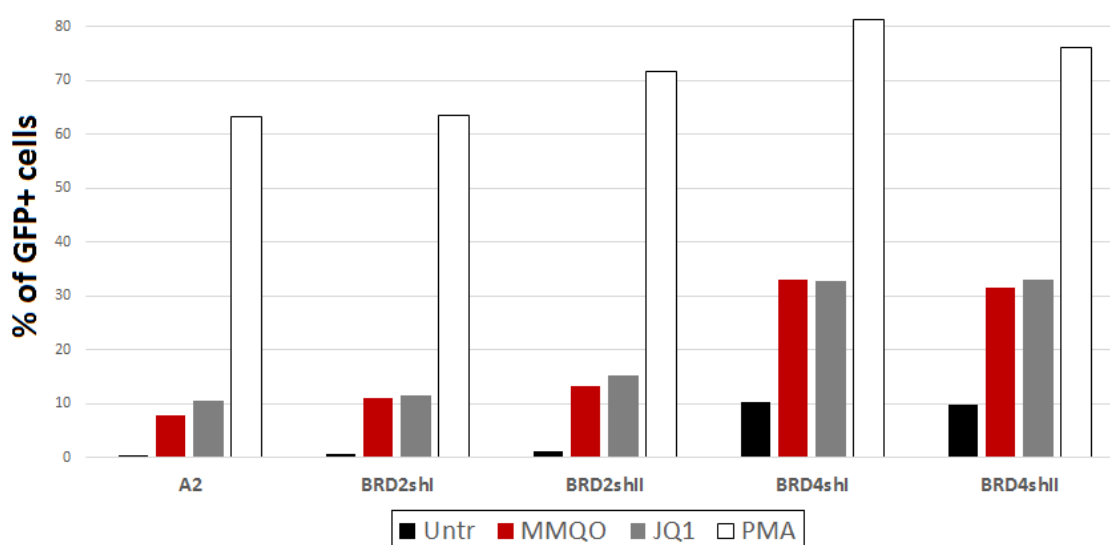


Figure 41: Flow cytometry results following BRD2 or BRD4 knockdowns and treatments with various latency reactivating agents in Jurkat A2 clones. 4 days following an infection with the knockdown vector, cells were treated with either MMQO (160 μ M), JQ1 (1 μ M), PMA (10nM) or left untreated for 24h and the cells were analyzed by forward scatter (FSC) and side scatter (SSC), by the GFP expressing percentage among the viable sample. Similar ratios were obtained measuring the fluorescence intensity these GFP+ cells.

3.5 MMQO affects Brd4 binding to HIV-1 minigenome promoter

To observe how Brd4 behaves following MMQO or JQ1 treatment in the proviral chromatin we performed chromatin immunoprecipitations (ChIP) on latently infected HeLa heterogeneous populations. As expected the levels of Brd4 drastically dropped in response to a 24 hour treatment by either drug near the TSS (nt +455) of HIV-1 (Figure 42). This decrease is in concurrence with the previously published ChIP results that displayed an 8-

fold decline of Brd4 in the proximal promoter of A2 clones in response to a high dose of JQ1 treatment (Li et al. 2013) and the result confirms that, on a chromatin level, MMQO targets Brd4.

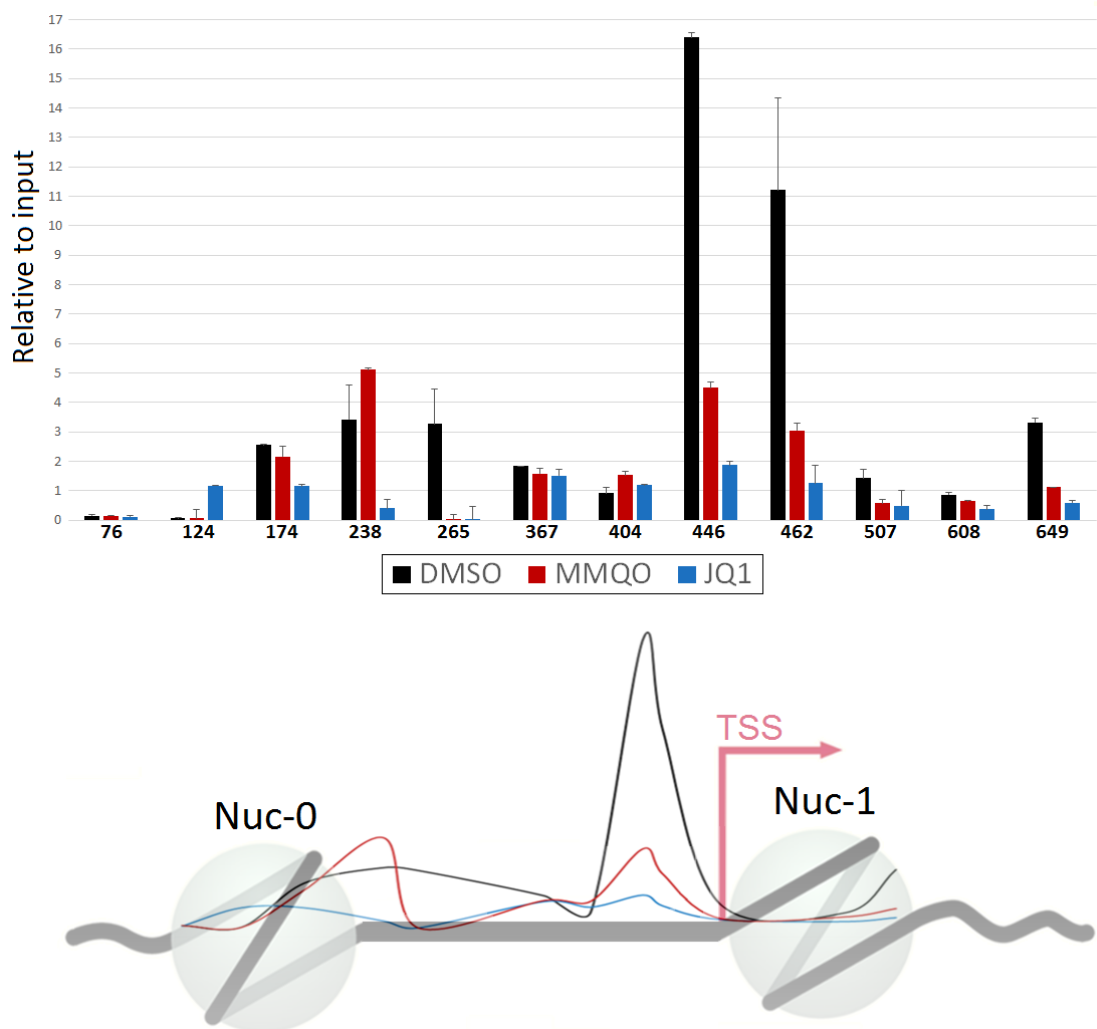


Figure 42: ChIP of Brd4 at the HIV-1 minigenome 5' LTR following MMQO or JQ1 treatment. (Above) Latently infected minigenome containing HeLa cells were treated 24h with MMQO (160 μ M), JQ1 (1 μ M) or equivalent volume of DMSO. Chromatin was crosslinked for 10 minutes, sonicated to an estimated 200-500bp size and used for immunoprecipitation against Brd4 or IgG as a negative control. The pulled down DNA was analyzed by qPCR. HIV 5' LTR was analyzed by 12 different pairs of primers producing amplicons with the average size of \sim 100bp. S.D. values (error bars) are shown from a representative experiment measured in duplicate. (Below) Illustration highlighting the abundance of Brd4 following the three different treatments (lines) in the 5' LTR of the minigenome.

3.6 MMQO specificity towards the different bromodomains of Brd4

In order to understand if MMQO preferably functions through the BD1 or BD2 domain of Brd4, we compared its function to the Brd4-BD2 inhibitor RVX-208 (Picaud et al. 2013). RVX-208 is a quinazolone scaffold based compound that was developed for the treatment of cardiovascular diseases associated with atherosclerosis (Bailey et al. 2010), but thus far has never been related to HIV latency.

Brd4-BD2 is considered to prefer different targets to those of the BD1 counterpart. For example it has been shown to have higher specificity for the KAc-310 of NF- κ B (Zhang et al. 2012), tri-acetylated cyclin T1 (Schröder et al. 2012) or to different core histone acetylations, preferring N-tails with multiple lysine acetylations simultaneously (Filippakopoulos et al. 2012). Since RVX-208 is a BET family inhibitor against a target that could display potential through different mechanisms against viral latency we were curious about its possible effect.

RVX-208 is described to have an IC₅₀ value of 0,5 μ M on the BD2 and become unspecific at around 87 μ M towards the BD1 site (Picaud et al. 2013). We therefore treated both Tat-positive and Tat-deficient latent models with varying doses of RVX-208 to determine if at a low dose the compound might have an effect on viral reactivation. Unfortunately we witnessed no effect of the drug at low doses and only at around 80 μ M did it start displaying an effect similar to MMQO (Figure 43). This suggests that the effect on the viral promoter is

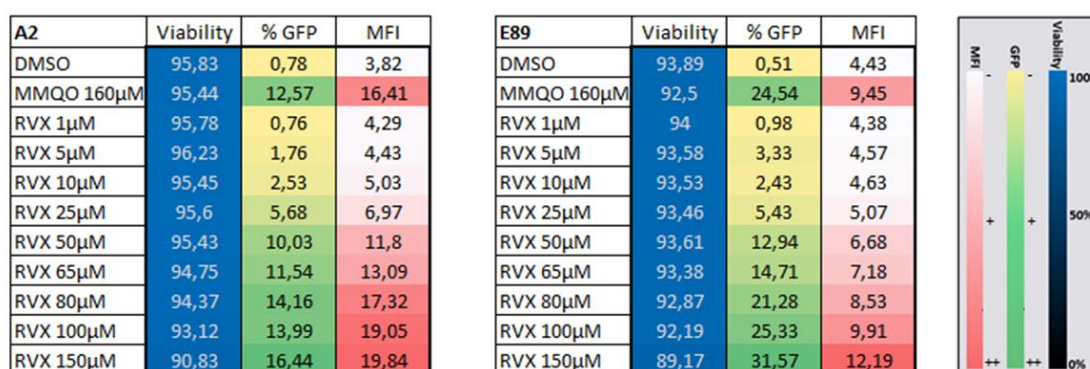


Figure 43: Effect of RVX-208 on latent Jurkat cells containing Tat-positive and Tat-negative minigenomes by flow cytometry. Jurkat A2 or E89 clones were incubated with MMQO (160 μ M) or varying doses of RVX-208 (1-150 μ M) for 24h and the cells were analyzed by forward scatter (FSC) and side scatter (SSC), by the GFP expressing percentage among the viable sample and their GFP expression intensity (Mean Fluorescence Intensity – MFI, depicted in arbitrary units). The color code indicates the intensity of the value within the dataset.

not due to its specific interaction with BD2 but probably due to its effect on BD1 of Brd4 at unspecific concentrations. Nevertheless, to our knowledge this is the first time RVX-208 has been shown to have an effect on HIV-1 transcription. This dose dependent response also tells us that the BD2 domain of the BET proteins aren't as much of determining factors for viral latency as the BD1 domains.

RVX-208 has a unique structure amongst the different BET inhibitors that are otherwise mostly based on triazolodiazepine scaffold structures. Due to the similarity of its basal structure to MMQO's quinoline skeleton it could be possible that MMQO also has higher specificity towards the BD2 domains of the BET family proteins. In addition to their design similarities the two drugs also display similar IC₅₀ values in terms on their effect on the viral reactivation. This hypothesis is also supported by the *in silico* docking of both drugs to the BD2 domain of Brd4, confirming they have very similar chemical characteristics, with strong affinity for the same Asparagine-429 amino acid (Figure 44). Due to the stabilizing secondary structure RVX-208 demonstrates a considerably higher affinity towards the domain (energy shift score of -9,005 versus -6,745). Considering this predicted interaction, we wanted to understand if MMQO also displays any specific traits characteristic to RVX-208.

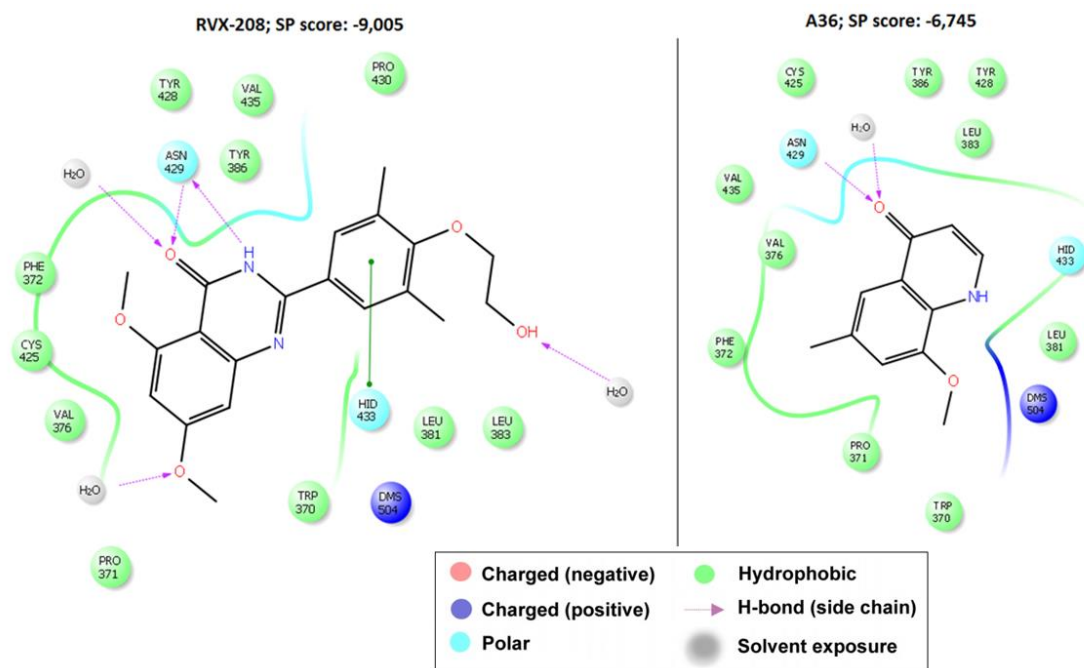


Figure 44: *In silico* docking models of RVX-208 and MMQO in the Brd4-BD2. MMQO was docked in the Brd4 BD-2 domain (right). RVX-208 was docked as control (left). PDB code: 4MR6. Illustration created by Salvador Guardiola, IRB.

It has been shown that RVX-208 leads to an increase of plasma levels of the high-density lipid protein APOA1, whose expression is regulated by BET proteins. The chemical inhibition of BET bromodomains has been associated with *ApoA1* upregulation on transcriptional and protein levels in HepG2 cells (Bailey et al. 2010). In our microarrays MMQO was able to dysregulate the expressions of various other members of the apolipoprotein family, such as *APOA*, *APOBR* and *APOL3*, suggesting it might have an effect on the family in other cell lines as well.

We examined the gene expression in human liver carcinoma HepG2 cells, analyzing the effect of both drugs on *APOA1*. We additionally measured *HEXIM1* as a control gene known to be upregulated by BD1 inhibition and *IRF7* as an MMQO target gene. HepG2 cells were treated for 48 hours with low doses (10 μ M MMQO or 5 μ M RVX-208), with high doses (80 μ M MMQO or 60 μ M RVX-208) and with the high dose combination of both compounds to measure the maximum of the gene expression (Figure 45). The results didn't confirm the hypothesis of MMQO preferentially targeting BD2 domains. MMQO had no effect on *APOA1* at low dosages, in contrast to RVX-208 that already at a concentration of 5 μ M shows the previously described mRNA upregulation. Concurrently, *HEXIM1* responded only at higher doses confirming the specificity of RVX-208 towards BD-2.

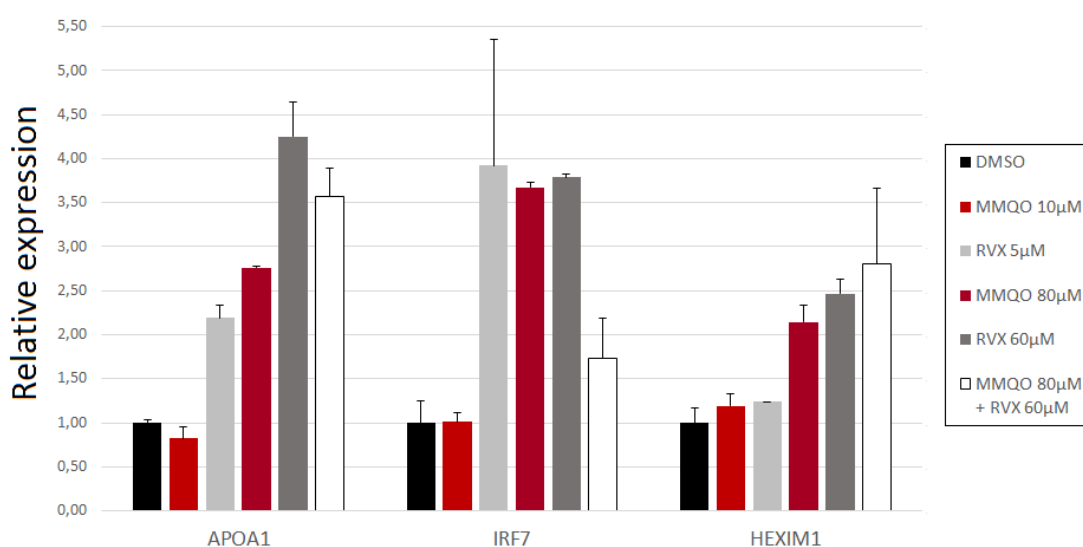


Figure 45: qPCR results depicting effects of MMQO or RVX-208 on HepG2 cells. HepG2 cells were treated for 2 days either with MMQO (10 μ M / 80 μ M), RVX-208 (5 μ M / 60 μ M), their high dose combination or equivalent volume of DMSO as vehicle. *GAPDH* was measured for normalization and results are represented relative to results from the DMSO treated cells. Genes were chosen by their specificity to RVX-208, MMQO (*IRF7*) or JQ1 (*HEXIM1*, described in Picaud et al. 2013). Means and S.D. values (error bars) are shown from a representative experiment measured in duplicate.

3.7 MMQO targets BETi specific genes

Understanding the kinetics of RVX-208 allowed us to perform one final control to distinguish if MMQO preferably displays HDACi- or BETi-like behavior. To that end we compared the effect of known BET and HDAC inhibitors on the MMQO-specific genes identified previously. For this assay we specifically concentrated on genes that showed an opposite regulation by TSA in the three hour microarray. As a control for the proper functioning of the compounds we also included universally dysregulated genes like *IRF7*, *MYC*, *RAG1* and *CXCR7*. Indeed, following a three hour treatment by the five compounds we witnessed MMQO displaying BET inhibitor-like behavior (Figure 46).

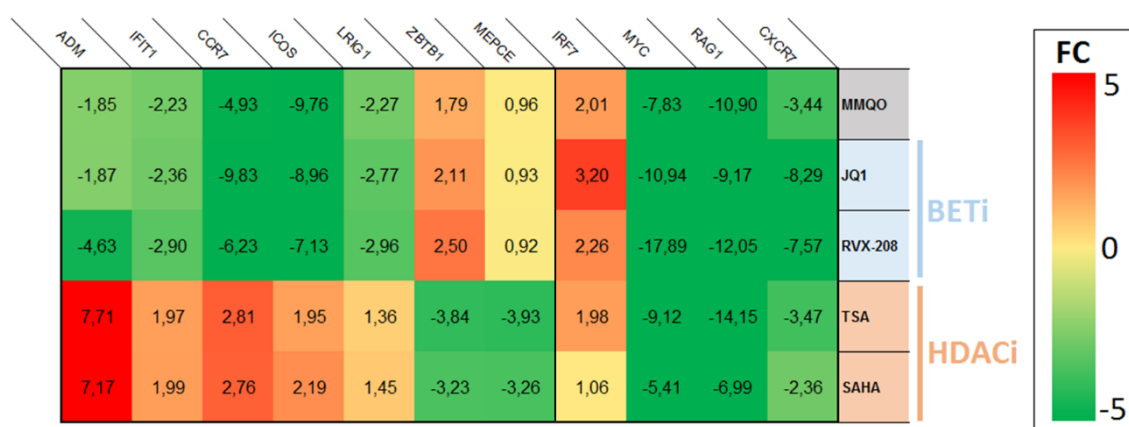


Figure 46: qPCR results depicting effects BET inhibitors and HDAC inhibitors on MMQO target genes. Jurkat cells were treated for 3h with either MMQO (160 μ M), RVX-208 (80 μ M), JQ1 (1 μ M), SAHA (5 μ M) TSA (200nM) or left untreated. GAPDH was measured for normalization and results are represented relative to results from the untreated cells. Heat map results were measured in duplicate and only genes that had reliable S.D. values are depicted in the figure.

As expected, we observed that HDAC inhibitors shared similar expression patterns to BET bromodomain inhibitors on the universal target genes, like *IRF7* that was upregulated by both classes of drugs. Also *MYC*, *CXCR7* and *RAG1* showed a strong downregulation by all drugs, further confirming the similarities between the two classes of compounds. In addition, genes like *ADM*, *IFIT1*, *CCR7*, *ICOS*, *LRIG1* were downregulated by bromodomain inhibitors but were upregulated by HDAC inhibitors. *ZBTB1* and *MEPCE* displayed a potent downregulation by TSA and SAHA, while being up- or unregulated by bromodomain inhibitors, respectively. According to this assay all the chosen genes displayed expected differential regulations by the corresponding class of drugs.

More importantly, these results illustrate that MMQO has same effect on gene expression as other bromodomain inhibitors. We can observe that genes that are differentially regulated by MMQO, are specifically also dysregulated by JQ1 and RVX-208. This is consistent with the hypothesis that they are implicated in the same molecular mechanism. In addition we also observed MMQO hindering protein expression of cMyc and Bcl-2 to a similar degree as JQ1, confirming the similarities between MMQO and BET inhibition also on protein level (Figure 38B). Most importantly, we also witnessed MMQO behaving similarly to bromodomain inhibitors on the proviral activity, either by overlapping with their induction, by synergizing similarly with other direct viral activators or by displacing the Brd4 protein from the 5'LTR of HIV-1 minigenome and chromatin in general. After comparing MMQO to a BD2 specific inhibitor, RVX-208, we can conclude that MMQO preferentially functions through the BD1 domain of Brd4.

3.8 Biotin tagging MMQO

BET proteins and their bromodomains are known to exhibit a high degree of conservation between the different members of the family (Figure 47) (Vollmuth et al. 2009). The high similarity of these acetyl-lysine interacting domains makes it difficult to design chemical probes that only target one specific domain on only one protein family member, so most of the BET inhibitors also express inspecificities towards other BD sites (Filippakopoulos & Knapp, 2014). Considering the simplistic structure of MMQO and the molecular promiscuity of other BET family inhibitors, it is probable that MMQO also targets other bromodomains that we haven't been able to identify due to the constrained mRNA and protein expression detection based methods.

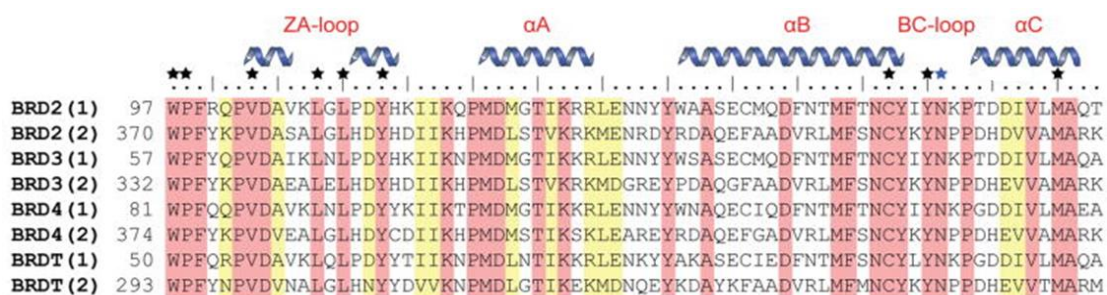
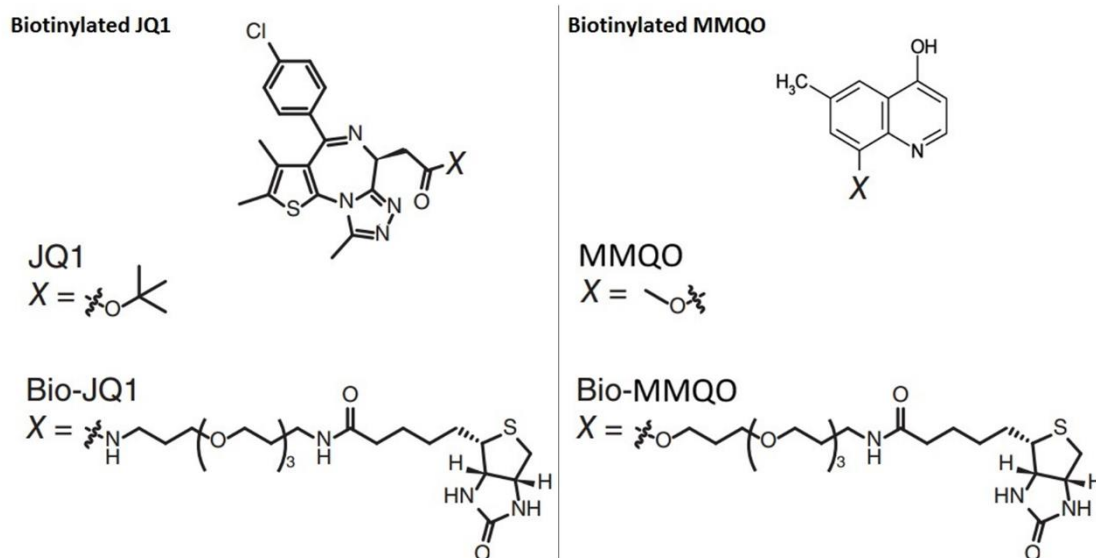


Figure 47: Protein sequence alignment of the human BET subfamily highlighting conserved (red) and similar (yellow) residues. Major bromodomain structural elements are shown above the sequence alignment. The side-chain contacts with JQ1 are annotated with a black star. The family conserved asparagine is indicated by a blue star. Illustration adapted from Filippakopoulos et al. 2010.

A powerful tool for determining a ligand's target(s) is to label it with a chemical tag. This requires the removal of a non-essential functional group from the original compound and replacing it with a required detectable structure. This method has been previously used successfully to determine the localization of small molecules in chromatin by fluorescent labelling for microscopy (Rodriguez et al. 2012), native protein pull down assays (Ohana et al. 2015) and even for chromatin immunoprecipitation through a biotin moiety (Jin et al. 2014). Recently a biotinylated JQ1 (Bio-JQ1) was also designed and used successfully in a "Chem-Seq" experiment that identified with high precision the DNA loci the tagged compound got crosslinked to (Anders et al. 2014). Besides showing near perfect correlation with Brd4 enrichment throughout the genome, Bio-JQ1 also overlapped considerably with Brd2 (96%) and Brd3 (63%). Inspired by the successful biotin tag on JQ1, we decided to utilize a similar strategy to determine the specific binding partners of MMQO. In collaboration with the Synthetic Chemistry Unit in Barcelona Science Park a biotin tag was synthesized on the methoxy group located at the predicted inert face of MMQO (Figure 48). This biotinylated derivative of MMQO was termed Bio-MMQO. To ensure that the biotin group was sufficiently prolonged from the core quinoline structure the polymer chain was triple pegylated. As an intermediate product of the synthesis a new stock of MMQO was produced for the following phases. This intermediate MMQO was confirmed to function with the same activity as the previously used stocks of MMQO by flow cytometry, thus validating biologically the functionality of the synthesis product (data not shown).



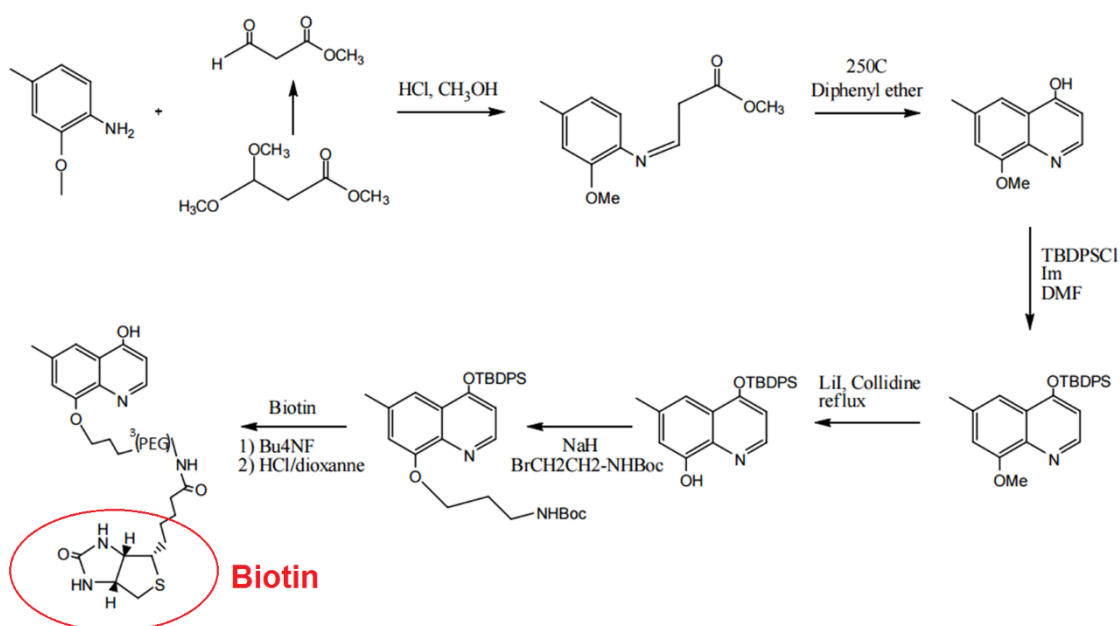


Figure 48: Illustration Bio-JQ1 and Bio-MMQO and *de novo* synthesis scheme for Bio-MMQO. The triple pegylated biotin was synthesized to the methoxy group predicted to face the exterior of the pocket (Figure 36). Different protective groups were added to the functional groups of MMQO and its successive structures to ensure the perseverance of these groups. Synthesis protocol designed and performed by Miriam Royo's group.

Anders *et al.* demonstrated Bio-JQ1 to have lower biological activity and required to be used at doses around 3-5 times higher than unmodified JQ1. Due to the possible steric interference of the biotin structure and decreased stability of the drug binding caused by the increased molecular weight we decided to first control Bio-MMQO's functionality on the minigenome expression by flow cytometry. To our discontent the biotinylated MMQO showed no effect on the minigenome, even up to doses as high as 2,5mM (Figure 49A).

Biotinylated compounds sometimes demonstrate limited cell permeability so we decided to control the functionality of Bio-MMQO following a chemical permeabilization of the cells. Following a short permeabilization by Triton X-100 and a treatment with either MMQO or Bio-MMQO we again did not witness any effect by Bio-MMQO (Figure 49B). We are currently still in process of evaluating the functionality of this compound by chromatin immunoprecipitation, fluorescence microscopy, flow cytometry and pull down assays.

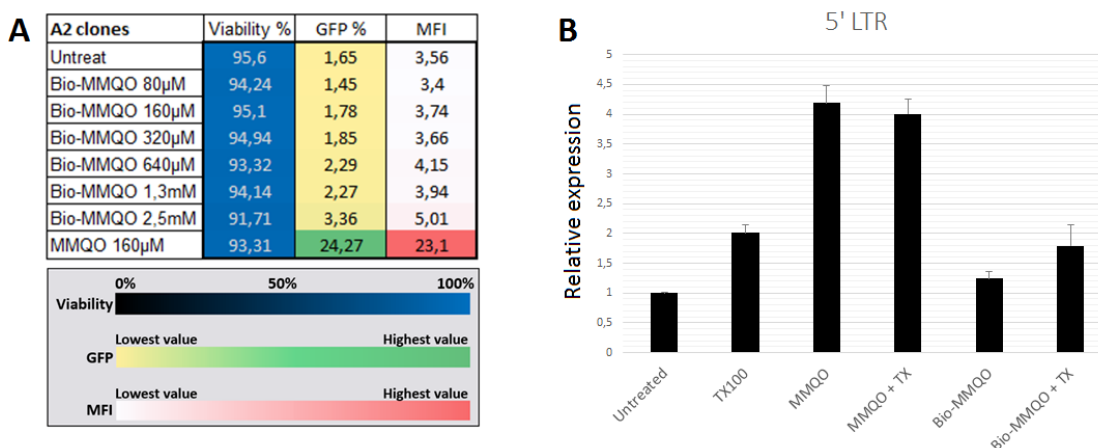


Figure 49: Bioactivity of Bio-MMQO. (A) Jurkat A2 clones were incubated with MMQO (160µM), with varying doses of Bio-MMQO (80µM-2,5mM) or left untreated for 24h and the cells were analyzed by forward scatter (FSC) and side scatter (SSC), by the GFP expressing percentage among the viable sample and their GFP expression intensity (Mean Fluorescence Intensity – MFI, depicted in arbitrary units). The color code indicates the intensity of the value within the dataset. (B) Highly responsive latent HeLa cells were treated for 12 minutes with 0,17mM TX100, washed twice and treated with MMQO (160µM) or Bio-MMQO (1mM) for 4 hours. *GAPDH* was measured for normalization and results are represented relative to the untreated cells.

3.9 Testing MMQO derivatives

In order to better understand the importance of the functional groups of MMQO, specifically the 6-methyl group considered to be on the inert face of the compound and the 8-methoxy group where the biotin-tag was synthesized before, we tested two different MMQO derived compounds lacking those moieties. Jurkat A2 clones were treated with varying doses of HMQ (4-Hydroxy-8-MethoxyQuinoline) and MQD (6-Methyl-4,8-QuinolineDiol) and we observed their effect on the minigenome based GFP production. While both of the compounds did show moderate function, they still displayed less activity and required higher doses than MMQO to function (Figure 50). Surprisingly the removal of the 6-methyl group, previously considered to be inactive and only functioning as an additional stabilizing unit for the MMQO, implied to be more crucial for the functioning of the quinoline structure than the removal of the more reactive methoxy group from 8th position. This substitution suggests that the previous *in silico* docking models might have predicted the exact interaction between MMQO and Brd4 incorrectly.

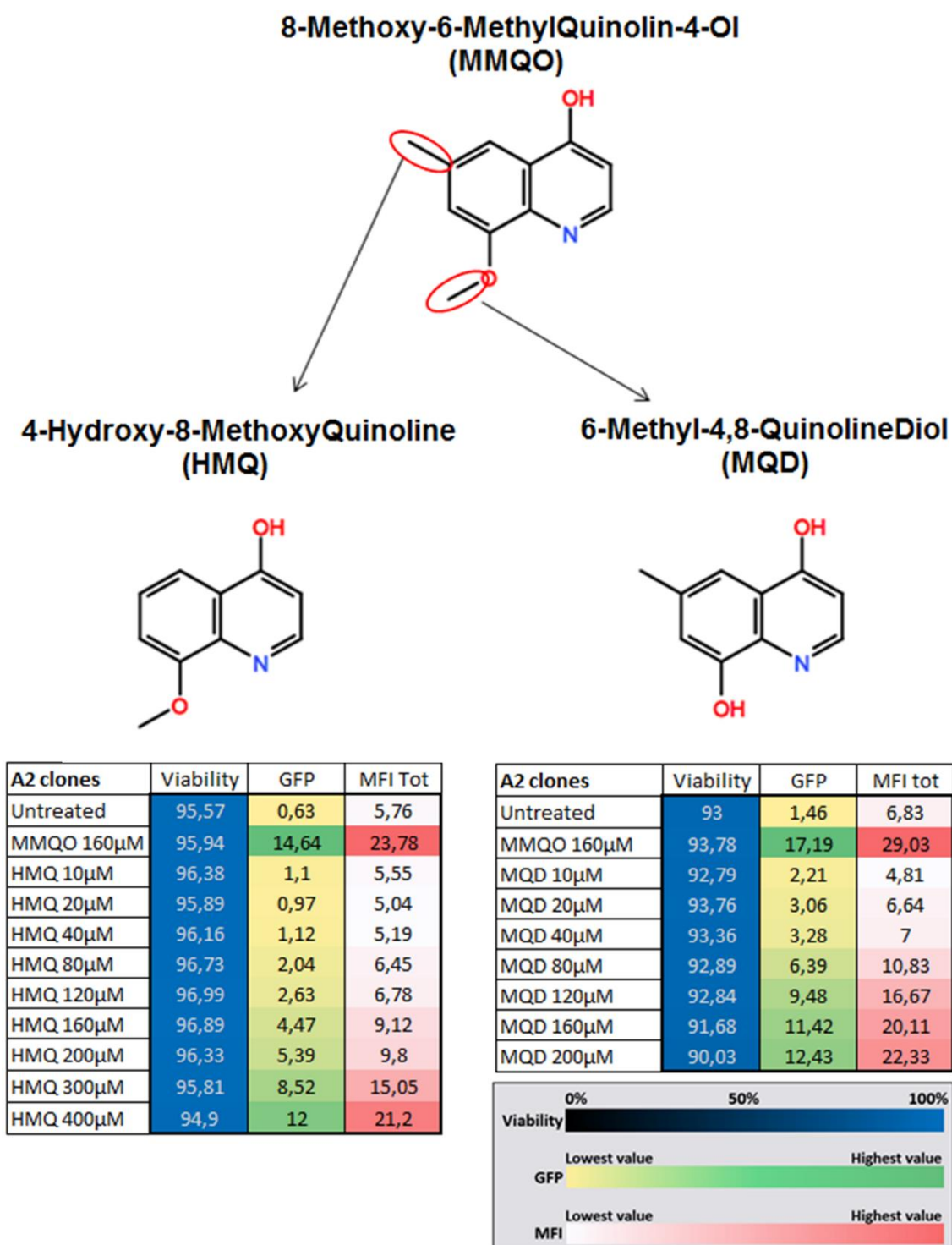


Figure 50: Biological functionality of MMQO derivatives. Jurkat A2 clones were incubated with MMQO (160µM) or varying doses of HMQ (10µM-400 µM), MQD (10µM-200µM) or left untreated for 24h and the cells were analyzed by forward scatter (FSC) and side scatter (SSC), by the GFP expressing percentage among the viable sample and their GFP expression intensity (Mean Fluorescence Intensity – MFI, depicted in arbitrary units). The color code indicates the intensity of the value within the dataset.

3.10 MMQO has a higher affinity for Brd9

Due to the lack of experience on bromodomain proteomics in our group we established a collaboration with the Structural Genomics Consortium in Oxford, who previously have identified and developed various bromodomain inhibitors, including JQ1. The main purpose of this cooperation was to confirm MMQO's binding to Brd4 *in vitro* and to identify any additional binding partners it might present among the human bromodomain families. Utilizing Homogeneous Time Resolved Fluorescence (HTRF) assays the group of Dr. John Porter discovered MMQO to have a higher affinity towards a Class IV family BET protein (Brd9) with an IC₅₀ value of ~16μM, rather than to Class II family (Brd4) (Table 11A). The assay also included the bromodomains of CECR2A and FALZA, two structurally related sites that have been previously shown to interact mildly with other Brd7/9 inhibitors (Hohmann et al. 2016). MMQO showed no affinity towards those two bromodomains, suggesting that its scaffold structure is unique enough for further optimization. In addition, the TAF1 domain has also been described to resemble the Brd4-BD1, yet MMQO showed to preference to that site neither (Crawford et al. 2016).

A	Target ID	IC50	Class
	CECR2A	>100	I
CECR2A	>100	I	
FALZA	>100	I	
FALZA	>100	I	
BRD4A	>100	II	
BRD4A	77,56	II	
CREBBPA	>100	III	
BRD9A	11,54	IV	
BRD9A	21,47	IV	
TAF1A	>100	VII	
TAF1A	>100	VII	

B	BRD4-BD1	BRD9	BRD7	
	1 TRP81	GLY43	ALA154	WPF motif
2 PRO82	PHE44	PHE155	WPF motif	
3 PHE83	PHE45	PHE156	WPF motif	
4 GLN84	ALA46	SER157	ZA channel	
5 GLN85	PHE47	PHE158	ZA channel	
6 PRO86	PRO48	PRO159	ZA channel	
7 VAL87	VAL49	VAL160	ZA channel	
8 ASP88	THR50	THR161	ZA loop	
9 ALA89	ASP51	ASP162	ZA loop	
10 LYS91	INS	INS	ZA loop	
11 LEU92	INS	INS	ZA loop	
12 ASN93	ILE53	ILE164	ZA loop	
13 LEU94	ALA54	ALA165	ZA loop	
14 TYR97	TYR57	TYR168	Water-binding Tyr	
15 TYR98	SER58	SER169		
16 ILE101	ILE61	ILE172		
17 MET132	MET92	MET203		
18 ASN135	ASN95	ASN206		
19 CYS136	ALA96	ALA207	Conserved Ala	
20 TYR139	TYR99	TYR210	Conserved Tyr	
21 ASN140	ASN100	ASN211	Conserved Asn	
22 ASP144	THR104	THR215		
23 ASP145	VAL105	ILE216		
24 ILE146	TYR106	TYR217	Gatekeeper	
25 VAL147	TYR107	TYR218		
26 MET149	LEU109	ALA220		
27 ALA150	ALA110	ALA221		

Table 11: Identification of BRD9 as a preferred target by MMQO. (A) Homogeneous time resolved fluorescence selectivity assay with MMQO on six bromodomain proteins from five different BD families after excitation at 337 nm, energy transfer at 620 nm, and fluorescence emission at 665 nm. (B) Sequence Similarity between the Residues of the Acetyl-Lysine Binding Sites of Brd4-BD1, Brd9, and Brd7. Colors represent residue properties: dark green = aromatic, light green = hydrophobic, red = acidic, blue = basic, orange = polar, purple = proline, white = small. INS = indel. Illustration (B) adapted from Theodoulou et al. 2016.

Bromodomain containing protein 9 (Brd9) is a poorly characterized member of the human bromodomain protein family. It consists of a single bromodomain and of a DUF region with a still unknown function (Theodoulou et al. 2016). These basic domains are especially conserved on the highly related Brd7 protein, sharing about 85% in sequence homology (Table 11B). The two paralog proteins have been described to primarily function as members of the SWI/SNF complexes. Unfortunately we weren't able to perform any FRET assays on the Brd7 protein, due to the low stability of the crystallized protein and its low functioning rates with weakly binding compounds. Nevertheless, taking into account the near identical structure of its bromodomain to that of Brd9, in combination with molecular promiscuity of MMQO, we speculate Brd7 also to be a possible target of MMQO.

3.11 Effect of Brd9 inhibition on HIV-1 expression

Last year the first of its class Brd7/9 dual-inhibitory compound, LP99, was introduced (Clark et al. 2015). LP99 is a quinoline scaffold based compound that in accordance with our results uses the minimalist heterocyclic core moiety to interact with the interior of the bromodomain pocket (Figure 51), while the external hydrophobic tail serves the purpose of stabilizing the active head of the compound within the pocket. It's worth to note that this compound was shown to exhibit immunosuppressive characteristics by limiting the IL-6 production in response to LPS treatment in human monocytes.

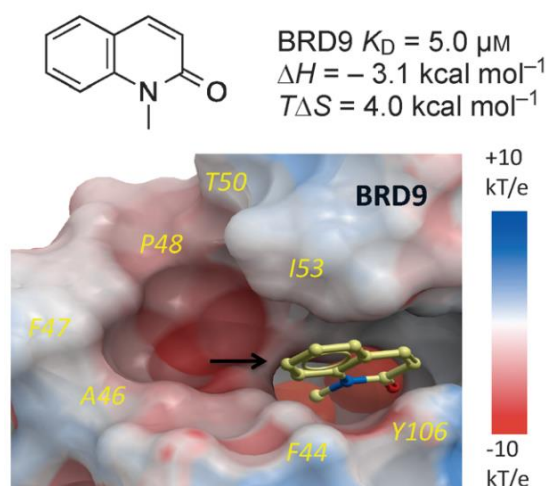


Figure 51: The quinoline hit used for designing LP99 within the Brd9 bromodomain. Electrostatic surface representation of Brd9 overlaid with the compound. The black arrow indicates the attachment point targeted for the design of selective inhibitors. Figure adapted from Clark et al. 2015.

In addition to LP99, few other compounds have been developed recently, such as BI-7273 and BI-9564. These two inhibitors are based on the original quinoline structure of LP99 and have been modified to be even more potent than the original compound. In a series of elegant experiments utilizing bromodomain swapping between Brd9 and Brd4 proteins, it has been shown that both BI-7273 and BI-9564 decrease cell proliferation among AML and multiple myeloma cells Brd9-dependently (Hohmann et al. 2016, Martin et al. 2016). In addition to these two quinoline scaffold based compounds, a novel thienopyridone scaffold compound was also described, termed I-BRD9. The unique structure of this inhibitor allows it to be the most potent among the currently available Brd9 inhibitors (Theodoulou et al. 2016).

Considering that Brd9 is a major carcinogenic factor of leukemia cell lines via the latency promoting transcription factor cMyc and that Brd9 been shown to be an irreplaceable member of the HIV-1 repressive BAF complex (Kadoch et al. 2013), the chemical inhibition of Brd9 could possibly serve an anti-latency function. If that hypothesis holds true, then it is probable that MMQO enforces its effects against HIV-1 latency through two separate mechanisms.

To clarify the effect Brd9 has on the GFP-expressing minigenome we performed a dose dependent treatment with I-BRD9 on Tat-expressing and Tat-deficient latent Jurkat clones (Figure 52). I-BRD9 is described to function at nanomolar range effectively and have an IC₅₀

A2 clones	Viability %	GFP %	MFI	E89 clones	Viability %	GFP %	MFI
DMSO	94,14	1,34	1,14	DMSO	82,21	0,76	3,85
MMQO 160µM	84,49	23,05	6,38	MMQO 160µM	79,16	17,99	5,72
JQ1 1µM	83,96	30,48	7,74	JQ1 1µM	77,08	18,47	5,60
I-BRD9 1µM	85,39	2,51	3,18	I-BRD9 1µM	81,54	0,97	3,77
I-BRD9 5µM	87,11	3,98	3,30	I-BRD9 5µM	80,29	1,79	3,74
I-BRD9 10µM	87,45	10,28	4,37	I-BRD9 10µM	79,96	9,38	4,58
I-BRD9 15µM	83,44	14,78	5,11	I-BRD9 15µM	76,92	18,17	5,67
I-BRD9 20µM	78,43	19,38	6,47	I-BRD9 20µM	66,88	30,29	7,70
I-BRD9 30µM	70,04	22,51	8,00	I-BRD9 30µM	52,74	48,73	12,73
I-BRD9 40µM	61,62	21,32	8,16	I-BRD9 40µM	47,02	60,72	16,83
I-BRD9 50µM	70,04	21,82	7,44	I-BRD9 50µM	45,3	70	20,96

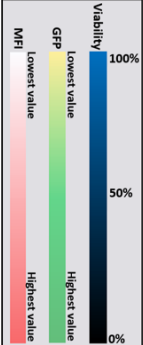


Figure 52: Effect of Brd9 inhibition on HIV-1 minigenome expression. Jurkat Jurkat A2 and E89 clones were incubated with MMQO (160µM) or varying doses of I-BRD9 (1µM-50µM), JQ1 (1µM) or treated with the equivalent volume of DMSO for 24h and the cells were analyzed by forward scatter (FSC) and side scatter (SSC), by the GFP expressing percentage among the viable sample and their GFP expression intensity (Mean Fluorescence Intensity – MFI, depicted in arbitrary units). The color code indicates the intensity of the value within the dataset.

value against Brd4 at around 5 μ M by *in vitro* assays. The minigenomes responding to canonical Brd4 inhibitors failed to respond against Brd9 inhibition at low doses suggesting that Brd9 inhibition alone cannot rescue HIV-1 from quiescence.

3.12 Comparing Brd4 and Brd9 inhibition by gene expressions

Similarly to the previously carried out assay to compare BETi and HDACi (Figure 47), we hoped to quantify the difference of MMQO target genes in response to Brd4 inhibition (JQ1) and Brd9 inhibition (I-BRD9). Since we hypothesize MMQO to function against Brd9 at lower doses and against Brd4 at higher ones, a distinct pattern of genes should be regulated by I-BRD9 and MMQO at lower doses, while remaining unaffected by JQ1 treatment. In addition to concentrating on the already established MMQO target genes (*IRF7*, *MYC*, *IL7R* etc), we also chose genes that might respond to Brd9 inhibition (*VAV3*, *SORL1*, *DDX46* etc). These genes were differentially regulated by MMQO in our first microarray and were additionally regulated in the microarrays published by Theodoulou et al. 2016. These datasets identified I-BRD9 specific genes in comparison to I-BET151 (an already established Brd4 specific inhibitor) in Kasumi-1 AML cell lines after six hour treatments.

We treated Jurkat cells for six hours with I-BRD9, and a low and a high dose of MMQO or JQ1 and analyzed the mRNA expression by qPCR. The time and dose for I-BRD9 were chosen based on gene expression data described by Theodoulou et al. 2016, the low dose for MMQO was chosen to saturate Brd9 bromodomain (40 μ M) and high dose to saturate the Brd4 bromodomains (200 μ M). 1 μ M JQ1 was used as a control for the Brd4 saturation and a 10-times lower dose was used to quantify the partial effect of Brd4 inhibition. Unfortunately we were not able to establish any concrete similarities between I-BRD9 and MMQO following a qPCR from six hour treated Jurkat cells (Figure 53). Based on the expressional responses the genes can roughly be categorized into four categories: genes where MMQO behaves somewhat like JQ1 (gene names marked yellow), genes where MMQO resembles more I-BRD9 (blue), genes that failed to respond or cannot be used for conclusions (gray) and *CXCR7*, a gene that displayed higher regulation in response to MMQO than with the other compounds.

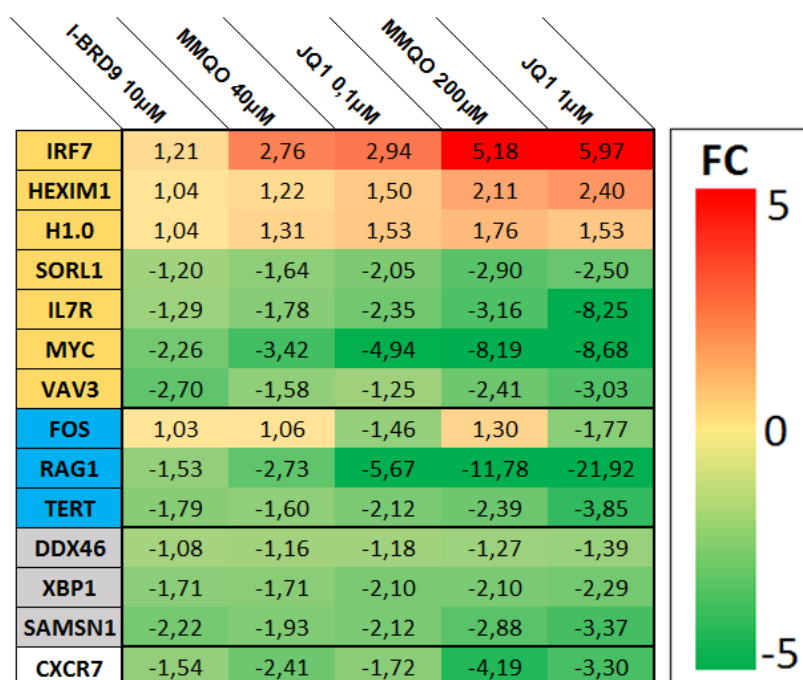


Figure 53: qPCR results depicting effects MMQO, BET inhibitor JQ1 and Brd9 inhibitor I-BRD9 on MMQO target genes. Jurkat cells were treated for 6h with either MMQO (40 μ M or 200 μ M), I-BRD9 (10 μ M), JQ1 (0,1 μ M or 1 μ M), or equivalent amount of DMSO. GAPDH was measured for normalization and results are represented relative to results from the untreated cells. Heat map results were measured in duplicate and only genes that had reliable S.D. values are depicted in the figure.

Based on the genes chosen for this assay it is unfortunately difficult to draw conclusions MMQO's preferred role. While most of the genes did respond to MMQO one way or another, the fold change values in almost all the cases fall between those of JQ1 and I-BRD9.

DISCUSSION

One of the principal reasons for the persistence of HIV-1 is its capability to remain latently hidden within the host. Even though last three decades have proven to be extremely successful in producing various antiretroviral drugs, none of them are directed against this quiescent form of HIV-1. However, the suggested “shock and kill” strategy aims to wake the dormant virus and eradicate it with a combination of conventional HAART and the patient’s own immune system.

The novel lead compound MMQO has been proven to achieve this “shocking” task (Gallastegui et al. 2012). Previous results by our group have shown its efficacy against latently infected HIV-1 in both cellular models and primary patient derived cells.

In this study we set out to pinpoint the molecular mechanism of MMQO in reactivating HIV-1 from latency, in hopes of elucidating the compound’s function and possibly to identify new pathways suppressing viral expression. Combining *in vitro* and *in silico* methods we determined that MMQO targets bromodomain proteins Brd4 and Brd9, with Brd4 inhibition probably playing the primary role in combating HIV-1 latency.

1. MMQO as a dual bromodomain inhibitor

Due to the potential of BET bromodomain inhibition in numerous diseases, including in the reactivation of HIV-1 from latency, intense efforts are directed towards the identification of new compounds of that class. The chemical inhibition of Brd9 is a relatively new concept, with only a few compounds being described in doing so. MMQO provides a new platform to design inhibitors against Brd9 and Brd4, both proteins being clinically significant targets in a variety of cancers. Though bromodomain inhibitors that can simultaneously affect those proteins have been described previously, these compounds proved to be too promiscuous by additionally targeting CECR2, CREBBP and TAF1 (Fedorov et al. 2014). The FRET assay carried out by our collaborators showed that MMQO does not affect these representatives of other bromodomain classes, confirming it to be more precise in its affinities (Table 11A). In addition to its unique target specificity, another advantage of MMQO is its minimalistic structure when compared to conventional bromodomain inhibitors, possibly allowing it to be further optimized for higher affinity and/or specificity. Numerous 8-hydroxyquinoline based compounds have been described to cross the blood-brain barrier (reviewed in Song et al. 2014), further increasing the potential of MMQO to be developed into a more potent

reagent. Finally, the low molecular weight scaffold may also play an importance in the time and cost efficiency of *de novo* synthesis of its chemical derivatives.

Although MMQO displays potential as a new class of bromodomain inhibitor, a broader assay targeting the whole bromodomain family should be carried out in order to evaluate its specificity. Most importantly, the possible relationship between Brd7 and MMQO should be further investigated, since the bromodomains of Brd7 and Brd9 are sequentially nearly identical (Table 11B), yet they both display considerable functional differences. Likewise, Brd4 inhibitors are oftentimes known to function non-specifically by additionally targeting the other BET subfamily members. Due to the low stability of bromodomain proteins crystals *in vitro*, the methodical approaches to determine MMQO's specificity should rather concentrate on cell culture methods.

At the initial phases of the project we were considering a variety of methods to identify MMQO's protein binding partners, including pulldown assays with MMQO-coated sepharose beads, Alexa-labelling of MMQO or radioactive tritium-tagging of MMQO. We eventually decided to perform biotin-tagging, due to ease of use, cost efficiency and potential applications. The biotin-tagging of MMQO unfortunately has thus far not yielded any results, suggesting that either the affinity of the novel compound has drastically decreased or is lacking completely, even following cell membrane permeabilization (Figure 49).

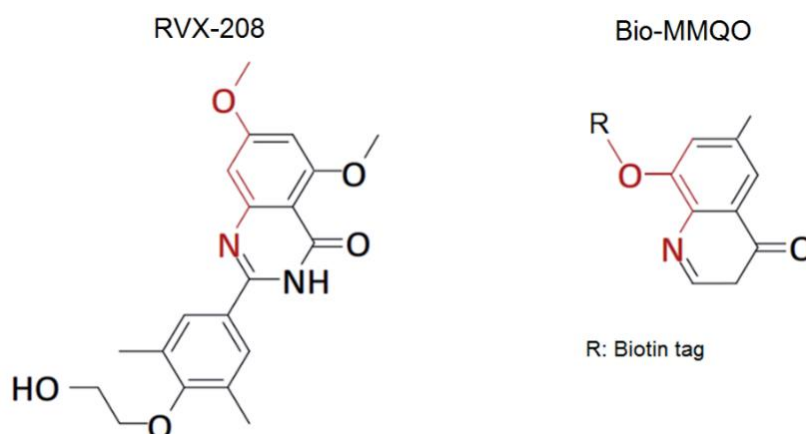


Figure 54: Structures of Bio-MMQO and RVX-208. The hypothesized alternative acetyl-lysine-mimetic element of MMQO and the known reactive domain of RVX-208 are highlighted in red. Figure adapted from Wang & Filippakopoulos, 2015.

The biotin moiety was designed to extend out of the bromodomain pocket via the methoxy-group based on the *in silico* predictions. Nevertheless it cannot be ruled out that MMQO

interacts with the bromodomain in a different conformation than predicted. A comparison of the similar BD-2 interacting domain of RVX-208 and MMQO molecular structures supports this presumption (Figure 54).

Further *in silico* analysis based on the NMR results is required to determine MMQO's exact interaction with bromodomains. Additional experiments carried out with point-mutations on the bromodomains might additionally help determine MMQO's binding partners. Although the biotin tag in its current format hasn't yielded in any practical application *in vitro*, the fact that it is inactive might hint towards structural properties that could still be used for future optimization *in silico*.

The depletion of individual bromodomain proteins should elaborate which MMQO target genes are affected by which factors. Since knockdown and knockout experiments with Brd2 and Brd4 have been shown to result in cell cycle arrest in lymphocyte cell lines, alternative BET inhibitor independent cell lines could be used to identify MMQO's reliance on BET family members. Various breast cancer cell lines like T47D, HCC-1395, MDA-MB-436 and SUM185PE have demonstrated high resistance against BET inhibitors (Hohmann et al. 2016). Nevertheless, it is not clear if the viability of these cells is autonomous of the inhibitory effects of BETi-s or completely independent from the BET proteins entirely. An alternative approach to describe MMQO's specificity in cell lines could be achieved by fluorescence recovery after photobleaching (FRAP). Observing the dissociation time and intensity of GFP-fused bromodomain proteins has indeed been previously shown to be a powerful tool in characterizing the affinities of bromodomain inhibitors (Patel et al. 2013).

2. MMQO as an anticancer drug

As Brd9 inhibition has been demonstrated to target specific cancers, the additional Brd4 hindrance dual inhibitory effect of MMQO could function synergistically. The transcriptional upregulation of chromatin readers has previously been demonstrated as a predictive marker for the cell types to respond to bromodomain inhibition (Barretina et al. 2012). In accordance with the published data about bromodomain protein dependency among the hematopoietic derived tumors, the Cancer Cell Line Encyclopedia datasets display a considerable increase of both Brd4 and Brd9 mRNA among the "Hematopoietic and Lymphoid Tissue" cells (Figure 55). Interestingly, also renal carcinoma (e.g. SLR20/21/23/24/25; UMRC2/6; SKRC20/31), meningioma (e.g. IOMM-Lee; F5; CH157MN)

and numerous lung derived cancer cell lines displayed a considerable upregulation of both bromodomain proteins mRNAs, suggesting their dependency of these factors. Indeed, RAS-dependent lung cancer cell lines were indeed recently described to be sensitive towards Brd4 inhibition (Garcia-Carpizo et al. 2016). Our IPA analysis of MMQO microarrays predicted the most inhibited transcription factor to be hypoxia inducible factor 1-alpha (HIF1 α) based on the regulation of its target genes in Jurkat cells (z-score:-3,003; p -value < 0,005). HIF1 α is known to be a crucial determinant for renal cell carcinoma tumorigenesis and has been demonstrated to be overexpressed in majority of renal cancers (reviewed in Gudas et al. 2014). In addition, Brd4 has been shown to be enriched and be depletable with JQ1 in the enhancer regions of both cMyc and HIF1 α triple-negative breast cancer cell lines (Shu et al. 2016). Thus, analyzing the viability, proliferation and cell cycle changes after targeting these cell lines with MMQO could provide information for developing new therapies. Further studies will have to be carried out to determine how the functioning and stability of the SWI/SNF complex, cMyc / HIF1 α expression and the global transcriptome will be affected in response to Brd9 inhibition to establish its significance in cancer.

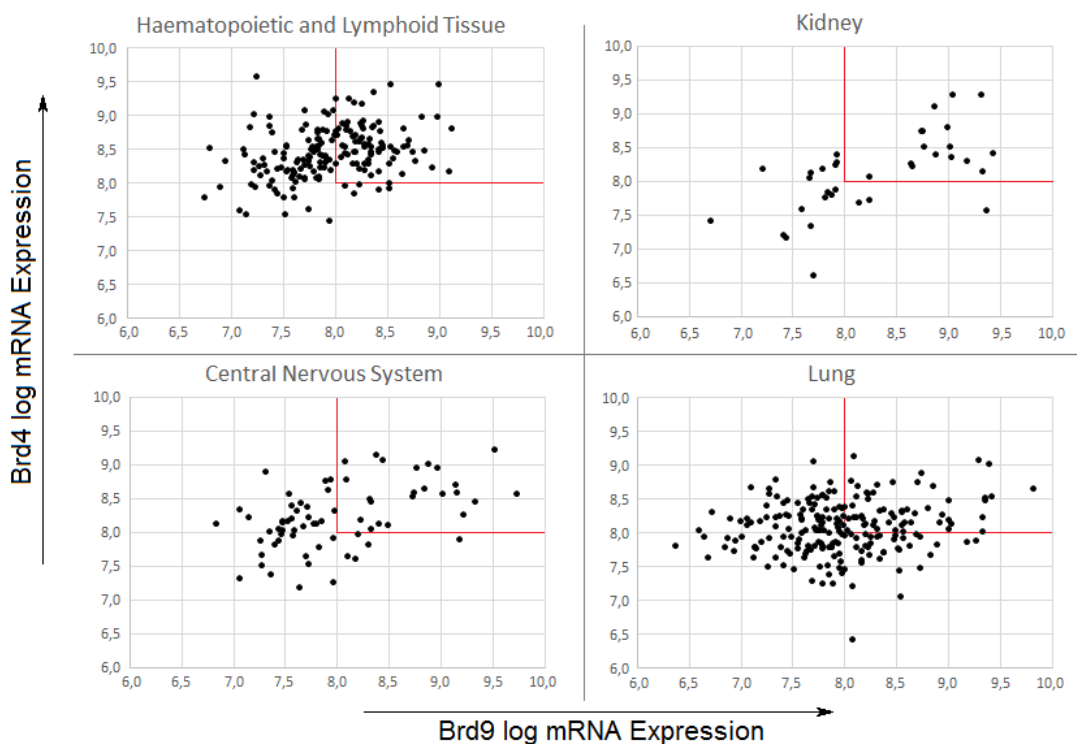


Figure 55: Expression levels of Brd4 and Brd9 mRNAs among different cancer cell lines. Data is based on Cancer Cell Line Encyclopedia microarray datasets. mRNA expression is represented in Robust Multi-array Average (RMA) units. A log value higher than 8,0 is considered to be highly expressed and is highlighted with red lines.

BET inhibitors like JQ1 are primarily being characterized by the downregulation of cMyc transcription, while their alternative effects on the transcriptome might be overlooked. Larger microarray datasets are oftentimes omitted from in-depth analyses, since the dysregulated secondary factors are known generate excessive background signal. These difficultly identifiable gene sets were also problematic in the microarrays carried for this project. From the first eight hour microarray we were not able to identify any specific molecular pathway being affected, aside from a vast cMyc related gene sets and a broadly immunosuppressive background, which we later were able to trace to NF- κ B inhibition (Figure 56). Combining the information from a follow up array with a shorter treatment time allowed us to pinpoint the genes directly affected by MMQO. Nevertheless, in retrospect we realize that in addition to utilizing cancer cells like Jurkats for this type of an assay we should have included a normal healthy sample as a comparison, to filter out significant cMyc independent signals.

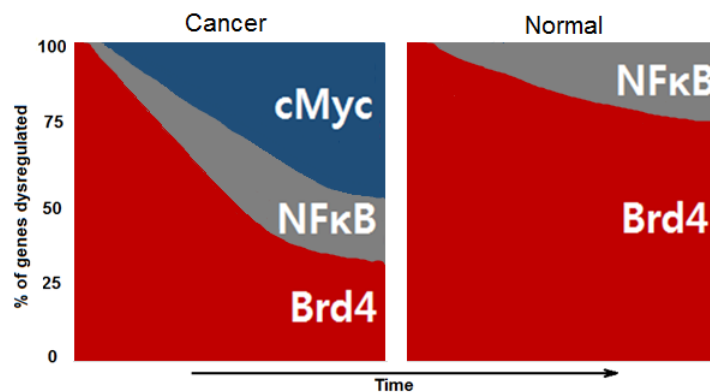


Figure 56: Proportions of genes affected by different factors observed in Jurkat cells and expected signal from healthy cells.

Recently, the group of Johannes Zuber elaborated which cancer related targets of Brd4 inhibition are additionally affecting acute myeloid leukemia cells utilizing nascent RNA-Seq. The benefit of identifying nascent pre-mRNAs within a few hours after treatment allowed them to identify the specific target genes downregulated by Brd4 inhibition, rather than detecting secondary unspecific products by other factors such as cMyc. These included tumorigenesis related transcription factors GATA2, TFAP4, Myb or intracellular kinases like PIK3IP1 and Cdk6 (data unpublished), demonstrating that although the downregulation of cMyc is a crucial hallmark in combating cancer with bromodomain inhibitors, understanding how the remodelling of the regulatory landscapes changes by utilizing more specific methods will be as crucial.

3. Role of bromodomains and MMQO in HIV-1 reactivation

Our results confirmed how bromodomain inhibitors like MMQO are able to function even in Tat-negative HIV minigenomes (Figure 52). This stochastic expression further supports the hypothesis of BET inhibitors inducing viral transcription independently of the Tat-Brd4 competition for P-TEFb sequestration (Boehm et al. 2013). As described by Razoogy et al. even minimal “shocking” events of latent HIV-1 could be enough to establish efficient positive feedback loop by Tat. This observation suggests that perhaps the “shock” capable drugs should concentrate on inducing the initial stage of viral transcription when no Tat is available, rather than inducing synergistic activation of the viral transcription at later phases. A more sensible method for reverting repressive transcription in physiological settings might then be with lower doses of compounds to minimize side effects from the compounds, while still crossing the threshold for Tat production.

In addition to Brd4 bromodomain inhibition functioning on the release of P-TEFb, we can hypothesize MMQO to function with alternative mechanisms against viral latency. Based on our microarray data, experimental results and a combination of previously suggested hypotheses the possible explanations for the functioning of MMQO through host factors include:

Depletion of Brd2 from the viral promoter. JQ1 is known to target Brd2 and counteract viral repression by inhibiting its ability to recruit HDACs. MMQO’s interaction with Brd2 has never been investigated, but due to the high similarities of the bromodomains of Brd2 and Brd4, it is highly likely for MMQO also to function on Brd2. Though Brd2 remains the less studied protein of the two, it is known to sequester the P-TEFb complex similarly to Brd4 (Malovannaya et al. 2011), thus probably further assisting in the hindrance of this factor from the 5’LTR. Alternatively, the Brd2 protein is hypothesized to associate with the SWI/SNF complex (Denis et al. 2006), though this interaction has not been demonstrated in the HIV-1 promoter.

BAF inhibition. The SWI/SNF BAF sub-complex has been demonstrated to position the repressive Nuc-1 nucleosome immediately downstream of the TSS to promote viral latency (Rafati et al. 2011). The chemical inhibition of BAF by targeting it with caffeic acid phenethyl ester and pyrimethamine has been shown to displace the BAF complex from the 5’LTR (Stoszko et al. 2015) and it can be hypothesized that the inhibition of bromodomains like

Brd9 will assist in this repression. The effect of Brd9 localization and possible displacement from the promoter needs to be further elaborated, though our initial screening suggests it to have little effect on the viral reactivation.

In addition to targeting the BAF complex via Brd9, MMQO could affect the function of BAF via Brd4. A poorly characterized member of the BAF complex is the glioma tumor suppressor candidate region gene 1 (GLTSCR1) protein (Middeljans et al. 2012), that coincidentally has been shown to interact with Brd4 (Rahman et al. 2011). Interestingly, the interaction between Brd4 and GLTSCR1 was shown to be necessary for the activation of bovine papillomavirus long control region independently of P-TEFb and the bromodomains of Brd4. Furthermore, Brd4 inhibition by JQ1 and a knockdown of BRG1, the central catalytic ATPase of the BAF complex, is known to yield in similar changes of the transcriptome and both proteins co-localize almost identically at the *MYC* enhancer in RN2 leukemia cells (Shi et al. 2013) (Figure 57A). According to the author's knowledge, the interaction of BAF and Brd4 in context of HIV latency has not been investigated.

BET inhibitors release Brd4 from the NF- κ B. Brd4 is known to interact with the NF- κ B subunit RelA at KAc-310 and enhance its global transcriptional activity. Though the repressive NF- κ B p50 homodimer is known to recruit HDACs to 5'LTR and suppress transcription initiation (Williams et al. 2006), no such mechanism has been described for the active p50-RelA heterodimer. Nevertheless, it could be hypothesized that Brd4 masks the RelA subunit, rendering the NF- κ B complex inactive within the 5'LTR. This rationale was suggested visually by Battistini & Sgarbanti, though unfortunately it went unelaborated (Battistini & Sgarbanti, 2014; Figure 3).

Another possible hypothetical mechanism for NF- κ B's activity might involve P-TEFb. Though P-TEFb abundance is tightly controlled in the nucleus, it is possible that in absence of viral Tat, an alternative mechanism might assist in the sequestration of P-TEFb to the viral promoter. For example the phosphorylation of Ser276 of the RelA subunit of the NF- κ B complex has been shown to allow the complex to interact with the CDK9 subunit of P-TEFb (Nowak et al. 2008). Coincidentally the same phosphorylation is also required for the binding of Brd4 (Brasier et al. 2011). It can be hypothesized that the release of Brd4 from NF- κ B can facilitate its introduction of the P-TEFb complex to the transcriptional machinery, albeit at a lower efficiency than with the viral catalyst Tat.

BET inhibitors release Brd4 from other transcription factors needed for HIV-1 transcription. HIF1 α has been shown to induce viral transcription (Deshmane et al. 2011). Considering that our microarrays predict it to be the most inhibited transcription factor following MMQO treatment, it can be hypothesized that Brd4 directly interacts with HIF1 α and induces its transcriptional activity, while the inhibition of Brd4 by MMQO increases the free pool of HIF1 α to function on HIV-1.

Other transcription factors predicted by IPA to be inhibited in MMQO-treated Jurkat cells included runt-related transcription factor 1 (RUNX1) and GATA3 (data not shown). GATA3 has been described to be a viral activator (Yang & Engel, 1993). Interestingly, the transcriptional activity of the GATA protein family is known to be regulated by acetylation of its C-terminus, interaction to BET proteins and has been shown to be diminished upon BET inhibition (Gamsjaeger et al. 2011), though no direct link to this mechanism has been shown in the context of HIV-1.

The T cell specific transcription factor RUNX1 has been described as a repressor of HIV-1 (Klase et al. 2014). It has been implied that Brd4 and RUNX1 co-localize to the same loci throughout the genome (Richard Young, unpublished data), suggesting their direct interaction. Inhibition of this hypothesized interaction at the 5'LTR could be assisting HIV-1 reactivation.

Yin yang1 (YY1) was among the first transcription factors discovered to facilitate repressive chromatin modifications on Nuc-1 by recruiting HDAC1 immediately downstream of the HIV-1 TSS and its knockdown is known to result in reversal of HIV-1 quiescence (Coull et al. 2000, Barton & Margolis, 2012). YY1 has been shown to interact with Brd4 in pulldown experiments with purified YY1 expressed from *Escherichia coli* (Wu et al. 2013). Considering the proximity of Nuc-1 to the YY1 and the enrichment of Brd4 at Nuc-1 (Figure 42), the interaction between Brd4 and YY1 could be possible, though this interaction has never been witnessed. Taking in mind that the pulldown proteins were expressed in *E.coli* experiments carried out by Wu et al., it is likely that YY1 was not acetylated thus increasing the likelihood of it interacting with Brd4 bromodomain independently.

Indirect dysregulation of HIV-1 transcriptional modifiers. Boehm et al. hypothesize how BET inhibition can reprogram the expression profiles of chromatin modifying and transcription factor genes, thus indirectly affecting viral latency (Boehm et al. 2013). In our

assays, co-treatment of MMQO with PMA yielded a synergistic activation of viral transcription within only one hour, thus rendering this option unlikely (Figure 25). The only known protein that could be downregulated this rapidly in our assays is cMyc, a transcription factor that is known to exhibit a short protein and mRNA half-life. Importantly, cMyc has been shown to engage with HDACs on the 5' LTR (Jiang et al. 2007). Though BETi are known to downregulate cMyc rapidly and potently in leukemia cell lines, it is not clear if this reduction could affect viral expression within an hour on the 5' LTR. Furthermore, the physiological significance of cMyc regulation in context of HIV-1 latency can also be questioned, since the expression of *MYC* in primary cells is known not to be affected by BET inhibitors.

Interestingly, pulldowns with purified cMyc protein have demonstrated Brd4 to interact with it directly (Wu et al. 2013), and cMyc and Brd4 do considerably co-localize genome wide in CUTLL1 lymphoma cell lines (Figure 57B). Nevertheless, the nature of this interaction and its dependency on the bromodomains of Brd4 remains unresolved, as does its significance in context of HIV-1 latency.

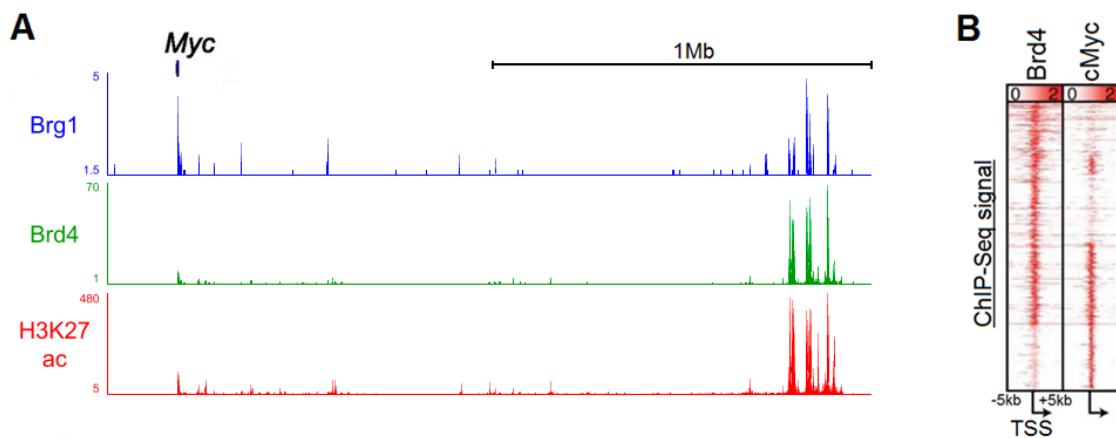


Figure 57: cMyc and Brd4 overlap from literature. (A) ChIP-seq occupancy profiles of Brg1, Brd4 and H3K27ac, obtained in RN2 cells (in reads per million). Image adapted from Shi et al. 2013. (B) ChIP-Seq signal density heat maps show Brd4 and cMyc at detected gene loci. Genes are clustered based on Brd4 signal density. Scale represents reads per million (RPM). Image adapted from King et al. 2013.

Steric hindrance of 5'LTR by Brd4. Although Brd4 in its chromatin binding is often depicted to bridge two different nucleosomes while connecting enhancer regions with promoters (Liu et al. 2013), this type of dinucleosomal interaction has never been validated experimentally. It could be hypothesized that the dual-bromodomain BET proteins, which have been

demonstrated thoroughly to have high affinities to acetylated lysines of the core histones, could be able to bridge different nucleosomes. Though Brd4 is primarily an activating mark for host genes, in case of HIV-1 could compress the 5'LTR (Figure 58). BET proteins have been shown to homo- and hetero-dimerize with each other, which could further stabilize this transcriptionally repressive structure (Gutierrez et al. 2012). A similar repression model has been described with the participation of HDACs (Rasmussen et al. 2013).

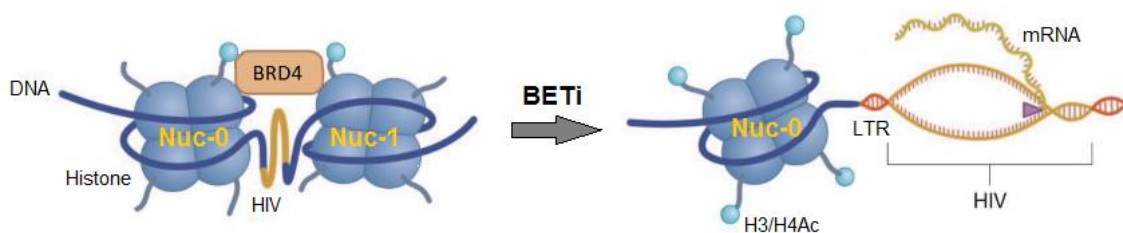


Figure 58: Model depicting Brd4 bridging Nuc-0 and Nuc-1 in the 5' LTR genome. Brd4 monomer is depicted to interact with two acetylated histone tails from different nucleosomes. Upon inhibition with BET inhibitors, chromatin loosens, Brd4 and Nuc-1 are evicted from the promoter and active transcription may ensue.

Since the BET family is known to interact with a wide variety of proteins, the steric repression by BET proteins could additionally be mediated by other determinants. Brd4 was recently shown to interact with and acetylate the linker histone H1.0 (Devaiah et al. 2016), a factor known to function as condensation of nucleosomes into a higher-order structures. Fittingly, H1.0 is known to be enriched in condensed chromatin (Morales et al. 2016), various H1 variants have been demonstrated to be enriched in HIV core promoter (Brendan Bell, unpublished data) and introduction of exogenous H1 proteins to latent cells has been shown to severely inhibit PMA induced HIV-1 transcription (Kozlowski et al. 2016). Examining the localization of H1 variants in the latent 5'LTR and if their enrichment changes in response to different LRAs should help elucidate if an inhibitory effect is carried out by these linker histones and if their function is related to BET proteins.

Brd4 associates with G-quadruplex structures. G-quadruplex (G4) structures are tertiary structures of DNA that form in guanine rich areas of the genome, often localized within functional regions of the genome and displaying high conservation between different species (reviewed in Rhodes & Lipps, 2015). Curiously, the formation of the quadruplexes has been described in loci that are often associated with Brd4, though the correlation between them has never been proposed. Examples of such sites include gene enhancer regions (Hegy, 2015), promoters of oncogenes like cMyc and HIF1 α (Siddiqui-Jain et al.

2002, Chen et al. 2014) and most importantly in the 5'LTR of HIV-1 (Perrone et al. 2013, Tosoni et al. 2015, De Nicola et al. 2016). Although Brd4 is not known to bind DNA itself, it possesses an extensive protein interactome through its various functional domains. Consistent with the idea of Brd4 associating with G4 structures, we witnessed a strong dysregulation of genes containing a high amount of guanine rich transcription factor motifs among the promoters (up to -1000bp from TSS). In fact, out of 89 highly enriched TRANSFAC motifs predicted by the g:profiler software, around 70 can be considered to contain four or more consecutive guanines within, a prerequisite for the formation of G4 structures. The motifs included the Sp1/2/6, WT1, AP-2, Egr1, ZF5, BTEB2, ETF, MAZ and KROX sites, suggesting the predictions to be nondiscriminatory and biologically random. Similar observations were made with other popular microarray analysis software tools, like DAVID and AMADEUS (data not shown). In fact the motifs for Sp1, AP-2, KROX, ZF5 and MAZ have been shown to be able to form G4 structures or at least correlate with them (Kumar et al. 2011, Raiber et al. 2012). Therefore it could be postulated that Brd4 associates with G4 structures and functions as a regulator in their stability. Further analysis of genome wide putative G4 structures, Brd4 ChIP-Seq and interactome datasets is needed to support this correlation.

The canonical model of Brd4 inhibition proposes that upon inhibiting its bromodomains, P-TEFb is released and sequestered by the viral Tat protein for viral elongation. However previous results, which were confirmed by our assays with Tat-negative minigenomes, suggest that alternative host-dependent and Tat-independent mechanisms are responsible for HIV-1 reactivation upon BET inhibition. In addition to functioning as a chromatin reader, Brd4 was recently demonstrated to function as an acetyltransferase by acetylating H3K122 (Devaiah et al. 2016) and phosphorylate RNA Polymerase II at Ser2 (Devaiah et al. 2012). H3K122 acetylation has been shown to be needed for evicting the affected nucleosome from the chromatin to facilitate transcription initiation, while the Ser2 phosphorylation of Pol-II is needed for transcription elongation. Contrary to these functions, Brd4 is not known to carry out those processes within the HIV-1 promoter and rather than collaborating with HIV-1 as an activating member, it paradoxically represses viral transcription. Although the negative hindrance of HIV by Brd4 is known for ten years already (Bisgrove et al. 2007), further studies are needed to explain its exact role in the viral promoter in a Tat-

independent manner. Here we proposed new models on how Brd4 could affect viral latency and global gene expression.

A prominent concern for the application of chromatin regulator inhibitors like MMQO is their unspecific targeting of the chromatin. HDAC inhibitors have been shown to be excessively immunosuppressive by restraining the effector functions of cytotoxic T-lymphocytes and possibly counteract against the “shock and kill” strategy (Jones et al. 2014). In response, bromodomain inhibitors have surged as a new method to combat HIV-1 latency. Concomitantly to our microarray results, Brd4 inhibitors are known to interfere less with the cellular transcriptome and thus present considerable potential as clinical therapeutics (Figure 33). Though no clinical trials have been established with bromodomain inhibitors against HIV-1, it is a prospect in consideration since BETi-s largely affect the virus at similar levels to HDAC inhibitors *ex vivo* yet preserving the host’s transcriptome from overly drastic dysregulations (Laird et al. 2015). Understanding the exact molecular mechanisms employed by bromodomain inhibitors will be crucial in assessing their efficacy in a clinical setting.

CONCLUSIONS

Results

1. Based on the FRET assays MMQO has the highest affinity towards the bromodomain of the SWI/SNF complex member Brd9. In the same assays MMQO also displays affinity towards the first bromodomain of the chromatin reader protein Brd4, but at 4-5 times lower doses.
2. MMQO releases the highly enriched Brd4 from the TSS of the repressed promoter, which probably is the main cause for the reactivation of viral transcription in the latency models used in our experiments.
3. Inhibition of Brd9 by chemical inhibitors has no effect on viral expression, suggesting that the reactivating effect witnessed with MMQO probably derives from its ability to inhibit Brd4.
4. MMQO is able to reactivate HIV transcription Tat-independently. Although the exact process for this activity remains unresolved, we proposed various possible molecular mechanisms that could reactivate viral transcription in a Brd4-dependent and Tat-independent manner.
5. MMQO displays a potent immunosuppressive behaviour, characterized by the downregulation of genes coding various CXCR, TNF and IL receptor family members. This immunoregulatory effect is caused by MMQO antagonizing the interaction between Brd4 and NF- κ B.
6. MMQO rapidly and potently downregulates cMyc expression in Jurkat cells, leading to a broad scale transcriptional dysregulation, thus inhibiting the proliferation of these cells. This downregulation can originate from both Brd4 and Brd9 inhibition, allowing us to hypothesize that MMQO-like compounds could be used against a variety of cancers displaying dependency for bromodomain proteins.
7. Though bromodomain inhibition transcriptome of MMQO resembles that of HDAC inhibition, it targets a considerably more limited set of genes and highlights the potential of BET inhibitors having less side effects than HDAC inhibitors.
8. Brd4 inhibitors and HDAC inhibitors can be identified and profiled by characterising the differential expressions of their target genes.

9. The inhibition of BRD4-BD2 with RVX-208 has minimal effect on viral reactivation, though the compound does exhibit a positive effect at higher doses, suggesting towards an unspecific function against other BET family bromodomains.
10. Clioquinol, an antimalarial compound known to additionally function as an HDAC inhibitor, was not able to induce viral reactivation.

Annex

11. Bromodomain inhibition by MMQO does not induce the MAPK pathways as previously published. Our results could not confirm any transcriptional similarities between JNK inducing stimuli and MMQO. We neither witnessed any phosphorylation of JNK or its downstream members in response to MMQO treatment.
12. MMQO does not induce any phosphorylation of Akt Ser473, an activating mark for this kinase, suggesting MMQO to function independently of this pathway.
13. MMQO does not induce any release of the transcription factor β -catenin and probably functions in an independent pathway. Although MMQO synergistically induced HIV-1 transcription in combination with LiCl, a β -catenin inducer, MMQO antagonized the upregulation of other LiCl target genes.
14. The increase of cAMP by forskolin synergistically induces HIV transcription in combination with MMQO.

MATERIALS AND METHODS

1. Materials

1.1 Reagents

Name	Working Concentration	Company
BAY11-7085	20 μ M	Sigma
Bio-MMQO	x	Custom
Camptothecin	5 μ M	Acros Organics
Clioquinol	10-30 μ M	Sigma
DMSO	Solvent	Sigma
HMQ	200-400 μ M	Sigma
I-BRD9	10 μ M	Selleckchem
JQ1 (+)	1 μ M	Cayman
MMQO	80-200 μ M	Custom
MQD	200-400 μ M	Custom
Nocodazole	50ng/ml	Selleckchem
PMA	10nM	Sigma
RVX-208	80 μ M	Selleckchem
SAHA	5 μ M	Selleckchem
TSA	400nM	Sigma

1.2 Plasmids

pEV731 Lentiviral plasmid that expresses the Tat-positive HIV minigenome LTR-Tat-Ires-GFP-LTR, generously donated by Dr. Eric Verdin (Gladstone Institutes, San Francisco, USA).

pEV658 Lentiviral plasmid that expresses the Tat-negative HIV minigenome LTR-Ires-GFP-LTR, generously donated by Dr. Eric Verdin (Gladstone Institutes, San Francisco, USA).

pVSVG Plasmid that codes for the viral capsid proteins, acquired from Clontech.

pCMV Δ R8.91 Plasmid that contains the viral *gag* and *pol* genes, necessary for lentiviral particle production. Generously donated by Dr. Didier Trono

1.3 Primers

Oligonucleotides for gene expression

Name	Sequence
ADMfw	TGCCCAGACCCTTATTCGG
ADMrev	AGTTGTTTCATGCTCTGGCGG
APOA1fw	ATGAAAGCTGCGGTGCTGA
APOA1rev	TCACTGGGTGTTGAGCTTC
CCR7fw	TGGTTTTACCGCCCAGAGAG

CCR7rev	GACACAGGCATACCTGGAAA
CD28fw	CGGACCTTCTAAGCCCTTTT
CD28rev	ATAGGGCTGGTAATGCTTGC
CD83fw	CGGTCTCCTGGGTCAAGTTA
CD83rev	AGAACCATTTTGCCCCTTCT
CXCR3fw	ACACCTTCCTGCTCCACCTA
CXCR3rev	G TTCAGGTAGCGGTCAAAGC
CXCR7fw	TGGGTGGTCAGTCTCGT
CXCR7rev	CCGGCAGTAGGTCTCAT
DDX46fw	GATGAGGATGCTGCAGTTGA
DDX46rev	TGGAGCAGGAACACTTGATG
EGR1fw	TGAACAACGAGAAGGTGCTG
EGR1rev	TGGGTTGGTCATGCTCACTA
FOSfw	AACTTCATTCCCACGGTCAC
FOSrev	GGCCTCCTGTCATGGTCTT
GAPDHfw	GAGTCAACGGATTTTGGTCGT
GAPDHrev	TTGATTTTGGAGGGATCTCG
H1.0fw	CCTGCGGCAAGCCCAAGCG
H1.0rev	AACTTGATCTGCGAGTCAGC
H1xfw	TTCCTTCAAGCTCAACCG
H1xrev	TGCCTTCTTCGCTTTGTG
HEXIM1fw	GACCTGGGAAGAGAAGAAAAG
HEXIM1rev	GAGGAACTGCGTGGTGTATAG
HIV_3'_fw	ATCCACTGACCTTTGGATGG
HIV_3'_rev	G TACTCCGGATGCAGCTCTC
HIV_5'_fw	AGTAGTGTGTGCCCGTCTGT
HIV_5'_rev	TCGCTTTCAGGTCCCTGTTCG
ICOSfw	GGATGTGCAGCCTTTGTTGT
ICOSrev	GGTCACATCTGTGAGTCTAGATTTT
IFIT1fw	GCCTCCTTGGGTTCGTCTATAA
IFIT1rev	TCAAAGTCAGCAGCCAGTCTCA
IL2RG fw	GCCTACCAACCTCACTCTGC
IL2RG rev	TAGCATCTGTGTGGCCTGTC
IL7Rfw	CGCCAGGAAAAGGATGAAA
IL7Rrev	ATACATTGCTGCCGGTTGG
IRF7fw	ACAGACCCCCAGCAGGTAG
IRF7rev	CCACCTCCCAGTACACCTTG
ISG15fw	CAGATCACCCAGAAGATCG
ISG15rev	CCCTTGTTATTCTCACCAG
LAT fw	AGCCGGGAGTATGTGAATGT
LAT rev	CTCTCACCAGGCCCTCAGT
LMO1 fw	AAGGACCGCTATCTGCTGAA
LMO1 rev	GTGCCAAAGAGCCTCAGGTA
LRIG1fw	GGTGAGCCTGGCCTTATGTGAATA
LRIG1rev	CACCACCATCCTGCACCTCC

MAFBfw	CATAGAGAACGTGGCAGCAA
MAFBrev	GAATGGGGATAAGGGAAGGA
MEPCEfw	GCCAGAGCAGTTCAGTTCCT
MEPCErev	CAGGACGCTGGAAGCCTTTA
MYCfw	TCAGAGAAGCTGGCCTCCTA
MYCrev	CTGTCGTTGAGAGGGTAGGG
OAS2fw	GAGTGGCCATAGGTGGCTC
OAS2rev	ACCACTTCGTGAACAGACAGA
RAG1fw	CTGCTGAGCAAGGTACCTCAGCCAG
RAG1rev	GAGAGGGTTTCCCCTCAAAGGAATC
SAMSN1fw	TCAACTGAGGCACATGAAGG
SAMSN1rev	TGGGCATTCTCTCCATCTTC
SORL1fw	AAAGGTGGTGCATCTCTTGG
SORL1rev	GGCTGACACACACAAACACC
SP1fw	TGCAGCAGAATTGAGTCACC
SP1rev	ACTGCTGCCACTCTGTTCT
STAT5Afw	GGCCATCCTAGGTTTTGTGA
STAT5Arev	ATGGTTTCAGGTTCCACAGG
TERTfw	TGTTTCTGGATTTGCAGGTG
TERTrev	GTTCTTGGCTTTCAGGATGG
TRAILfw	ACCAACGAGCTGAAGCAGAT
TRAILrev	CAGCAGGGGCTGTTCACTACT
TUBB3fw	AACGAGGCCTCTTCTCACAA
TUBB3rev	GGGTCTGCCATCAGAGCTT
VAV3fw	CATGAAGGACCCCTTTACA
VAV3rev	GCTTGACTGCATCACTTGGA
XBP1fw	CGAATGAGTGAGCTGGAACA
XBP1rev	CCAAGCGCTGTCTTAAGTCC
ZBTB1fw	ATGGCCAGTGGTGAAATAGGG
ZBTB1rev	GGAAGACAGAAAAGATGGTGCC

Oligonucleotides used for HIV 5'LTR chromatin immunoprecipitation

Primer pair	Sequence	Position
15-137	AAGGGCTAATTCCTCCCAA	76
	AGCACCATCCAAAGGTCACT	
75-172	CCTGATTGGCAGAACTACACAC	124
	TCTACTTGCTCTGGTTCAACTGG	
124-224	CCTTTGGATGGTGTCTCAAGTTAG	174
	ATGCTGGCTCATAGGGTGTAAAC	
182-293	GTGGCGCCCGAACAGG	238
	CACCAGTCGCCGCC	
215-314	GAGCCAGCATGGGATGG	265
	CTCCGGATGCAGCTCTC	
315-419	TACTACAAAGACTGCTGACATCG	367

	TCTGAGGGCTCGCCACTC	
350-457	GGGACTTTCCGCTGGGGAC	404
	AGAGACCCAGTACAGGCAAAA	
379-513	GGTGTGGCCTGGGCGGGA	446
	GTTCCCTAGTTAGCCAGAGAGC	
403-521	AGTGCGGAGCCCTCAGATG	462
	AGCAGTGGGTTCCCTAGTTAGC	
442-572	TTGCCTGTA CTGGGTCTCTCTGG	507
	AGACGGGCACACACTACTTTG	
552-663	AGTAGTGTGTGCCCGTCTGT	608
	TCGCTTTCAGGTCCTGTTCG	
583-714	GGTAACTAGAGATCCCTCAGAC	649
	CTTCAGCAAGCCGAGTCC	
GD1fw	CATCCCTGGACTGATTGTCA	
GD1rev	GGTTGGCCAGGTACATGTTT	

1.4 Antibodies

Target	Western blot working concentration	Company	Reference
α -cleaved Casp3	1/1000	Cell Signal	9664S
Anti Mouse perox	1/4000	GE	#NA931V
Anti Rabbit perox	1/4000	GE	#NA934V
Anti Mouse Odyssey	1/10000	LI-COR	32210
Anti Rabbit Odyssey	1/10000	LI-COR	68021
α -Tubulin	1/3333	Sigma	9026
Bcl2 (50E3)	1/1000	Cell Signal	2870
Brd4	1/2000	Bethyl Labs	A301-985A50
cMyc	1/1000	Santa Cruz	sc-764
H3	1/1000	Abcam	ab1791
H3Ac	1/5000	Upstate	06-599
H4Ac	1/2000	Upstate	06-866
PARP p25	1/1000	Abcam	ab32064
γ -H2AX (Ser139)	1/2500	Millipore	07-164

1.5 shRNA sequences

shRNA	Plasmid ID	Sequence
BRD4 I	TRCN0000021428	CCGGCCAGAGTGATCTATTGTCAATCTCGAGATTGACAATAGATCACTCTGGTTTTT
BRD4 II	TRCN0000021427	CCGGCCTGGAGATGACATAGTCTTACTCGAGTAAGACTATGTCATCTCCAGGTTTTT
BRD2 I	TRCN0000006308	CCGGCCCTTTGCTGTGACACTTCTTCTCGAGAAGAAGTGTCACAGCAAAGGGTTTTT
BRD2 II	TRCN0000006309	CCGGGCCCTCTTACGTGATTCAAACCTCGAGTTTGAATCACGTAAAGAGGGCTTTTT

2. Methods

2.1 Cell culturing

Jurkat cells or latently infected derivatives carrying pEV731 or pEV658, were grown at 37°C with 5% CO₂ in RPMI 1640 medium (Sigma, R8758), supplemented with 10% fetal bovine serum (FBS), without additional antibiotics. Jurkat clones were previously described by Jordan et al. 2001, while heterogeneous populations were described in Gallastegui et al. 2012. HEK293T, HepG2 and HeLa cell lines were grown at 37°C with 5% CO₂ in Dulbecco's modified Eagle's medium GlutaMax medium containing 10% FBS, supplemented with 100U/ml penicillin and 100µg/ml streptomycin. The heterogeneous HeLa populations were created during this project.

When indicated, cells were treated with reagents, concentrations and durations indicated in the figure legends. All reagents were dissolved in DMSO and when possible, DMSO treatment was used as a negative control. When possible, the concentration of DMSO did not increase above 1µl/1ml in treatment experiments.

2.2 Microarray

Total RNA was extracted using High Pure RNA isolation Kit (Roche) according to the manufacturer's instructions. High RNA integrity was assessed by Bioanalyzer nano 6000 assay. Sample preparation was previously described by Millán-Ariño et al. 2014. For each sample, 100ng of total were reverse transcribed into cDNA with a T7 promoter and the cDNA was in vitro transcribed into cRNA in the presence of Cy3-CTP using the Low input quick Amp kit (Agilent). Labeled samples were purified using RNeasy mini spin columns (Qiagen). Then, 600ng of cRNA were preblocked and fragmented in Agilent fragmentation buffer and mixed with Agilent GEx Hybridization mix. Hybridization mix was laid onto each sector of subarray gasket slide and sandwiched against an 8 × 65K format oligonucleotide microarray (Human v1 Sureprint G3 Human GE 8x60k Microarray, Agilent design ID 028004) inside a hybridization chamber, which was hybridized overnight at 65°C. Subsequently array chambers were disassembled submerged in Agilent Gene Expression Buffer 1 and washed 1 min in another dish with the same solution with a magnetic stirrer at 200 rpm at room temperature, followed by 1 min in Agilent Gene Expression Buffer 2 with a magnetic stirrer at 200 rpm at 37°C and immediate withdrawal from the

solution and air drying. Fluorescent signal was captured into TIF images with an Agilent scanner using recommended settings with Scan Control software (Agilent). Signal intensities were extracted into a tabulated text file using Feature Extraction software (Agilent) using the appropriate array configuration and annotation files. The normalized log₂ intensities were obtained using quantile method with normalized expression background correction the Bioconductor Limma package in R. The microarray sample preparations and experiments were carried out by the lab of Dr. Lauro Sumoy, IMPPC.

2.3 Microarray analysis

Genes were sorted and organized for further analysis based on the obtained log₂ values. Transcripts with a q -value > 0,05 were considered insignificant and transcripts represented in multiples had their fold change calculated to a mean value. Datasets were organized by fold changes, where FC > 1,5 or FC < -1,5 was considered significantly differentially expressed, and analyzed utilizing the following software tools:

g:profiler: Public tool used to determine overrepresentation among GO, KEGG, Reactome and TRANSFAC annotations. Data analysis was carried out with strong hierarchical sorting.

AMADEUS: Public tool used specifically to determine overrepresentation among TRANSFAC transcription factor motif gene sets.

DAVID: Database for Annotation, Visualization, and Integrated Discovery. Popular but slightly outdated public tool used for gene ontology analysis. Useful since it compiles information from most major bioinformatics sources and was used as a control for g:profiler.

GSEA: Gene Set Enrichment Analysis. Public tool developed by Broad Institute, where the raw target datasets are compared against other curated gene sets, corresponding to biological pathways, transcription factor motifs, gene proximal locations on genome *etc.*

IPA: Ingenuity Pathway Analysis. Microarray analysis platform where the raw target datasets are compared against curated gene sets that are constantly updated by Ingenuity Systems (Qiagen). Useful especially for transcription factor (TF) analysis, since the TF activity is not only predicted by the enrichment of binding motifs, but is

additionally based on other experimental data (microarrays, knockdowns or knockins, chemical inhibitors *etc*).

R: Used to calculate correlation matrices and scatterplots of our arrays. Calculations were performed Andrea Izquierdo-Bouldstridge.

2.4 RNA extraction, reverse transcription and Real Time PCR

Total RNA was extracted using either the High Pure RNA isolation kit (Roche Applied Science) or the TRIzol kit (Ambion). cDNA was generated from 50-100ng of RNA using the Superscript VILO cDNA Synthesis kit (Invitrogen) or iScript cDNA synthesis kit (Bio-Rad). Gene products were analyzed by qPCR using SYBR Green master mix (Invitrogen) and specific oligonucleotides in a Roche Applied Science 480 light cycler machine on 96-well plates. Each value in gene expression experiments was corrected by human GAPDH and represented as relative units. Each experiment was performed in duplicate and standard error of the mean was used to express variability.

2.5 Protein extraction, gel electrophoresis, and immunoblotting

Cells were washed once with PBS and proteins extracted in the lysis buffer indicated in the figure legends. Lysis buffer was supplemented with 1x Protease inhibitor cocktail (Roche), 1mM Na₃VO₄, 5 mM NaF, 1 µg/ml leupeptin, 0.5 µg/ml pepstatin, 0.5 µg/ml aprotinin, 20mM β-glycerophosphate and 1 mM PMSF to block product degradation. Protein concentration was determined by BCA assay (Pierce) and 10-30µg of protein was boiled in Laemmli buffer and electrophoresed in 7,5-15% SDS-polyacrylamide gels. Separated proteins were transferred to nitrocellulose or PVDF membranes (constant 400mA; 4°C) for 1,5h. Blots were blocked in Tris-buffered saline (TBS) solution containing 0.1% Tween 20 (TBST) and either 5% nonfat dry milk, 3% bovine serum albumin or 1:1 Odyssey blocking buffer for 1h, incubated with primary antibodies at room temperature for 1h or overnight at 4°C, followed by 3x 10 minutes washes with TBST and incubated with secondary antibodies for 1h at room temperature. Following 3x washes of the secondary antibodies, the immunodetection of specific proteins was carried out with primary antibodies using an ECL system (GE Healthcare) or Odyssey® Infrared Imaging System (LI-COR).

RIPA buffer is previously described (Abcam protocols), while the High Salt Extraction protocol was described in Ai et al. 2011.

2.6 Virus production and infection

3×10^6 HEK-293T cells were transfected with the plasmids of interest (10 μ g), pCMV Δ R8.91 (15 μ g) and pVSVG (5 μ g) using calcium phosphate (BD Bioscience) according to manufacturer's instructions. Medium was collected every 48h for 4 days and ultracentrifuged for 1h 30min at 26.000 rpm and 4°C in a sucrose gradient to concentrate the viral particles. Pellet containing the viruses was dissolved in target cell line medium and used for the infection. Cells were infected via spinoculation at 1200rpm for 2h at room temperature at different multiplicity of infection values. For knockdown experiments the positively infected cells were sorted by 24h puromycin treatment (10 μ g/ml).

2.7 Flow cytometry

GFP fluorescence was measured in Cytomics FC500 MPL flow cytometer or CytoFLEX system (Beckman Coulter). A two-parameter analysis was used to distinguish viable cells (identified by forward and side scatter) containing GFP-derived fluorescence (525nm) from the background utilizing. Fluorescence was represented in a logarithmic scale and on average 10000+ events were observed per sample. Optical calibration was carried out using 10nm fluorescent beads (Flow-Check fluorospheres, Beckman Coulter). Cell sorting was carried out with FACS Aria cell sorter (BD Biosciences). 5 days post infection cells were treated with 10nM PMA for 24h and the GFP+ cells were sorted out. 5 days post sorting the GFP-negative cells were sorted out to represent the latent population.

2.8 Bliss independence model

Lack of synergy between JQ1 and MMQO was calculated according the Bliss independence model, described previously by Laird et al. 2015. The Bliss independence assumes that two different drugs act through separate molecular mechanisms and therefore in an additive manner, first described by Bliss, 1956.

2.9 In silico docking

Crystal structures for the analysis were obtained from RCSB Protein Data Bank and structures only of human origin were used for predictions. PDB names for each analysis are listed in the figure description. The following software was used:

Swissdock: Simple and fast to use public software useful for initial hypothesis confirmation. Protein-ligand interaction is predicted without concentrating on specific protein domains.

AutoDock Vina: Public software for more specific protein-ligand predictions, that allows to change multiple aspects in the protocol, such as narrowing down the prediction to a certain domain or presence of solvents.

Maestro: Most sophisticated and commercial software from the programs used. Similar to AutoDock Vina, but with more complex visualization tools and prediction algorithms. Predictions with Maestro were carried out by Salvador Guardiola, IRB Barcelona.

2.10 Nuclear Magnetic Resonance of MMQO with Brd4-BD1

The 2D ^1H - ^{15}N HSQC spectroscopy was carried out according to the published protocol in Gacias et al. 2014 in the laboratory Dr. Ming-Ming Zhou and at the NMR facility at the New York Structural Biology Center, USA.

2.11 Homogeneous Time Resolved Fluorescence

HTRF assays were carried on the Cisbio platforms in the laboratory of Dr. John Porter in Structural Genomics Consortium Oxford, UK.

2.12 Chromatin Immunoprecipitation

Sample preparation: Chromatin extraction was carried out as described previously (Anders et al. 2014). Cells were fixed by adding 1% formaldehyde for 15min in cell culture medium at 37°C. Chemical cross-linking was terminated by addition of TRIS buffer, pH 7.5, to a final concentration of 300mM TRIS at room temperature for 5min. Cells were washed three times with PBS containing protease inhibitors (detailed in the protein extraction methods), harvested using a silicon scraper, centrifuged, and the derived pellets were centrifuged. Cells were lysed in Lysis buffer and cell nuclei were washed with Nuclear wash buffer. Nuclei were resuspended in Sonication buffer and sonicated using Diagenode Bioruptor for 20 cycles (30s each)

on ice with 30s intervals between cycles to generate chromatin fragments between 200 and 500bp. After sonication material was centrifuged at maximum speed 10min at 4°C, and cell debris / SDS-free supernatant was recovered.

Determining concentration: 50µl of the chromatin was treated with Proteinase K overnight at 65°C to de-crosslink and digest the protein. DNA was recovered by phenol/chloroform extraction for DNA concentration quantification. The efficiency of the sonication was confirmed in a 1,2% agarose gel.

Chromatin immunoprecipitation: 30µg of chromatin was diluted IP buffer (0,01% SDS; 1,1% Triton X-100; 1,2mM EDTA pH8,0; 16,7mM Tris-HCl pH8,1; 167mM NaCl) with 5µg of antibody and protease inhibitors until final volume of 1ml. Immunocomplexes were recovered using 20µl of Protein A magnetic beads (Millipore) rotating overnight at 4°C, with IgG (Santa Cruz Biotechnology) being used as a control for non-specific interaction of DNA. Input was prepared with 10% of the chromatin material used for an immunoprecipitation. Beads with antibody/protein/DNA complexes were washed for 5min at 4°C in rotation with Washing buffers 1 (0,1% SDS; 1% Triton X-100; 2mM EDTA pH8,0; 20mM Tris-HCl pH8,1; 150mM NaCl), 2 (same as Wash buffer 1 but NaCl concentration increased to 500mM) and 3 (0,25M LiCl; 1% NP-40; 1% sodium deoxycholate; 1mM EDTA pH8,0; 10mM Tris-HCl pH8,1), and then twice with 1x Tris-EDTA buffer. Samples were de-crosslinked overnight at 65°C and recovered according to the IPure Kit manual. Samples were analysed according to real time PCR protocol, with corresponding input samples used for correction.

ANNEX

The c-jun N-terminal kinases (JNK) transmit the intracellular stress response, in response to extracellular stimuli such as those osmotic shock, UV irradiation or cytokines. JNK kinases have been shown to also be phosphorylated in response to extracellular TLR3 stimulation, leading to NF- κ B activation and eventual HIV-1 transcription (Bhargavan et al. 2016). Our previous results hinted at MMQO functioning via the MAPK pathway, specifically through the JNK (Gallastegui et al. 2012). Chemical inhibition of JNK proteins resulted in decreased levels of HIV-1 expression, while JNK itself became phosphorylated in response to treatment 15 minute treatment with MMQO (Figure 59). The phosphorylations of JNK Thr183/Tyr185 residues is considered its canonical activation signal, leading to its nuclear localization and kinase activity on TFs and other transcriptional regulators.

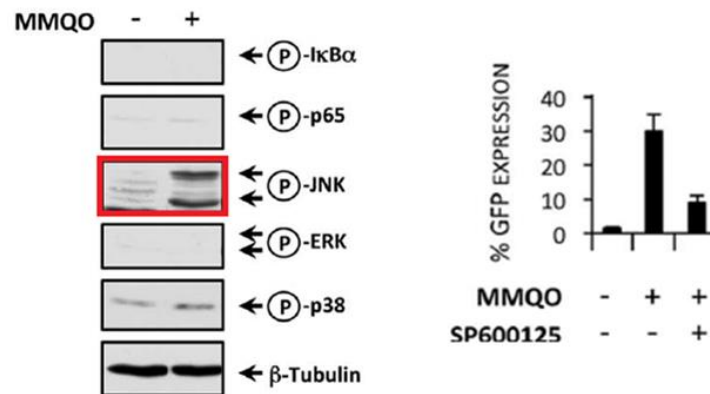


Figure 59: MMQO activity on JNK. (left) Native Jurkat cells were stimulated with MMQO (160 μ M) or left unstimulated for 15min. Total protein was extracted and immunoblotted against various phosphorylated forms of MAPKs and NF- κ B complex. (right) Flow cytometry of a heterogeneous latent Jurkat population treated 18h with MMQO (80 μ M), in combination with 1 μ M of SP600125 (a direct chemical JNK inhibitor), or left untreated. Y-axis represents the percentage of GFP-positive cells.

In addition to hypothesizing MMQO to functioning through immunosuppressive pathways as described in the „Results“ chapter of this dissertation, we initially were trying to find an overlap between MAPK pathways and the functioning of MMQO.

1. Comparison of MMQO target genes to MAPK pathway target genes

MAPK pathway activating agents TNF α , NaCl or Anisomycin induce specific MAPK pathway target gene expression by 15-30 fold on microarray platforms (Ferreiro et al. 2010). Strikingly we didn't witness any intense dysregulations of specific genes in either cell line after MMQO treatment in the first eight hour microarray, with only five genes being upregulated more than 4-fold (Figure 17C and Figure 18C). The highest upregulated gene (*EFR3B*) presented a fold change of +7,3 and the most repressed gene (*RAG1*) became

downregulated -8,06 times when compared to the untreated samples in Jurkat cells. To estimate the overlap between MAPK pathway activity and MMQO response we treated Jurkat cells for 3h and 8h with MMQO or anisomycin and compared the expression of target genes by qPCR. Anisomycin is a potent chemical inducer of both p38 and JNK pathways, displaying a more potent effect on the JNK family members (Ogawa et al. 2004). Measuring the levels of target genes at two different treatment time points would allow us to interpret the kinetic profile of each drug, since the activity of MAPKs is known to oscillate in response to anisomycin. Genes like *EGR1*, *JUN*, *FOS* and *MYC* are all known JNK pathway targets, while the rest of the genes were chosen based on their previous response to MMQO. To our surprise, majority of the genes tested exhibited markedly contrasting responses (Figure 60A-B). As expected, the fold change of *EGR1*, *JUN* and *FOS* all increased dramatically in response to anisomycin, while the effect of MMQO was minimal. Moreover, the target genes of MMQO, e.g., *RAG1*, *IL7R* and *CD28*, displayed a striking negative correlation anisomycin.

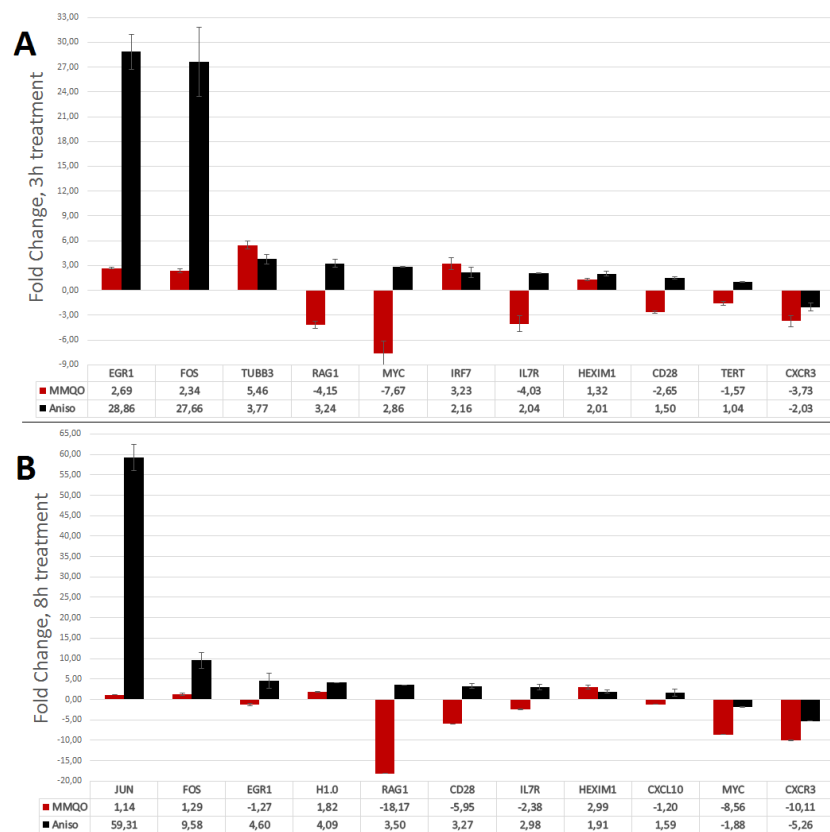


Figure 60: qPCR for target gene dysregulations by MMQO or Anisomycin. Jurkat cells were treated either 3h or 8h with MMQO (160 μ M), Anisomycin (10 μ g/ml) or left untreated. Genes were chosen based on their specificity towards previously published MAPK and MMQO responses. *GAPDH* was measured for normalization and results are represented relative to results from untreated cells. The means and S.D. values (error bars) are shown from a representative experiment measured in duplicate (mean values displayed separately below the bars).

Further analysis of the microarray with GSEA didn't suggest any strong MAPK pathway participation neither. Only three gene sets related to MAPK pathways had a reliable correlation to MMQO treatment (False Discovery Rate (FDR) q -value $<0,05$ but FamilyWise Error Rate (FWER) p -value $>0,05$), while the majority and the more prominent MAPK related pathways, such as "ACTIVATION_OF_JNK_ACTIVITY", "JNK_CASCADE" and "ACTIVATION_OF_MAPK_ACTIVITY", didn't present any enrichment. A selection of MAPK related gene sets is exhibited in Table 12.

NAME	Size	NES	FDR q -value	FWER p -value
REACTOME_MAP_KINASE_ACTIVATION_IN_TLR_CASCADE	49	1,99	0,007	0,119
REACTOME_NFKB_AND_MAP_KINASES_ACTIVATION_MEDIATED	69	1,88	0,015	0,598
REACTOME_JNK_C_JUN_KINASES_PHOSPHORYLATION_AND_ACTIVATION	16	1,707	0,049	1
ST_JNK_MAPK_PATHWAY	40	1,669	0,062	1
RESPONSE_TO_UV	25	1,51	0,186	1
BIOCARTA_STRESS_PATHWAY	25	1,243	0,342	1
RESPONSE_TO_OXIDATIVE_STRESS	46	1,19	0,503	1
HAN_JNK_SINGALING_UP	35	1,147	0,455	1
RESPONSE_TO_STRESS	505	1,12	0,542	1
ST_P38_MAPK_PATHWAY	37	1,07	0,562	1
BIOCARTA_P38MAPK_PATHWAY	39	0,998	0,666	1
HUI_MAPK14_TARGETS_UP	21	-0,959	0,699	1
REACTOME_GASTRIN_CREB_SIGNALING_PATHWAY_VIA_PKC_AND_MAPK	199	-0,962	0,692	1
MAPKKK_CASCADE_GO_0000165	104	-1,189	0,563	1
POSITIVE_REGULATION_OF_JNK_ACTIVITY	18	-1,192	0,352	1
REGULATION_OF_JNK_ACTIVITY	20	-1,194	0,352	1
STRESS_ACTIVATED_PROTEIN_KINASE_SIGNALING_PATHWAY	49	-1,217	0,567	1
JNK_CASCADE	47	-1,261	0,552	1
ACTIVATION_OF_JNK_ACTIVITY	16	-1,266	0,542	1
ACTIVATION_OF_MAPK_ACTIVITY	41	-1,356	0,543	1

Table 12: Table of MAPK related gene sets available and regulated by MMQO in Jurkat cells based on GSEA. In total 198 gene sets correlated positively with MMQO treatment with a significant q -value. Genes with a q -value $<0,05$ are highlighted. (NES, normalized enrichment score)

2. The lack of response by MAPKs following MMQO treatment

To further elucidate the role of MAPKs in MMQO's functioning we resorted to western blot analysis of phosphorylated forms of JNK, p38 and their downstream kinases. Peculiarly we were not able to witness any previously reported stress activation of JNK by MMQO in Jurkat cells, nor any of the JNK specific downstream specific transcription factors, such as cJun and JunD (Gallastegui et al. 2012, Lamb et al. 2003) (Figure 61A). Taking into account that the previous results by Gallastegui 2012 *et al.* were performed with different stimuli (Anisomycin and TNF α) than the one used in the current experiment (UV), we followed up with a treatment series of different mitogenic stress factors and compared them to the response by MMQO. Recurrently we did not observe any MAPK phosphorylation in response

to MMQO treatment when compared to UV, osmotic, translational or cytokine induced stress (Figure 61B).

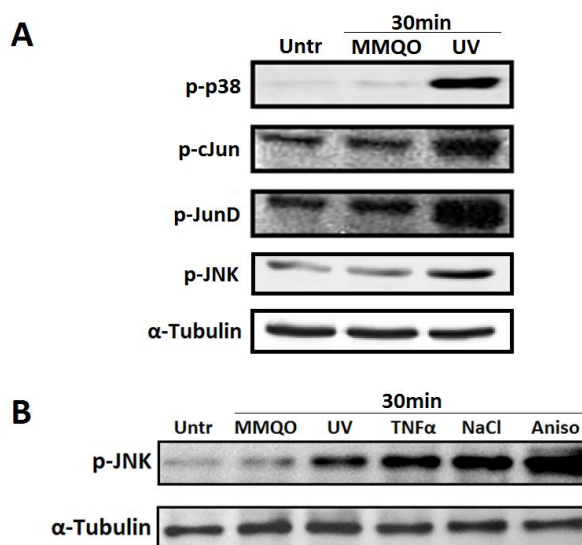


Figure 61: Western blot analysis of various MAPK pathway member phosphorylations in response to different stress stimuli. (A) Jurkat cells were incubated 30min with UV (20s, 20 J/m²), MMQO (160μM) or left untreated. Total protein was extracted with RIPA buffer and analyzed by immunoblotting against various MAPKs, their downstream transcription factors and α-Tubulin as a loading control. (B) Jurkat cells were incubated 30min with UV (20s, 20 J/m²), TNFα (10ng/ml), NaCl (1M), Anisomycin (10μg/ml), MMQO (160μM) or left untreated. Total protein was extracted with RIPA buffer and analyzed by immunoblotting against the phosphorylated form of JNK and α-Tubulin as a loading control.

3. MMQO in combination with MAPK inhibitors

To confirm the results obtained by immunoblotting we decided to study how MMQO functions in combination with various intracellular chemical inhibitors known to hinder the MAPK pathways. To block the JNK axis we utilized the previously applied inhibitor SP600125 to target the JNK family directly (Gallastegui et al. 2012), the upstream kinase MKK4 inhibitor myricetin (Kim et al. 2009), curcumin and betulinic acid to inhibit the direct downstream transcription factors C/EBP and AP-1 that are also known to function as HIV-1 activator (Huang et al 1991, Stein et al. 1989, Liu et al. 2009, Prasad & Tyagi, 2015).

In parallel we utilized the ligand-target prediction program LASSO (Ligand Activity by Surface Similarity Order) to speculate the protein target of MMQO, based on its surface properties (Reid et al. 2008). MMQO was juxtaposed against the active sites from total of 40 different receptor families provided by the program. Based on LASSO MMQO's conformation has the

highest possible affinity to the platelet derived growth factor receptor kinase family (PDGFR), with a bioactivity score of 0,69 (Table 13).

Category	Target	LASSO Score
Kinases	PDGFRb, platelet derived growth factor receptor kinase	0.69
Kinases	EGFr, epidermal growth factor receptor	0.06
Kinases	P38 MAP, P38 mitogen activated protein	0.03
Nuclear Hormone Receptors	PPARg, peroxisome proliferator activated receptor	0.03
Other Enzymes	HIVRT, HIV reverse transcriptase	0.02
Other Enzymes	InhA, enoyl ACP reductase	0.02
Serine Proteases	FXa, factor Xa	0.02
Kinases	SRC, tyrosine kinase SRC	0.01
Other Enzymes	HMGR, hydroxymethylglutaryl-CoA reductase	0.01
Metalloenzymes	PDE5, phosphodiesterase 5	0.01

Table 13: Top 10 predicted protein targets of MMQO. MMQO was translated into a numeric surface point descriptor sequence and juxtaposed against surface points of common protein active sites. The score indicates a normalized result ranging from 0 to 1, with 0 having no similarity to active molecules and 1 having the highest level of similarity.

The participation of PDGFRs was weakly supported by GSEA analysis, where among the most highly enriched related gene sets correlating to the upregulated genes was “PDGF_UP.V1.UP” with a *q*-value of 0,032. The tyrosine kinase PDGF receptor family are cell-surface ligand binding receptors that function by forming homo- or heterodimers between their alpha and beta polypeptides. Intriguingly, among the canonical affected targets of growth factor receptors (including PDGFRs) are the PI3K and MAPK pathways (Figure 62). These mechanisms are mostly needed for promoting cell proliferation, differentiation and are also known to participate in viral transcription (Veracini et al. 2005, Ostendorf et al. 2014, Trejo-Sol et al. 2013).

Epidermal growth factor receptors (EGFRs) are considered among the principal inducers of JNK pathway (Zhao et al. 2015). Previous experiments with the HIV-1 luciferase reporter also showed an induction to almost an equal level between MMQO and the epidermal growth factors (EGF). EGF was included as a positive control in the experiments, where HEK-293T cells were transfected with an HIV-1 LTR-Luc reporter plasmid and treated with various HIV-1 stimulating substances, since EGF is known to induce the effect of transfected plasmids. However, the possibility of EGFRs inducing the expression of the HIV-1 minigenome specifically thus far has been overlooked (Gallastegui et al. 2012). Indeed EGFR targeting agents were recently described to reactivate latent HIV (Calvanese et al. 2013). GSEA

pathway analysis suggested the dataset “V\$ETF_Q6”, a designation for the EGFR-specific transcription factor (ETF) motif, to be the most significantly positively correlating transcription factor specific geneset with MMQO treatment (q -value 0,004; Normalized Enrichment Score (NES) = 1,81). Though LASSO did not support the similarity of EGFR active site to MMQO’s profile, they have been described to share considerable similarities to PDGFRs (Wang et al. 2004) and we decided to involve these receptors in our study. In total we included three different extracellular inhibitors against membrane receptors – AG490, AG1296, AG1478. The aforementioned drugs were analyzed in combination with MMQO by qPCR and flow cytometry.

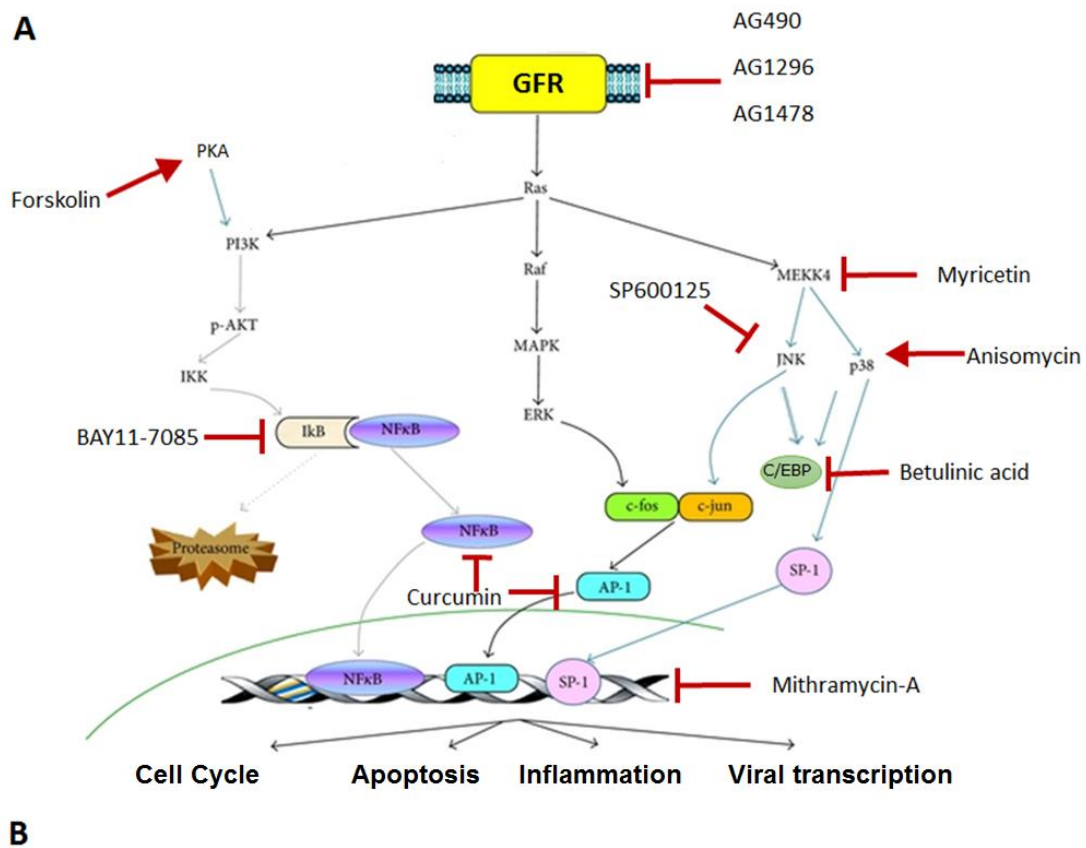
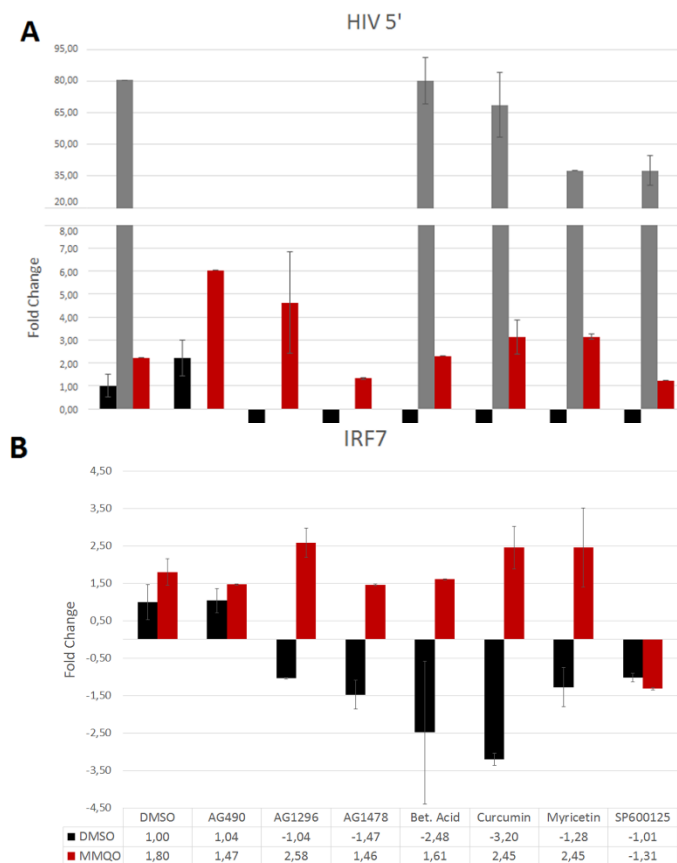


Figure 62: Illustration depicting various intra -and extracellular activators and inhibitors used in this study to investigate the role of MAPK and PKA pathways. (A) Simplified model of growth factor

dependent pathways that activate both MAPK and NF- κ B related transcription. The downstream transcription factors are all known HIV-1 activating factors as well. Image adapted from Trejo-Solis 2013. (B) Table listing the drugs depicted in the illustration 7A listing their specific targets, dosages at which they were applied for qPCR and the mechanisms of action.

First, for the qPCR we preincubated Jurkat E89 clones with the inhibitors listed in Figure 62B for one hour and then followed up with a six hour treatment with either MMQO, PMA as a positive control or DMSO as a negative control. We favored to use the Tat-negative E89 cells to avoid any secondary transcriptional mechanisms by Tat since MAPK pathways have been shown to overlap with it before (Prasad & Tyagi, 2015, Soo Youn et al. 2015, Youn et al. 2014, Ju et al. 2012). We left out the combination treatments between PMA and the extracellular inhibitors, since PMA is known to function intracellularly on the PKC pathway (Myers et al. 1985) and extracellularly functioning compounds wouldn't prohibit its functionality. In line with the immunoblot results, no substantial effect of the inhibitors on MMQO's target genes by qPCR was observed. The two drugs to seemingly have hindered MMQO's ability to reactivate HIV transcription – AG1478 and SP600125 – also decreased the basal level of 5' LTR expression, implying that their effect isn't specific to MMQO's mechanism (Figure 63A). The same remark can be made also about the expressions of *IRF7* and *MYC*, genes that were among the most potently dysregulated by MMQO in the previous experiments yet remained unaffected by the addition on inhibitors (Figure 63B-C).



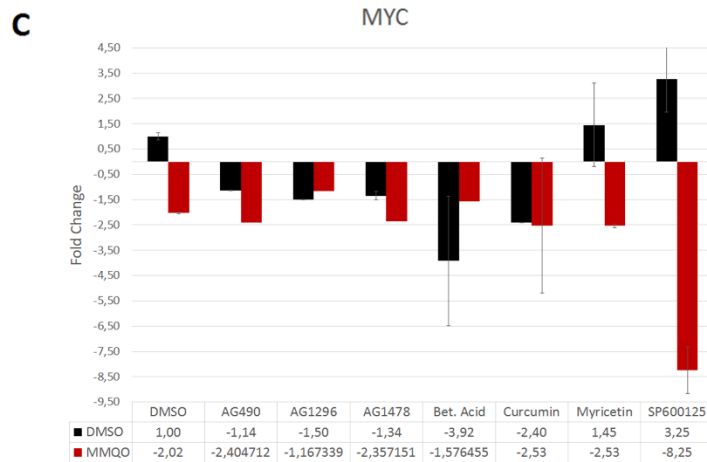


Figure 63: Effect of JNK pathway inhibitors on MMQO target genes by qPCR. (A-C) Jurkat E89 clones were treated 6h either with MMQO (160µM), PMA (10nM) or equivalent volume of DMSO. Cells were preincubated for 1h with the designated inhibitor. The three genes were chosen based on their specificity towards MMQO responses. GAPDH was measured for normalization and results are represented relative to results from the DMSO cells. The means and S.D. values (error bars) are shown from a representative experiment measured in duplicate (mean values displayed separately below the bars).

As a confirmatory approach we decided to examine the effect of those inhibitors via flow cytometry. Jurkat A2 clones were treated with various doses of inhibitors in combination with a low dose of MMQO. The low dose of MMQO was to assure a low toxicity, since the combination of different drugs might decrease viability, which might lead to interference in GFP expression. Though all the inhibitors used here were chosen based on their primary function at the lowest dose, a number of those compounds have been described to exhibit alternative inhibitory functions at higher doses (Figure 64A-F). In addition to the kinase inhibitors we also tested a compound named Mithramycin-A that binds directly the Sp1 motifs, thus blocking the effect of this crucial MAPK downstream transcription factor. Mithramycin-A was able to inhibit the MFI of MMQO but also the response of positive control compound PMA, thus exhibiting a total inhibitory effect on the minigenome (data not shown). In agreement with the qPCR and immunoblotting results, we didn't observe any blocking effect of these inhibitors on MMQO activation of HIV promoter in flow cytometry.

A	AG1296	% Viability	% GFP	MFI
	Untreated	90,79	23,03	11,8
	MMQO 40µM	92,75	27,46	13,19
	1µM AG1296 + MMQO	90,67	29,14	15,4
	2µM AG1296 + MMQO	90,99	30,89	15,1
	3µM AG1296 + MMQO	90,66	29,52	15,4
	4µM AG1296 + MMQO	91,28	29,21	15
	5µM AG1296 + MMQO	91,05	25,5	17,9
	10µM AG1296 + MMQO	89,37	30,44	15,9
	20µM AG1296 + MMQO	63,22	26,78	15
	AG1296 10µM	74,38	25,3	13,8

B	AG1478	% Viability	% GFP	MFI
	Untreated	91,15	23,11	11,8
	MMQO 40µM	92,75	27,46	13,19
	20µM AG1478 + MMQO	92,21	27,31	14,6
	40µM AG1478 + MMQO	90,74	26,92	14,1
	60µM AG1478 + MMQO	89,06	26,13	15
	80µM AG1478 + MMQO	78,47	26,26	14,9
	100µM AG1478 + MMQO	67,89	23,89	14,7
	AG1478 100µM	75,89	22,63	13,4

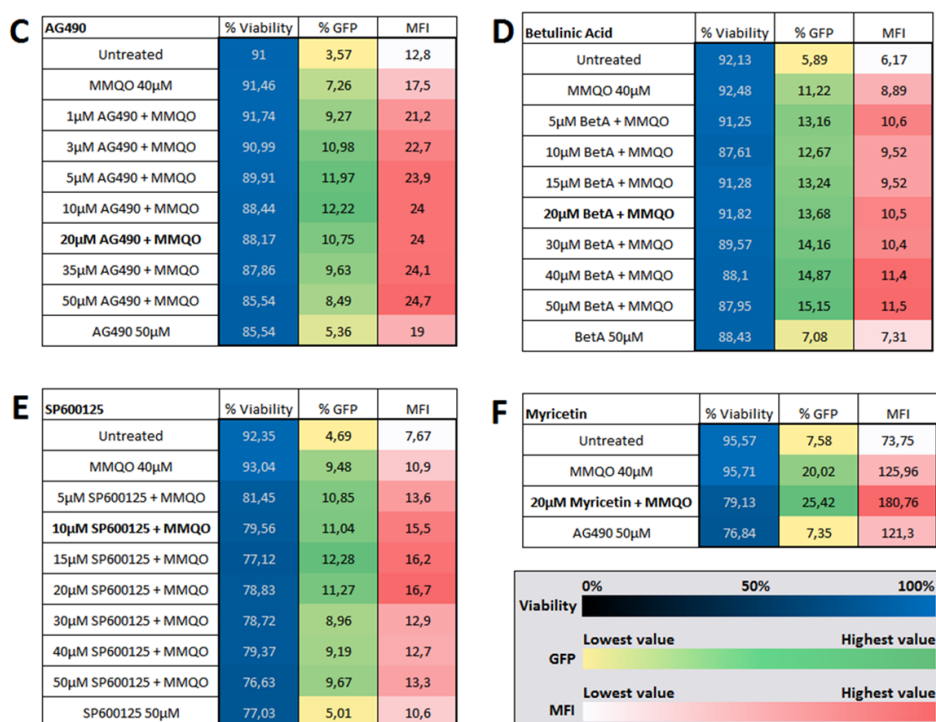


Figure 64: Effect of JNK pathway inhibitors on MMQO minigenome expression by flow cytometry. Jurkat A2 clones were co-incubated with MMQO and MAPK pathway inhibitors for 24h and the cells were analyzed by forward scatter (FSC) and side scatter (SSC), by the GFP expressing percentage among the viable sample and their GFP expression intensity (Mean Fluorescence Intensity – MFI, depicted in arbitrary units). The color code indicates the intensity of the value within the dataset. Drug concentration highlighted in bold annotates the ideal concentration for functioning on the intended target.

Though the microarray analysis and *in silico* predictions weakly supported the idea of MAPK pathways being involved in MMQO's function, we were not able to witness any such effect experimentally. We did not observe any similar gene expression patterns between MMQO and the MAPK pathway activating compound anisomycin and on a protein level we neither witnessed any previously described JNK activation following treatments with different mitogens. Further analysis confirmed that also the downstream targets of JNK activity remained unaffected by MMQO. Finally, in a series of qPCR and flow cytometry experiments utilizing chemical inhibition of various members of the JNK axis, we again failed to report any correlation between the MMQO and MAPK signaling. In light of the negative immunoblotting, qPCR and flow cytometry results we decided to abandon the hypothesis of MMQO reactivating HIV-1 transcription via MAPK pathways and began probing for other potential pathways implicated in the microarray.

4. Cross-reaction of MMQO and PI3K/Akt pathway in HIV expression and T cell receptor signaling

As an alternative approach we considered a different mechanism that is known to transduce an activating signal to viral promoter – namely the PI3K/Akt pathway (Figure 62A) (Zhao et al. 2015; Wollin et al. 2015; Plesec, 2011). Akt is a known initiator of HIV-1 reactivation from latency and has been shown to be chemically inducible by disulfiram (Xing et al. 2011; Doyon et al. 2013). This compound has recently been evaluated as a latency reactivating compound in a clinical setting, but thus far it has failed to show a stable decrease of the latent reservoir in clinical settings (Rasmussen et al. 2016). It's mechanism of action is by drastic depletion of PTEN, an inhibitory partner of the Akt kinase. The increased activity of Akt allows it to disassociate the P-TEFb complex from the repressive 7SK snRNP structure, thus inducing HIV-1 elongation (Contreras et al. 2007). Among the most intriguing facts about disulfiram is that it is able to induce viral transcription without global T cell activation since it is capable of inhibiting the proinflammatory transcription factor NF- κ B (Wang et al. 2003; Ramakrishnan et al. 2015). This immunosuppressive characteristic of Akt is generally considered to be the result of the PKA signaling. Interestingly, the microarray data further confirmed MMQO's anti-TCR signalling and general immunosuppressive quality, which could be a trait shared with AKT pathway (Figure 65). The Akt kinase is also known to phosphorylate the CREB transcription factor, which is known to co-operate with Tat in viral reactivation and aid viral expression via cyclic adenosine monophosphate (cAMP) response elements in HIV promoter (Rabbi et al. 1997, Du & Montminy, 1998, Wen et al. 2010, Rohr et al. 1999). GSEA pathway analysis suggests the datasets "REACTOME_PI3K_AKT_ACTIVATION" and "REACTOME_PI_3K_CASCADE" to be among the highest positively correlating genesets with MMQO treatment (q -value 0,012; NES=1,954 and 0,019; NES=1,851 respectively). Considering the microarray data and previously published immunosuppressive characteristics of MMQO, we hypothesised that it might function through the Akt axis instead, either by transmitting the signal through the protein directly or through an alternative upstream mechanism, such as the PKA pathway.

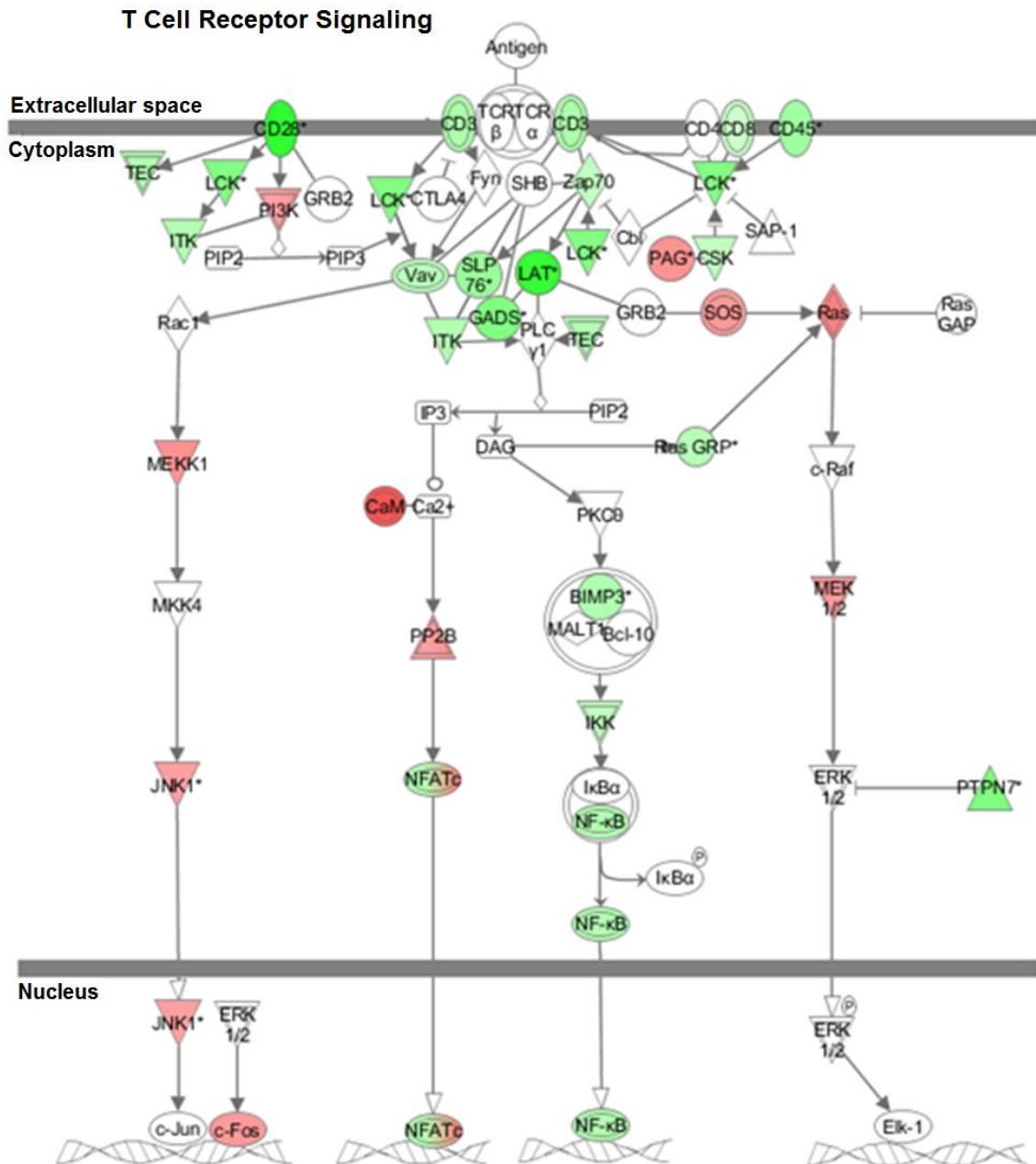


Figure 65: Regulation of T-cell receptor (TCR) signaling genes by MMQO. Transcriptional pathway analysis of T-cell receptor signaling in MMQO treated Jurkat cells. Green and red symbols represent significantly down- or upregulated genes, respectively; white symbols are not differentially expressed between subsets. Figure was created using the IPA software.

Starting upstream of Akt activation, we questioned if the activation of PKA pathway participates in the functioning of MMQO. To that end we utilized the chemical compound forskolin, an immunosuppressive molecule that induces the Protein Kinase A (PKA) pathway by activating the enzyme adenylyl cyclase (AC) and increases the intracellular levels of cAMP (Seamon & Daly, 1981). Employing combinatory treatments between MMQO and forskolin we first observed their effect on the LTR-GFP expression in latently infected Jurkat clones.

We witnessed a considerable dose dependent synergy in the co-treated Tat-positive cells, while forskolin alone barely had any effect on the number of GFP-positive cells (Figure 66A). Nevertheless, forskolin did present a trivial response on the fluorescence intensity in these cells, suggesting that the activation of cAMP/PKA axis assists an already reactivated minigenome, rather than functioning as an independent anti-latency mechanism. The percentage of synergistically activated cells in combination with the two drugs was corroborated in a heterogeneous latent Jurkat population (Figure 66B) and also in the E89 Tat-negative clones (Figure 66C). As expected the synergy of fluorescence intensity scaled markedly higher in the Tat-positive clones, supporting the previous assessment that transcription factors of the PKA pathway require Tat for having an effect on the viral promoter.

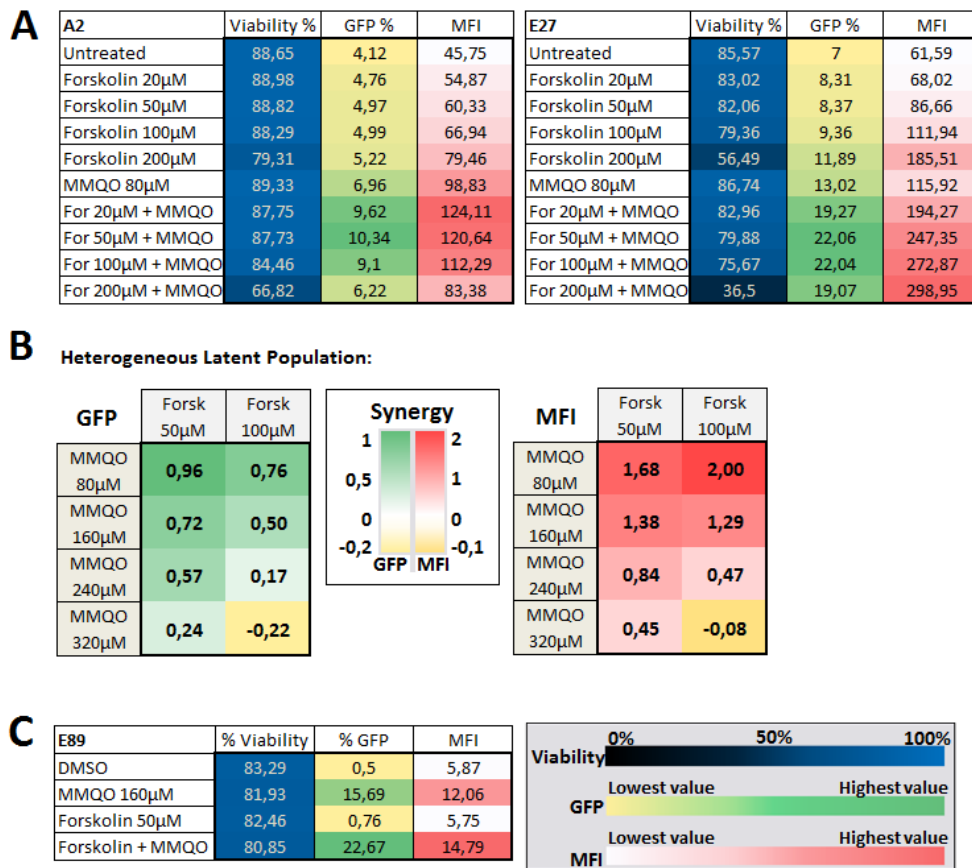


Figure 66: Forskolin synergy on MMQO minigenome expression by flow cytometry. Listed Jurkat cells were treated with various doses of forskolin alone or in combination with MMQO for 24h and the cells were analyzed by forward scatter (FSC) and side scatter (SSC), by the GFP expressing percentage among the viable sample and their GFP expression intensity (MFI, depicted in arbitrary units). The color code in bottom indicates the intensity of the value within the (A) and (C) datasets (A) Tat-expressing latent Jurkat A2 and E27 clones. (B) Heat map illustration of Bliss interaction index of Tat-positive minigenome containing latent heterogeneous Jurkat population treated with various doses of MMQO and forskolin. (C) Latent Jurkat E89 clones (Tat-negative) were treated with forskolin, MMQO or their combination for 24h.

Although the additional production of cAMP acts as a supportive condition for the activity of MMQO, the fact that it functions synergistically suggest that these two mechanisms function independently of each other. PKA pathway is known to also activate the NFAT transcription factor family, which in turn can have an effect on HIV-1 proviral induction (Romanchikova et al. 2003, Chow & Davis, 2000). We therefore decided exclude PKA pathway activity from the targets of MMQO and continue downstream on the pathway axis.

A hallmark of Akt activity is its ability to both phosphorylate and deactivate the glycogen synthase kinase 3 proteins (GSK3) and independently activate GSK3's substrate β -catenin, which are central players in Wnt signaling pathways (Fang et al. 2007, Manning & Cantley 2007). It is worth noting that the HIV-1 promoter is capable of recruiting β -catenin as a repressive unit together with other Wnt pathway transcription factors, such as TCF4, to the four different binding motifs of TCF4 on the 5' LTR (Al-Harhi, 2012). If MMQO indeed functions on the Akt pathway, this effect could also shift the intracellular equilibrium of β -catenin, thus affecting viral reactivation.

The β -catenin transcription factor is maintained at low levels through degradation and its abundance is tightly controlled by the GSK3 kinases within the cytosol. Upon external stimuli GSK3 becomes phosphorylated, becoming inactive and releasing the β -catenin from their repressive complex. This process can be provoked by canonical Wnt pathway, insulin signaling or GSK3 can directly be inhibited by lithium (Lizcano & Alessi, 2002, Cohen & Frame, 2001). The additional β -catenin in turn has to be phosphorylated to be rendered active after which it can participate in regulating transcription. GSEA pathway analysis suggests the β -catenin specific dataset "REACTOME_CTNNB1_PHOSPHORYLATION_CASCADE" to be significantly and positively correlating genesets with MMQO treatment (q -value 0,012, NES=1,728).

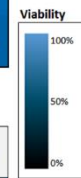
To elaborate if the GSK3/ β -catenin axis overlaps with MMQO's function we co-treated various latent Jurkat populations with LiCl, a known β -catenin activator and measured the results by flow cytometry. In terms of percentage of GFP and fluorescence intensity the Tat-positive latent populations responded synergistically (Figure 67A), while the Tat-negative latent clones we witnessed only minimal effect from LiCl (Figure 67B). This response suggests that MMQO and GSK3/ β -catenin function independently from each other and that the inhibition of GSK3 only benefits the second phase of HIV minigenome transcription.

A Heterogeneous Latent Jurkat Population

GFP		MMQO			
		0	40uM	80uM	160uM
LiCl	0	0,98	3,85	8,25	14,64
	5mM	1,05	6,31	13,35	19,65
	15mM	1,77	7,4	12,95	19,28
	30mM	1,62	6,63	10,3	13,66

MFI		MMQO			
		0	40uM	80uM	160uM
LiCl	0	5,76	7,65	13,7	23,78
	5mM	5,51	10,12	18,65	29,66
	15mM	6,69	12,58	18,1	29,29
	30mM	7,24	12,8	17,66	24,58

Viability		MMQO			
		0	40uM	80uM	160uM
LiCl	0	95,57	96,47	97,05	95,94
	5mM	95,44	96,32	95,9	94,32
	15mM	93,1	95,27	94,05	91,97
	30mM	88,7	91,21	90,13	86,85

**B** E89 Jurkat Clones

GFP		MMQO			
		0	40uM	80uM	160uM
LiCl	0	0,48	1,68	4,79	9,93
	5mM	0,75	2,26	4,76	11,27
	15mM	0,57	2,55	4,45	10,52
	30mM	0,6	2,4	4,3	10,99

MFI		MMQO			
		0	40uM	80uM	160uM
LiCl	0	6,73	6,73	7,8	9,31
	5mM	6,63	7,28	7,8	10,12
	15mM	7,14	7,38	8,14	9,8
	30mM	7,54	7,73	8,58	10,92

Viability		MMQO			
		0	40uM	80uM	160uM
LiCl	0	91,72	92,05	92,39	91,81
	5mM	91,15	91,9	92,23	91,13
	15mM	90,14	91,09	90,92	89,43
	30mM	86,63	88,27	89,99	86,83

Figure 67: Flow cytometry of LiCl and MMQO. Listed Jurkat cells were treated with various doses of LiCl in combination with MMQO for 24h and the cells were analyzed by forward scatter (FSC) and side scatter (SSC), by the GFP expressing percentage among the viable sample and their GFP expression intensity (MFI, depicted in arbitrary units). The color code on the side indicates the intensity of the value within the datasets (A) Tat-expressing latent heterogeneous Jurkat population. (B) Tat-negative latent E89 Jurkat clones

In an attempt to characterize the synergy between LiCl and MMQO by qPCR, we discovered MMQO to actually inhibit the response from LiCl (Figure 68). *AXIN2* and *DKK1* are considered to be the canonical targets of Wnt pathway signaling. Although they both potently responded to LiCl, MMQO displayed a potent antagonistic effect against the expression of these genes.

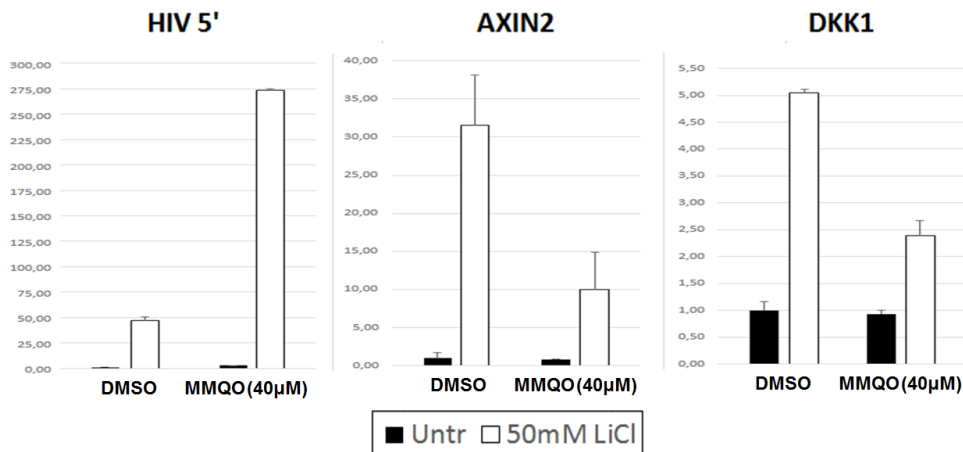


Figure 68: Effect of JNK pathway inhibitors on MMQO target genes by qPCR. Jurkat A2 clones were treated 24h either with MMQO (40µM), LiCl (50mM), their combination or equivalent volume of DMSO. GAPDH was measured for normalization and results are represented relative to results from the DMSO cells. The means and S.D. values (error bars) are shown from a representative experiment measured in duplicate (mean values displayed separately below the bars).

The independence of β -catenin-axis from MMQO was also confirmed on protein level – as opposed to LiCl inhibition, the MMQO treatment did not induce any accumulation of β -catenin within total extracts (Figure 69A). We neither witnessed any β -catenin build-up on total chromatin extracts (Figure 69B), thus confirming that MMQO functions entirely independent of the GSK3/ β -catenin axis.

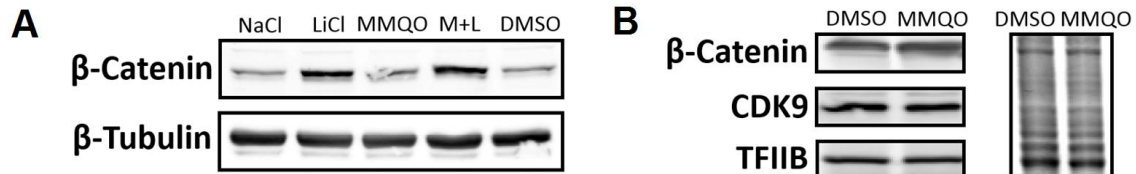


Figure 69: β -catenin accumulation in response to LiCl and MMQO. (A) Cells were incubated 6h with LiCl (30mM), MMQO (160 μ M), NaCl (30mM), MMQO and LiCl combination or equivalent volume of DMSO as vehicle. Total protein was immunoblotted against total β -catenin or β -Tubulin as a loading control. (B) Cells were treated for 24h with either MMQO (160 μ M) or equivalent volume of DMSO. Crosslinked chromatin was extracted, sonicated, de-crosslinked and run in an acrylamide gel. Protein was immunoblotted against β -catenin, CDK9 or TFIIB. Coomassie from a similar molecular weight (MW) was used as a loading confirmation.

The phosphorylation of the serine-473 residue on the Akt kinase is considered a compulsory post-translational modification necessary for the protein's activity and can be induced either by insulin treatment within thirty minutes or by disulfiram after two hours by downregulating the PTEN protein (Tan et al. 2010, Vincent et al. 2011, Doyon et al. 2013).

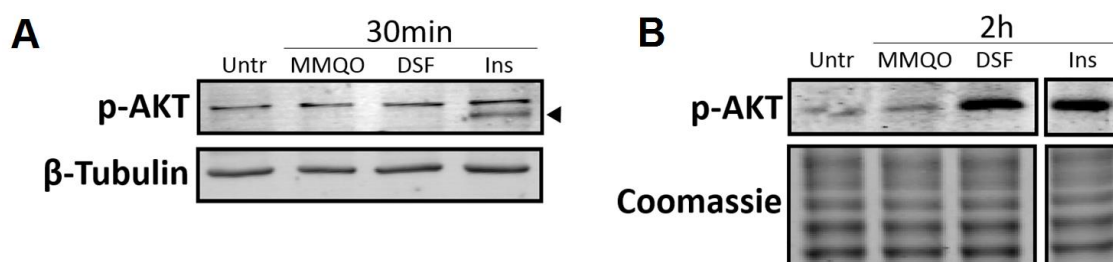


Figure 70: β -catenin accumulation and Akt phosphorylation in response to various stimuli. (E) Cells were incubated 30min with Disulfiram (20 μ M), MMQO (160 μ M), insulin (100nM) or left untreated. Samples were analyzed by immunoblotting against the phosphorylated Ser473 Akt protein or β -Tubulin as a loading control. The correct p-Akt band is highlighted with the triangle. (F) Cells were incubated 2h with Disulfiram (20 μ M), MMQO (160 μ M), insulin (100nM) or left untreated. Protein samples extracted from HeLa cells and analyzed by immunoblotting on a nitrocellulose membrane against the phosphorylated Ser473 Akt protein. Below as a loading control is a section of an untransferred coomassie staining of a gel from the same MW region as Akt. The insulin treated sample has been cropped from the same image as the other samples without any further tampering in contrast, brightness or other quality determining factors. Membrane (A) was plotted on PVDF, while membrane (B) was plotted on nitrocellulose.

For the experiments requiring disulfiram we avoided using Jurkat lymphocytes, since they have been described to be PTEN-negative and probably wouldn't respond to the treatment (Shan et al. 2000). While both insulin and disulfiram phosphorylated Akt (Figure 70A-B), MMQO failed to do so in native HeLa cells neither at the thirty minute time point, nor after a two hour long treatment.

In addition to previously excluding the JNK participation, we also demonstrated that neither Akt, β -catenin nor their upstream regulators probably have an effect on MMQO's impact at the viral reactivation. Thereafter we concentrated on further analysis of the microarrays and identifying the immunosuppressive pathways MMQO was inhibiting.

ABBREVIATIONS

7SK snRNP	7SK small nuclear ribonucleoprotein
8-HQ	8-hydroxyquinoline
AC	adenylyl cyclase
AIDS	acquired immune deficiency syndrome
Akt	protein kinase B
AML	acute myeloid leukemia
AP-1	activator protein 1
ART	anti-retroviral therapy
AZT	azidothymidine
BET	bromodomain and extraterminal domain
BETi	BET inhibitor
BRD	bromodomain-containing protein
cAMP	cyclic adenosine monophosphate
CBP	CREB binding protein
CD	cluster of differentiation
CDK9	cyclin-dependent kinase 9
ChIP	chromatin immunoprecipitation
cMYC	v-myc avian myelocytomatosis viral oncogene homolog
CTD	C-terminal domain
CXCR	C-X-C chemokine receptor
DSF	disulfiram
DSIF	DRB sensitivity inducing factor
ETF	EGFR-specific transcription factor
FBS	fetal bovine serum
FDR	false discovery rate
FRAP	fluorescence recovery after photobleaching
FRET	fluorescence resonance energy transfer
FSC	forward scatter
FWER	FamilyWise Error Rate
G4	g-quadruplex
GFP	green fluorescence protein
GLTSCR1	glioma tumor suppressor candidate region gene 1
GO	Gene Ontology
GSEA	Gene Set Enrichment Analysis
GSK3	glycogen synthase kinase 3
HAART	see ART
HAT	histone acetyltransferase
HDAC	histone deacetylase
HDACi	HDAC inhibitor
HIF1α	hypoxia inducible factor 1-alpha
HIV-1	human immunodeficiency virus type 1

HMQ	4-hydroxy-8-methoxyquinoline
HMT	histone lysine methyltransferase
HSQC	heteronuclear single quantum coherence
HTRF	homogeneous time resolved fluorescence
IL	interleukin
IPA	Ingenuity Pathway Analysis
JNK	c-jun N-terminal
KAc	acetylated lysine
LASSO	Ligand Activity by Surface Similarity Order
LAT	linker for activation of T-cells
LEDGF/p75	lens epithelium-derived growth factor
LEF-1	lymphoid enhancer binding factor 1
LiCl	lithium chloride
lincRNA	long intergenic non-coding RNA
LRA	latency reactivating agent
LTR	long terminal repeat
MAPK	mitogen-activated protein kinase
MFI	mean fluorescence intensity
MMQO	8-methoxy-6-methylquinolin-4-ol
MQD	6-methyl-4,8-quinolinediol
MW	molecular weight
nef	negative regulatory factor
NELF	negative elongation factor
NES	normalized enrichment score
NFAT	nuclear factor of activated T-cells
NF-κB	nuclear factor kappa B
NK	natural killer
NMR	nuclear magnetic resonance
Nuc	nucleosome
ORF	open reading frame
PBMC	peripheral blood mononuclear cells
PDGFR	platelet derived growth factor receptor
PEP	post-exposure prophylaxis
PIC	pre-integration complex
PKA	protein kinase A
PKC	protein kinase C
PMA	phorbol-12-myristate-13-acetate
PoI II	RNA polymerase II
P-TEFb	positive transcription elongation factor b
PTEN	phosphatase and tensin homolog
REAC	Reactome
rev	regulator of expression of virion

RUNX1	runt-related transcription factor 1
SAHA	suberoylanilide hydroxamic acid
SEC	super elongation complex
shRNA	small hairpin RNA
SSC	side scatter
ssRNA	single-stranded RNA
SWI/SNF	switch/sucrose non-fermentable
T-ALL	T-cell acute lymphoblastic leukemia
TAR	trans-activation response element
Tat	trans-activator of transcription
TCR	T cell receptor
TF	transcription factor
TLR	toll-like receptor
TNF-α	tumor necrosis factor alpha
TSA	trichostatin A
TSS	transcription start site
vif	viral infectivity factor
VPA	valproic acid
vpr	viral protein R
vpu	viral protein unique
YY1	yin yang 1

REFERENCES

- Acuto, Oreste, and Frédérique Michel. "CD28-Mediated Co-Stimulation: A Quantitative Support for TCR Signalling." *Nature Reviews Immunology* 3, no. 12 (December 2003): 939–51.
- Afzal, Obaid, Suresh Kumar, Md Rafi Haider, Md Rahmat Ali, Rajiv Kumar, Manu Jaggi, and Sandhya Bawa. "A Review on Anticancer Potential of Bioactive Heterocycle Quinoline." *European Journal of Medicinal Chemistry* 97 (June 5, 2015): 871–910.
- Ai, Nanping, Xiangming Hu, Feng Ding, Bingfei Yu, Huiping Wang, Xiaodong Lu, Kai Zhang, et al. "Signal-Induced Brd4 Release from Chromatin Is Essential for Its Role Transition from Chromatin Targeting to Transcriptional Regulation." *Nucleic Acids Research* 39, no. 22 (December 1, 2011): 9592–9604.
- Al-Harhi, Lena. "Interplay between Wnt/ β -Catenin Signaling and HIV: Virologic and Biologic Consequences in the CNS." *Journal of Neuroimmune Pharmacology: The Official Journal of the Society on Neuroimmune Pharmacology* 7, no. 4 (December 2012): 731–39.
- Archin, Nancie M., Julia Marsh Sung, Carolina Garrido, Natalia Soriano-Sarabia, and David M. Margolis. "Eradicating HIV-1 Infection: Seeking to Clear a Persistent Pathogen." *Nature Reviews. Microbiology* 12, no. 11 (November 2014): 750–64.
- Arshad, Zeeshaan, James Smith, Mackenna Roberts, Wen Hwa Lee, Ben Davies, Kim Bure, Georg A. Hollander, Sue Dopson, Chas Bountra, and David Brindley. "Open Access Could Transform Drug Discovery: A Case Study of JQ1." *Expert Opinion on Drug Discovery* 11, no. 3 (March 3, 2016): 321–32.
- Bailey, Dana, Ravi Jahagirdar, Allan Gordon, Anouar Hafiane, Steven Campbell, Safia Chatur, Gregory S. Wagner, et al. "RVX-208: A Small Molecule That Increases Apolipoprotein A-I and High-Density Lipoprotein Cholesterol In Vitro and In Vivo." *Journal of the American College of Cardiology* 55, no. 23 (June 8, 2010): 2580–89.
- Banerjee, Camellia, Nancie Archin, Daniel Michaels, Anna C. Belkina, Gerald V. Denis, James Bradner, Paola Sebastiani, David M. Margolis, and Monty Montano. "BET Bromodomain Inhibition as a Novel Strategy for Reactivation of HIV-1." *Journal of Leukocyte Biology* 92, no. 6 (December 2012): 1147–54.
- Barboric, Matjaz, and Tina Lenasi. "Kick-sTARting HIV-1 Transcription Elongation by 7SK snRNP deportATion." *Nature Structural & Molecular Biology* 17, no. 8 (August 2010): 928–30.
- Barré-Sinoussi, F., J. C. Chermann, F. Rey, M. T. Nugeyre, S. Chamaret, J. Gruest, C. Dautet, et al. "Isolation of a T-Lymphotropic Retrovirus from a Patient at Risk for Acquired Immune Deficiency Syndrome (AIDS)." *Science (New York, N.Y.)* 220, no. 4599 (May 20, 1983): 868–71.

- Barretina, Jordi, Giordano Caponigro, Nicolas Stransky, Kavitha Venkatesan, Adam A. Margolin, Sungjoon Kim, Christopher J. Wilson, et al. "The Cancer Cell Line Encyclopedia Enables Predictive Modelling of Anticancer Drug Sensitivity." *Nature* 483, no. 7391 (March 28, 2012): 603–7.
- Barkett, M., and T. D. Gilmore. "Control of Apoptosis by Rel/NF-kappaB Transcription Factors." *Oncogene* 18, no. 49 (November 22, 1999): 6910–24.
- Bartholomeeusen K, Xiang Y, Fujinaga K, Peterlin BM (2012) Bromodomain and extraterminal (BET) bromodomain inhibition activate transcription via transient release of positive transcription elongation factor b (P-TEFb) from 7SK small nuclear ribonucleoprotein. *J Biol Chem* 287(43):36609–36616.
- Barton, Kirston, and David Margolis. "Selective Targeting of the Repressive Transcription Factors YY1 and cMyc to Disrupt Quiescent Human Immunodeficiency Viruses." *AIDS Research and Human Retroviruses* 29, no. 2 (February 2013): 289–98.
- Belkina, Anna C., Barbara S. Nikolajczyk, and Gerald V. Denis. "BET Protein Function Is Required for Inflammation: Brd2 Genetic Disruption and BET Inhibitor JQ1 Impair Mouse Macrophage Inflammatory Responses." *The Journal of Immunology* 190, no. 7 (April 1, 2013): 3670–78.
- Bennett, B. L., D. T. Sasaki, B. W. Murray, E. C. O'Leary, S. T. Sakata, W. Xu, J. C. Leisten, et al. "SP600125, an Anthrapyrazolone Inhibitor of Jun N-Terminal Kinase." *Proceedings of the National Academy of Sciences of the United States of America* 98, no. 24 (November 20, 2001): 13681–86.
- Bhadury, Joydeep, Lisa M. Nilsson, Somsundar Veppil Muralidharan, Lydia C. Green, Zhoulei Li, Emily M. Gesner, Henrik C. Hansen, Ulrich B. Keller, Kevin G. McLure, and Jonas A. Nilsson. "BET and HDAC Inhibitors Induce Similar Genes and Biological Effects and Synergize to Kill in Myc-Induced Murine Lymphoma." *Proceedings of the National Academy of Sciences* 111, no. 26 (July 1, 2014): E2721–30.
- Bisgrove, Dwayne A., Tokameh Mahmoudi, Peter Henklein, and Eric Verdin. "Conserved P-TEFb-Interacting Domain of BRD4 Inhibits HIV Transcription." *Proceedings of the National Academy of Sciences of the United States of America* 104, no. 34 (August 21, 2007): 13690–95.
- Bliss, C. I. "THE CALCULATION OF MICROBIAL ASSAYS." *Bacteriological Reviews* 20, no. 4 (December 1956): 243–58.
- Boehm, D., Calvanese, V., Dar, R.D., Xing, S., Schroeder, S., Martins, L., Aull, K., Li, P.C., Planelles, V., Bradner, J.E., et al. (2013). BET bromodomain-targeting compounds reactivate HIV from latency via a Tat-independent mechanism. *Cell Cycle* 12, 452–462.

- Boehm, Daniela, Ryan J. Conrad, and Melanie Ott. "Bromodomain Proteins in HIV Infection." *Viruses* 5, no. 6 (June 21, 2013): 1571–86.
- Bouchat, Sophie, Nadège Delacourt, Anna Kula, Gilles Darcis, Benoit Van Driessche, Francis Corazza, Jean-Stéphane Gatot, et al. "Sequential Treatment with 5-Aza-2'-Deoxycytidine and Deacetylase Inhibitors Reactivates HIV-1." *EMBO Molecular Medicine* 8, no. 2 (February 1, 2016): 117–38.
- Brasier, Allan R., B. Tian, M. Jamaluddin, Mridul K. Kalita, Roberto P. Garofalo, and Muping Lu. "RelA Ser276 Phosphorylation-Coupled Lys310 Acetylation Controls Transcriptional Elongation of Inflammatory Cytokines in Respiratory Syncytial Virus Infection." *Journal of Virology* 85, no. 22 (November 2011): 11752–69.
- Brooks, David G., Philip A. Arlen, Lianying Gao, Christina M. R. Kitchen, and Jerome A. Zack. "Identification of T Cell-Signaling Pathways That Stimulate Latent HIV in Primary Cells." *Proceedings of the National Academy of Sciences of the United States of America* 100, no. 22 (October 28, 2003): 12955–60.
- Brown, Jonathan D., Charles Y. Lin, Qiong Duan, Gabriel Griffin, Alexander J. Federation, Ronald M. Paranal, Steven Bair, et al. "NF- κ B Directs Dynamic Super Enhancer Formation in Inflammation and Atherogenesis." *Molecular Cell* 56, no. 2 (October 23, 2014): 219–31.
- Calvanese, Vincenzo, Leonard Chavez, Timothy Laurent, Sheng Ding, and Eric Verdin. "Dual-Color HIV Reporters Trace a Population of Latently Infected Cells and Enable Their Purification." *Virology* 446, no. 1–2 (November 2013): 283–92.
- Cao, Biyin, Jie Li, Jingyu Zhu, Mingyun Shen, Kunkun Han, Zubin Zhang, Yang Yu, et al. "The Antiparasitic Cloroquinol Induces Apoptosis in Leukemia and Myeloma Cells by Inhibiting Histone Deacetylase Activity." *Journal of Biological Chemistry* 288, no. 47 (November 22, 2013): 34181–89.
- Cary, Daniele C., Koh Fujinaga, and B. Matija Peterlin. "Molecular Mechanisms of HIV Latency." *The Journal of Clinical Investigation* 126, no. 2 (February 2016): 448–54.
- Chaitanya, Ganta Vijay, Jonathan S. Alexander, and Phanithi Prakash Babu. "PARP-1 Cleavage Fragments: Signatures of Cell-Death Proteases in Neurodegeneration." *Cell Communication and Signaling* 8 (2010): 31.
- Chen R, Liu M, Zhang K, Zhou Q (2011) Isolation and functional characterization of P-TEFb-associated factors that control general and HIV-1 transcriptional elongation. *Methods* 53(1):85–90.
- Chen, Ruichuan, Jasper H. N. Yik, Qiao Jing Lew, and Sheng-Hao Chao. "Brd4 and HEXIM1: Multiple Roles in P-TEFb Regulation and Cancer." *BioMed Research International* 2014 (2014): 232870.

- Chen, Han, Haitao Long, Xiaojie Cui, Jiang Zhou, Ming Xu, and Gu Yuan. "Exploring the Formation and Recognition of an Important G-Quadruplex in a HIF1 α Promoter and Its Transcriptional Inhibition by a Benzo[c]phenanthridine Derivative." *Journal of the American Chemical Society* 136, no. 6 (February 12, 2014): 2583–91.
- Chow, Chi-Wing, and Roger J. Davis. "Integration of Calcium and Cyclic AMP Signaling Pathways by 14-3-3." *Molecular and Cellular Biology* 20, no. 2 (January 2000): 702–12.
- Chun, T. W., D. Engel, S. B. Mizell, L. A. Ehler, and A. S. Fauci. "Induction of HIV-1 Replication in Latently Infected CD4+ T Cells Using a Combination of Cytokines." *The Journal of Experimental Medicine* 188, no. 1 (July 6, 1998): 83–91.
- Chun, T. W., D. Engel, S. B. Mizell, C. W. Hallahan, M. Fischette, S. Park, R. T. Davey, et al. "Effect of Interleukin-2 on the Pool of Latently Infected, Resting CD4+ T Cells in HIV-1-Infected Patients Receiving Highly Active Anti-Retroviral Therapy." *Nature Medicine* 5, no. 6 (June 1999): 651–55.
- Chung, Chun-Wa, Anthony W. Dean, James M. Woolven, and Paul Bamborough. "Fragment-Based Discovery of Bromodomain Inhibitors Part 1: Inhibitor Binding Modes and Implications for Lead Discovery." *Journal of Medicinal Chemistry* 55, no. 2 (January 26, 2012): 576–86.
- Clark, Peter G. K., Lucas C. C. Vieira, Cynthia Tallant, Oleg Fedorov, Dean C. Singleton, Catherine M. Rogers, Octovia P. Monteiro, et al. "LP99: Discovery and Synthesis of the First Selective BRD7/9 Bromodomain Inhibitor." *Angewandte Chemie (Weinheim an Der Bergstrasse, Germany)* 127, no. 21 (May 18, 2015): 6315–19.
- Cohen, P., and S. Frame. "The Renaissance of GSK3." *Nature Reviews. Molecular Cell Biology* 2, no. 10 (October 2001): 769–76.
- Cohen, Jon. "Drug Flushes out Hidden AIDS Virus." *Science (New York, N.Y.)* 347, no. 6226 (March 6, 2015): 1056.
- Coiras, Mayte, María Rosa López-Huertas, Joaquín Rullas, Maria Mittelbrunn, and José Alcamí. "Basal Shuttle of NF-kappaB/I kappaB Alpha in Resting T Lymphocytes Regulates HIV-1 LTR Dependent Expression." *Retrovirology* 4 (2007): 56.
- Contreras, Xavier, Matjaz Barboric, Tina Lenasi, and B. Matija Peterlin. "HMBA Releases P-TEFb from HEXIM1 and 7SK snRNA via PI3K/Akt and Activates HIV Transcription." *PLoS Pathogens* 3, no. 10 (October 2007).
- Contreras, Xavier, Marc Schweneker, Ching-Shih Chen, Joseph M. McCune, Steven G. Deeks, Jeffrey Martin, and B. Matija Peterlin. "Suberoylanilide Hydroxamic Acid Reactivates HIV from Latently Infected Cells." *Journal of Biological Chemistry* 284, no. 11 (March 13, 2009): 6782–89.

Coull, J. J., F. Romerio, J. M. Sun, J. L. Volker, K. M. Galvin, J. R. Davie, Y. Shi, U. Hansen, and D. M. Margolis. "The Human Factors YY1 and LSF Repress the Human Immunodeficiency Virus Type 1 Long Terminal Repeat via Recruitment of Histone Deacetylase 1." *Journal of Virology* 74, no. 15 (August 2000): 6790–99.

Coutsoudis, Anna, Leith Kwaan, and Mairi Thomson. "Prevention of Vertical Transmission of HIV-1 in Resource-Limited Settings." *Expert Review of Anti-Infective Therapy* 8, no. 10 (October 2010): 1163–75.

Crawford, Terry D., Vickie Tsui, E. Megan Flynn, Shumei Wang, Alexander M. Taylor, Alexandre Côté, James E. Audia, et al. "Diving into the Water: Inducible Binding Conformations for BRD4, TAF1(2), BRD9, and CECR2 Bromodomains." *Journal of Medicinal Chemistry* 59, no. 11 (June 9, 2016): 5391–5402.

Dar, Roy D., Nina N. Hosmane, Michelle R. Arkin, Robert F. Siliciano, and Leor S. Weinberger. "Screening for Noise in Gene Expression Identifies Drug Synergies." *Science (New York, N.Y.)* 344, no. 6190 (June 20, 2014): 1392–96.

Dawson, M.A., Prinjha, R.K., Dittmann, A., Giotopoulos, G., Bantscheff, M., Chan, W.I., Robson, S.C., Chung, C.W., Hopf, C., Savitski, M.M., et al. (2011). Inhibition of BET recruitment to chromatin as an effective treatment for MLL-fusion leukaemia. *Nature* 478, 529–533.

De Nicola, Beatrice, Christopher J. Lech, Brahim Heddi, Sagar Regmi, Ilaria Frasson, Rosalba Perrone, Sara N. Richter, and Anh Tuân Phan. "Structure and Possible Function of a G-Quadruplex in the Long Terminal Repeat of the Proviral HIV-1 Genome." *Nucleic Acids Research* 44, no. 13 (July 27, 2016): 6442–51.

Deeney, Jude T., Anna C. Belkina, Orian S. Shirihai, Barbara E. Corkey, and Gerald V. Denis. "BET Bromodomain Proteins Brd2, Brd3 and Brd4 Selectively Regulate Metabolic Pathways in the Pancreatic β -Cell." *PloS One* 11, no. 3 (2016): e0151329.

Deeks, Steven G. "HIV: Shock and Kill." *Nature* 487, no. 7408 (July 26, 2012): 439–40.

Deeks, Steven G., Sharon R. Lewin, Anna Laura Ross, Jintanat Ananworanich, Monsef Benkirane, Paula Cannon, Nicolas Chomont, et al. "International AIDS Society Global Scientific Strategy: Towards an HIV Cure 2016." *Nature Medicine* 22, no. 8 (August 2016): 839–50.

Delmore, J.E., Issa, G.C., Lemieux, M.E., Rahl, P.B., Shi, J., Jacobs, H.M., Kastiris, E., Gilpatrick, T., Paranal, R.M., Qi, J., et al. (2011). BET bromodomain inhibition as a therapeutic strategy to target c-Myc. *Cell* 146, 904–917.

Denis GV (2010) Bromodomain coactivators in cancer, obesity, type 2 diabetes, and inflammation. *Discov Med* 10(55):489–499.

- Deshmane, Satish L., Shohreh Amini, Satarupa Sen, Kamel Khalili, and Bassel E. Sawaya. "Regulation of the HIV-1 Promoter by HIF-1 α and Vpr Proteins." *Virology Journal* 8 (October 24, 2011): 477.
- Devaiah, Ballachanda N., Brian A. Lewis, Natasha Cherman, Michael C. Hewitt, Brian K. Albrecht, Pamela G. Robey, Keiko Ozato, Robert J. Sims, and Dinah S. Singer. "BRD4 Is an Atypical Kinase That Phosphorylates serine2 of the RNA Polymerase II Carboxy-Terminal Domain." *Proceedings of the National Academy of Sciences of the United States of America* 109, no. 18 (May 1, 2012): 6927–32.
- Devaiah, Ballachanda N., Chanelle Case-Borden, Anne Gegonne, Chih Hao Hsu, Qingrong Chen, Daoud Meerzaman, Anup Dey, Keiko Ozato, and Dinah S. Singer. "BRD4 Is a Histone Acetyltransferase That Evicts Nucleosomes from Chromatin." *Nature Structural & Molecular Biology* 23, no. 6 (June 2016): 540–48.
- Dey, A., Chitsaz, F., Abbasi, A., Misteli, T., and Ozato, K. (2003). The double bromodomain protein Brd4 binds to acetylated chromatin during interphase and mitosis. *Proc. Natl. Acad. Sci. USA* 100, 8758–8763.
- Dey A, Nishiyama A, Karpova T, McNally J, Ozato K (2009) Brd4 marks select genes on mitotic chromatin and directs postmitotic transcription. *Mol Biol Cell* 20(23):4899–4909.
- Dhalluin, C., J. E. Carlson, L. Zeng, C. He, A. K. Aggarwal, and M. M. Zhou. "Structure and Ligand of a Histone Acetyltransferase Bromodomain." *Nature* 399, no. 6735 (June 3, 1999): 491–96.
- Donnell, Deborah, Jared M. Baeten, James Kiarie, Katherine K. Thomas, Wendy Stevens, Craig R. Cohen, James McIntyre, Jairam R. Lingappa, Connie Celum, and Partners in Prevention HSV/HIV Transmission Study Team. "Heterosexual HIV-1 Transmission after Initiation of Antiretroviral Therapy: A Prospective Cohort Analysis." *Lancet (London, England)* 375, no. 9731 (June 12, 2010): 2092–98.
- Doyon, Geneviève, Jennifer Zerbato, John W. Mellors, and Nicolas Sluis-Cremer. "Disulfiram Reactivates Latent HIV-1 Expression through Depletion of the Phosphatase and Tensin Homolog." *AIDS (London, England)* 27, no. 2 (January 14, 2013): F7–11.
- Drost, Jarno, Fiamma Mantovani, Francesca Tocco, Ran Elkon, Anna Comel, Henne Holstege, Ron Kerkhoven, et al. "BRD7 Is a Candidate Tumour Suppressor Gene Required for p53 Function." *Nature Cell Biology* 12, no. 4 (April 2010): 380–89.
- Du, K., and M. Montminy. "CREB Is a Regulatory Target for the Protein Kinase Akt/PKB." *The Journal of Biological Chemistry* 273, no. 49 (December 4, 1998): 32377–79.
- Duh, E. J., W. J. Maury, T. M. Folks, A. S. Fauci, and A. B. Rabson. "Tumor Necrosis Factor Alpha Activates Human Immunodeficiency Virus Type 1 through Induction of Nuclear

- Factor Binding to the NF-Kappa B Sites in the Long Terminal Repeat." *Proceedings of the National Academy of Sciences of the United States of America* 86, no. 15 (August 1989): 5974–78.
- Engelman, Alan, and Peter Cherepanov. "The Structural Biology of HIV-1: Mechanistic and Therapeutic Insights." *Nature Reviews. Microbiology* 10, no. 4 (April 2012): 279–90.
- Fang, Dexing, David Hawke, Yanhua Zheng, Yan Xia, Jill Meisenhelder, Heinz Nika, Gordon B. Mills, Ryuji Kobayashi, Tony Hunter, and Zhimin Lu. "Phosphorylation of β -Catenin by AKT Promotes β -Catenin Transcriptional Activity." *Journal of Biological Chemistry* 282, no. 15 (April 13, 2007): 11221–29.
- Faria, Nuno R., Andrew Rambaut, Marc A. Suchard, Guy Baele, Trevor Bedford, Melissa J. Ward, Andrew J. Tatem, et al. "HIV Epidemiology. The Early Spread and Epidemic Ignition of HIV-1 in Human Populations." *Science (New York, N.Y.)* 346, no. 6205 (October 3, 2014): 56–61.
- Fedorov, Oleg, Hannah Lingard, Chris Wells, Octovia P. Monteiro, Sarah Picaud, Tracy Keates, Clarence Yapp, et al. "[1,2,4]triazolo[4,3-A]phthalazines: Inhibitors of Diverse Bromodomains." *Journal of Medicinal Chemistry* 57, no. 2 (January 23, 2014): 462–76.
- Fenouil, Romain, Pierre Cauchy, Frederic Koch, Nicolas Descostes, Joaquin Zacarias Cabeza, Charlène Innocenti, Pierre Ferrier, et al. "CpG Islands and GC Content Dictate Nucleosome Depletion in a Transcription-Independent Manner at Mammalian Promoters." *Genome Research* 22, no. 12 (December 2012): 2399–2408.
- Fernandez, Paula C., Scott R. Frank, Luquan Wang, Marianne Schroeder, Suxing Liu, Jonathan Greene, Andrea Cocito, and Bruno Amati. "Genomic Targets of the Human c-Myc Protein." *Genes & Development* 17, no. 9 (May 1, 2003): 1115–29.
- Ferreiro, Isabel, Manel Joaquin, Abul Islam, Gonzalo Gomez-Lopez, Montserrat Barragan, Luís Lombardía, Orlando Domínguez, et al. "Whole Genome Analysis of p38 SAPK-Mediated Gene Expression upon Stress." *BMC Genomics* 11 (2010): 144.
- Filippakopoulos, Panagis, Jun Qi, Sarah Picaud, Yao Shen, William B. Smith, Oleg Fedorov, Elizabeth M. Morse, et al. "Selective Inhibition of BET Bromodomains." *Nature* 468, no. 7327 (December 23, 2010): 1067–73.
- Filippakopoulos, P., Picaud, S., Mangos, M., Keates, T., Lambert, J.P., Barsyte-Lovejoy, D., Felletar, I., Volkmer, R., Müller, S., Pawson, T., et al. (2012). Histone recognition and large-scale structural analysis of the human bromodomain family. *Cell* 149, 214–231.
- Filippakopoulos, Panagis, and Stefan Knapp. "Targeting Bromodomains: Epigenetic Readers of Lysine Acetylation." *Nature Reviews Drug Discovery* 13, no. 5 (May 2014): 337–56.

Fowler, Trent, Payel Ghatak, David H. Price, Ronald Conaway, Joan Conaway, Cheng-Ming Chiang, James E. Bradner, Ali Shilatifard, and Ananda L. Roy. "Regulation of MYC Expression and Differential JQ1 Sensitivity in Cancer Cells." *PLOS ONE* 9, no. 1 (January 23, 2014): e87003.

Gabay, Meital, Yulin Li, and Dean W. Felsher. "MYC Activation Is a Hallmark of Cancer Initiation and Maintenance." *Cold Spring Harbor Perspectives in Medicine* 4, no. 6 (June 2014).

Gacias, Mar, Guillermo Gerona-Navarro, Alexander N. Plotnikov, Guangtao Zhang, Lei Zeng, Jasbir Kaur, Gregory Moy, et al. "Selective Chemical Modulation of Gene Transcription Favors Oligodendrocyte Lineage Progression." *Chemistry & Biology* 21, no. 7 (July 17, 2014): 841–54.

Gallastegui, Edurne, Brett Marshall, David Vidal, Gonzalo Sanchez-Duffhues, Juan A. Collado, Carmen Alvarez-Fernández, Neus Luque, et al. "Combination of Biological Screening in a Cellular Model of Viral Latency and Virtual Screening Identifies Novel Compounds That Reactivate HIV-1." *Journal of Virology* 86, no. 7 (April 1, 2012): 3795–3808.

Gamsjaeger R, et al. (2011) Structural basis and specificity of acetylated transcription factor GATA1 recognition by BET family bromodomain protein Brd3. *Mol Cell Biol* 31(13):2632–2640.

Gianotti, N., F. Moretti, G. Tambussi, B. Capiluppi, M. Ferrari, and A. Lazzarin. "The Rationale for a Study on HIV-1 Reverse Transcriptase Mutations and Outcome of Antiretroviral Therapy with Two Nucleoside Analogs." *Journal of Biological Regulators and Homeostatic Agents* 13, no. 3 (September 1999): 158–62.

Goodsell, David S. "Illustrating the Machinery of Life: Viruses." *Biochemistry and Molecular Biology Education* 40, no. 5 (September 1, 2012): 291–96.

Gregory, Mark A., and Stephen R. Hann. "C-Myc Proteolysis by the Ubiquitin-Proteasome Pathway: Stabilization of c-Myc in Burkitt's Lymphoma Cells." *Molecular and Cellular Biology* 20, no. 7 (April 1, 2000): 2423–35.

Gudas, Lorraine J., Leiping Fu, Denise R. Minton, Nigel P. Mongan, and David M. Nanus. "The Role of HIF1 α in Renal Cell Carcinoma Tumorigenesis." *Journal of Molecular Medicine (Berlin, Germany)* 92, no. 8 (August 2014): 825–36.

Garcia-Gutierrez, Pablo, Maria Mundi, and Mario Garcia-Dominguez. "Association of Bromodomain BET Proteins with Chromatin Requires Dimerization through the Conserved Motif B." *Journal of Cell Science* 125, no. Pt 15 (August 1, 2012): 3671–80.

- Hakre, Shweta, Leonard Chavez, Kotaro Shirakawa, and Eric Verdin. "HIV Latency: Experimental Systems and Molecular Models." *FEMS Microbiology Reviews* 36, no. 3 (May 1, 2012): 706–16.
- Hamer, Dean H. "Can HIV Be Cured? Mechanisms of HIV Persistence and Strategies to Combat It." *Current HIV Research* 2, no. 2 (April 2004): 99–111.
- Hartmann, Tanja Nicole, Valentin Grabovsky, Ronit Pasvolsky, Ziv Shulman, Eike C. Buss, Asaf Spiegel, Arnon Nagler, Tsvee Lapidot, Marcus Thelen, and Ronen Alon. "A Crosstalk between Intracellular CXCR7 and CXCR4 Involved in Rapid CXCL12-Triggered Integrin Activation but Not in Chemokine-Triggered Motility of Human T Lymphocytes and CD34+ Cells." *Journal of Leukocyte Biology* 84, no. 4 (October 1, 2008): 1130–40.
- Hegy, Hedi. "Enhancer-Promoter Interaction Facilitated by Transiently Forming G-Quadruplexes." *Scientific Reports* 5 (March 16, 2015): 9165.
- Henderson, Angus, Adele Holloway, Raymond Reeves, and David John Tremethick. "Recruitment of SWI/SNF to the Human Immunodeficiency Virus Type 1 Promoter." *Molecular and Cellular Biology* 24, no. 1 (January 2004): 389–97.
- Herrick, D. J., and J. Ross. "The Half-Life of c-Myc mRNA in Growing and Serum-Stimulated Cells: Influence of the Coding and 3' Untranslated Regions and Role of Ribosome Translocation." *Molecular and Cellular Biology* 14, no. 3 (March 1994): 2119–28.
- Ho, D. D. "Time to Hit HIV, Early and Hard." *The New England Journal of Medicine* 333, no. 7 (August 17, 1995): 450–51.
- Hohmann, Anja F., Laetitia J. Martin, Jessica L. Minder, Jae-Seok Roe, Junwei Shi, Steffen Steurer, Gerd Bader, et al. "Sensitivity and Engineered Resistance of Myeloid Leukemia Cells to BRD9 Inhibition." *Nature Chemical Biology* 12, no. 9 (September 2016): 672–79.
- Hollis, Angela, Bianca Sperl, Martin Gräber, and Thorsten Berg. "The Natural Product Betulinic Acid Inhibits C/EBP Family Transcription Factors." *ChemBioChem* 13, no. 2 (January 23, 2012): 302–7.
- Huang, T. S., S. C. Lee, and J. K. Lin. "Suppression of c-Jun/AP-1 Activation by an Inhibitor of Tumor Promotion in Mouse Fibroblast Cells." *Proceedings of the National Academy of Sciences of the United States of America* 88, no. 12 (June 15, 1991): 5292–96.
- Huang, Ming-Jer, Yuan-chih Cheng, Chien-Ru Liu, Shufan Lin, and H. Eugene Liu. "A Small-Molecule c-Myc Inhibitor, 10058-F4, Induces Cell-Cycle Arrest, Apoptosis, and Myeloid Differentiation of Human Acute Myeloid Leukemia." *Experimental Hematology* 34, no. 11 (November 2006): 1480–89.

Huang, Bo, Xiao-Dong Yang, Ming-Ming Zhou, Keiko Ozato, and Lin-Feng Chen. "Brd4 Coactivates Transcriptional Activation of NF- κ B via Specific Binding to Acetylated RelA." *Molecular and Cellular Biology* 29, no. 5 (March 1, 2009): 1375–87.

Huth, Jeffrey R., Liping Yu, Irene Collins, Jamey Mack, Renaldo Mendoza, Binumol Isaac, Demetrios T. Braddock, et al. "NMR-Driven Discovery of Benzoylanthranilic Acid Inhibitors of Far Upstream Element Binding Protein Binding to the Human Oncogene c-Myc Promoter." *Journal of Medicinal Chemistry* 47, no. 20 (September 1, 2004): 4851–57.

Jang, Moon Kyoo, Kazuki Mochizuki, Meisheng Zhou, Ho-Sang Jeong, John N. Brady, and Keiko Ozato. "The Bromodomain Protein Brd4 Is a Positive Regulatory Component of P-TEFb and Stimulates RNA Polymerase II-Dependent Transcription." *Molecular Cell* 19, no. 4 (August 19, 2005): 523–34.

Januchowski, Radosław, and Paweł P. Jagodzinski. "Trichostatin A down-Regulates ZAP-70, LAT and SLP-76 Content in Jurkat T Cells." *International Immunopharmacology* 7, no. 2 (February 2007): 198–204.

Jiang, Guochun, Amy Espeseth, Daria J. Hazuda, and David M. Margolis. "C-Myc and Sp1 Contribute to Proviral Latency by Recruiting Histone Deacetylase 1 to the Human Immunodeficiency Virus Type 1 Promoter." *Journal of Virology* 81, no. 20 (October 15, 2007): 10914–23.

Jiang, Guochun, Erica A. Mendes, Philipp Kaiser, Daniel P. Wong, Yuyang Tang, Ivy Cai, Anne Fenton, et al. "Synergistic Reactivation of Latent HIV Expression by Ingenol-3-Angelate, PEP005, Targeted NF- κ B Signaling in Combination with JQ1 Induced P-TEFb Activation." *PLOS Pathog* 11, no. 7 (July 30, 2015): e1005066.

Jin, Zhe, Daisuke Nagakubo, Aiko-Konno Shirakawa, Takashi Nakayama, Akiko Shigeta, Kunio Hieshima, Yasuaki Yamada, and Osamu Yoshie. "CXCR7 Is Inducible by HTLV-1 Tax and Promotes Growth and Survival of HTLV-1-Infected T Cells." *International Journal of Cancer* 125, no. 9 (November 1, 2009): 2229–35.

Jones, Richard Brad, Rachel O'Connor, Stefanie Mueller, Maria Foley, Gregory L. Szeto, Dan Karel, Mathias Lichterfeld, et al. "Histone Deacetylase Inhibitors Impair the Elimination of HIV-Infected Cells by Cytotoxic T-Lymphocytes." *PLoS Pathogens* 10, no. 8 (August 14, 2014).

Jordan, Albert, Patricia Defechereux, and Eric Verdin. "The Site of HIV-1 Integration in the Human Genome Determines Basal Transcriptional Activity and Response to Tat Transactivation." *The EMBO Journal* 20, no. 7 (April 2, 2001): 1726–38.

Jordan, Albert, Dwayne Bisgrove, and Eric Verdin. "HIV Reproducibly Establishes a Latent Infection after Acute Infection of T Cells in Vitro." *The EMBO Journal* 22, no. 8 (April 15, 2003): 1868–77.

Ju, Sung Mi, Ah Ra Goh, Dong-Joo Kwon, Gi Soo Youn, Hyung-Joo Kwon, Yong Soo Bae, Soo Young Choi, and Jinseu Park. "Extracellular HIV-1 Tat Induces Human Beta-Defensin-2 Production via NF-kappaB/AP-1 Dependent Pathways in Human B Cells." *Molecules and Cells* 33, no. 4 (April 2012): 335–41.

Jung, Yun-Jin, Jennifer S. Isaacs, Sunmin Lee, Jane Trepel, and Len Neckers. "Microtubule Disruption Utilizes an NFkB-Dependent Pathway to Stabilize HIF-1 α Protein." *Journal of Biological Chemistry* 278, no. 9 (February 28, 2003): 7445–52.

Kaesler, Matthias D., Aaron Aslanian, Meng-Qiu Dong, John R. Yates, and Beverly M. Emerson. "BRD7, a Novel PBAF-Specific SWI/SNF Subunit, Is Required for Target Gene Activation and Repression in Embryonic Stem Cells." *The Journal of Biological Chemistry* 283, no. 47 (November 21, 2008): 32254–63.

Kaufman, J. D., G. Valandra, G. Roderiquez, G. Bushar, C. Giri, and M. A. Norcross. "Phorbol Ester Enhances Human Immunodeficiency Virus-Promoted Gene Expression and Acts on a Repeated 10-Base-Pair Functional Enhancer Element." *Molecular and Cellular Biology* 7, no. 10 (October 1987): 3759–66.

Kim, Jong-Eun, Jung Yeon Kwon, Dong Eun Lee, Nam Joo Kang, Yong-Seok Heo, Ki Won Lee, and Hyong Joo Lee. "MKK4 Is a Novel Target for the Inhibition of Tumor Necrosis Factor-Alpha-Induced Vascular Endothelial Growth Factor Expression by Myricetin." *Biochemical Pharmacology* 77, no. 3 (February 1, 2009): 412–21.

King, Bryan, Thomas Trimarchi, Linsey Reavie, Luyao Xu, Jasper Mullenders, Panagiotis Ntziachristos, Beatriz Aranda-Orgilles, et al. "Regulation of Leukemia-Initiating Cell Activity by the Ubiquitin Ligase FBXW7." *Cell* 153, no. 7 (June 20, 2013): 1552–66.

Klase, Zachary, Venkat S. R. K. Yedavalli, Laurent Houzet, Molly Perkins, Frank Maldarelli, Jason Brenchley, Klaus Strebel, Paul Liu, and Kuan-Teh Jeang. "Activation of HIV-1 from Latent Infection via Synergy of RUNX1 Inhibitor Ro5-3335 and SAHA." *PLOS Pathog* 10, no. 3 (March 20, 2014): e1003997.

Knoechel, Birgit, Justine E. Roderick, Kaylyn E. Williamson, Jiang Zhu, Jens G. Lohr, Matthew J. Cotton, Shawn M. Gillespie, et al. "An Epigenetic Mechanism of Resistance to Targeted Therapy in T Cell Acute Lymphoblastic Leukemia." *Nature Genetics* 46, no. 4 (April 2014): 364–70.

Kovalenko, M., A. Gazit, A. Böhmer, C. Rorsman, L. Rönnstrand, C. H. Heldin, J. Waltenberger, F. D. Böhmer, and A. Levitzki. "Selective Platelet-Derived Growth Factor

Receptor Kinase Blockers Reverse Sis-Transformation." *Cancer Research* 54, no. 23 (December 1, 1994): 6106–14.

Kozlowski, Hannah N., Eric T. L. Lai, Pierre C. Havugimana, Carl White, Andrew Emili, Darinka Sakac, Beth Binnington, Anton Neschadim, Stephen D. S. McCarthy, and Donald R. Branch. "Extracellular Histones Identified in Crocodile Blood Inhibit in-Vitro HIV-1 Infection." *AIDS (London, England)* 30, no. 13 (August 24, 2016): 2043–52.

Krakower, Douglas S., Sachin Jain, and Kenneth H. Mayer. "Antiretrovirals for Primary HIV Prevention: The Current Status of Pre- and Post-Exposure Prophylaxis." *Current HIV/AIDS Reports* 12, no. 1 (March 2015): 127–38.

Kroesen, Michiel, Paul Gielen, Ingrid C. Brok, Inna Armandari, Peter M. Hoogerbrugge, and Gosse J. Adema. "HDAC Inhibitors and Immunotherapy; a Double Edged Sword?" *Oncotarget* 5, no. 16 (July 31, 2014): 6558–72.

Kumar, Pankaj, Vinod Kumar Yadav, Aradhita Baral, Parveen Kumar, Dhurjhoti Saha, and Shantanu Chowdhury. "Zinc-Finger Transcription Factors Are Associated with Guanine Quadruplex Motifs in Human, Chimpanzee, Mouse and Rat Promoters Genome-Wide." *Nucleic Acids Research* 39, no. 18 (October 2011): 8005–16.

Kulkosky, J., D. M. Culnan, J. Roman, G. Dornadula, M. Schnell, M. R. Boyd, and R. J. Pomerantz. "Prostratin: Activation of Latent HIV-1 Expression Suggests a Potential Inductive Adjuvant Therapy for HAART." *Blood* 98, no. 10 (November 15, 2001): 3006–15.

Laird, Gregory M., C. Korin Bullen, Daniel I. S. Rosenbloom, Alyssa R. Martin, Alison L. Hill, Christine M. Durand, Janet D. Siliciano, and Robert F. Siliciano. "Ex Vivo Analysis Identifies Effective HIV-1 Latency-Reversing Drug Combinations." *The Journal of Clinical Investigation* 125, no. 5 (May 2015): 1901–12.

Lamb, Jennifer A., Juan-Jose Ventura, Patricia Hess, Richard A. Flavell, and Roger J. Davis. "JunD Mediates Survival Signaling by the JNK Signal Transduction Pathway." *Molecular Cell* 11, no. 6 (June 2003): 1479–89.

Lehrman, Ginger, Ian B Hogue, Sarah Palmer, Cheryl Jennings, Celsa A Spina, Ann Wiegand, Alan L Landay, et al. "Depletion of Latent HIV-1 Infection in Vivo: A Proof-of-Concept Study." *Lancet* 366, no. 9485 (August 13, 2005): 549–55.

Li, Zichong, Jia Guo, Yuntao Wu, and Qiang Zhou. "The BET Bromodomain Inhibitor JQ1 Activates HIV Latency through Antagonizing Brd4 Inhibition of Tat-Transactivation." *Nucleic Acids Research* 41, no. 1 (January 7, 2013): 277–87.

Lin, L., M.-M. Han, F. Wang, L.-L. Xu, H.-X. Yu, and P.-Y. Yang. "CXCR7 Stimulates MAPK Signaling to Regulate Hepatocellular Carcinoma Progression." *Cell Death & Disease* 5, no. 10 (October 23, 2014): e1488.

- Liu, Yujie, Michael R. Nonnemacher, and Brian Wigdahl. "CCAAT/enhancer-Binding Proteins and the Pathogenesis of Retrovirus Infection." *Future Microbiology* 4, no. 3 (April 2009): 299–321.
- Liu, Wen, Qi Ma, Kaki Wong, Wenbo Li, Kenny Ohgi, Jie Zhang, Aneel K. Aggarwal, and Michael G. Rosenfeld. "Brd4 and JMJD6-Associated Anti-Pause Enhancers in Regulation of Transcriptional Pause Release." *Cell* 155, no. 7 (December 19, 2013): 1581–95.
- Lizcano, Jose M., and Dario R. Alessi. "The Insulin Signalling Pathway." *Current Biology* 12, no. 7 (April 2, 2002): R236–38.
- Los Alamos National Laboratory HIV Database: HIV Sequence Database <https://www.hiv.lanl.gov/content/sequence/HIV/MAP/landmark.html>
- Lovén, Jakob, Heather A. Hoke, Charles Y. Lin, Ashley Lau, David A. Orlando, Christopher R. Vakoc, James E. Bradner, Tong Ihn Lee, and Richard A. Young. "Selective Inhibition of Tumor Oncogenes by Disruption of Super-Enhancers." *Cell* 153, no. 2 (April 11, 2013): 320–34.
- Manning, Brendan D., and Lewis C. Cantley. "AKT/PKB Signaling: Navigating Downstream." *Cell* 129, no. 7 (June 29, 2007): 1261–74.
- Malovannaya, Anna, Rainer B. Lanz, Sung Yun Jung, Yaroslava Bulynko, Nguyen T. Le, Doug W. Chan, Chen Ding, et al. "Analysis of the Human Endogenous Coregulator Complexome." *Cell* 145, no. 5 (May 27, 2011): 787–99.
- Martin, Laetitia J., Manfred Koegl, Gerd Bader, Xiao-Ling Cockcroft, Oleg Fedorov, Dennis Fiegen, Thomas Gerstberger, et al. "Structure-Based Design of an in Vivo Active Selective BRD9 Inhibitor." *Journal of Medicinal Chemistry* 59, no. 10 (May 26, 2016): 4462–75.
- Maruyama T, et al. (2002) A mammalian bromodomain protein, Brd4, interacts with replication factor C and inhibits progression to S phase. *Mol Cell Biol* 22(18):6509–6520.
- Maxmen, Amy. "Cancer Research: Open Ambition." *Nature* 488, no. 7410 (August 8, 2012): 148–50.
- Mazur, Pawel K, Alexander Herner, Stephano S Mello, Matthias Wirth, Simone Hausmann, Francisco J Sánchez-Rivera, Shane M Lofgren, et al. "Combined Inhibition of BET Family Proteins and Histone Deacetylases as a Potential Epigenetics-Based Therapy for Pancreatic Ductal Adenocarcinoma." *Nature Medicine* 21, no. 10 (October 2015): 1163–71.
- Mbonye, Uri, and Jonathan Karn. "Transcriptional Control of HIV Latency: Cellular Signaling Pathways, Epigenetics, Happenstance and the Hope for a Cure." *Virology* 454–455 (April 2014): 328–39.

McCarthy, Davis J., and Gordon K. Smyth. "Testing Significance Relative to a Fold-Change Threshold Is a TREAT." *Bioinformatics* 25, no. 6 (March 15, 2009): 765–71.

Mertz, J.A., Conery, A.R., Bryant, B.M., Sandy, P., Balasubramanian, S., Mele, D.A., Bergeron, L., and Sims, R.J., 3rd. (2011). Targeting MYC dependence in cancer by inhibiting BET bromodomains. *Proc. Natl. Acad. Sci. USA* 108, 16669–16674.

Middeljans, Evelien, Xi Wan, Pascal W. Jansen, Vikram Sharma, Hendrik G. Stunnenberg, and Colin Logie. "SS18 Together with Animal-Specific Factors Defines Human BAF-Type SWI/SNF Complexes." *PloS One* 7, no. 3 (2012): e33834.

Mishra, Alok, Rakesh Kumar, Abhishek Tyagi, Indu Kohaar, Suresh Hedau, Alok C Bharti, Subhodeep Sarker, Dipankar Dey, Daman Saluja, and Bhudev Das. "Curcumin Modulates Cellular AP-1, NF- κ B, and HPV16 E6 Proteins in Oral Cancer." *Ecancermedicalscience* 9 (April 23, 2015).

Mu, Qitian, Qiuling Ma, Shasha Lu, Ting Zhang, Mengxia Yu, Xin Huang, Jian Chen, and Jie Jin. "10058-F4, a c-Myc Inhibitor, Markedly Increases Valproic Acid-induced Cell Death in Jurkat and CCRF-CEM T-lymphoblastic Leukemia Cells." *Oncology Letters*, June 24, 2014.

Myers, M. A., L. C. McPhail, and R. Snyderman. "Redistribution of Protein Kinase C Activity in Human Monocytes: Correlation with Activation of the Respiratory Burst." *Journal of Immunology (Baltimore, Md.: 1950)* 135, no. 5 (November 1985): 3411–16.

Nicodeme, Edwige, Kate L. Jeffrey, Uwe Schaefer, Soren Beinke, Scott Dewell, Chun-Wa Chung, Rohit Chandwani, et al. "Suppression of Inflammation by a Synthetic Histone Mimic." *Nature* 468, no. 7327 (December 23, 2010): 1119–23.

Nilsson, Jonas A., and John L. Cleveland. "Myc Pathways Provoking Cell Suicide and Cancer." *Oncogene* 22, no. 56 (2003): 9007–21.

Nowak, David E., Bing Tian, Mohammad Jamaluddin, Istvan Boldogh, Leoncio A. Vergara, Sanjeev Choudhary, and Allan R. Brasier. "RelA Ser276 Phosphorylation Is Required for Activation of a Subset of NF- κ B-Dependent Genes by Recruiting Cyclin-Dependent Kinase 9/cyclin T1 Complexes." *Molecular and Cellular Biology* 28, no. 11 (June 2008): 3623–38.

Offersen, Rasmus, Sara Konstantin Nissen, Thomas A. Rasmussen, Lars Østergaard, Paul W. Denton, Ole Schmeltz Sjøgaard, and Martin Tolstrup. "A Novel Toll-Like Receptor 9 Agonist, MGN1703, Enhances HIV-1 Transcription and NK Cell-Mediated Inhibition of HIV-1-Infected Autologous CD4+ T Cells." *Journal of Virology* 90, no. 9 (May 2016): 4441–53.

Ogawa, Takahiko, Tomonori Hayashi, Seishi Kyoizumi, Yoichiro Kusunoki, Kei Nakachi, Donald G. MacPhee, James E. Trosko, Katsuko Kataoka, and Noriaki Yorioka.

“Anisomycin Downregulates Gap-Junctional Intercellular Communication via the p38 MAP-Kinase Pathway.” *Journal of Cell Science* 117, no. 10 (April 15, 2004): 2087–96.

Ohana, Rachel Friedman, Thomas A. Kirkland, Carolyn C. Woodroffe, Sergiy Levin, H. Tetsuo Uyeda, Paul Otto, Robin Hurst, et al. “Deciphering the Cellular Targets of Bioactive Compounds Using a Chloroalkane Capture Tag.” *ACS Chemical Biology* 10, no. 10 (October 16, 2015): 2316–24.

Ostendorf, Tammo, Peter Boor, Claudia R. C. van Roeyen, and Jürgen Floege. “Platelet-Derived Growth Factors (PDGFs) in Glomerular and Tubulointerstitial Fibrosis.” *Kidney International Supplements* 4, no. 1 (November 2014): 65–69.

Ott, Christopher J., Nadja Kopp, Liat Bird, Ronald M. Paranal, Jun Qi, Teresa Bowman, Scott J. Rodig, Andrew L. Kung, James E. Bradner, and David M. Weinstock. “BET Bromodomain Inhibition Targets Both c-Myc and IL7R in High-Risk Acute Lymphoblastic Leukemia.” *Blood* 120, no. 14 (October 4, 2012): 2843–52.

Ou, Tian-Miao, Yu-Jing Lu, Chi Zhang, Zhi-Shu Huang, Xiao-Dong Wang, Jia-Heng Tan, Yuan Chen, et al. “Stabilization of G-Quadruplex DNA and Down-Regulation of Oncogene c-Myc by Quindoline Derivatives.” *Journal of Medicinal Chemistry* 50, no. 7 (April 1, 2007): 1465–74.

Patel, Mira C., Maxime Debrosse, Matthew Smith, Anup Dey, Walter Huynh, Naoyuki Sarai, Tom D. Heightman, Tomohiko Tamura, and Keiko Ozato. “BRD4 Coordinates Recruitment of Pause Release Factor P-TEFb and the Pausing Complex NELF/DSIF to Regulate Transcription Elongation of Interferon-Stimulated Genes.” *Molecular and Cellular Biology* 33, no. 12 (June 2013): 2497–2507.

Peart, Melissa J., Gordon K. Smyth, Ryan K. van Laar, David D. Bowtell, Victoria M. Richon, Paul A. Marks, Andrew J. Holloway, and Ricky W. Johnstone. “Identification and Functional Significance of Genes Regulated by Structurally Different Histone Deacetylase Inhibitors.” *Proceedings of the National Academy of Sciences of the United States of America* 102, no. 10 (March 8, 2005): 3697–3702.

Peng, Cong, Jie Zhou, Hua Ying Liu, Ming Zhou, Li Li Wang, Qiu Hong Zhang, Yi Xin Yang, et al. “The Transcriptional Regulation Role of BRD7 by Binding to Acetylated Histone through Bromodomain.” *Journal of Cellular Biochemistry* 97, no. 4 (March 1, 2006): 882–92.

Perkins, N. D., A. B. Agranoff, C. S. Duckett, and G. J. Nabel. “Transcription Factor AP-2 Regulates Human Immunodeficiency Virus Type 1 Gene Expression.” *Journal of Virology* 68, no. 10 (October 1994): 6820–23.

Perrone, Rosalba, Matteo Nadai, Ilaria Frasson, Jerrod A. Poe, Elena Butovskaya, Thomas E. Smithgall, Manlio Palumbo, Giorgio Palù, and Sara N. Richter. “A Dynamic G-

Quadruplex Region Regulates the HIV-1 Long Terminal Repeat Promoter." *Journal of Medicinal Chemistry* 56, no. 16 (August 22, 2013): 6521–30.

Persaud, Deborah, Yan Zhou, Janet M. Siliciano, and Robert F. Siliciano. "Latency in Human Immunodeficiency Virus Type 1 Infection: No Easy Answers." *Journal of Virology* 77, no. 3 (February 2003): 1659–65.

Picaud, Sarah, Christopher Wells, Ildiko Felletar, Deborah Brotherton, Sarah Martin, Pavel Savitsky, Beatriz Diez-Dacal, et al. "RVX-208, an Inhibitor of BET Transcriptional Regulators with Selectivity for the Second Bromodomain." *Proceedings of the National Academy of Sciences of the United States of America* 110, no. 49 (December 3, 2013): 19754–59.

Pierre, Sandra, Thomas Eschenhagen, Gerd Geisslinger, and Klaus Scholich. "Capturing Adenylyl Cyclases as Potential Drug Targets." *Nature Reviews Drug Discovery* 8, no. 4 (April 2009): 321–35.

Philpott, Martin, Catherine M. Rogers, Clarence Yapp, Chris Wells, Jean-Philippe Lambert, Claire Strain-Damerell, Nicola A. Burgess-Brown, Anne-Claude Gingras, Stefan Knapp, and Susanne Müller. "Assessing Cellular Efficacy of Bromodomain Inhibitors Using Fluorescence Recovery after Photobleaching." *Epigenetics & Chromatin* 7 (2014): 14.

Plesec, Thomas P. "Gastrointestinal Mesenchymal Neoplasms Other than Gastrointestinal Stromal Tumors: Focusing on Their Molecular Aspects." *Pathology Research International* 2011 (February 16, 2011): e952569.

Prasad, Sahdeo, and Amit K. Tyagi. "Curcumin and Its Analogues: A Potential Natural Compound against HIV Infection and AIDS." *Food & Function* 6, no. 11 (November 2015): 3412–19.

Qin, Z. H., R. W. Chen, Y. Wang, M. Nakai, D. M. Chuang, and T. N. Chase. "Nuclear Factor kappaB Nuclear Translocation Upregulates c-Myc and p53 Expression during NMDA Receptor-Mediated Apoptosis in Rat Striatum." *The Journal of Neuroscience: The Official Journal of the Society for Neuroscience* 19, no. 10 (May 15, 1999): 4023–33.

Rabbi, M. F., L. Al-Harhi, and K. A. Roebuck. "TNFalpha Cooperates with the Protein Kinase A Pathway to Synergistically Increase HIV-1 LTR Transcription via Downstream TRE-like cAMP Response Elements." *Virology* 237, no. 2 (October 27, 1997): 422–29.

Rafati, Haleh, Maribel Parra, Shweta Hakre, Yuri Moshkin, Eric Verdin, and Tokameh Mahmoudi. "Repressive LTR Nucleosome Positioning by the BAF Complex Is Required for HIV Latency." *PLoS Biology* 9, no. 11 (November 29, 2011).

Rahl PB, et al. (2010) c-Myc regulates transcriptional pause release. *Cell* 141(3): 432–445.

Rahman, Shaila, Mathew E. Sowa, Matthias Ottinger, Jennifer A. Smith, Yang Shi, J. Wade Harper, and Peter M. Howley. "The Brd4 Extraterminal Domain Confers Transcription Activation Independent of pTEFb by Recruiting Multiple Proteins, Including NSD3." *Molecular and Cellular Biology* 31, no. 13 (July 2011): 2641–52.

Raiber, Eun-Ang, Ramon Kranaster, Enid Lam, Mehran Nikan, and Shankar Balasubramanian. "A Non-Canonical DNA Structure Is a Binding Motif for the Transcription Factor SP1 in Vitro." *Nucleic Acids Research* 40, no. 4 (February 2012): 1499–1508.

Ramakrishnan, Rajesh, Hongbing Liu, and Andrew P. Rice. "Short Communication: SAHA (Vorinostat) Induces CDK9 Thr-186 (T-Loop) Phosphorylation in Resting CD4+ T Cells: Implications for Reactivation of Latent HIV." *AIDS Research and Human Retroviruses* 31, no. 1 (January 1, 2015): 137–41.

Rasmussen, Thomas A., Martin Tolstrup, Anni Winckelmann, Lars Østergaard, and Ole S. Sjøgaard. "Eliminating the Latent HIV Reservoir by Reactivation Strategies: Advancing to Clinical Trials." *Human Vaccines & Immunotherapeutics* 9, no. 4 (April 2013): 790–99.

Rasmussen, Thomas Aagaard, Martin Tolstrup, and Ole Schmeltz Sjøgaard. "Reversal of Latency as Part of a Cure for HIV-1." *Trends in Microbiology* 24, no. 2 (February 2016): 90–97.

Rasmussen, Thomas A., and Sharon R. Lewin. "Shocking HIV out of Hiding: Where Are We with Clinical Trials of Latency Reversing Agents?" *Current Opinion in HIV and AIDS* 11, no. 4 (July 2016): 394–401.

Ratner, L., W. Haseltine, R. Patarca, K. J. Livak, B. Starcich, S. F. Josephs, E. R. Doran, J. A. Rafalski, E. A. Whitehorn, and K. Baumeister. "Complete Nucleotide Sequence of the AIDS Virus, HTLV-III." *Nature* 313, no. 6000 (January 24, 1985): 277–84.

Razooky, Brandon S., Anand Pai, Katherine Aull, Igor M. Rouzine, and Leor S. Weinberger. "A Hardwired HIV Latency Program." *Cell* 160, no. 5 (February 26, 2015): 990–1001.

Reeder, Jonathan E, Youn-Tae Kwak, Ryan P McNamara, Christian V Forst, and Iván D'Orso. "HIV Tat Controls RNA Polymerase II and the Epigenetic Landscape to Transcriptionally Reprogram Target Immune Cells." *eLife* 4. Accessed September 3, 2016.

Reid, Darryl, Bashir S. Sadjad, Zsolt Zsoldos, and Aniko Simon. "LASSO—ligand Activity by Surface Similarity Order: A New Tool for Ligand Based Virtual Screening." *Journal of Computer-Aided Molecular Design* 22, no. 6–7 (January 18, 2008): 479–87.

RIVER Protocol.

http://www.ctu.mrc.ac.uk/research/documents/hiv_protocols/river_protocol.

Rhodes, Daniela, and Hans J. Lipps. "G-Quadruplexes and Their Regulatory Roles in Biology." *Nucleic Acids Research* 43, no. 18 (October 15, 2015): 8627–37.

Rohr, O., C. Schwartz, D. Aunis, and E. Schaeffer. "CREB and COUP-TF Mediate Transcriptional Activation of the Human Immunodeficiency Virus Type 1 Genome in Jurkat T Cells in Response to Cyclic AMP and Dopamine." *Journal of Cellular Biochemistry* 75, no. 3 (December 1, 1999): 404–13.

Romanchikova, Nadezhda, Victorija Ivanova, Carsten Scheller, Eriks Jankevics, Christian Jassoy, and Edgar Serfling. "NFAT Transcription Factors Control HIV-1 Expression through a Binding Site Downstream of TAR Region." *Immunobiology* 208, no. 4 (2003): 361–65.

Romani, Bizhan, Susan Engelbrecht, and Richard H. Glashoff. "Functions of Tat: The Versatile Protein of Human Immunodeficiency Virus Type 1." *Journal of General Virology* 91, no. 1 (2010): 1–12.

Rosser, Edward M., Simon Morton, Kate S. Ashton, Philip Cohen, and Alison N. Hulme. "Synthetic Anisomycin Analogues Activating the JNK/SAPK1 and p38/SAPK2 Pathways." *Organic & Biomolecular Chemistry* 2, no. 1 (December 17, 2004): 142–49.

Sáez-Ciri3n, Asier, Charline Bacchus, Laurent Hocqueloux, Véronique Avettand-Fenoel, Isabelle Girault, Camille Lecuroux, Valerie Potard, et al. "Post-Treatment HIV-1 Controllers with a Long-Term Virological Remission after the Interruption of Early Initiated Antiretroviral Therapy ANRS VISCONTI Study." *PLoS Pathogens* 9, no. 3 (March 2013): e1003211.

Sample Preparation for Western Blot | Abcam.

<http://www.abcam.com/protocols/sample-preparation-for-western-blot>.

Saussede-Aim, Jennifer, Charles Dumontet. "Regulation of tubulin expression: Multiple overlapping mechanisms." *International Journal of Medicine and Medical Sciences* Vol 1.(8) pp. 290-296, August, 2009.

Schneider, H., A. Cohen-Dayag, and I. Pecht. "Tyrosine Phosphorylation of Phospholipase C Gamma 1 Couples the Fc Epsilon Receptor Mediated Signal to Mast Cells Secretion." *International Immunology* 4, no. 4 (April 1992): 447–53.

Scripture-Adams, Deirdre D., David G. Brooks, Yael D. Korin, and Jerome A. Zack. "Interleukin-7 Induces Expression of Latent Human Immunodeficiency Virus Type 1 with Minimal Effects on T-Cell Phenotype." *Journal of Virology* 76, no. 24 (December 2002): 13077–82.

Seamon, K. B., and J. W. Daly. "Forskolin: A Unique Diterpene Activator of Cyclic AMP-Generating Systems." *Journal of Cyclic Nucleotide Research* 7, no. 4 (1981): 201–24.

- Schröder, Sebastian, Sungyoo Cho, Lei Zeng, Qiang Zhang, Katrin Kaehlcke, Lily Mak, Joann Lau, et al. "Two-Pronged Binding with Bromodomain-Containing Protein 4 Liberates Positive Transcription Elongation Factor B from Inactive Ribonucleoprotein Complexes." *The Journal of Biological Chemistry* 287, no. 2 (January 6, 2012): 1090–99.
- Serrao, Erik, Bikash Debnath, Hiroyuki Otake, Yuting Kuang, Frauke Christ, Zeger Debyser, and Nouri Neamati. "Fragment-Based Discovery of 8-Hydroxyquinoline Inhibitors of the HIV-1 Integrase-Lens Epithelium-Derived Growth factor/p75 (IN-LEDGF/p75) Interaction." *Journal of Medicinal Chemistry* 56, no. 6 (March 28, 2013): 2311–22.
- Shan, Xiaochuan, Michael J. Czar, Stephen C. Bunnell, Pinghu Liu, Yusen Liu, Pamela L. Schwartzberg, and Ronald L. Wange. "Deficiency of PTEN in Jurkat T Cells Causes Constitutive Localization of Itk to the Plasma Membrane and Hyperresponsiveness to CD3 Stimulation." *Molecular and Cellular Biology* 20, no. 18 (September 2000): 6945–57.
- Shang, Enyuan, Helen D. Nickerson, Duancheng Wen, Xiangyuan Wang, and Debra J. Wolgemuth. "The First Bromodomain of Brdt, a Testis-Specific Member of the BET Sub-Family of Double-Bromodomain-Containing Proteins, Is Essential for Male Germ Cell Differentiation." *Development (Cambridge, England)* 134, no. 19 (October 2007): 3507–15.
- Sharif, Jafar, Takaho A. Endo, Tetsuro Toyoda, and Haruhiko Koseki. "Divergence of CpG Island Promoters: A Consequence or Cause of Evolution?" *Development, Growth & Differentiation* 52, no. 6 (August 2010): 545–54.
- Sheridan, P. L., C. T. Sheline, K. Cannon, M. L. Voz, M. J. Pazin, J. T. Kadonaga, and K. A. Jones. "Activation of the HIV-1 Enhancer by the LEF-1 HMG Protein on Nucleosome-Assembled DNA in Vitro." *Genes & Development* 9, no. 17 (September 1, 1995): 2090–2104.
- Shi, Junwei, Warren A. Whyte, Cinthya J. Zepeda-Mendoza, Joseph P. Milazzo, Chen Shen, Jae-Seok Roe, Jessica L. Minder, et al. "Role of SWI/SNF in Acute Leukemia Maintenance and Enhancer-Mediated Myc Regulation." *Genes & Development* 27, no. 24 (December 15, 2013): 2648–62.
- Shu, Shaokun, Charles Y. Lin, Housheng Hansen He, Robert M. Witwicki, Doris P. Tabassum, Justin M. Roberts, Michalina Janiszewska, et al. "Response and Resistance to BET Bromodomain Inhibitors in Triple-Negative Breast Cancer." *Nature* 529, no. 7586 (January 21, 2016): 413–17.
- Siddiqui-Jain, Adam, Cory L. Grand, David J. Bearss, and Laurence H. Hurley. "Direct Evidence for a G-Quadruplex in a Promoter Region and Its Targeting with a Small

Molecule to Repress c-MYC Transcription." *Proceedings of the National Academy of Sciences of the United States of America* 99, no. 18 (September 3, 2002): 11593–98.

Simon, Viviana, and David D. Ho. "HIV-1 Dynamics in Vivo: Implications for Therapy." *Nature Reviews. Microbiology* 1, no. 3 (December 2003): 181–90.

Smith, Steven G., and Ming-Ming Zhou. "The Bromodomain: A New Target in Emerging Epigenetic Medicine." *ACS Chemical Biology* 11, no. 3 (March 18, 2016): 598–608.

Snyder, R. C., R. Ray, S. Blume, and D. M. Miller. "Mithramycin Blocks Transcriptional Initiation of the c-Myc P1 and P2 Promoters." *Biochemistry* 30, no. 17 (April 30, 1991): 4290–97.

Soo Youn, Gi, Sung Mi Ju, Soo Young Choi, and Jinseu Park. "HDAC6 Mediates HIV-1 Tat-Induced Proinflammatory Responses by Regulating MAPK-NF-kappaB/AP-1 Pathways in Astrocytes." *Glia*, June 1, 2015.

Spencer, W., H. Kwon, P. Crépieux, N. Leclerc, R. Lin, and J. Hiscott. "Taxol Selectively Blocks Microtubule Dependent NF-kappaB Activation by Phorbol Ester via Inhibition of IkkappaBalpha Phosphorylation and Degradation." *Oncogene* 18, no. 2 (January 14, 1999): 495–505.

Stein, B., H. J. Rahmsdorf, A. Steffen, M. Litfin, and P. Herrlich. "UV-Induced DNA Damage Is an Intermediate Step in UV-Induced Expression of Human Immunodeficiency Virus Type 1, Collagenase, c-Fos, and Metallothionein." *Molecular and Cellular Biology* 9, no. 11 (November 1989): 5169–81.

Stellbrink, Hans-Jürgen, Jan van Lunzen, Michael Westby, Eithne O'Sullivan, Claus Schneider, Axel Adam, Lutwin Weitner, et al. "Effects of Interleukin-2 plus Highly Active Antiretroviral Therapy on HIV-1 Replication and Proviral DNA (COSMIC Trial)." *AIDS (London, England)* 16, no. 11 (July 26, 2002): 1479–87.

Stoszko, Mateusz, Elisa De Crignis, Casper Rokx, Mir Mubashir Khalid, Cynthia Lungu, Robert-Jan Palstra, Tsung Wai Kan, et al. "Small Molecule Inhibitors of BAF; A Promising Family of Compounds in HIV-1 Latency Reversal." *EBioMedicine* 3 (November 27, 2015): 108–21.

Tan, Shi-Xiong, Yvonne Ng, and David E. James. "Akt Inhibitors Reduce Glucose Uptake Independently of Their Effects on Akt." *Biochemical Journal* 432, no. 1 (November 15, 2010): 191–98.

Theodoulou, Natalie H., Paul Bamborough, Andrew J. Bannister, Isabelle Becher, Rino A. Bit, Ka Hing Che, Chun-wa Chung, et al. "Discovery of I-BRD9, a Selective Cell Active Chemical Probe for Bromodomain Containing Protein 9 Inhibition." *Journal of Medicinal Chemistry* 59, no. 4 (February 25, 2016): 1425–39.

- Thomas, Lance R., and William P. Tansey. "MYC and Chromatin." *The Open Access Journal of Science and Technology* 3 (2015).
- Thompson, Martin. "Polybromo-1: The Chromatin Targeting Subunit of the PBAF Complex." *Biochimie* 91, no. 3 (March 2009): 309–19.
- Torres, Fernando C., M. Eugenia García-Rubiño, César Lozano-López, Daniel F. Kawano, Vera L. Eifler-Lima, Gilsane L. von Poser, and Joaquín M. Campos. "Imidazoles and Benzimidazoles as Tubulin-Modulators for Anti-Cancer Therapy." *Current Medicinal Chemistry* 22, no. 11 (2015): 1312–23.
- Torres, Cristina Morales, Alva Biran, Matthew J. Burney, Harshil Patel, Tristan Henser-Brownhill, Ayelet-Hashahar Shapira Cohen, Yilong Li, et al. "The Linker Histone H1.0 Generates Epigenetic and Functional Intratumor Heterogeneity." *Science* (New York, N.Y.) 353, no. 6307 (September 30, 2016).
- Tosoni, Elena, Ilaria Frasson, Matteo Scalabrin, Rosalba Perrone, Elena Butovskaya, Matteo Nadai, Giorgio Palù, Dan Fabris, and Sara N. Richter. "Nucleolin Stabilizes G-Quadruplex Structures Folded by the LTR Promoter and Silences HIV-1 Viral Transcription." *Nucleic Acids Research* 43, no. 18 (October 15, 2015): 8884–97.
- Trejo-Solí, Cristina S, Pedraza-Chaverrí, Jose, Mó Torres-Ramos, nica, Jimé, et al. "Multiple Molecular and Cellular Mechanisms of Action of Lycopene in Cancer Inhibition, Multiple Molecular and Cellular Mechanisms of Action of Lycopene in Cancer Inhibition." *Evidence-Based Complementary and Alternative Medicine, Evidence-Based Complementary and Alternative Medicine* 2013, 2013 (July 21, 2013): e705121.
- Tsatsanis, C., C. Tsiriyotis, and D. A. Spandidos. "Hexamethylene Bisacetamide and Cis-Platin Stimulate the Expression from the HIV-1 Long Terminal Repeat Sequence in Human MCF-7 Cells." *In Vivo (Athens, Greece)* 6, no. 2 (April 1992): 145–49.
- UNAIDS. Global AIDS Update 2016.
- Van Lint, Carine, Sophie Bouchat, and Alessandro Marcello. "HIV-1 Transcription and Latency: An Update." *Retrovirology* 10 (2013): 67.
- Veracini, L., M. Franco, A. Boueux, V. Simon, S. Roche, and C. Benistant. "Two Functionally Distinct Pools of Src Kinases for PDGF Receptor Signalling." *Biochemical Society Transactions* 33, no. 6 (October 26, 2005): 1313–15.
- Verdin, E., P. Paras, and C. Van Lint. "Chromatin Disruption in the Promoter of Human Immunodeficiency Virus Type 1 during Transcriptional Activation." *The EMBO Journal* 12, no. 8 (August 1993): 3249–59.

- Vidler, Lewis R., Panagis Filippakopoulos, Oleg Fedorov, Sarah Picaud, Sarah Martin, Michael Tomsett, Hannah Woodward, Nathan Brown, Stefan Knapp, and Swen Hoelder. "Discovery of Novel Small-Molecule Inhibitors of BRD4 Using Structure-Based Virtual Screening." *Journal of Medicinal Chemistry* 56, no. 20 (October 24, 2013): 8073–88.
- Vincent, E E, D J E Elder, E C Thomas, L Phillips, C Morgan, J Pawade, M Sohail, M T May, M R Hetzel, and J M Tavaré. "Akt Phosphorylation on Thr308 but Not on Ser473 Correlates with Akt Protein Kinase Activity in Human Non-Small Cell Lung Cancer." *British Journal of Cancer* 104, no. 11 (May 24, 2011): 1755–61.
- Volberding, Paul A., and Steven G. Deeks. "Antiretroviral Therapy and Management of HIV Infection." *Lancet (London, England)* 376, no. 9734 (July 3, 2010): 49–62.
- Vollmuth, Friederike, Wulf Blankenfeldt, and Matthias Geyer. "Structures of the Dual Bromodomains of the P-TEFb-Activating Protein Brd4 at Atomic Resolution." *The Journal of Biological Chemistry* 284, no. 52 (December 25, 2009): 36547–56.
- Wang F, et al. (2010) Brd2 disruption in mice causes severe obesity without Type 2 diabetes. *Biochem J* 425(1):71–83.
- Wang, Yi, Steven D. Pennock, Xinmei Chen, Andrius Kazlauskas, and Zhixiang Wang. "Platelet-Derived Growth Factor Receptor-Mediated Signal Transduction from Endosomes." *Journal of Biological Chemistry* 279, no. 9 (February 27, 2004): 8038–46.
- Wang, Weiguang, Howard L. McLeod, and James Cassidy. "Disulfiram-Mediated Inhibition of NF-kappaB Activity Enhances Cytotoxicity of 5-Fluorouracil in Human Colorectal Cancer Cell Lines." *International Journal of Cancer* 104, no. 4 (April 20, 2003): 504–11.
- Wang, Chen-Yi, and Panagis Filippakopoulos. "Beating the Odds: BETs in Disease." *Trends in Biochemical Sciences* 40, no. 8 (August 2015): 468–79.
- Wen, Andy Y., Kathleen M. Sakamoto, and Lloyd S. Miller. "The Role of the Transcription Factor CREB in Immune Function." *Journal of Immunology (Baltimore, Md.: 1950)* 185, no. 11 (December 1, 2010): 6413–19.
- Williams, Samuel A, Lin-Feng Chen, Hakju Kwon, Carmen M Ruiz-Jarabo, Eric Verdin, and Warner C Greene. "NF-κB p50 Promotes HIV Latency through HDAC Recruitment and Repression of Transcriptional Initiation." *The EMBO Journal* 25, no. 1 (January 11, 2006): 139–49.
- Wilson, Boris G., and Charles W. M. Roberts. "SWI/SNF Nucleosome Remodellers and Cancer." *Nature Reviews. Cancer* 11, no. 7 (July 2011): 481–92.

- Whitehouse, I., A. Flaus, B. R. Cairns, M. F. White, J. L. Workman, and T. Owen-Hughes. "Nucleosome Mobilization Catalysed by the Yeast SWI/SNF Complex." *Nature* 400, no. 6746 (August 19, 1999): 784–87.
- Wollin, Lutz, Eva Wex, Alexander Pautsch, Gisela Schnapp, Katrin E. Hostettler, Susanne Stowasser, and Martin Kolb. "Mode of Action of Nintedanib in the Treatment of Idiopathic Pulmonary Fibrosis." *European Respiratory Journal*, March 5, 2015, ERJ-01749-2014.
- Wyce, Anastasia, Gopinath Ganji, Kimberly N. Smitheman, Chun-wa Chung, Susan Korenchuk, Yuchen Bai, Olena Barbash, et al. "BET Inhibition Silences Expression of MYCN and BCL2 and Induces Cytotoxicity in Neuroblastoma Tumor Models." *PLOS ONE* 8, no. 8 (August 23, 2013): e72967.
- Xia, Z., J. W. DePierre, and L. Nässberger. "Dysregulation of Bcl-2, c-Myc, and Fas Expression during Tricyclic Antidepressant-Induced Apoptosis in Human Peripheral Lymphocytes." *Journal of Biochemical Toxicology* 11, no. 4 (1996): 203–4.
- Xing, Sifei, Cynthia K. Bullen, Neeta S. Shroff, Liang Shan, Hung-Chih Yang, Jordyn L. Manucci, Shridhar Bhat, et al. "Disulfiram Reactivates Latent HIV-1 in a Bcl-2-Transduced Primary CD4+ T Cell Model without Inducing Global T Cell Activation." *Journal of Virology* 85, no. 12 (June 2011): 6060–64.
- Yang, Z., and J. D. Engel. "Human T Cell Transcription Factor GATA-3 Stimulates HIV-1 Expression." *Nucleic Acids Research* 21, no. 12 (June 25, 1993): 2831–36.
- Yang, Zhiyuan, Jasper H. N. Yik, Ruichuan Chen, Nanhai He, Moon Kyoo Jang, Keiko Ozato, and Qiang Zhou. "Recruitment of P-TEFb for Stimulation of Transcriptional Elongation by the Bromodomain Protein Brd4." *Molecular Cell* 19, no. 4 (August 19, 2005): 535–45.
- Youn, Gi Soo, Dong-Joo Kwon, Sung Mi Ju, Hyangshuk Rhim, Yong Soo Bae, Soo Young Choi, and Jinseu Park. "Celastrol Ameliorates HIV-1 Tat-Induced Inflammatory Responses via NF-kappaB and AP-1 Inhibition and Heme Oxygenase-1 Induction in Astrocytes." *Toxicology and Applied Pharmacology* 280, no. 1 (October 1, 2014): 42–52.
- Zhang, Weishi, Celine Prakash, Calvin Sum, Yue Gong, Yinghui Li, Jeffrey J. T. Kwok, Nina Thiessen, et al. "Bromodomain-Containing Protein 4 (BRD4) Regulates RNA Polymerase II Serine 2 Phosphorylation in Human CD4+ T Cells." *The Journal of Biological Chemistry* 287, no. 51 (December 14, 2012): 43137–55.
- Zhang, Guangtao, Ruijie Liu, Yifei Zhong, Alexander N. Plotnikov, Weijia Zhang, Lei Zeng, Elena Rusinova, et al. "Down-Regulation of NF-κB Transcriptional Activity in HIV-Associated Kidney Disease by BRD4 Inhibition." *The Journal of Biological Chemistry* 287, no. 34 (August 17, 2012): 28840–51.

- Wong, Victor C., Linda E. Fong, Nicholas M. Adams, Qiong Xue, Siddharth S. Dey, and Kathryn Miller-Jensen. "Quantitative Evaluation and Optimization of Co-Drugging to Improve Anti-HIV Latency Therapy." *Cellular and Molecular Bioengineering* 7, no. 3 (September 1, 2014): 320–33.
- Wu, Shwu-Yuan, A-Young Lee, Hsien-Tsung Lai, Hong Zhang, and Cheng-Ming Chiang. "Phospho Switch Triggers Brd4 Chromatin Binding and Activator Recruitment for Gene-Specific Targeting." *Molecular Cell* 49, no. 5 (March 7, 2013): 843–57.
- Zhao, Hua-Fu, Jing Wang, and Shing-Shun Tony To. "The Phosphatidylinositol 3-kinase/Akt and c-Jun N-Terminal Kinase Signaling in Cancer: Alliance or Contradiction? (Review)." *International Journal of Oncology* 47, no. 2 (August 2015): 429–36.
- Zhou, Meisheng, Keven Huang, Kyung-Jin Jung, Won-Kyung Cho, Zach Klase, Fatah Kashanchi, Cynthia A. Pise-Masison, and John N. Brady. "Bromodomain Protein Brd4 Regulates Human Immunodeficiency Virus Transcription through Phosphorylation of CDK9 at Threonine 29." *Journal of Virology* 83, no. 2 (January 2009): 1036–44.
- Zhou, Qiang, Tiandao Li, and David H. Price. "RNA Polymerase II Elongation Control." *Annual Review of Biochemistry* 81 (2012): 119–43.
- Zhu, Jian, Gaurav D. Gaiha, Sinu P. John, Thomas Pertel, Christopher R. Chin, Geng Gao, Hongjing Qu, Bruce D. Walker, Stephen J. Elledge, and Abraham L. Brass. "Reactivation of Latent HIV-1 by Inhibition of BRD4." *Cell Reports* 2, no. 4 (October 25, 2012): 807–16.
- Zuber, J., Shi, J., Wang, E., Rappaport, A.R., Herrmann, H., Sison, E.A., Magoon, D., Qi, J., Blatt, K., Wunderlich, M., et al. (2011). RNAi screen identifies Brd4 as a therapeutic target in acute myeloid leukaemia. *Nature* 478, 524–528.